Physiological mechanisms involved in the contamination and long retention of the amnesic shellfish poisoning toxin, domoic acid, in the king scallop Pecten maximus

José Luis García-Corona

COLLEGE SCIENCES DOCTORAL DE LA MER BRETAGNE ET DU LITTORAL

UBO Université de Bretagne Occidentale

THÈSE DE DOCTORAT DE

L'UNIVERSITE DE BRETAGNE OCCIDENTALE

ECOLE DOCTORALE N° 598
Sciences de la Mer et du Littoral
Spécialité : *Biologie marine*

Par

José Luis GARCÍA-CORONA

Mécanismes physiologiques impliqués dans la contamination et la lente dépuration de la toxine amnésiante, l'acide domoïque, chez la coquille Saint-Jacques P*ecten maximus*.

Thèse présentée et soutenue à Plouzané, le 07 juillet 2023
Unité de recherche : Laboratoire des sciences de l'environnement marin (LEMAR UMR 6539)

Rapporteurs avant soutenance :

Antonio J. PAZOS-CASTELOS	Professor, Department of Biochemistry and Molecular Biology, University of Santiago de Compostela, Santiago de Compostela, Spain.
Pascal FAVREL	Professeur, UMR BOREA Biologie des Organismes et des Écosystèmes Aquatiques, Université de Caen-Normandie, Caen, France.

Composition du Jury :

Président : Pascal FAVREL	Professeur, UMR BOREA Biologie des Organismes et des Écosystèmes Aquatiques, Université de Caen-Normandie, Caen, France.
Examinateurs :	
Antonio J. PAZOS-CASTELOS	Professor, Department of Biochemistry and Molecular Biology, University of Santiago de Compostela, Santiago de Compostela, Spain.
Patricia Mirella da SILVA SCARDUA	Professor, Department of Molecular Biology, Federal University of Paraíba, Joao Pessoa, PB, Brazil.
Juan BLANCO	Senior Researcher, Marine Research Center (CIMA), Vilanova de Arousa, Spain.
Dir. de thèse : Caroline FABIOUX	Maîtresse de conférences, Université de Brest, Institut Universitaire Européen de la Mer, UMR 6539 LEMAR, Plouzané, France.
Co-dir. de thèse : Hélène HEGARET	Directrice de Recherche CNRS, Institut Universitaire Européen de la Mer, UMR 6539 LEMAR Plouzané, France.

Invité(s)

Malwenn LASSUDRIE	Chercheuse, IFREMER ODE/UL/LER Bretagne Occidentale, Station de Biologie Marine, Concarneau, France.
Elodie FLEURY	Chercheuse IFREMER RBE-PHYTNESS, UMR 6539 LEMAR, Plouzané, France

Remerciements

Au Laboratoire des Sciences de l'Environnement Marin (LEMAR), de l'Institut Universitaire Européen de la Mer (IUEM), et à l'Université de Bretagne Occidentale (UBO) pour m'avoir accueilli et mis à disposition l'infrastructure pour mener à bien mes études doctorales, ainsi qu'un grand merci a une bonne partie du personnel du laboratoire, car il n'y a pas eu un seul jour au cours de ces quatre dernières années sans qu'ils ne m'aient fait me sentir chez moi.

Je tiens particulièrement à remercier Luis Tito de Morais (ancien directeur du LEMAR) pour son l'accueil chaleureux à mon arrivée au laboratoire et parce qu'il a toujours été au courant de mon bon état d'esprit pendant mon doctorat. Ainsi qu'à Géraldine Sarthou (actuelle directrice du LEMAR) pour sa disponibilité à m'aider pour toutes sortes de demandes auprès du laboratoire.

Au Consejo Nacional de Ciencia y Tecnología (CONACyT) du Mexique pour la bourse (REF: 2019-000025-01EXTF-00067) accordée pour payer mes études doctorales en France entre la période 2019-II et 2023-I.

Au projet de recherche «MaSCoET» (Mainten du Stock de Coquillages en lien avec la problématique des Efflorescences Toxiques) financé par France Filière Pêche et Brest métropole, et porté par le laboratoire DYNECO PELAGOS (Ifremer, Brest) dont le LEMAR (IUEM, UBO) est partenaire, pour le financement d'une grande partie des consommables et réactifs nécessaires pour developer ma recherche doctorale, ainsi que le financement pour ma participation à des congrès nationaux et internationaux.

Je ne peux pas aller plus loin sans remercier à mes deux directrices de thèse, mes deux chefs, Caroline Fabioux et Hélène Hegaret. Je n'ai jamais trouvé les mots pour exprimer l'énorme honneur que cela a été pour moi de travailler sous la direction de

deux personnes que j'admire beaucoup depuis que j'écrivais ma première thèse pour être biologiste marin, quand l'idée de travailler avec vous n'était qu'un rêve. Votre présence m'a toujours valu un grand respect et une grande admiration, mais vous, en plus de diriger magistralement mon travail de doctorat, m'avez appris deux grandes leçons qui me serviront pour le reste de ma vie professionnel : 1) comment mener à bien le travail scientifique d'une facon objective et correcte, et 2) le parfait exemple de ce que devrait être un directeur de thèse. Merci pour ces quatre années incroyables au cours desquelles vous m'avez aidé à grandir scientifiquement et humainement, merci de m'avoir fait confiance avec ce magnifique sujet de thèse, pour toute votre patience face à mon anxiété, et pour toute votre bienveillance depuis je suis arrivé en France. Carmen Rodriguez m'avait dit un jour que je méritais d'avoir les meilleurs directeurs de thèse pour mon doctorat, je ne sais pas si je le méritais vraiment, mais je les ai définitivement eus.

Je tiens à remercier a Malwenn Lassudrie et Elodie Fleury d'avoir accepté d'être co-encadrantes de cette thèse, pour toujours avoir être prêtes à m'aider avec tout ce dont je pourrais avoir besoin, et de m'avoir toujours encouragé pour la suite. Une petite parenthèse pour te remercier, Elo, d'avoir toujours été là pour m'aider pendant mes crises d'angoisse à 4h00 du matin, d'avoir toujours cru en moi et de m'avoir motivé en tout moment. Il n'y a eu aucun moment où tu ne m'as pas fait confiance. Pour moi, rencontrer Elodie Fleury (ma Brittney Spears scientifique) n'était qu'un rêve quand j'étais etudiant de licence, et j'ai fini par rencontrer l'une des plus belles personnes que j'ai pu croisser sur mon chemin. Ton amitié et ta bienveillance sont l'un des plus beaux cadeaux que la France pouvait me faire.

Ici je veux faire une autre parenthèse pour remercier énormément à Edouard Kraffe de m'avoir motivé pour faire un doctorat en France, et d'avoir toujours été au courant

de toute ma progression professionnelle et de mon intégration au sein du LEMAR. Ce doctorat à était sans aucun doute l'une des meilleures opportunités que j'ai eues dans ma vie. Merci vraiment Doudou.

Merci à Jonathan Flye-Sainte-Marie, Valentin Foulon, Juan Blanco, et Guillaume Rivière, qui ont accepté d'être membres de mon jury de thèse. Merci pour vos bonnes idées et pour vos encouragements.

Je tiens à remercier Antonio J. Pazos-Castello et Pascal Favrel d'avoir accepté d'être rapporteurs de thèse pré-soutenance, ansi que Juan Blanco et Patricia Mirella da Silva pour leur participation en tant qu'examinateurs pensant la soutenance de ce travail.

Je tiens à remercier tout particulièrement Juan Blanco, qui s'est activement impliqué dans l'interprétation correcte des résultats de ma recherche dès le début de mon doctorat, de m'avoir reçu dans son laboratoire en Galice pour collaborer avec lui et son équipe (Araceli, Carmen et Helena, a qui je remercie beaucoup aussi), pour le développement d'une partie importante des expériences de cette thèse, et pour sa volonté et sa toujours pour répondre toujours à mes questions de toutes sortes. Parler avec toi, Juan, c'était toujours comme lire un énorme livre plein de connaissances et d'expériences.

Un grand merci à l'Ecole Doctorale des Sciences de la Mer et du Littoral (EDSML), mais particulièrement à Elisabeth Bondou et Aurélie Claude pour m'avoir toujours aidé avec une bonne disposition avec mes mille questions.

Merci vraiment à l'ensamble de personnes du LEMAR, IUEM, UBO, et de l'IFREMER qui m'ont donné leur soutien technique pendant la partie analytique et expérimentale de mon travail de thèse, comme Margot Deléglise, Jean Vanmaldergem, Valentin Foulon, Philippe Elies, Eric Dabas, Amélie Derrien, Sylvain Petek, Aouregan Terre-

Terrillon, Virgille Quillen, et Christine Dubreuil. Mais je tiens particulièrement à remercier enormement à Nelly Le Goic, Christophe Lamber, et Adeline Bidault qui ont toujours répondu instantanément et avec une bonne disposition à mes millions de "j'ai une petite question". Ma thèse n'aurait pas été possible sans toute votre aide.

Je dois une part très importante de ce travail de thèse à mes stagiers Adeline Marzari, Marie Calvez, Laura Bressolier, Eva Calvo et Tomé Delaire, pour le travail incroyable qu'ils ont fait pour m'aider à mener à bien ce travail. Vous m'avez aussi appris une leçon importante que je garderai toujours à l'esprit: comment travailler avec mes futurs étudiants si un jour je deviens chercheur.

Je suis profondément reconnaissant à Sylvain Enguehard (Novakits, Nantes) d'avoir fourni les anticorps primaires non commerciaux nécessaires à la réalisation de cette étude après une rupture de stock internationale.

Un merci particulier à l'ecloserie du Tinduff et à Florian Breton pour leur aide avec son expertise dans certaines expériences de ce travail doctoral.

Merci à Carmen Rodríguez de CIBNOR, La Paz, pour tous ses conseils pour mener à bien des étapes cruciales de certaines des expériences de ce travail, et pour avoir toujours gardé un œil sur moi à distance.

Merci également à toute l'équipe administrative et financière du LEMAR. Particulièrement à Gene, Estelle, Nathalie, Sonia, Elodie, Delphine et Anne-Sophie, pour m'avoir aidé avec toute la paperasse que j'ai eu à faire pendant mon doctorat au laboratoire. Votre aide m'a sauvé à plusieurs fois.

Merci à The Interdisciplinary Graduate School for the Blue Planet, et au Groupe de recherche Phycotox, d'avoir financé des bourses de mobilité pour effectuer des séjours

de recherche ou participer à des réunions scientifiques au niveau national et international durant mon doctorat.

Merci au légendaire bureau A107 et a ses membres qui sont passés par ici pendant mon doctorat: Clément, Léna, Mallori, Laura, Maeva, Clémentine, Valentin, Manon, Justine et Bastian pour les bons moments et les bonbons.

Merci à tous les amis et personnes incroyables que j'ai eu l'occasion de rencontrer au laboratoire (Nathalia, Marc, Maria, Marcos, David, Vero, Anais, Lucie, Whenshen, Lisa, Nathasha, Eleonora, Charles, Cynthia, Elyne, Fernandihno, Danielle, Rafa, Justine (ma chouquette), Morgan S, Morgane G, Briva, Julien, Aude, Manon, Mickael, Seb H et Seb A, Gauthier (cabron), ainsi que à la bande des fous Brestois (Angela, Marin, Momo, Lena, Nora, Maggie, Estelle, Anto, Gwendo, Margaux, Pierre) pour toutes ces fêtes, soirées, repas, rires et bons souvenirs qui resteront à jamais. Vous avez joué un rôle important dans l'équilibre de ma santé mentale tout au long de ce processus.

Merci à mes élèves du cours de Génomique Marine (mes loulous) Laura, Axel, Alix, Helias, Eryne et Sylvain pour tous les repas et bons moments partagés. Vous m'avez vraiment soulagé dans certains des moments les plus difficiles du doctorat.

Merci infiniment à Brigitte, Gilles, Noelle, Vero, et Anne-Christine pour tous ces repas et bons moments qu'on a passé ensemble, et pour toujours m'avoir faire sentir chez moi et en famille lorsque j'étais loin de chez moi. Je vous considère comme la famille que la France m'a donnée pendant cette étape de ma vie doctorale dans ce pays.

Un merci tres special à Tati et Raúl, pour tous ces repas, voyages et moments incroyables que nous avons partagés ensemble lors de la dernière année de mon doctorat à Brest. J'ai trouvé une amitié incroyable en vous que j'espère garder encore de nombreuses années.

À mes amis mexicains (Caro, Paulina, Abel, Maritza, Raul, Ana Nader, Salwa, Pamela, Fabz, Coral) qui sont restés en contact tres prochaiment de moi tout au long de ces quatre années et qui m'ont donné l'impression que mon temps au Mexique ne s'est pas arrêté.

Merci à ma cousine Norma Corona (ma sœur aînée) et à toute la famille pour le soutien qu'ils m'ont apporté quand j'étais embarqué dans cette aventure, et pour tout leur soutien tout au long de ces quatre années d'absence.

Un immense merci à Ludovic Fougeroux pour toute sa bienveillance, ses conseils avisés, et son soutien durant les semaines avant et après la réalisation de cette étape professionnelle, et pour avoir rendu mon départ de France beaucoup moins difficile que je l'avais imaginé.

Finalement, mais l’un des plus importants remerciements dans cette thèse est pour ma famille. Mes parents (Blas García et Gloria Corona) et mes petits frères (Osvaldo et Francis), Merci infiniment d’avoir accepté mon absence loin de notre famille pendant ces quatre dernières années, et pour m'avoir toujours soutenu et motivé pour poursuivre mes rêves professionnels, même si cela impliquait de ne pas se voir pendant longtemps.

INTRODUCTION GENERALE & OBJECTIFS DE LA THESE

Les proliférations de microalgues toxiques et nuisibles (ou “Harmful Algal Blooms” HAB, pour ces sigles en anglais) sont des proliférations massives de de micro-algues dans les environnements côtiers ayant des conséquences majeures sur les écosystèmes marins et la santé humaine dans le monde entier (Turner *et al.,* 2021). Sur environ 5 000 espèces de microalgues marines répertoriées, environ 300 sont connues pour former des HAB, communément appelés «marées rouges», car les efflorescences de microalgues varient énormément en couleur et en densité cellulaire (Hallegraeff, 1995). Dans les écosystèmes marins, les organismes responsables des HAB sont principalement des dinoflagellés et des diatomées (Lassus *et al.,* 2016*;* Turner *et al.,* 2021*;* Tewari, 2022). La fréquence des HAB a augmenté dans le monde au cours des dernières décennies (Anderson *et al.,* 2012*;* Tewari, 2022). Depuis la dernière décennie, la Commission océanographique intergouvernementale de l'UNESCO a sonné l’alarme sur les HAB qui représentent maintenant l’une des préoccupations écologiques et socio-économiques majeures au niveau mondial (Kudela *et al.,* 2015).

Les microalgues peuvent être considérées comme toxiques ou nuisibles lorsque certaines microalgues naturellement présentes dans l'environnement prolifèrent avec des effets qui peuvent être délétères pour les organismes marins, soit parce qu'une forte biomasse induit une hypoxie sévère dans l'eau, soit parce que les microalgues produisent des composées toxiques qui endommagent physiquement les tissus des organismes qui les ingèrent, soit enfin parce que ces microalgues produisent des phycotoxines, qui affectent les organismes qui les consomment directement, soir les consommateurs supérieurs par transfert trophique (Fernández *et al.,* 2003*;* Hoagland & Scatasta, 2006*;* Turner, 2021). Ainsi, les phycotoxines représentent également une préoccupation importante pour la santé humaine, car certaines sont nocives, voire

mortelles pour les mammifères, dont l'Homme, souvent par le biais de la consommation de coquillages contaminés (Grattan *et al.,* 2016). Les efflorescences de microalgues toxiques et nuisibles, peuvent ainsi induire des pertes économiques de plusieurs millions de dollars dans les secteurs du tourisme et de l'industrie (Shumway, 1990*;* Van Dolah, 2000*;* Hoagland *et al.,* 2002*;* Hallegraeff, 2014). De plus, ces événements représentent un problème critique pour les écosystèmes marins car ils peuvent perturber les structures des communautés et du réseau trophique (Hallegraeff, 2010).

La plupart des phycotoxines ont été classées selon leurs effets toxiques et les syndromes qu'elles provoquent chez l'homme après la consommation de coquillages contaminés (Lassus *et al.,* 2016). Les intoxications les plus connues sont l'intoxication par des toxines paralysantes (Paralytic Shellfish Poisoning : PSP), l'intoxication par des toxines diarrhéiques (Diarrheic Shellfish Poisoning : DSP), l'intoxication par des toxines neurotoxiques (Neurologic Shellfish Poisoning : NSP), l'intoxication à la ciguatera (CP), l'intoxication par l'azaspiracide (AZP) et l'intoxication par des toxines amnésiantes (Amnesic Shellfish Poisoning : ASP) (Hallegraeff 2004*;* Lawrence *et al.* 2011, Lassus *et al.* 2016). Ce dernier, «Amnesic Shellfish Poisoning (ASP)» est causé par la phycotoxine acide domoïque (AD) (Fig. 1), un acide aminé cyclique hydrosoluble neuroexcitateur chez les mammifères, homologue de l'acide glutamique.

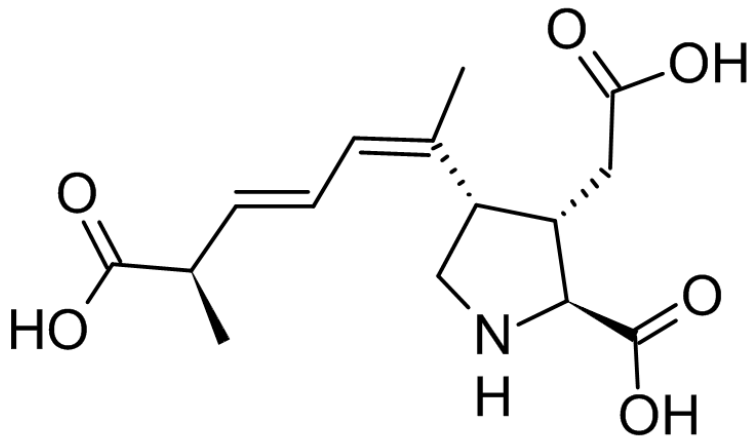

Figure 1. Structure chimique de l'acide domoïque.

L'AD est produit par au moins 29 souches de diatomées du genre *Pseudo-nitzschia* (Fig. 2) (Lundholm *et al.,* 2009; Trainer *et al.,* 2012; Grattan *et al.,* 2016; Bates *et al.,* 2018), où l'espèce *P. australis* semble être l'une des plus toxiques de toutes (Lelong *et al.,* 2012; La Barre *et al.,* 2014).

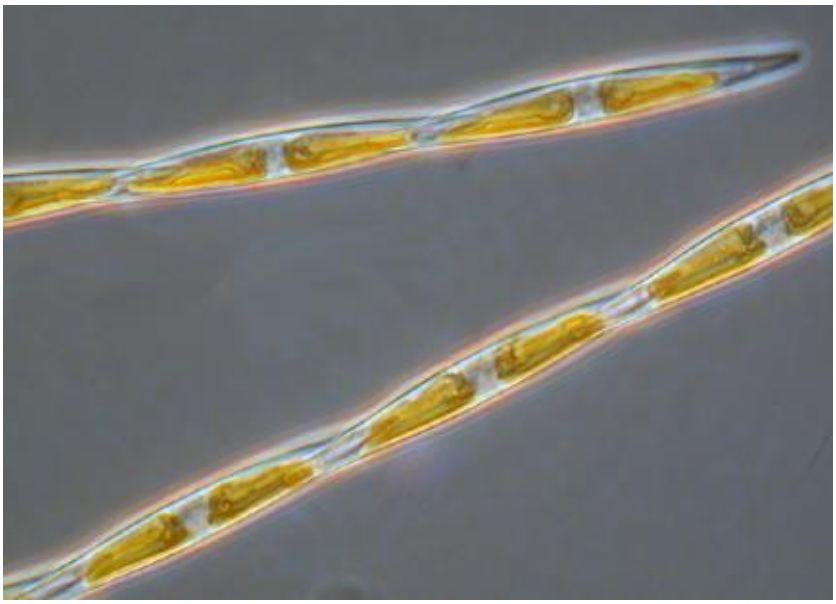

Figure 2. *Pseudo-nitzschia sp*. Photo prise par Dr Rozalind Jester.

Chez les mammifères, les principaux symptômes toxicologiques de l'ASP comprennent les nausées, la gastro-entérite et les vomissements, suivis de signes

neurologiques tels que la confusion, la léthargie, la désorientation, la paresthésie, la perte de mémoire à court terme et, dans les cas extrêmes, le coma et la mort (Pulido, 2008; La Barre *et al.,* 2014; Miller *et al.,* 2021). Les effets critiques de neurotoxicité de l'AD sont médiés par son activité de liaison et d'agoniste de haute affinité sur certaines formes de récepteurs du glutamate dans certaines régions du cerveau (par exemple, l'hippocampe), entraînant la mort des cellules neuronales (Perl *et al.,* 1990; Lerma *et al.,* 1993; Ramsdell, 2007; Pulido, 2008). L'événement ASP le plus meurtrier jamais enregistré à ce jour s'est produit à l'Île-du-Prince-Édouard, au Canada, en 1987, où près de 100 personnes sont décédées et au moins 150 autres sont tombées malades après avoir consommé des moules bleues *Mytilus edulis* contaminées avec l'AD (Bates *et al.,* 1998; Trainer *et al.,* 2008; La Barre *et al.,* 2014).

En tant qu'organismes filtreurs des microalgues, les bivalves sont sujets à la contamination et à l'accumulation rapide de grandes quantités de neurotoxines produites par les HAB, comme c'est le cas pour l'AD. Ainsi, la consommation des coquillages et de poissons est le principal vecteur de problèmes en santé humaine liés aux HAB comme l'ASP (Lelong *et al.,* 2012; Grattan *et al.,* 2016). En Europe, la réglementation a interdit la commercialisation des coquillages lorsque la concentration en AD est supérieure à 20 mg kg^{-1} de chair totale sur l'ensemble ou sur des parties individuelles de l'animal (McKenzie et Bavington, 2002; Wekell *et al.,* 2004). Néanmoins, les concentrations en AD mesurées dans les tissus des bivalves au cours des programmes de surveillance varient considérablement d'une espèce à l'autre, principalement en raison de différences importantes dans la vitesse de dépuration de la toxine (Blanco *et al.,* 2002, 2021b). Ces différences dans les taux d'excrétion des toxines ont conduit les bivalves à être classés comme dépurateurs «rapides» ou «lents» de l'AD. La plupart des bivalves, comme les moules et les huîtres (Novaczek

et al., 1992; Blanco *et al.,* 2002a; Mafra *et al.,* 2010), plusieurs espèces des clams et palourdes (Blanco *et al.,* 2010; Álvarez *et al.,* 2015; Dusek-Jennings *et al.,* 2020), et certains pétoncles (Wohlgeschaffen *et al.,* 1992; Douglas *et al.,* 1997; Álvarez *et al.,* 2020) dépurent l'AD en quelques heures/jours ou en quelques semaines, suite à des efflorescences de *Pseudo-nitzschia spp.* toxique, ayant ainsi un impact relativement faible sur leur récolte et leur commercialisation. Cependant, d'autres espèces telles que la coquille Saint-Jacques *Pecten maximus* (Blanco *et al.,* 2002a; 2006; García-Corona *et al.,* in prep a) et le couteau *Siliqua patula* (Horner *et al.,* 1993; Dusek Jennings *et al.,* 2020) sont catalogués comme les dépurateurs de l'AD les plus lents parmi les bivalves.

Cela est particulièrement problématique pour les flottes de pêche et l'industrie aquacole de *P. maximus*, puisque cette espèce est capable d'accumuler jusqu'à 3200 mg AD kg^{-1} dans la glande digestive (DG), et ~2900 mg AD kg^{-1} dans la chair totale, en le retenant dans les tissus pendant de longues périodes, jusqu'à des années dans certains cas (Blanco *et al.,* 2002a, 2006; García-Corona in prep a). Dans le cas de plusieurs efflorescences consécutives de *Pseudo-nitzschia* toxiques, cette dépuration lente peut conduire à une ré-intoxication des coquilles avant qu'elles aient dépuré les charges d'AD de la première efflorescence (Blanco *et al.,* 2006b; Mauriz et Blanco, 2010; Blanco *et al.,* 2021b). Au cours des trente dernières années, des fermetures prolongées de la pêche à la coquille Saint-Jacques ont eu lieu en Irlande (Bogan *et al.,* 2007a,b), en Écosse (Campbell *et al.,* 2001), en Espagne (Arévalo *et al.,* 1998; Blanco *et al.* , 2002a, 2006, 2020, 2021b), au Portugal (Vale et Sampayo 2001) et en France (Amzil *et al.,* 2001; Nézan *et al.,* 2006; Husson *et al.,* 2016), entraînant des impacts économiques négatifs sur l'exploitation des coquilles Saint-Jacques sauvages et d'élevage (Blanco *et al.,* 2002a, 2006a, 2021b; Husson *et al.,* 2016). Parallèlement,

la surveillance en France a révélé que les efflorescences toxiques de *Pseudo-nitzschia* sont devenues plus fréquentes depuis l'année 2000 (Amzil *et al.,* 2001; Husson *et al.,* 2016). De même, au Royaume-Uni, les données sur l'occurrence de l'AD et les événements toxiques associés ont montré une augmentation de la fréquence depuis l'année 2008 (Rowland-Pilgrim *et al.,* 2019). La presence d'espèces de *Pseudo-nitzschia* toxique est répertoriée dans le monde entier (Lelong *et al.,* 2012) (Fig. 3).

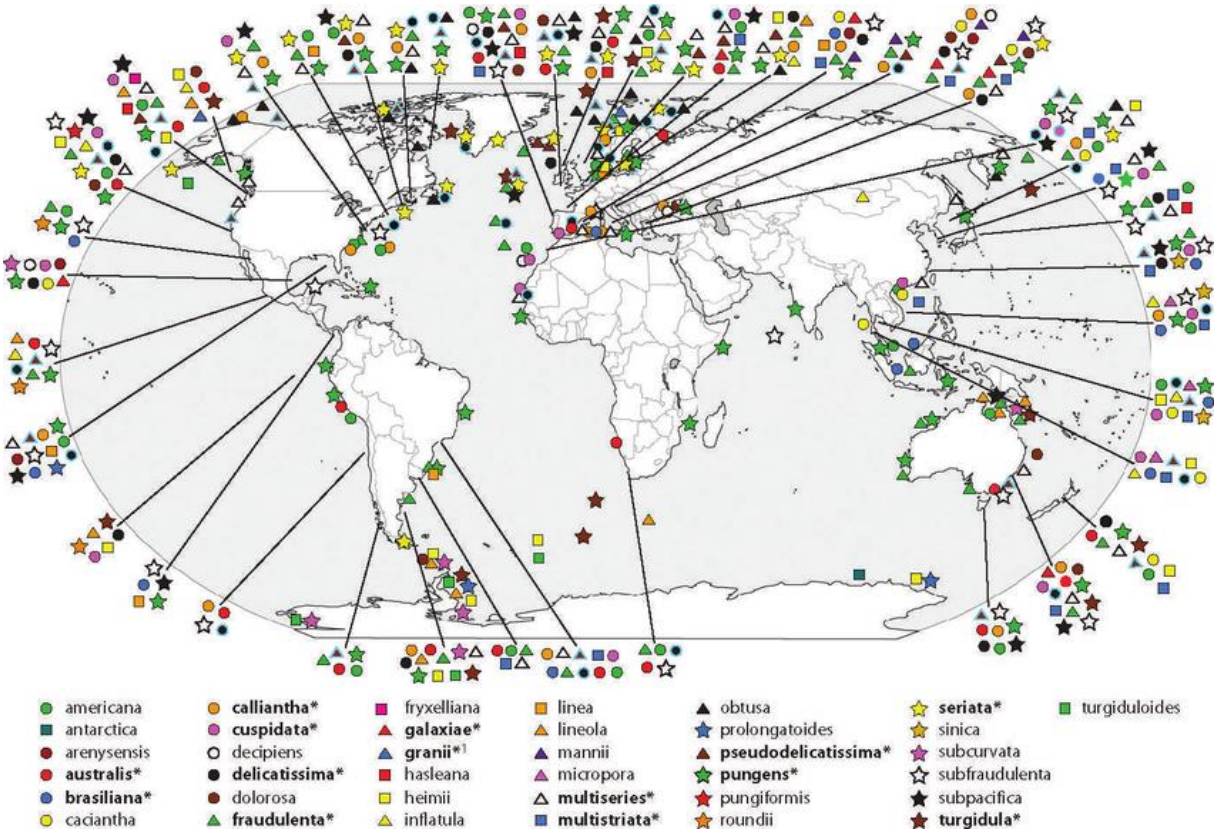

Figure. 3. Répartition mondiale des *Pseudo-nitzschia* spp. Les espèces toxigues sont en gras et signalées par un * ; il est à noter que seules certaines souches de ces espèces sont toxigues dans certains endroits (Lelong *et al.,* 2012

La durée des fermetures de pêche est principalement modulée par le taux de dépuration des organismes, qui semble être spécifique à l'espèce (Blanco *et al.,* 2002a). Jusqu'au travail présenté dans cette thèse, seules quelques études ont permis la formulation d'hypothèses pouvant expliquer les différences profondes dans la cinétique de dépuration entre les dépurateurs rapides et les dépurateurs lents d'AD.

D'une part, Mauriz et Blanco (2010) ont constaté que la glande digestive de *P. maximus* accumule plus de 80 % des charges totales d'AD, et que près de 90% de l'AD accumulé dans la glande digestive était libre sous une forme soluble dans le cytoplasme des cellules digestives. Ils en ont ainsi déduit que les taux d'accumulation élevés d'AD et sa dépuration lente pourraient être dus à l'absence de transporteurs membranaires efficaces pour excréter la toxine chez *P. maximus,* Chez d'autres espèces, telles que le couteau *Siliqua patula*, la présence de plusieurs formes de récepteurs au glutamate, avec des affinités et des sensibilités différentes pour l'AD a été identifiée, suggère que l'activation différentielle de récepteurs à forte affinité mais faible sensibilité à l'AD dans des tissus précis pourrait expliquer que les couteaux retiennent l'AD pendant de longues périodes sans effets toxigènes significatifs (Trainer et Bill, 2004). Chez le pétoncle chilien *Argopecten purpuratus*, la clé de la dépuration rapide de l'AD pourrait reposer sur le transfert rapide de la plupart des charges de toxines accumulées dans la glande digestive vers d'autres organes capables de l'excréter avec une plus grande efficacité (Álvarez *et al.,* 2020). Néanmoins, aucune de ces hypothèses n'a encore été entièrement confirmée.

Après quelques analyses transcriptomiques chez la moule *Mytilus galloprovincialis* (Pazos *et al.,* 2017) et le pétoncle blanc *Aequipecten opercularis* (Ventoso *et al.,* 2019) *in vivo* exposés à des cellules de *Pseudo-nitzschia* productrices de l'AD, la régulation différentielle de certaines protéines codant pour des transporteurs membranaires de la famille des transporteurs de solutés (SLC) et des enzymes impliquées dans le système antioxydant et de détoxification ont été trouvées. Dans une autre analyse RNA-seq, Ventoso *et al.* (2021) ont découvert que l'injection intramusculaire d'AD chez *P. maximus* conduisait à l'augmentation du taux de transcrits de plusieurs récepteurs du glutamate, ainsi qu'à la surexpression de certains gènes liés à l'autophagie, au

transport médié par les vésicules, à la réponse antioxydante et à certains transporteurs SLC dans les cellules digestives des coquilles Saint-Jacques. De plus, la caractérisation des mécanismes d'absorption de l'AD dans la GD de *M. galloprovincialis* réalisée par Blanco *et al.* (2021a) ont suggéré que le mécanisme de transport de l'AD ne serait pas dépendant de Na^+, H^+ ou de l'ATP, mais impliquerait la présence de transporteurs membranaires dépendants de Cl^- (ou des autres anions$^-$), responsables de l'entrée de l'AD dans les cellules digestives. Toutes ces évidences nous ont amenés à émettre l'hypothèse que la reconnaissance et le transport de l'AD au niveau moléculaire dans les cellules digestives pourraient être des processus à l'origine de la forte accumulation et de la lente dépuration de cette toxine chez *P. maximus*.

La proposition de méthodes pour accélérer la dépuration d'AD chez *P. maximus* a été énormément entravée par le manque de connaissances sur les mécanismes physiologiques impliqués dans la longue rétention de cette toxine chez cette espèce. Jusqu'à présent, aucune étude n'a pu fournir de données robustes sur la localisation précise de l'AD dans les tissus de bivalves contaminés. Cette thèse a donc permis la localisation précise de l'AD dans les tissus des coquilles Saint-Jacques, mais aussi d'autres espèces d'invertébrés contaminés, en comparant les fortes différences intra- et interspécifiques de la toxicocinétique de l'AD mentionnées ci-dessus à partir d'une approche englobant différentes échelles d'organisation: individuelle, tissulaire, cellulaire, et moléculaire.

Ainsi, l'approche méthodologique de cette thèse s'appuie sur l'assemblage multidisciplinaire des domaines scientifiques précités visant à répondre à la question principale de recherche: quels sont les principaux mécanismes physiologiques impliqués dans la cinétique d'accumulation et de dépuration lente de l'AD chez la

coquille Saint-Jacques *P. maximus* après des efflorescences toxiques de *Pseudo-nitzschia spp.*? Pour répondre à cette question, cette thèse s'articule autour de cinq objectifs (Fig. 4).

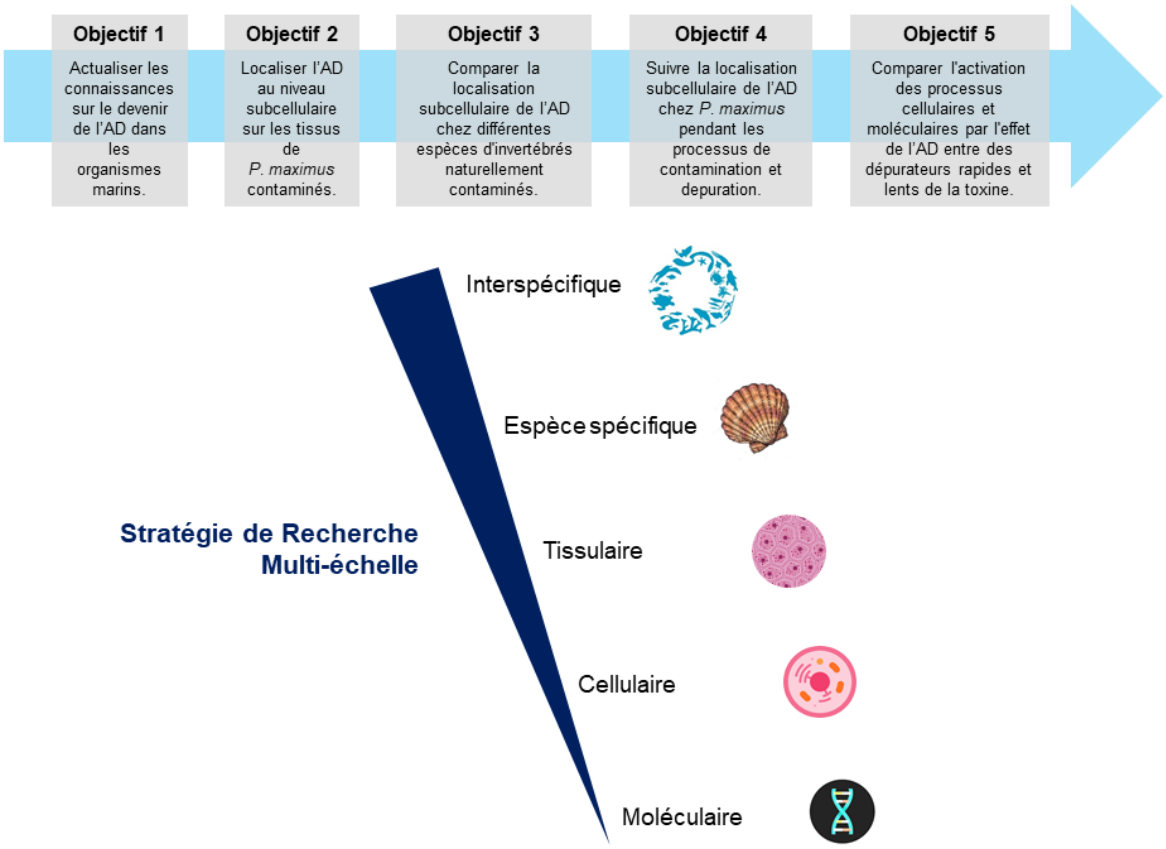

Figure 4. Objectifs de la thèse et stratégie de recherche multi-échelle.

Afin d'atteindre ces objectifs et de répondre à la question principale de recherche, cette thèse est structurée en sept parties.

Le **Chapitre 1**, qui complète cette introduction, est une revue qui se veut la plus exhaustive possible, de la littérature sur les connaissances actuelles sur le devenir de l'AD dans les écosystèmes marins, abordant les questions concernant 1) une liste actualisée des espèces *Pseudo-nitzschia* responsables de l'ASP, ainsi que les principales espèces de poissons et de coquillages qui accumulent de l'AD; 2) des informations spécifiques sur la toxicité de l'AD chez les vertébrés marins; 3) des détails

sur l'accumulation de l'AD dans les poissons et les invertébrés marins en mettant l'accent sur le transport trophique de la toxine; 4) les connaissances disponibles sur les taux d'accumulation et de dépuration de l'AD entre les espèces de poissons et de coquillages, 5) les effets de l'exposition à l'AD ou à *Pseudo-nitzschia* toxique sur certains traits physiologiques des bivalves à différents stades de vie; et 6) l'impact de *Pseudo-nitzschia* toxique et de l'AD sur les écosystèmes marins.

Le **Chapitre 2** présente les résultats d'une innovante technique immunohistochimique (IHC) développée au cours de la première partie de cette thèse pour réaliser la localisation de l'AD au niveau subcellulaire sur des coupes histologiques de *P. maximus* contaminées après des efflorescences naturelles de *Pseudo-nitzschia spp*.

Le **Chapitre 3** traite de la comparaison de la localisation subcellulaire de l'AD dans les tissus de cinq espèces d'invertébrés contaminés après des efflorescences naturelles ASP en appliquant la technique IHC développée dans le chapitre 2 de cette thèse.

Le **Chapitre 4** est consacré à l'étude de la cinétique de localisation subcellulaire de l'AD dans les glandes digestives de *P. maximus,* en utilisant la technique IHC anti-DA mentionnée précédemment, dans un scénario de contamination naturelle lors des efflorescences de *P. australis* productrice de l'AD, ainsi que lors de la dépuration contrôlée de l'AD au laboratoire chez des coquilles Saint-Jacques fortement contaminées collectées sur le terrain après des efflorescences de *P. australis*.

Le **Chapitre 5** vise à comparer l'activation des principaux mécanismes subcellulaires et moléculaires activés par l'exposition *in vitro* à l'AD dissoute dans les glandes digestives de deux espèces de bivalves, le dépurateur lent *P. maximus* vs le dépurateur rapide *Mytilus edulis*.

Enfin, la dernière partie de cette thèse présente une discussion générale des résultats obtenus dans ce travail, associée à un ensemble de perspectives qui font émerger de nouvelles questions/hypothèses, ainsi que des pistes de recherche futures potentielles pour poursuivre l'étude de ce phénomène et avancer dans la proposition de méthodes pour accélérer la dépuration de l'AD chez *P. maximus* .

Cette thèse s'intègre dans le projet de recherche «MaSCoET» (Maintien du Stock de Coquillages en lien avec la problématique des Efflorescences Toxiques) financé par France Filière Pêche et Brest métropole, et porté par le laboratoire DYNECO PELAGOS (Ifremer, Brest) dont le LEMAR (IUEM, UBO) est partenaire. Plus precisement, cette thèse s'insère en particulier dans l'objectif n°2 du projet visant à mieux comprendre pourquoi la décontamination des coquilles Saint-Jacques en AD est très lente par rapport à d'autres pectinidés.

Chacun des cinq chapitres de ce manuscrit fait l'objet d'un article scientifique, en préparation pour les chapitres 1, 3, 4 et 5 et publié pour le chapitre 2.

Les chapitres étant présentés sous la forme d'articles publiés ou près à être soumis, la numérotation des figures est indépendante dans chacun des chapitres (1, 2, 3, 4 et 5). Pour les parties « introduction », « préambules » et « discussion », la numérotation des figures se suit.

CHAPTER 1

THE FATE OF THE AMNESIC TOXIN, DOMOIC ACID, IN MARINE ORGANISMS

PREAMBLE

The first and deadliest ASP event ever recorded up to date occurred in Prince Edward Island, Canada, in 1987 where nearly 100 people died, and at least 150 others got sick after consuming blue mussels *Mytilus edulis* contaminated with DA (Bates *et al.,* 1998; Trainer *et al.,* 2008; La Barre *et al.,* 2014). Following this fatal ASP event, *Pseudo-nitzschia* DA-producers have been detected in all oceans of the world (Trainer *et al.,* 2012; Lelong *et al.,* 2012; McCabe *et al.,* 2016; Bates *et al.,* 2018). Beside the deleterious effects of DA on human health causing up to death in most severe cases (Pulido, 2008; Lefebvre & Robertson, 2010; Basti *et al.,* 2018), DA can also have highly detrimental effects on entire marine ecosystems (Bejarano *et al.,* 2008). DA can affect marine organisms through the food web, which has even resulted into massive mortality events of marine wildlife in several areas and potentially leading to an imbalance of the coastal ecosystem structure (Trainer *et al.,* 2012; La Barre *et al.,* 2014; Lefebvre *et al.,* 2018).

Up to date there are nearly 24 literature reviews and more than 300 scientific articles on the interaction between marine organisms and DA-producing diatoms of the genus *Pseudo-nitzschia*, but there is none that compiles updated information on accumulation, anatomical distribution, and depuration of DA, as well as its potential effects on marine organisms accumulating this toxin. Hence, there is a need to encompass the updated and latest information on the fate of DA on marine biodiversity. In this review we summarize current knowledge about 1) the latest list of species responsible for ASP, as well as the main fish and shellfish species that accumulate DA; 2) specific information of DA toxicity in marine vertebrates; 3) details on DA accumulation in marine fish and invertebrates with emphasis on the trophic transport of toxin; 4) available knowledge on toxin accumulation and depuration rates between

fish and shellfish species, 5) effects of DA or toxic *Pseudo-nitzschia* exposure on some physiological traits of bivalves at different life stages; and 6) the impact of toxic *Pseudo-nitzschia spp.,* and DA on marine ecosystems.

The fate of the Amnesic Shellfish Poisoning (ASP) toxin, domoic acid, in marine fish and invertebrates.

José Luis Garcia-Corona[1]*, Caroline Fabioux[1], Juan Blanco[2], Raúl O. Martínez-Rincón[3], Hélène Hegaret[1]*

[1]Institut Universitaire Européen de la Mer, Laboratoire des Sciences de l'Environnement Marin (UMR6539 CNRS/UBO/IFREMER/IRD) Technopôle Brest-Iroise, Plouzané 29280, France.

[2]Centro de Investigacións Mariñas (CIMA), Xunta de Galicia, Pedras de Coron s/n, 36620 Vilanova de Arousa, Spain.

[3]Centro de Investigaciones Biológicas del Noroeste (CIBNOR), Mar Bermejo 195, Col. Playa Palo de Santa Rita, La Paz, B.C.S. 23090, Mexico.

*Corresponding autor: José Luis García-Corona, Hélène Hegaret

Institut Universitaire Européen de la Mer, Laboratoire des Sciences de l'Environnement Marin (UMR6539 CNRS/UBO/IFREMER/IRD) Technopôle Brest-Iroise 29280, Plouzané, France.

e-mail: jose.corona@univ-brest.fr, helene.hegaret@univ-brest.fr

ABSTRACT

Domoic acid (DA), the phycotoxin responsible for the amnesic shellfish poisoning (ASP), is an excitatory amino acid naturally produced by bloom-forming marine diatoms *Pseudo-nitzschia spp.* The increase in frequency, intensity and global distribution of DA-producing harmful algal blooms is a growing problem worldwide. Filter feeders, such as bivalve molluscs, can accumulate and lengthy retain high amounts of DA in their tissues, threatening human health and leading to extensive-prolonged fishery and aquaculture closures. This paper reviews sources of DA, as well as variations in toxicity, accumulation, anatomical distribution, detoxification kinetics and physiological effects of DA in marine invertebrates.

Twenty-nine species of the genus *Pseudo-nitzschia* are show to be toxigenic with the production of DA. Monitoring networks have therefore been implemented to detect the presence of *Pseudo-nitzschia* cells in the water, as well as the presence of DA in tissues of bivalves, as these filter feeders concentrate and bioaccumulate the highest concentrations of DA. The total toxic burden is not distributed evenly throughout the tissues of contaminated animals; more DA is concentrated in non-edible tissues, as the digestive gland, remaining highly toxic even throughout months or even years. Nevertheless, so far no constant correlation between tissues can be established due to the influence of factors that affect DA anatomical partitioning. Moreover, DA appears not to be biotransformed or translocated to any tissue for storage in fish and shellfish organs.

Marine invertebrates can be broadly classified as rapid or slow DA depurators. The former takes weeks to detoxify; the latter takes months to years. Depuration rate of DA does not seem to be related to several variables, as microhabitat differences and shell length; furthermore, toxin biotransformation seems not lead to changes in net DA

burden. Profound inter and intra-specific differences in the toxicokinetics of DA have been identified in a wide variety of species; nonetheless, a better understanding of the fate of DA is necessary for greater accuracy in the prediction of shellfish toxicity during *Pseudo-nitzschia* outbreaks, and to propose alternatives for depuration in contaminated fish and shellfish catches.

The present work also reviews the toxicokinetics of DA in other marine organisms, such as fish, cephalopods, crabs, and ascidians. Despite very few publications relating effects of *Pseudo-nitzschia spp*. or DA on filter feeders, literature indicates that DA uptake disrupts behavioural and complex metabolic, molecular and physiological processes in bivalves, including those based upon antioxidant/detoxification enzyme pathways, oxidative stress, and non-specific immune responses, making them more vulnerable to environmental stress-inducing agents. DA accumulation also compromises onset development (embryo-larval growth and survival) of bivalves, which suggests that this toxin could affect natural recruitment and aquaculture.

Key words: Amnesic shellfish poisoning, *Pseudo-nitzschia* outbreaks, domoic acid, toxicokinetics, decontamination strategies, fish and shellfish.

1. Impacts of *Pseudo-nitzschia* and domoic acid transfer in marine ecosystems

The Amnesic Shellfish Poisoning (ASP) syndrome is caused by domoic acid (DA) an extremely dangerous neurotoxin produced mainly by bloom-forming species of diatoms of the genus *Pseudo-nitzschia* (Table I). Currently, there are 58 species of diatoms belonging to the genus *Pseudo-nitzschia*, of which 29 have been identified as DA-producing species (Lelong *et al.,* 2012; Trainer *et al.,* 2012; Bates *et al.,* 2018).

Until the late 1990s, early records suggested that DA-producing *Pseudo-nitzschia* outbreaks only occurred along the occidental coasts of North America and Europe (Lundholm *et al.,* 1994; Rhodes *et al.,* 1998; Bates *et al.,* 2000). Notwithstanding, in the last thirty years, blooms of DA-producing *Pseudo-nitzschia spp.* have spread and occur abruptly in tropical areas around the world between 40° N and 40° S (Bates & Trainer, 2006; Lelong *et al.,* 2012; Bates *et al.,* 2018). New records of toxic *Pseudo-nitzschia* include countries like Turkey (Ayaz *et al.,* 2018), Vietnam (Kotaki *et al.,* 2000; Lundholm & Moestrup, 2000), Malaysia (Teng *et al.*, 2014; Tan *et al.,* 2016; Suriyanti *et al.,* 2017), Thailand (Romero *et al.,* 2008), Indonesia (Romero *et al.,* 2011; Thoha *et al.,* 2012), the Phillippines (Romero *et al.,* 2012), China (Li *et al.,* 2017; Kim *et al.,* 2018), Japan (Kotaki *et al.,* 2008; Zheng *et al.,* 2022), Australia (Higgins *et al.,* 2003), Brazil (Cavalcante, 2011), and Mexico (Santiago-Morales *et al.,* 2011; Teng *et al.,* 2015; Rivera-Vilarelle *et al.,* 2018; Clark *et al.,* 2019). As a consequence of the extended distribution and increasing number of toxigenic species worldwide, it is now possible to osberve DA more pervasively within the food web, contaminating new marine organisms of higher trophic levels (Bejarano *et al.,* 2008; Trainer *et al.,* 2012; Zabaglo *et al.,* 2016).

In this review we list all DA-synthesizing *Pseudo-nitzschia* species including an updated list of new toxicity records on fish and invertebrates (Table I). Here, only basic aspects of toxic *Pseudo-nitzschia* species, new toxicity records, and outbreaks occurrence are highlighted. Other aspects as the historical and physicochemical background of DA, as well as biology, ecotoxicology, geographical distribution, toxicity and metabolism of the genus *Pseudo-nitzschia* are reviewed elsewhere (Bates, 1998; Mos, 2001; Fryxell and Hasle, 2002; Lelong *et al.,* 2012; Trainer *et al.,* 2012; La barre *et al.,* 2014; Zabaglo *et al.,* 2016; Hallegraeff, 2017; Basti *et al.,* 2018; Bates *et al.,* 2018; Lundholm, 2018). As seen in Fig. 1, DA is accumulated in the vast majority by marine bivalves (around 200 species), but also in small fish like sardines and anchovies, or large pelagic predators, as tuna and mackerel (~50 species), as well as crustaceans (~30 species) and other invertebrates, ranging from zooplankton copepods to other mollusks as gastropods and cephalopods, polychaetes, ascidians, and echinoderms (Table I, Fig.1).

Within the list of species of the genus *Pseudo-nitzschia* able to produce DA, *P. australis* and *P. multiseries* seem to be the species with the highest number of records of toxic bloom occurrence around the world (Lelong *et al.,* 2012; Bates *et al.,* 2018). Hence, it is not surprising that the highest number of fish and invertebrate species affected by DA-accumulation corresponds to those two toxic species (73 species affected by *P. australis* and 60 species by *P. multiseries*), followed by *P. delicatissima*, *P. pseudodelicatissima*, and *P. pungens*, with ~24 animal species affected by each diatom species (Fig. 1, Table I). As shown below (subsection 4) when DA burdens are above the regularty threshold (20 µg g^{-1}) in seafood, the causative species are frequently *P. australis* and *P. multiseries* (Fig. 1). Unfortunately, in most cases, when toxin levels are monitored, the *Pseudo-nitzschia* species responsible for DA production

is not determined. Since bivalves are commonly used as sentinels to detect the presence of DA in marine ecosystems, it is not surprising that for some *Pseudo-nitzschia* species ≥ 90% of toxicity events correspond to this group of invertebrates, as is the case of *P. cuspidata*, *P. fraudulenta*, and *P. turgida* (Fig. 1, Table I). Furthermore, in the last 6 years, 11 other *Pseudo-nitzschia* species (*P. abrensis, P. batesiana, P. bipertita, P. fukuyoi, P. hasleana, P. lundohlniae, P. obtusa, P. plurisecta, P. simulans, P. subcurvata,* and *P. subfraudulenta*) have been discovered to be capable of producing DA. However, there are still no records of accumulation by any species of fish or invertebrates from these species (Table I).

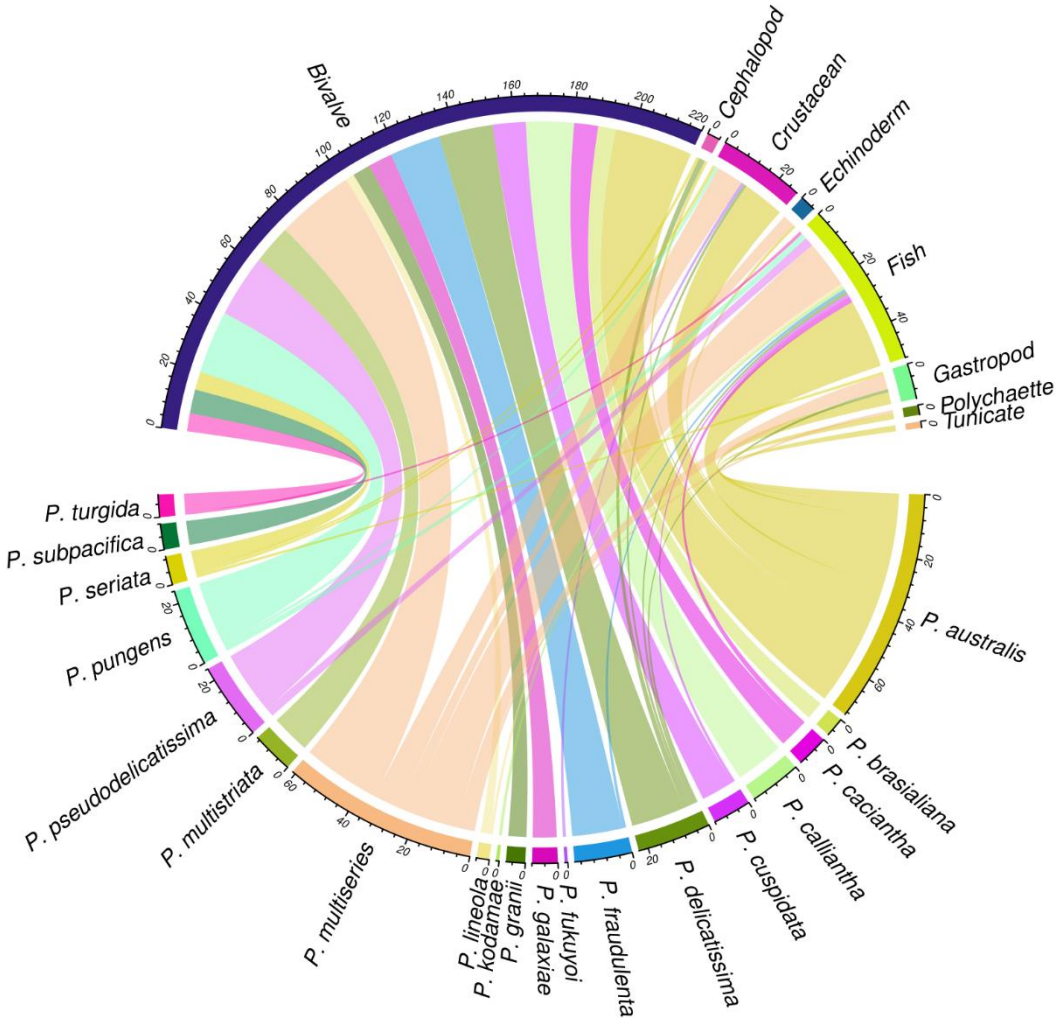

Figure 1. Chrod plot of summed linkages of toxicity among affected fish and invertebrate species and DA-producing *Pseudo-nitzschia spp*. reported in the literature. The width of the connecting chords indicates the number of species affected by each *Pseudo-nitzschia spp.* (Table I), denoted by the size of each circle segment.

Table I. List of primary-described species of the genus *Pseudo-nitzschia* causative of the ASP toxin domoic acid (DA) as well as the main marine fish and invertebrate species used for human consumption commonly contaminated with DA during ASP outbreaks.

DA producing species	References for *Pseudo-nitzschia spp.* toxicity	DA contaminated fish and shellfish species	References for DA contamination in marine fish and invertebrates
P. abrensis	Orive *et al.,* 2013; Teng *et al.,* 2016		
P. australis	Fritz *et al.,* 1992; Garrison *et al.* 1992; Sison-Mangus *et al.,* 2014; Thorel *et al.,* 2014; Álvarez *et al.,* 2015; Woods, 2016; Lema *et al.,* 2017; Zhu *et al.,* 2017b; Gai *et al.,* 2018. Nishimura *et al.,* 2021.	***Bivalves*** *Aequipecten opercularis, Argopecten purpuratus, Aulacomya ater, Cerastoderma edule, Crassostrea gigas, Crassostrea spp, Donax trunculus, Ensis siliqua, Ensis spp., Mesodesma donacium, Mytilus californianus, Mytilus chilensis, Mytilus edulis, Mytilus galloprovincialis, Mytilus sp., Ostrea edulis, Panopea abrupta, Pecten maximus, Pecten novaezelandiae, Perna canaliculus, Protothaca staminea, Protothaca theca, Ruditapes decusata, Scrobicularia plana, Siliqua patula, Venerupis pullastra,* ***Gastropods*** *Crepidula fornicata, Haliotis sp., Nassarius fossatus, Olivella biplicata,* ***Cephalopods*** *Loligo opalescens,* ***Crustaceans*** *Acartia clausi, Callianassa californiensis, Callinectes sapidus, Cancer antennarius, Cancer magister, Cancer pagurus, Emerita analoga, Euphausia pacifica, Menippe adina, Metacarcinus magister, Neotrypaea californiensis, Pagurus samuelis,*	Buck *et al.* 1992; Fritz *et al.,* 1992; Drum *et al.,* 1993; Horner *et al.,* 1993; Horner & Postel, 1993; Wekell *et al.,* 1994a,b; Altwein *et al.,* 1995; McGinness *et al.* 1995; Sierra-Beltrán *et al.* 1997; Arévalo *et al.,* 1998; Fraga *et al.,* 1998; Lefebvre *et al.* 1999; Hay *et al.,* 2000; Scholin *et al.,* 2000; Trainer *et al.,* 2000; Campbell *et al.* 2001; Gallacher *et al.,* 2001; Lefebvre *et al.,* 2001; Vale & Sampayo, 2001; Bargu *et al.* 2002; Blanco *et al.,* 2002; Ferdin *et al.,* 2002; Lefebvre *et al.,* 2002a,b; Naar *et al.,* 2002; Powell *et al.,* 2002; Vale & Sampayo, 2002; Wekell *et al.,* 2002; Bargu & Silver, 2003; Costa *et al.,* 2003; Goldberg, 2003; Bill *et al.* 2004; Costa & Garrido 2004; Negri *et al.* 2004; Fire & Silver 2005; James *et al.,* 2005; Maneiro *et al.,* 2005; Bill *et al.,* 2006; Blanco *et al.,* 2006; Busse *et al.,* 2006; Nézan *et al.,* 2006; Bogan *et al.,* 2007a,b; Trainer *et al.,* 2007; Vigilant & Silver, 2007; Bargu *et al.* 2008; Kvitek *et al.* 2008; Trainer *et al.,* 2008; López-Rivera *et al.* 2009; Nézan *et al.*

		Palinurus elephas, *Polybus henslowii,* ***Polychaetes*** *Poeobius meseres,* *Urechis caupo,* ***Echinoderms*** *Dendraster excentricus,* ***Tunicates*** *Asterocarpa spp.,* *Pyura chilensis,* ***Fishes*** *Atherinopsis californiensis,* *Citharichthys sordidus,* *Engraulis anchoita,* *Engraulis mordax,* *Eopsetta exilis,* *Eopsetta jordan,* *Eopsetta jordani,* *Errex zachirus,* *Genyonemus lineatus,* *Gymnocanthus tricupsis,* *Hippoglossus stenolepis,* *Hyperprosopon argenteum,* *Leptocottus armatus,* *Microstomus pacificus,* *Pleuronectes decurrens,* *Pleuronectes vetulus,* *Psettichthys melanostictus,* *Sardina pilchardus,* *Sardinops sagax,* *Scomber japonicus,* *Thunnus alalunga,* *Trachurus symmetricus,* *Zaniolepis latipinnis,*	2010; Reizopoulou *et al.,* 2012; Malhi *et al.,* 2014; Álvarez *et al.,* 2015; McCabe *et al.,* 2016; Bresnan *et al.,* 2017; Pazos *et al.,* 2017; Louw *et al.,* 2018; Blanco *et al.,* 2020; Álvarez *et al.,* 2020; García-Corona *et al.,* in prep a, b.
P. batesiana	Lim *et al.,* 2013; Teng *et al.,* 2015		
P. bipertita	Dong *et al.,* 2020		
P. brasiliana	Sahraoui *et al.,* 2011; Lim *et al.,* 2014; Sakka Hlaili *et al.,* 2016	***Bivalves*** *Argopecten irradians,* *Atrina rigida,* *Crassostrea virginica,* *Donax variabilis,* *Modiolus americanus,* *Trachycardium egmontainum,*	O'Dea *et al.,* 2012, 2013
P. caciantha	Dao *et al.,* 2014; Dong *et al.,* 2020	***Bivalves*** *Acanthocardia tuberculata,* *Argopecten irradians,* *Atrina rigida,* *Challista chione,* *Crassostrea virginica,* *Donax variabilis,* *Modiolus americanus,* *Trachycardium egmontainum,*	O'Dea *et al.,* 2012, 2013; Leblad *et al.,* 2013; Louw *et al.,* 2018

		Fishes *Brevoortia patronus,* *Sardinops sagax,*	
P. calliantha	Martin *et al.,* 1990; Besiktepe *et al.,* 2008; Ryabushko *et al.,* 2008; Álvarez *et al.,* 2015; Sakka Hlaili *et al.,* 2016	***Bivalves*** *Acanthocardia tuberculata,* *Argopecten irradians,* *Atrina rigida,* *Challista chione,* *Crassostrea virginica,* *Crenomytilus grayanus,* *Donax variabilis,* *Mesodesma donacium,* *Mizuhopecten yessoensis,* *Modiolus americanus,* *Mya arenaria,* *Mytilus edulis,* *Mytilus trossulus,* *Perna perna,* *Placopecten magellanicus,* *Trachycardium egmontainum,*	Martin *et al.,* 1990; Del Rio *et al.,* 2010; O'Dea *et al.,* 2012, 2013; Fernandes, 2013; Leblad *et al.,* 2013; Álvarez *et al.,* 2015; Stonik *et al.,* 2019
P. cuspidata	Bill *et al.,* 2005; Schnetzer *et al.,* 2007; Auro and Cochlan, 2013; Ajani *et al.,* 2013a; Dong *et al.,* 2020	***Bivalves*** *Acanthocardia tuberculata,* *Argopecten irradians,* *Atrina rigida,* *Challista chione,* *Crassostrea virginica,* *Donax deltoides,* *Donax variabilis,* *Modiolus americanus,* *Modiolus proclivis,* *Saccostrea glomerata,* *Trachycardium egmontainum,* ***Fishes*** *Sardinops sagax*	Takahashi *et al.,* 2007; O'Dea *et al.,* 2012, 2013; Leblad *et al.,* 2013; Louw *et al.,* 2018
P. delicatissima	Rhodes *et al.,* 1996; Baugh *et al.,* 2006; Sahraoui *et al.,* 2011; Fuentes and Wikfors, 2013; Penna *et al.,* 2013; Fernandes *et al.,* 2014	***Bivalves*** *Argopecten irradians,* *Atrina rigida,* *Aulacomya atra,* *Chlamys vitrea,* *Crassostrea virginica,* *Crenomytilus grayanus,* *Donax variabilis,* *Mizuhopecten yessoensis,* *Modiolus americanus,* *Mytilus chilensis,* *Mytilus edulis,* *Mytilus galloprovincialis,* *Mytilus trossulus,* *Pecten novaezelandiae,* *Perna canaliculus,* *Siliqua patula,* *Trachycardium egmontainum,* ***Gastropods*** *Haliotis sp.,*	Hay *et al.,* 2000; Trainer *et al.,* 2000; Trainer and Bill *et al.* 2004; Mazzillo *et al.,* 2011; Lage *et al.,* 2012; O'Dea *et al.,* 2012, 2013; Malhi *et al.,* 2014; Pizarro *et al.,* 2017; Louw *et al.,* 2018; Stonik *et al.,* 2019

		Cephalopods *Dosidicus gigas,* *Octopus vulgaris* ***Crustaceans*** *Emerita analoga* ***Fishes*** *Sardinops sagax*	
P. fraudulenta	Rhodes *et al.,* 1998; Tatters *et al.,* 2012; Fernandes *et al.,* 2014; Sison-Mangus *et al.,* 2014; Lema *et al.,* 2017; Dong *et al.,* 2020	***Bivalves*** *Acanthocardia tuberculata,* *Argopecten irradians,* *Atrina rigida,* *Challista chione,* *Crassostrea virginica,* *Donax deltoides,* *Donax variabilis,* *Modiolus americanus,* *Modiolus proclivis,* *Mytilus edulis,* *Panopea abrupta,* *Pecten novaezelandiae,* *Perna canaliculus,* *Protothaca staminea,* *Saccostrea glomerata,* *Siliqua patula,* *Trachycardium egmontainum,* ***Fishes*** *Sardinops sagax*	Hay *et al.,* 2000; Trainer and Bill *et al.* 2004, 2006; Takahashi *et al.,* 2007; Trainer *et al.,* 2007; O'Dea *et al.,* 2012, 2013; Leblad *et al.,* 2013; Louw *et al.,* 2018
P. fukuyoi	Lim *et al.,* 2013; Dao *et al.,* 2014; Dong *et al.,* 2020	***Crustaceans*** *Artemia salina*	Dong *et al.,* 2020
P. galaxiae	Lundholm & Moestrup, 2002; Cerino *et al.,* 2005; Moschandreou *et al.,* 2012	***Bivalves*** *Acanthocardia tuberculata,* *Argopecten irradians,* *Atrina rigida,* *Challista chione,* *Crassostrea virginica,* *Donax variabilis,* *Modiolus americanus,* *Trachycardium egmontainum,*	O'Dea *et al.,* 2012, 2013; Leblad *et al.,* 2013
P. granii	Trick *et al.,* 2010; Fuentes & Wikfors, 2013	***Bivalves*** *Argopecten irradians,* *Atrina rigida,* *Crassostrea virginica,* *Donax variabilis,* *Modiolus americanus,* *Trachycardium egmontainum,*	O'Dea *et al.,* 2012, 2013
P. hasleana	Sakka Hlaili *et al.,* 2016		
P. kodamae	Teng *et al.,* 2014	***Fishes*** *Sardinops sagax*	Louw *et al.,* 2018
P. lineola	Takahashi *et al.,* 2007; Huang *et al.,* 2019	***Bivalves*** *Donax deltoides,* *Modiolus proclivis,* *Saccostrea glomerata*	Takahashi *et al.,* 2007; Louw *et al.,* 2018

		Fishes	
		Sardinops sagax	
P. lundholniae	Teng *et al.,* 2015; Huang *et al.,* 2019; Dong *et al.,* 2020		
P. multiseries	Bates *et al.,* 1989; Kotaki *et al.,* 2008; Lelong *et al.,* 2012; Pitcher *et al.,* 2014; Woods, 2016; Huang *et al.,* 2019; Dong *et al.,* 2020; Nishimura *et al.,* 2021	***Bivalves*** *Acanthocardia tuberculata, Argopecten irradians, Atrina rigida, Challista chione, Crassostrea gigas, Crassostrea virginica, Donax trunculus, Donax variabilis, Modiolus americanus, Mya arenaria, Mytilus californianus, Mytilus edulis, Mytilus galloprovincialis, Nuttallia obscurata, Panopea abrupta, Pecten maximus, Pecten novaezelandiae, Perna canaliculus, Placopecten magellanicus, Protothaca staminea, Ruditapes decussata, Ruditapes philippinarum, Siliqua patula, Spondylus squamosus, Spondylus versicolor, Trachycardium egmontainum,* ***Gastropods*** *Aporrhais pespelecani, Haliotis sp., Nassarius fossatus, Nassarius reticulatus, Olivella biplicata,* ***Crustaceans*** *Acartia tonsa, Calanus finmarchicus, Callianassa californiensis, Cancer magister, Emerita analoga, Neotrypaea californiensis, Pagurus samuelis, Pleuroncodes planipes, Temora longicornis,* ***Polychaetes*** *Urechis caupo,* ***Echinoderms*** *Amphiura chiajei, Cucumaria sp., Dendraster excentricus,*	Bates *et al.* 1989; Novaczek *et al.* 1992; Silvert and Subba 1992; Wohlgeschaffen *et al.,* 1992; Drum *et al.,* 1993; Horner *et al.,* 1993; Horner & Postel, 1993; Roelke *et al.,* 1993; Wekell *et al.,* 1993; 1994a,b; Jones *et al.,* 1995; Douglas *et al.,* 1997; Bates, 1997; Bates *et al.,* 1998; Stewart *et al.* 1998; REPHY ifremer; Bates & Richard, 2000; Hay *et al.,* 2000; Trainer *et al.,* 2000; Amzil *et al.* 2001; Lefebvre *et al.,* 2001; Lincoln *et al.,* 2001; Ferdin *et al.* 2002; Lefebvre *et al.,* 2002a; Naar *et al.,* 2002; Powell *et al.,* 2002; Wekell *et al.,* 2002; Goldberg, 2003; Bates, 2004; Bill *et al.,* 2004, 2006; Busse *et al.* 2006; Nézan *et al.,* 2006; Vigilant & Silver *et al.,* 2007; Kvitek *et al.,* 2008; Stewart *et al.,* 2008; Takata *et al.,* 2009; Leandro *et al.,* 2010; Mafra *et al.* 2010; Nézan *et al.* 2010; O'Dea *et al.,* 2012; Reizopoulou *et al.,* 2012; Leblad *et al.,* 2013; O'Dea *et al.,* 2013; Malhi *et al.,* 2014; Pazos *et al.,* 2017; Louw *et al.,* 2018; Dusek Jennings *et al.,* 2020

		Ophiura ophiura ***Fishes*** *Atherinopsis californiensis,* *Citharichthys sordidus,* *Engraulis mordax,* *Eopsetta exillis,* *Eopsetta jordani,* *Errex zachirus,* *Hippoglossus stenolepis,* *Microstomus pacificus,* *Pleuronectes decurrens,* *Pleuronectes vetulus,* *Psettichthys melanostictus,* *Sardinops sagax,* *Scomber japonicus,* *Thunnus alalunga,* *Trachurus symmetricus,* *Zaniolepis latipinnis,*	
P. multistriata	Rhodes *et al.,* 2000; Sarno *et al.,* 2000; Orsini *et al.,* 2002; Pistocchi *et al.,* 2012; Ajani *et al.,* 2013; Tenorio *et al.,* 2021	***Bivalves*** *Acanthocardia tuberculata,* *Argopecten irradians,* *Atrina rigida,* *Challista chione,* *Crassostrea virginica,* *Crenomytilus grayanus,* *Donax variabilis,* *Mizuhopecten yessoensis,* *Modiolus americanus,* *Mytilus trossulus,* *Pecten novaezelandiae,* *Perna canaliculus,* *Trachycardium egmontainum*	Hay *et al.,* 2000; O'Dea *et al.,* 2012, 2013; Leblad *et al.,* 2013; Stonik *et al.,* 2019
P. obtusa	Harðardóttir *et al.,* 2015; Lundholm *et al.,* 2018		
P. plurisecta	Orive *et al.,* 2013; Fernandes *et al.,* 2014; Teng *et al.,* 2014; Gai *et al.,* 2018; Caruana *et al.,* 2019		
P. pseudodelicatissima	Martin *et al.,* 1990; Lundholm *et al.,* 1997; Lapworth *et al.,* 2001; Pan *et al.,* 2001; Moschandreou *et al.,* 2012; Huang *et al.,* 2019	***Bivalves*** *Acanthocardia tuberculata,* *Argopecten irradians,* *Atrina rigida,* *Challista chione,* *Crassostrea virginica,* *Donax trunculus,* *Donax variabilis,* *Mesodesma donacium,* *Modiolus americanus,* *Mya arenaria,* *Mytilus edulis,* *Mytilus galloprovincialis,* *Panopea abrupta,* *Pecten novaezelandiae,* *Perna canaliculus,* *Perna perna,* *Placopecten magellanicus,* *Protothaca staminea,*	Gilgan *et al.,* 1990; Martin *et al.,* 1990, 1993; Haya *et al.,* 1991; Bates, 1997; Adams *et al.* 2000; Hay *et al.,* 2000; Scholin *et al.,* 2000; Trainer *et al.,* 2000; Amzil *et al.* 2001; Wekell *et al.,* 2002; Bill *et al.,* 2004, 2006; Trainer *et al.,* 2007; Del Rio *et al.,* 2010; O'Dea *et al.,* 2012, 2013; Fernandes *et al.,* 2013; Leblad *et al.,* 2013;

		Ruditapes decussata, *Siliqua patula,* *Trachycardium egmontainum* ***Fishes*** *Brevoortia patronus,* *Engraulis mordax,* *Sardinops sagax*	Álvarez *et al.,* 2015; Louw *et al.,* 2018
P. pungens	Rhodes *et al.,* 1996; Fernandes *et al.,* 2014; Lim *et al.,* 2014; Woods, 2016; Lema *et al.,* 2017; Pednekar *et al.,* 2018	***Bivalves*** *Acanthocardia tuberculata,* *Argopecten irradians,* *Atrina rigida,* *Challista chione,* *Crassostrea gigas,* *Crassostrea virginica,* *Crenomytilus grayanus,* *Donax deltoides,* *Donax variabilis,* *Mizuhopecten yessoensis,* *Modiolus americanus,* *Modiolus proclivis,* *Mytilus edulis,* *Mytilus trossulus,* *Panopea abrupta,* *Pecten novaezelandiae,* *Perna canaliculus,* *Protothaca staminea,* *Saccostrea glomerata,* *Silicua patula,* *Trachycardium egmontainum* ***Crustaceans*** *Cancer magister* ***Fishes*** *Brevoortia patronus,* *Sardinops sagax*	Drum *et al.,* 1993; Horner *et al.,* 1993; Horner & Postel, 1993; Wekell *et al.,* 1993; 1994a,b; Bates *et al.* 1998; Hay *et al.,* 2000; Wekell *et al.,* 2002; Bill *et al.,* 2006; Takahashi *et al.,* 2007; Del Rio *et al.,* 2010; O'Dea *et al.,* 2012, 2013; Leblad *et al.,* 2013; Louw *et al.,* 2018; Stonik *et al.,* 2019
P. seriata	Lundholm *et al.,* 1994; Tammilehto *et al.,* 2012, 2015; Fernandes *et al.,* 2014; Harðardóttir *et al.,* 2015; Lundholm *et al.,* 2018	***Bivalves*** *Aulacomya atra,* *Chlamys vitrea,* *Chlamys vítrea,* *Mytilus chilensis,* *Mytilus edulis,* *Mytilus galloprovincialis,* ***Gastropods*** *Haliotis spp.,* ***Cephalopods*** *Octopus vulgaris* ***Crustaceans*** *Emerita analoga*	Bill *et al.* 2004; Fehling *et al.,* 2004; Lundholm *et al.,* 2005; Lage *et al.,* 2012; Malhi *et al.,* 2014; Pizarro *et al.,* 2017 ; Bates *et al.,* 2018
P. simulans	Li *et al.,* 2017		
P. subcurvata	Olesen *et al.,* 2021		
P. subfraudulenta	Teng *et al.,* 2015		

P. subpacifica	Fernandes *et al.,* 2014	***Bivalves*** *Acanthocardia tuberculata,* *Argopecten irradians,* *Atrina rigida,* *Challista chione* *Crassostrea virginica,* *Donax variabilis,* *Modiolus americanus,* *Trachycardium egmontainum,*	O'Dea *et al.,* 2012, 2013; Leblad *et al.,* 2013
P. turgidula	Rhodes *et al.,* 1996; Fernandes *et al.,* 2014	***Bivalves*** *Argopecten irradians,* *Atrina rigida,* *Crassostrea virginica,* *Donax variabilis,* *Modiolus americanus,* *Trachycardium egmontainum,* ***Fishes*** *Sardinops sagax*	O'Dea *et al.,* 2012, 2013; Louw *et al.,* 2018

2. The toxicological impact of *Pseudo-nitzschia* and domoic acid on marine vertebrates (fish, mammals and seabirds)

DA is structurally and functionally similar to kainic acid (KA), another well-known phycotoxin in some macroalgae, and both are excitatory amino acids analogues of glutamate, which is a major excitatory neurotransmitter in the brain of vertebrates (Todd, 1993; Ramsdell, 2007). Glutamate receptors (GR) are mainly distributed in the central nervous system (CNS) and the cardiovascular system (CVS), and are activated by glutamate (Pulido, 2008). The negative neuroexcitatory and neurotoxic effects of DA on vertebrates are mainly attributed to the induction of a potent excitotoxicity by an integrative binding and activation of GR, including the major subtypes N-methyl-D-aspartate (NMDA), kainate (KA), and the α-amino-3-hydroxy-5-methyl-4-isoxazolepropionic acid (AMPA) receptors, for which DA has high affinity, triggering the excitatory neurotransmission at both presynaptic and postsynaptic plasma membranes (La Barre *et al.,* 2014). Particularly, in the brain of mammals, DA exhibits

a 3 to 100-fold higher affinity than its structural analogs (Pulido, 2008; Lefebvre & Robertson, 2010). As these receptors are distributed in all organs, DA can affect the functioning of the whole organism and not only the CNS (Miller *et al.,* 2021).

The high affinity of DA to GR in the brain is associated to strong clinical symptoms, explaining the vast literature on neurotoxic effects of ASP-events on vertebrates such as birds, but mainly mammals (Lefebvre *et al.,* 2002a; Pulido, 2008; La Barre *et al.,* 2014; Miller *et al.,* 2021). The excitotoxicity of DA damages mainly the neurons of the hippocampus and amygdaloid nucleus, which undergoes rapid swelling in both the soma and dendrites of the neurons (Ramsdell, 2007; McCabe *et al.,* 2016). Dendrites appear as preferential early target sites for DA excitotoxicity by the coactivation of AMPA/KA and NMDA receptors, causing a rapid desensitization at both sides of the synapse (Ramsdell, 2007). These receptors are ligand-gated ion channels selective to Na^{+}, K^{+} and Ca^{+2} that are activated by glutamate and its agonists, mediating a fast excitatory synaptic transmission (Pulido, 2008; McCabe *et al.,* 2016). The excitotoxicity of DA leads to the depolarization and release of glutamate into the synapse, causing an uncontrolled influx of Ca^{+2} into the cell. This excess of Ca^{+2} is highly toxic for the cells and triggers the activation of oxidative phosphorylation lowering function and energy production by the mitochondria, the activation of phospholipases, proteases, protein phosphatases and the production of free radicals. All these processes break the phospholipids in the membrane, destroying the cell and leading to degeneration and permanent neural damage (Ramsdell, 2007; Pulido, 2008; Zabaglo *et al.,* 2016). Glial cells and astrocytes are also targets for DA, where acute injury effects are characterized by vacuolation and necrosis (Silvagni *et al.,* 2005; Miller *et al.,* 2021).

The deleterious effects induced by DA in vertebrates are dose-dependent, as observed in numerous biological models (Schaffer *et al.,* 2016; Pulido, 2008). Nevertheless, as

described below, there is sufficient evidence that demonstrates a species-specific susceptibility to DA in marine organisms (Lefevbre *et al.,* 2002a; Silvagni *et al.,* 2005). Some studies suggested that the oral administration or the intracoelomic injection of DA could impact the behavior (*i.e.,* disorientation, spinning, inability to school) of some fish species like salmonids, anchovies and sardines (Lefebvre *et al.,* 2002a, 2002b). However, subsequent research based on field observations during ASP-outbreaks revealed that some pelagic fish like mackerel, albacore, and combfish are more tolerant to DA than their piscivorous predators (Lefevbre *et al.,* 2012). Moreover, Schaffer *et al.* (2006) found no histopathological or behavioral (swimming and feeding) changes in juvenile leopard sharks (*Triakis semifasciata*) exposed to DA doses as high as 30 mg kg^{-1}, which are lethal for other vertebrates like birds and mammals, despite the presence of GR in shark brains. Probably, *T. semifasciata* prevents DA toxicity by employing an endogenous specific ligand that can be effectively competitive with DA binding sites (Schaffer *et al.,* 2006), suggesting that some species have developed potential intrinsic protection mechanisms against DA intoxication. Thus, the currently available knowledge indicates that DA produced during blooms of *Pseudo-nitzschia* does not cause neurotoxicity, behavioral changes, or massive mortalities in fish populations (Lefebvre & Robertson, 2010; Lefebvre *et al.,* 2012).

The relevance of the role-played by GR as mediators of excitatory neurotransmission relays on their wide distribution outside the CNS, prompting the attention to other tissues as potential target sites (Pulido, 2008). In mammals, DA intoxication may also affects peripheral nervous system and different related organs such as kidney, even at levels considered safe for human consumption (Funk *et al.,* 2014), as well as the cardiovascular system (CVS), lungs, gastrointestinal tract, and retina (Miller *et al.,* 2021). Concerning marine fauna, ASP toxicity events have been confirmed in seabirds

(Work *et al.,* 1993; Shumway *et al.,* 2003; Lefevre *et al.,* 2012), whales (Lefevbre *et al.,* 2002a; D'Agostino *et al.,* 2017), seals (Silvagni *et al.,* 2005; McHuron *et al.,* 2013), sea lions (Rust *et al.,* 2014; Lefebvre *et al.,* 2018), and sea otters (Miller *et al.,* 2021) exposed to the toxin through the consumption of contaminated prey. Birds and mammals affected by ASP commonly exhibit signs of disorientation, regurgitation, erratic movements, tachycardia, convulsion, coma, and in severe cases, death (Work *et al.,* 1993; Silvagni *et al.,* 2005; Lefevre *et al.,* 2012; McHuron *et al.,* 2013). In humans, the clinical diagnosis by ASP includes gastrointestinal symptoms within the first 24 h, and neurological impairment within 48 h (Pulido, 2008). Symptoms of illness also include nausea, vomiting, abdominal cramps, diarrhea, headache, unstable blood pressure, and neurological dysfunction, including coma and memory loss (Perl, 1990; Pulido, 2008).

Recently, Miller *et al.* (2021) described the most detailed compendium of clinical pathologies associated with DA intoxication in a mammal. It was found that sea otters *(Enhydra lutris nereis)* with acute fatal DA intoxication had severe lesions in the CNS and CVS, typically presenting micro-hemorrhages in the brain, spinal cord, heart, and eyes, in addition to cellular necrosis and apoptosis in these organs. In cases of chronic DA exposure, tissue damage in the CVS (cardiomyocytes and coronary arterioles) was even more severe than the pathologies observed in the CNS. While in sea otters with acute, subacute, and chronic DA intoxication the most common histopathologies were found in the CNS mainly in the hippocampus, olfactory, entorhinal and parahippocampal cortex, periventricular neuropil, and ventricles, with a progressive loss of cardiomyocytes and the occurrence of arteriosclerosis in the CVS (Miller *et al.,* 2021). These findings showed that DA ingestion-related lesions are similar with acute exposure at high doses and with chronic exposure at low doses. Moreover, the

histopathological analysis of live-stranded harbor seals *Phoca vitulina richardii* (McHuron *et al.,* 2013), as well as Northern fur seals *Callorhinus ursinus*, and California sea lions *Zalophus californianus* (Silvagni *et al.,* 2005) revealed lesions associated with intoxication after consumption of DA-contaminated prey. The main pathologies were associated to brain damage, particularly of the hippocampal region, characterized by a high neuronal death (necrosis), degeneration within the neuropil of the hippocampus, amygdaloid nucleus, pyriform lobe, and other limbic structures. The fragmentation of the myocardial muscle and a high frequency of macrophages in the necrotic muscle cells were also observed.

The mentioned above raises concerns regarding possible increase in the risk of long term effects of ASP since it has been demonstrated that DA crosses the placenta of marine mammals and can be detected in maternal milk, with potential development (fetal) and neonatal neurotoxicity impairments occurring during pregnancy and lactation, respectively (Goldstein *et al.,* 2008; Lefebvre *et al.,* 2018). Sequestration of DA in fetal fluids and maternal milk have been documented in *Z. californianus* (Silvagni *et al.,* 2005; Rust *et al.,* 2014; Lefebvre *et al.,* 2018) and *P. vitulina* (McHuron *et al.,* 2013) with evidence of DA exposure of pups from both species in utero and during lactation, which prolong maternal and fetal toxicosis. Given the main vector of ASP is the consumption of contaminated shellfish and since seabirds and most marine mammals consume the same contaminated seafood as humans, all this contributes to facilitating the diagnosis of DA intoxication in other vertebrates and humans.

3. Bioaccumulation and transfer of DA across the trophic chain

Shellfish, mainly benthic species and filter-feeding foragers are the most directly exposed species to HABs and are the major source of human intoxications worldwide,

as they bioaccumulate phycotoxins (Bricelj & Shumway, 2013; Hallegraeff, 2017; Basti *et al.,* 2018). Bivalve molluscs are the primary consumers of toxic *Pseudo-nitzschia* cells, thus the first organisms to bioaccumulate DA. Toxic *Pseudo-nitzschia* cells can also be grazed by zooplankton (mainly copepods and krill) and small-herbivorous fish like sardines or anchovies (Bargu *et al.,* 2002; Lefevbre *et al.,* 2002a). Subsequently, DA can be transported across all trophic levels of the ocean food web (Granéli & Turner, 2006; Bejarano *et al.,* 2008; Schnetzer *et al.,* 2017) bioaccumulating in some invertebrate species like molluscs (cephalopods and gastropods), as well as crustaceans, echinoderms, urochordates, worms (Bargu *et al.,* 2002; Kvitek *et al.,* 2008; Zabaglo *et al.,* 2016; Baustian *et al.,* 2018, Basti *et al.,* 2018), carnivorous fishes and marine mammals (cetaceans, sea otters or sea lions), and birds (Shumway *et al.,* 2003; Trainer *et al.,* 2010). More than 50% of total DA accumulated in the whole body is concentrated in non-edible tissues of fishes and shellfish (Blanco *et al.,* 2020; Kvrgić *et al.,* 2022), such as the stomach and gut of fishes (Lefebvre *et al.,* 2002b; Costa & Garrido, 2004; Vigilant & Silver, 2007; Kudela *et al.,* 2015), and the digestive gland of bivalves (James *et al.,* 2005; Blanco *et al.,* 2006; Bogan *et al.,* 2007a; García-Corona *et al.,* 2022), gasteropods (Malhi *et al.,* 2014), cephalopods (Costa *et al.,* 2004, 2005a,b; Ben Haddouch *et al.,* 2016; Lopes *et al.,* 2018), crustaceans (Costa *et al.,* 2003), and ascidians (López-Rivera *et al.,* 2009).

The trophic transfer and biomagnification of this toxin through the food web from benthic invertebrates and planktivorous fish to top predators has demonstrated serious health risk to marine wildlife and humans, and have been responsible for dramatic mass mortality events, mainly involving vertebrates, such as sea birds and marine mammals (Zabaglo *et al.,* 2016).

4. Interspecific variability in accumulation and detoxification of DA in marine invertebrates and fish

Studies on DA accumulation and detoxification kinetics have been mainly performed on molluscs, especially bivalves, probably because they are the most contaminated primary consumers and represent a threat to human health, following consumption of contaminated seafood. Notwithstanding, there is a profound inter and intra-specific variability in the toxicokinetics of accumulation and detoxification rates of DA which does not seem to be linked to the influence of environmental (microhabitat differences) or endogenous (body size) factors between most of the bivalve species (James *et al.,* 2005; Bogan *et al.,* 2007a,b; Blanco *et al.,* 2021a) but rather to species-specific physiological mechanisms involved in the way the toxin is assimilated, distributed, and excreted (Section 5 below).

Table II summarizes the information on DA-accumulation in the whole body and/or in the digestive tissues of all species of fish and marine invertebrates susceptible ASP toxicity, as well as the conditions (natural or experimental) of exposure to DA reported in the literature for each case. The maximum amounts of DA accumulated in mussels (Bates *et al.,* 1989; Quilliam *et al.,* 1989; Blanco *et al.,* 2002b), clams (Horner *et al.,* 1993; Trainer *et al.,* 2007; Blanco *et al.,* 2010), oysters (Horner & Postel, 1993, Vale & Sampayo, 2001; Trainer *et al.,* 2007), and small scallops (Ventoso *et al.,* 2019; Álvarez *et al.,* 2020) range between 0.1 to 900 mg DA kg^{-1} in total tissues and in the DG. In contrast, bigger scallops such as the deep-sea scallop *Placopecten magellanicus* (Gilgan, 1990) and *P. maximus* (Blanco *et al.,* 2006; Bogan *et al.,* 2007a, b, c; García-Corona *et al.,* 2021) are capable to accumulate up to 4300 mg DA kg^{-1}, and 3200 mg DA kg^{-1}, respectively, in the DG, and ~ 460 to 2900 mg DA kg^{-1} in their whole tissues, respectively (Haya *et al.,* 1991; Ramsdell, 2007).

Table II. Maximum accumulation of ASP toxin domoic acid (DA) attained by several fish and shellfish species (adults unless indicated) used for human consumption, separated as (A) naturally or (B) experimentally exposed to DA produced by *Pseudo-nitzschia spp*. except when indicated. DA accumulation levels are expressed in µg DA g^{-1} (unless indicated). Action level for closure of fish-shellfish harvesting = 20 µg DA g^{-1}. FW = fresh weight, nd = not detected.

Species	µg DA g^{-1} accumulated (FW)		Accumulation conditions	Reference
	Toxicity of whole tissues	Toxicity of digestive tissue		
(A) Naturally exposed				
Mytilus galloprovincialis	—	153 µg· g^{-1}	Mussels exposed during *P. australis* blooms in estuaries of Galicia, Spain.	Blanco *et al.* (2002)
	—	0.86 µg· g^{-1}	Sampled during *Nitzschia bizertensis* outbreaks (10^6 cells L^{-1}; 7×10^{-3} pg $cell^{-1}$) in Bizerte Lagoon, Tunisia.	Bouchouicha Smida *et al.* (2015)
	2.2 µg· g^{-1}	—	Simultaneous sampling after an ASP outbreak in Fokida, Greece.	Kaniou-Grigoriadou *et al.* (2005)
	1.67 µg· g^{-1}		Animals collected by the Federal Agency for the Safety of the Food Chain, in Belgium (2004-2009).	Andjelkovic *et al.* (2012)
	3.7 µg· g^{-1}	—	Sampling after *P. delicatissima* and *P. seriata blooms* (81×10^9 cells L^{-1}) in Peniche, Portugal.	Lage *et al.* (2012)
	186 µg· g^{-1} —	— 3.9 µg· g^{-1}	Animals sampled after *P. multiseries* and *P. australis* blooms in Galicia, Spain.	Reizopoulou *et al.,* 2012; Pazos *et al.,* 2017
	1.5 µg· g^{-1}	—	Samples contaminated with DA after *Pseudo-nitzschia spp.* blooms (>10^6 cells L^{-1}) in the Croatian coast of the Adriatic Sea (2006-2008).	Ujević *et al.* (2010)
	49 µg· g^{-1}	—	Control monitoring program of ASP outbreaks in British waters during teen years (2008-2017).	Rowland-Pilgrim, *et al.* (2019)
Mytilus edulis	2.6 µg· g^{-1}	—	Mussels from the French coasts exposed to *P. multiseries* and *P. pseudodelicatissima* blooms (1×10^5 cells L^{-1}).	Amzil *et al.* (2001)
	0.8 µg· g^{-1}	—		
	0.18 µg· g^{-1}	—	DA contaminated animals sampled in Japan.	Kawatsu & Hamano, 2000
	0.9 µg· g^{-1}	—	Continuous monitoring of DA in cultivated molluscs for a period of 6 months in coastal areas of Ireland.	James *et al.* (2005)
	2 µg· g^{-1}	—	Samples obtained after a bloom of the toxic *P. australis* (~1.3×10^5 cells L^{-1}, ~75 pg DA $cell^{-1}$) and *P. pseudodelicatissima* (10^6 cells L^{-1}) in Santa Cruz, CA, USA.	Scholin *et al.,* 2000

5 µg· g^{-1}	—	Contaminated after a *P. australis* bloom (6.7 × 10^4 cells L^{-1}) in Portuguese coastal areas.	Costa *et al.* (2003)
7.6 µg· g^{-1}	—	Samples collected from suspended bags during *P. australis* blooms (6 × 10^5 cells L^{-1}) in Scotland.	Bresnan *et al.* (2017)
29 µg· g^{-1}	—	Samples obtained during a DA-related shellfish closure (*P. australis, P. pungens, P. pseudodelicatissima, P. fraudulenta* and *P. multiseries* 2.9 × 10^6 cells L^{-1}; 4.6 × 10^3 ng DA L^{-1}) in Washington, USA.	Bill *et al.,* 2006
32 µg· g^{-1}	—	Sampling during *P. seriata* blooms (5.3 × 10^4 cells L^{-1}; 490 ng DA L^{-1}) in Denmark.	Lundholm *et al.,* 2005
53 µg· g^{-1}	—	Mussels naturally contaminated with DA during blooms of *P. pseudodelicatissima* in Bay of Fundy, Canada.	Martin *et al.,* 1993
90 µg· g^{-1}	325 µg· g^{-1}	Simultaneous sampling after a *Pseudo-nitzschia sp.* bloom (400 ng DA L^{-1}) in Aveiro Lagoon, Portugal.	Vale & Sampayo (2001)
< 20 µg· g^{-1}	—	Animals contaminated with DA during a *P. pungens, P. multiseries* and *P. australis* outbreaks in 1991 inWashington, USA.	Horner & Postel, 1993
20 µg· g^{-1}	—	Monthly monitoring after a *Pseudo-nitzschia sp.* Outbreak in Neguac Bay, Canada.	Canadian Food Inspection Agency (CFIA)
46 µg· g^{-1}	—	Simultaneous sampling after a *Pseudo-nitzschia sp.* bloom in Penn Cove, US.	Trainer *et al.* (2007)
200 µg· g^{-1}	—	Exposed to blooms of *P. seriata* and P. *australis* (0.32 and 0.68 pg DA $cell^{-1}$, respectively) in Scottish waters.	Bates *et al.,* 2004; Fehling *et al.* (2004)
200 µg· g^{-1}	—	Monthly monitoring after a *Pseudo-nitzschia sp.* Outbreak in Nuevo Brunswick, Canada.	Canadian Food Inspection Agency (CFIA)
—	300 µg· g^{-1}	Exposed to *P. multiseries* blooms (1.2 × 10^6 cells L^{-1}) in Cardigan Bay, Canada.	Silvert and Subba (1992)
—	346 µg· g^{-1}	Mussels contaminated with DA harvested from Cardigan River, UK.	Grimmelt *et al.* (1990)
350 µg· g^{-1}	—	Sampling after ASP outbreak in Prince Edward Island, Canada.	Gilgan *et al.* (1990)
—	790 µg· g^{-1}	Animals contaminated with DA during *P. multiseries* blooms (15 × 10^6 cells L^{-1}, 21 ng DA L^{-1}) in Cardigan Bay, Canada.	Bates *et al.* (1989)

	900 µg· g^{-1}	—	Cultured mussels contaminated after an ASP outbreak in Prince Edward Island, Canada.	Quilliam *et al.,* 1989
	790 µg· g^{-1}	—	Sampling after a *Pseudo-nitzschia sp.* outbreack in Cardigan River, Canada.	Bates *et al.* (1998)
	—	60 µg· g^{-1}	Mussels exposed to *P. multiseries* blooms in New Scotland, Canada.	Stewart *et al.* (1998)
	—	0.92 µg· g^{-1}	Animals contaminated with DA in the North Black Sea, in Bulgaria.	Bates *et al.,* 2018
Mytilus californianus	2.5 µg· g^{-1}	—	Mussels contaminated with DA during ASP outbreaks.	Whyte *et al.* (1995)
	0.31 µg· g^{-1}	—	Mussels collected in a monthly basis during *P. australis* and *P. multiseries* blooms in Santa Cruz and Monterey Bay, CA, US.	Ferdin *et al.* (2002)
	—	5.8 µg· g^{-1}	Samples obtained during *P. australis* and *P. multiseries* blooms (7.7 × 10^4 cells L^{-1}) in San Diego, CA, USA.	Busse *et al.,* 2006
Crenomytilus grayanus *Mytilus trossulus* *Mizuhopecten yessoensis*	≤ 0.3 µg· g^{-1}		Bivalves collected during *P. multistriata, P. calliantha, P. delicatissima* and *P. pungens* (> 10^4 cells L^{-1}, 0.57 pg DA $cell^{-1}$) blooms in the northwestern sea of Japan-Russia.	Stonik *et al.,* 2019
Perna perna	98.5 µg· g^{-1}	—	Mussels sampled in shellfish farms during *Pseudo-nitzschia sp.* blooms (22.5 × 10^6 cells L^{-1}) through a year in the south brazilian coast.	Fernandes *et al.,* 2013
Perna canaliculus	187 µg· g^{-1}	—	Samples obtained during *Pseudo-nitzschia sp.* blooms (2.7 × 10^4 cells L^{-1}) in New Zealand.	Hay *et al.,* 2000
Perna viridis	0.5 µg· g^{-1}	—	Shellfish and fish samples collected bimonthly during a *Pseudo-nitzschia sp.* episode (1.2 × 10^4 cells L^{-1}, 13.2 ng DA L^{-1}) through a year in Sriracha bay, Thailand.	Veschasit *et al.,* 2017
Crassostrea lugubris	0.4 µg· g^{-1}	—		
Pinctada fucata	0.3 µg· g^{-1}	—		
Secutor megalolepis	44.2 µg· g^{-1}	—		
Saccostrea glomerata	43 µg· g^{-1}	—	Bivalves sampled for 24 consecutive months during *P. pungens, P. fraudulenta, P. lineola* and *P. cuspidata* blooms (70 cells L^{-1}) on the east coast of Australia.	Takahashi *et al.,* 2007
Donax deltoides	256 µg· g^{-1}	—		
Modiolus proclivis	147 µg· g^{-1}	—		
Tapes philippinarum	68 µg· g^{-1}	—	Simultaneous sampling after a *Pseudo-nitzschia sp.* bloom in Penn Cove, US.	Trainer *et al.* (2007)
Mya arenaria	2.5 µg· g^{-1}	165 µg· g^{-1}	Clams exposed to *P. multiseries* blooms in New Scotland, Canada.	Stewart *et al.* (1998)

	38 µg· g^{-1}	—	Contaminated with DA during *P. multiseries* blooms (1.7 × 10^5 cells L^{-1}, 21 ng DA L^{-1}) in Cardigan Bay, Canada.	Bates *et al.,* 1989
	53 µg· g^{-1}	—	Contaminated with DA during blooms of *P. pseudodelicatissima* in Bay of Fundy, Canada.	Martin *et al.,* 1993
Modiolus americanus	13.25 µg· g^{-1}	—	Continuous shellfish sampling during multiple *Pseudo-nitzschia sp.* blooms in Florida coastal waters (Gulf of Mexico) USA.	O'Dea *et al.,* 2012, 2013
Trachycardium egmontainum	0.27 µg· g^{-1}	—		
Donax variabilis	1.39 µg· g^{-1}	—		
Argopecten irradians	28.2 µg· g^{-1}	—		
Atrina rigida	52.1 µg· g^{-1}	—		
Crassostrea virginica	76 µg· g^{-1}	—		
	0.9 µg· g^{-1}	—	Monthly monitoring after a *Pseudo-nitzschia sp.* Outbreak in Neguac Bay, Canada.	Canadian Food Inspection Agency (CFIA)
Crassostrea gigas	< 20 µg· g^{-1}	—	Oysters contaminated with DA during a *P. pungens, P. multiseries* and *P. australis* outbreaks in 1991 inWashington, USA.	Horner & Postel, 1993
	> 20 µg· g^{-1}	—	Control monitoring programme of ASP outbreaks in British waters during teen years (2008-2017)	Rowland-Pilgrim, *et al.* (2019)
	30 µg· g^{-1}	—	Sampling after a *Pseudo-nitzschia sp.* outbreak in Sequim Bay, US.	Trainer *et al.* (2007)
	0.9 µg· g^{-1}	—	Continuous monitoring of DA in cultivated molluscs for a period of 6 months in coastal areas of Ireland.	James *et al.* (2005)
Ostrea edulis	≤ 4.9 µg· g^{-1}	—		
	—	1.04 µg· g^{-1}	Sampled during *Nitzschia bizertensis* outbreaks (3 ×10^6 cells L^{-1}; 7 × 10^{-3} pg $cell^{-1}$) in Bizerte Lagoon, Tunisia.	Bouchouicha Smida *et al.* (2015)
	5.6 µg· g^{-1}	—	Simultaneous sampling after a *Pseudo-nitzschia sp.* bloom (400 ng DA L^{-1}) in Aveiro Lagoon, Portugal.	Vale & Sampayo (2001)
	77 µg· g^{-1}		Oysters collected by the Federal Agency for the Safety of the Food Chain, in Belgium (2004-2009).	Andjelkovic *et al.* (2012)
	1.1 µg· g^{-1}		Samples contaminated with DA aftter *Pseudo-nitzschia spp.* blooms (>10^6 cells L^{-1}) in the Croatian coast of the Adriatic Sea (2006-2008).	Ujević *et al.* (2010)
	> 20 µg· g^{-1}	—	Control monitoring programme of ASP outbreaks in British waters during teen years (2008-2017)	Rowland-Pilgrim, *et al.* (2019)
	0.2 µg· g^{-1}	—	Seasonal monitoring of DA in the Northern Adriatic Sea (Croatia).	Kvrgic *et al.* (2022)

	0.3 µg· g^{-1}	—	Simultaneous sampling after a *Pseudo-nitzschia sp.* bloom in Fokida, Greece.	Kaniou-Grigoriadou *et al.* (2005)
Venus verrucosa	5.6 µg· g^{-1}	—		
Mesodesma donacium	10 µg· g^{-1}	—	Surf clams contaminated with ASP toxin during *P. australis* blooms (1.2 ×10^6 cells L^{-1}) in Coquimbo, Chile.	Álvarez *et al.,* 2015
Mytilus spp.	79 µg· g^{-1}	—	Mussels sampled after a *Pseudo-nitzschia sp.* bloom (400 ng DA L^{-1}) in Aveiro Lagoon, Portugal.	Vale *et al.,* 2008
	75 µg· g^{-1}	—	Shellfish monitoring after the largest recorded ASP outbreak (*P. australis*, 19.98 µg DA L^{-1}) along the North American west coast in early 2015.	McCabe *et al.,* 2016
Metacarcinus magister	270 µg· g^{-1}	—		
Cancer antennarius	1000 µg· g^{-1}	—		
Siliqua patula	170 µg· g^{-1}	—		
	295 µg· g^{-1}	—	Razor clams sampled after a *Pseudo-nitzschia sp.* outbreak in Kalaloch Beach, US.	Adams *et al.* (2000)
	260 µg· g^{-1}	—	Clams contaminated with DA from the Pacific Coast of the US.	Lund *et al.* (1997)
	308 µg· g^{-1}	—	Exposed to a bloom of *P. pseudodelicatissima* in the central Washington coast.	Trainer *et al.* (2000)
	0.6 µg· g^{-1}	—	Contaminated with DA during a *P. pungens, P. multiseries* and *P. australis* outbreaks in Washington, USA between 1991 and 1999. In some cases furnished by the Washington State Department of Fisheries (WDF).	Drum *et al.,* 1993; Horner *et al.,* 1993; Horner & Postel, 1993; Wekell *et al.,* 1993; 1994a,b; 2002
	160 µg· g^{-1}	—		
	106 µg· g^{-1}	—		
	147 µg· g^{-1}	—		
	50 µg· g^{-1}	—		
	12.3 µg· g^{-1}	10.4 µg· g^{-1}		
	295 µg· g^{-1}			
	> 20 µg· g^{-1}	—	Animals contaminated with DA in the Pacific coastline of the USA.	Altwein *et al.* (1996)
	68 µg· g^{-1}	—	Exposed to *P. australis, P. pseudodelicatissima* and *P. fraudulenta* (2.3 × 10^7 cells L^{-1}; 1.4 × 10^5 ng DA L^{-1}) blooms.	Trainer *et al.,* 2007
	68 µg· g^{-1}	—	Samples obtained during a DA-related shellfish closure (*P. australis, P. pungens, P. pseudodelicatissima, P. fraudulenta* and *P. multiseries,* 2.9 × 10^6 cells L^{-1}; 4.6 × 10^3 ng DA L^{-1}) in Washington, USA.	Bill *et al.,* 2006
Protothaca staminea	< 20 µg· g^{-1}	—		
Panopea abrupta	< 20 µg· g^{-1}	—		
Ensis siliqua	1.3 µg· g^{-1}	—	Continuous monitoring of DA in cultivated molluscs for a period of 6 months in coastal areas of Ireland.	James *et al.* (2005)

Pecten maximus	5 µg· g^{-1}	—	Simultaneous sampling after a *Pseudo-nitzschia spp.* bloom (400 ng DA L^{-1}) in Aveiro Lagoon, Portugal.	Vale & Sampayo (2001)
	34 µg· g^{-1}	—	Control monitoring programme of ASP outbreaks in British waters during teen years (2008-2017)	Rowland-Pilgrim, *et al.* (2019)
	230 µg· g^{-1} 2900 µg· g^{-1}	— —	Shellfish sampled after *Pseudo-nitzschia spp.* blooms in Canada.	Ramsdell (2007)
	1569 µg· g^{-1}	—	Scallops collected after a *Pseudo-nitzschia sp.* outbreak in Tobermory bay, Scotland.	Campbell *et al.* (2001)
	91.17 µg· g^{-1}	—	Sampling during a routinely ASP monitoring program in Scotland coastal areas.	Campbell *et al.* (2003)
	160 µg· g^{-1} 240 µg· g^{-1}	— 2280 µg· g^{-1}	Continuous monitoring of DA in cultivated molluscs for a period of 6 months in coastal areas of Ireland.	James *et al.* (2005)
	129 µg· g^{-1}	—	Contaminated scallops dredged from a closed fishing area in Scottish waters	Smith *et al.,* 2006
	4.3 µg· g^{-1}	28.3 µg· g^{-1}	Contaminated animals collected on a weekly basis during a year in in the Bay of Seine, Normandy France.	Amzil *et al.,* 2007
	8.45 µg· g^{-1} 9.59 µg· g^{-1} 154.3 µg· g^{-1} 29.5 µg· g^{-1}	1212.6 µg· g^{-1} 1348.1 µg· g^{-1} 1531 µg· g^{-1} 296.3 µg· g^{-1}	Scallops contaminated with DA, collected in a monthly basis during a year from a seabed, and aquaculture systems in Clew Bay, Ireland.	Bogan *et al.,* 2006; 2007a,b,c
	203.4 µg· g^{-1}	—	Animals collected by the Federal Agency for the Safety of the Food Chain, in Belgium (2004-2009).	Andjelkovic *et al.* (2012)
	5.77 µg· g^{-1}	9.88 µg· g^{-1}	Scallops contaminated with DA during a *P. australis* outbreak sampled from a natural bed in The Ría de Arousa, Galicia, Spain.	Blanco *et al.* (2002a)
	> 20 µg· g^{-1}	3200 µg· g^{-1}		Blanco *et al.* (2006)
	—	2007 µg· g^{-1}		Blanco *et al.* (2020)
	346 µg· g^{-1}	—	Samples collected from the sea floor during *P. australis* blooms (6×10^5 cells L^{-1}) in Scotland.	Bresnan *et al.* (2017)
	266 µg· g^{-1}	—	Sampling after a *Pseudo-nitzschia sp.* bloom (400 ng DA L^{-1}) in Aveiro Lagoon, Portugal.	Vale *et al.,* 2008
	445 µg· g^{-1}	—	Analysis of two decades of *Pseudo-nitzschia spp.* blooms (14×10^6 cells L^{-1}) along the French Atlantic and English Channel coasts.	Husson *et al.,* 2016
	nd	1070 µg· g^{-1}	Scallops dredged during a *P. australis* bautbreak (1.1×10^5 cells L^{-1}) in Camaret-sur-Mer, France.	García-Corona *et al.* (in prep)

	nd	1807 µg· g^{-1}	Cultured scallops in suspended cages during P. australis bloom (6×10^4 cells L^{-1}) in the Bay of Brest, France.	García-Corona *et al.* (in prep)
	—	446.6 µg· g^{-1}	Scallops contaminated with DA during a *Pseudo-nitzschia spp.* outbreak sampled from a natural bed in Northwest coast of Brittany, France.	García-Corona *et al.* (2022)
	—	638.6 µg· g^{-1}	Sampling after a *P. australis* bloom (1.1×10^5 cells L^{-1}) in Camaret-sur-Mer, France.	García-Corona *et al.* (in prep)
Crepidula fornicata	—	48.5 µg· g^{-1}		
Asterocarpa spp.	—	4.2 µg· g^{-1}		
Pecten novaezelandiae	210 µg· g^{-1}	—	Samples obtained during *Pseudo-nitzschia sp.* blooms (2.7×10^4 cells L^{-1}) in New Zealand.	Hay *et al.,* 2000
Placopecten magellanicus	460 µg· g^{-1}	4180 µg· g^{-1}	Clams collected during a toxic *P. pseudodelicatissima* bloom in Bay of Fundy, New Brunswick, Canada.	Haya *et al.,* 1991
	—	3400 µg· g^{-1}	Animals contaminated during a *P. multiseries* and *P. pseudodelicatissima* bloom in the Canadian east coast.	Bates, 1997
	10 µg· g^{-1} 150 µg· g^{-1} —	200 µg· g^{-1} 1300 µg· g^{-1} 4300 µg· g^{-1}	Contaminated with DA during *Pseudo-nitzschia sp.* blooms in Browns and Georges Bank, USA.	Gilgan (1990); Gilgan *et al.* (1996)
Ruditapes philippinarum	> 20 µg· g^{-1}	—	Control monitoring programme of ASP outbreaks in British waters during teen years (2008-2017)	Rowland-Pilgrim, *et al.* (2019)
Mercenaria mercenaria	> 20 µg· g^{-1}	—		
Spisula solida	> 20 µg· g^{-1}	—		
Lutraria lutraria	> 20 µg· g^{-1}	—		
Aequipecten opercularis	> 20 µg· g^{-1}	—		
	—	6.68 µg· g^{-1}	Scallops placed in aquaculture rafts during *Pseudo-nitzschia spp.* bloms in Galicia, Spain.	Ventoso *et al.* (2019)
	22 µg· g^{-1}	—	Continuous monitoring of DA contamination in Galicia, Spain.	Intecmar, Xunta de Galicia
	—	22.7 µg· g^{-1}	Sampling after a *P. australis* bloom (1.1×10^5 cells L^{-1}) in Camaret-sur-Mer, France.	García-Corona *et al.* (in prep)
	0.8 µg· g^{-1}	—	Seasonal monitoring of DA in the Northern Adriatic Sea (Croatia).	Kvrgic *et al.* (2022)
Microcosmus spp.	0.02 µg· g^{-1}	—		
Argopecten purpuratus	~ 60 µg· g^{-1}	~ 60 µg· g^{-1}	Scallops reared in the field during *P. australis blooms* (5.3×10^4 cells L^{-1}) in the Bay of Tongoy, Chile.	Álvarez *et al.* (2020)

Donax trunculus	—	12 µg· g^{-1}	Clams obtained during *P. australis* bloom (2.6 × 10^5 cells L^{-1}) in the Bay of Douarnenez, France.	García-Corona *et al.* (in prep)
Ruditapes decussata	53 µg· g^{-1}	—	Shellfish samples collected from different points along the French coasts during *P. multiseries* and *P. pseudodelicatissima* blooms (1 × 10^5 cells L^{-1})	Amzil *et al.* (2001)
	1.55 µg· g^{-1}	—		
	> 20 µg· g^{-1}	—	Control monitoring programme of ASP outbreaks in British waters during teen years (2008-2017)	Rowland-Pilgrim, *et al.* (2019)
	7 µg· g^{-1}	—	Shellfish simultaneously sampled after a *Pseudo-nitzschia sp.* bloom (400 ng DA L^{-1}) in Aveiro Lagoon, Portugal.	Vale *et al.,* 1998; Vale & Sampayo, 2001; 2002; Vale *et al.,* 2008
	160 µg· g^{-1}	—		
Scrobicularia plana	27.5 µg· g^{-1}	—		
Venerupis pullastra	17 µg· g^{-1}	—		
Acanthocardia tubercula	5.3 µg· g^{-1}	—		
Pollicipes pollicipes	0.5 µg· g^{-1}	1 µg· g^{-1}		
Cerastoderma edule	39 µg· g^{-1}	—		
	33 µg· g^{-1}	—	Control monitoring programme of ASP outbreaks in British waters during teen years (2008-2017)	Rowland-Pilgrim, *et al.* (2019)
Mactra veneriformis	4.13 µg· g^{-1}	—	Shellfish contaminated with DA collected from fish retail outlets in Korea.	Choi *et al.,* 2009
Peronidia venulosa	3.02 µg· g^{-1}	—		
Acanthocardia tuberculata	≤4.9 µg· g^{-1}		Cockels and clams sampled during *Pseudo-nitzschia spp.* blooms (1.6 × 10^5 cells L^{-1}) in M'diq Bay, Morocco. One year monthly monitoring from the estuarine central Adriatic Sea (Croatia)	Leblad *et al.,* 2013; Ujević *et al.* (2019)
Challista chione	≤2.1 µg· g^{-1}			
Dosinia orbignyi	25 µg· g^{-1}	—	Bivalves samples obtained from fisheries during ASP outbreaks (1401 ng DA L^{-1}) in Angola.	Blanco *et al.* (2010)
Venerupis corrugata	14 µg· g^{-1}	—		
Mactra glabrata	5 µg· g^{-1}	—		
Spondylus squamosus	88.16 µg· g^{-1}	—	Clams sampled during *P. multiseries* blooms (8.2 × 10^4 cells L^{-1}) in Phillipines, Vietnam, Thailand and Japan.	Takata *et al.* (2009)
Spondylus versicolor	42.17 µg· g^{-1}	—		
	3.6 µg· g^{-1}	146.8 µg· g^{-1}	Exposed to DA (12 pg L^{-1}) with seasonal samplings in Nha Phu Bay, Vietnam.	Dao *et al.* 2009;, 2015
Spondylus cruentus	2.7 µg· g^{-1}	—		
Flexopecten proteus	0.12 µg· g^{-1}	—	Contaminated with DA aftter *Pseudo-nitzschia spp.* blooms (>10^6 cells L^{-1}) in the Croatian coast (2006-2008).	Ujević *et al.* (2010)
Pecten jacobaeus	1.7 µg· g^{-1}	—		
Haliotis rubra	42 µg· g^{-1}	231 µg· g^{-1}	Abalone sampled during *Pseudo-nitzschia spp.* blooms (5^6 cells L^{-1}) in southern coast of Australia. Tissues were pooled for quantification analysis.	Malhi *et al.,* 2014
Haliotis laevigata				
Haliotis roei				
Haliotis conicopora				

Octopus vulgaris	—	26.6 µg· g^{-1}	Octopus sampled after *P. delicatissima* and *P. seriata blooms* (81 × 10^9 cells L^{-1}) in Peniche, Portugal.	Lage *et al.* (2012)
	7 µg· g^{-1}	166.2 µg· g^{-1}	Animals collected by commercial vessels in the Portuguese continental coast.	Costa *et al.* (2004)
Loligo opalescens	—	0.37 µg· g^{-1}	Squids obtained from the commercial fleet during a *P. australis* bloom in Monterey, CA, USA.	Bargu *et al.,* 2008
Eledone cirrhosa	—	18.8 µg· g^{-1}	Octopus contaminated after ASP outbreaks and collected along the Portuguese coast.	Costa *et al.* (2005a)
Eledone moschata	—	127 µg· g^{-1}		
Dosidicus gigas	—	0.3 µg· g^{-1}	Squid samples collected during *P. delicatissima* blooms (5.4 × 10^5 cells L^{-1}) La Jolla, CA, USA.	Mazzillo *et al.,* 2011
	—	0.23 µg· g^{-1}	Stranded animals contaminated with DA collected in Pacific Canada.	Braid *et al.,* 2012
Sepia officinalis	—	241.7 µg· g^{-1}	Simultaneous sampling after a *Pseudo-nitzschia sp.* blooms in Peniche, Portugal.	Costa *et al.* (2005b)
	16 µg· g^{-1}	50 µg· g^{-1}	Cuttlefish contaminated with DA sampled throughout 2014 and 2015 in southern Morocco.	Ben Haddouch *et al.,* 2016
	—	75.9 µg· g^{-1}	Animals contaminated with DA collected in British Columbia, Canada.	Lopes *et al.,* 2018
Cucumaria sp.	1.4 µg· g^{-1}	—	Benthic invertebrates contaminated with DA after blooms of *P. multiseries* in Ria de Vigo, Spain.	Reizopoulou *et al.,* 2012
Amphiura chiajei	0.83 µg· g^{-1}	—		
Ophiura ophiura	0.4 µg· g^{-1}	—		
Aporrhais pespelecani	2.2 µg· g^{-1}	—		
Nassarius reticulatus	41.1 µg· g^{-1}	—		
Callinectes sapidus	< 20 µg· g^{-1}	—	Crustaceans contaminated with DA during *P. australis* blooms in Washington and Oregon Pacific coast.	Altwein *et al.,* 1995
Cancer pagurus	< 20 µg· g^{-1}	—		
Menippe adina	> 30 µg· g^{-1}	—		
Palinurus elephas	24 µg· g^{-1}	—		
Cancer magister	—	495 µg· g^{-1}	Crabs sampled during *Pseudo-nitzschia sp.* blooms in the Pacific Coast of USA.	Villac *et al.,* 1993
	—	90 µg· g^{-1}	Animals collected during *P. australis* monitoring blooms in Washington and Oregon coast.	Wekell *et al.* (1994b)
	> 154 µg· g^{-1}	—	Crabs contaminated with DA during a *P. pungens, P. multiseries* and *P. australis* outbreaks in 1991 in Washington, USA.	Horner & Postel, 1993
Aulacomya atra	19.75 µg· g^{-1}		Samples of bivalves collected during *P. seriata* and *P. delicatissima* (1 × 10^4 cells L^{-1}) in Magellan, Chile.	Pizarro *et al.,* 2017
Chlamys vitrea	14 µg· g^{-1}			
Mytilus chilensis	1.53 µg· g^{-1}			

	6.4 µg· g^{-1}	—	Shellfish sampling during a *P. australis* bloom (50-90 × 10^4 cells L^{-1}) in Bahía Inglesa, Chile.	López-Rivera *et al.* (2009)
Aulacomya ater	5.4 µg· g^{-1}	—		
Pyura chilensis	15.5 µg· g^{-1}	32.7 µg· g^{-1}		
Protothaca thaca	4.7 µg· g^{-1}	—		
Emerita analoga	27.3 µg· g^{-1}		Sand crabs collected during a *Pseudo-nitzschia sp.* bloom (10^6 cells L^{-1}) in Sand City, CA, USA.	Shanks *et al.,* 2016
	13.4 µg· g^{-1}	—	Crabs collected in a monthly basis during *P. australis* and *P. multiseries* blooms in Santa Cruz and Monterey Bay, CA, US.	Ferdin *et al.* (2002); Powell *et al.* (2002)
	5 µg· g^{-1}	—		
	278 µg· g^{-1}	—	Benthic shellfish samples collected during and after an ASP outbreak (*P. australis* and *P. multiseries* ≤ 10^4 cells L^{-1}) during a year in Monterey Bay, CA, USA.	Lefebvre *et al.,* 2002a; Goldberg, 2003; Kvitek *et al.,* 2008
Callianassa californiensis	145 µg· g^{-1}	—		
Urechis caupo	751 µg· g^{-1}	—		
Nassarius fossatus	674 µg· g^{-1}	—		
Pagurus samuelis	56 µg· g^{-1}	—		
Neotrypaea californiensis	145 µg· g^{-1}	—		
Dendraster excentricus	15 µg· g^{-1}	—		
Olivella biplicata	3 µg· g^{-1}	—		
Citharichthys sordidus	515 µg· g^{-1}	—		
	—	7.2 µg· g^{-1}		
	—	50.1 µg· g^{-1}	Fish samples obtained during *P. australis* and *P. multiseries* blooms (7.7 × 10^4 cells L^{-1}) in the southern coastal area of California, and in Newport, Kentucky, USA.	Lefebvre *et al.,* 2002a; Naar *et al.,* 2002; Busse *et al.,* 2006
Scomber japonicus	—	7.3 µg· g^{-1}		
	—	1.4 µg· g^{-1}		
Trachurus symmetricus	—	5.5 µg· g^{-1}		
Zaniolepis latipinnis	—	9.7 µg· g^{-1}		
Brevoortia patronus	—	0.31 µg· g^{-1}	Fish samples obtained during a *Pseudo-nitzscia sp.* bloom (2 × 10^6 cells L^{-1}, 11 pg DA $cell^{-1}$, 371 ng DA L^{-1}) in Louisiana, USA.	Del Rio *et al.,* 2010
Polybus henslowii	323.1 µg· g^{-1}	571.6 µg· g^{-1}	Crabs contaminated after a *P. australis* bloom (6.7 × 10^4 cells L^{-1}) in Portugal.	Costa *et al.* (2003)
Euphausia pacifica	—	44 µg· g^{-1}	Krill samples collected during *P. australis* blooms (10 × 10^5 cells L^{-1}) in Monterey Bay, California, US.	Bargu *et al.,* 2002b; Bargu & Silver, 2003
Menticirrhus littoralis	0.14 µg· g^{-1}	—	Fish collected during *P. subfraudulenta* blooms (10^6 cells L^{-1}, 540 pg DA mL^{-1}, 5 months) in the northern Gulf of Mexico	Liefer *et al.,* 2013
Anchoa hepsetus	0.72 µg· g^{-1}	—		
Mugil curema	0.056 µg· g^{-1}	—		
Paralichthys californicus	2.5 µg· g^{-1}	—	Fish samples obtained during the largest and most toxic ASP outbreak recorded in the last 15 years in Monterey, CA. USA.	Kudela *et al.,* 2015
Ophiodon elongatus	0.5 µg· g^{-1}	—		
Engraulis mordax	35 µg· g^{-1}	2076 µg· g^{-1}		

	505 μg· g^{-1}	3239 μg· g^{-1}	Anchovies sampled after the largest recorded ASP outbreack (*P. australis*, 19.98 μg DA L^{-1}) along the North American west coast in early 2015.	McCabe *et al.,* 2016
	105 μg· g^{-1}	485 μg· g^{-1}	Commercially frozen anchovies contaminated with DA from Monterey Bay, California, US.	Wekell *et al.* (1994b)
	100 μg· g^{-1}	191 μg· g^{-1}	Samples obtained after a bloom of *P. australis* in Monterey Bay, CA. USA.	Fritz *et al.,* 1992
	77 μg· g^{-1}	275 μg· g^{-1}	Anchovies contaminated with DA during ASP outbreaks.	Quilliam *et al.* (1991)
	40 μg· g^{-1}	190 μg· g^{-1}		Work *et al.* (1993)
	55 μg· g^{-1}	223 μg· g^{-1}	Anchovies collected during a *P. australis* bloom in Monterey Bay, CA, US.	Lefebvre *et al.* (1999)
	—	71.3 μg· g^{-1}	Samples obtained after a bloom of the toxic *P. australis* (~1.3 × 10^5 cells L^{-1}, ~75 pg DA $cell^{-1}$) and *P. pseudodelicatissima* (10^6 cells L^{-1}) in Monterey Bay, CA, USA.	Scholin *et al.,* 2000
	2.2 μg· g^{-1}	1815 μg· g^{-1}	Field-exposed anchovies during a *P. australis* and *P. multiseries* blooms (5 × 10^5 cells L^{-1}) in Monterey Bay, California, US.	Lefebvre *et al.,* 2001; 2002b
	1.2 μg· g^{-1}	1175 μg· g^{-1}		
Engraulis encrasicolus	—	492.4 μg· g^{-1}	Sampling after a *Pseudo-nitzschia sp.* bloom (400 ng DA L^{-1}) in the coastal area of Portugal.	Vale & Sampayo (2001)
Sardina pilchardus	74.2 μg· g^{-1}	—		
	nd	128.5 μg· g^{-1}	Contaminated with DA after blooms of *P. australis* in the NW coast of Portugal.	Costa & Garrido (2004)
	0.2 μg· g^{-1}	728 μg· g^{-1}	Field-exposed fishes during a *P. australis* and P. *multiseries* blooms (5 × 10^5 cells L^{-1}) in Monterey Bay, California, US.	Lefebvre *et al.* (2002a)
Thunnus alalunga	—	4.6 μg· g^{-1}		
Atherinopsis californiensis	—	275 μg· g^{-1}		
Sardinops sagax	nd	72.2 μg· g^{-1}	Samples collected in 2011 during a mass mortality event in Redondo Beach, CA, USA.	Stauffer *et al.,* 2012
	nd	0.12 μg· g^{-1}	Samples collected in 2014 during a fish mortality event due to an ASP outbreak (*Pseudo-nitzschia sp.,* ~180 ng DA L^{-1}) the Nambian coast, Africa.	Louw *et al.,* 2018
Genyonemus lineatus	nd	2.4 μg· g^{-1}	Sample set of fish obtained during *P. australis* event in Monterey, CA, USA.	Fire & Silver, 2005
Leptocottus armatus	nd	2.8 μg· g^{-1}		
Citharichthys sordidus	—	3.4 μg· g^{-1}	Flatfish collected by trawl from depths of 30–180 m offshore of Davenport, USA, and within Monterey Bay, USA, on a monthly basis during DA-producing *P. australis* and *P. multiseries.* blooms between 2002 and 2003.	Vigilant & Silver (2007)
Eopsetta exillis	—	4.9 μg· g^{-1}		
Eopsetta jordani	—	6.7 μg· g^{-1}		
Psettichthys melanostictus	—	13.2 μg· g^{-1}		
Hippoglossus stenolepis	—	8.4 μg· g^{-1}		

Errex zachirus	—	24.3 µg· g^{-1}		
Microstomus pacificus	—	53.3 µg· g^{-1}		
Pleuronectes vetulus	—	15 µg· g^{-1}		
Pleuronectes decurrens	—	25.9 µg· g^{-1}		
Pleuronectes sp.	177.4 µg· g^{-1}	—	Fish samples collected randomly, not on a monthly basis and not during any HAB in Scottish waters.	Jensen *et al.,* 2015
Limanda limanda	51.1 µg· g^{-1}	—		
Gadhus morhua	2.7 µg· g^{-1}	—		
Hippoglossoides platessoides	2.8 µg· g^{-1}	—		
Merlangius merlangus	0.3 µg· g^{-1}	—		
Mugil cephalus	—	0.09 µg· g^{-1}	Fish samples obtained during an ASP outbreak (*Pseudo-nitzschia spp.,* 10^5 cells L^{-1}) and marine mass-mortality events in Florida (Gulf of Mexico) USA.	Twiner *et al.,* 2012
Lagodon rhomboides	—	0.039 µg· g^{-1}		
Orthopristis chrysoptera	—	0.076 µg· g^{-1}		
Eugerres plumieri	—	0.065 µg· g^{-1}		
Harengula jaguana	—	0.44 µg· g^{-1}		
(B) Experimentally exposed				
Mytilus edulis	—	13 µg· g^{-1}	Mussels fed with *P. multiseries* (4 – 8 × 10^6 cells L^{-1}) during 10 days.	Wohlgeschaffen *et al.* (1992)
	—	50 µg· g^{-1}	Animals fed with *P. multiseries*.	Novaczek *et al.* (1992)
	320 µg· g^{-1}	—	Juveniles exposed during two weeks to toxic *P. multiseries* (8.7 ng DA mL^{-1}).	Mafra *et al.* (2010a)
	4.8 µg· g^{-1}	460 µg· g^{-1}	Mussels exposed to *P. multiseries* at 3100 cells mL^{-1} for 2 days.	Mafra *et al.* (2010b)
	186.2 µg· g^{-1}	—	Fed with the toxic *P. multiseries* (1.7 × 10^6 cells mL^{-1}, 833 ng DA L^{-1}).	Stewart *et al.* (2008)
	—	42 µg· g^{-1}	Digestive gland slices incubated during 3h in seawater supplemented with dissolved DA (500-µg mL^{-1}).	Blanco *et al.* (2021a)
	—	84.3 µg· g^{-1}	Digestive gland slices incubated during 40 min in seawater supplemented with dissolved DA (200-µg mL^{-1}).	García-Corona *et al.* (in prep)
Mytilus californianus	2.5 µg· g^{-1}	3.6 µg· g^{-1}	Mussels exposed to *P. multiseries* (16 °C; 28 UPS; 335 × 10^3 cells mL^{-1}; 1.6 pg DA $cell^{-1}$) during 48 h.	Jones *et al.* (1995)
Crassostrea virginica	—	44 µg· g^{-1}	Oysters exposed during two weeks to toxic *P. multiseries* (9.8 pg $cell^{-1}$).	Mafra *et al.* (2010a)

	1.1 µg· g^{-1}	78.6 µg· g^{-1}	Animals exposed to *P. multiseries* at 3100 cells mL^{-1} for 2 days.	Mafra *et al.* (2010b)
	2 µg· g^{-1}	—	Exposed to *P. multiseries.*	Roelke *et al.* (1993)
Crassostrea gigas	4.4 µg· g^{-1}	36.3 µg· g^{-1}	Oysters exposed (48 h) to *P. multiseries* (16 °C; 28 UPS; 335 × 10^3 cells mL^{-1}; 1.6 pg DA $cell^{-1}$).	Jones *et al.* (1995)
Chlamys varia	—	68.2 µg· g^{-1}	Digestive gland slices incubated during 40 min in seawater supplemented with dissolved DA (200-µg mL^{-1}).	García-Corona *et al.* (in prep)
Pecten maximus	—	132.3 µg· g^{-1}		
	221 µg· g^{-1}	—	Scallops fed with 0.15 mL 100 µg mL^{-1} DA with 0.1 g formulated feed (1 g d^{-1} $scallop^{-1}$) at day 0, 12 and 32, respectively.	Liu *et al.,* 2007a
	117.7 µg· g^{-1}	—		
	262.5 µg· g^{-1}	—		
	5.21pg ind^{-1}		Scallop larvae exposed to a solution of 50 ng DA mL^{-1} and fed once a day with a blend of *Ishochrysis sp.* and *Pavlova lutheri* (1:1, 2 × 10^6 cells L^{-1}) during 25 days.	Lui *et al.,* 2007b
Placopecten magellanicus	36.7 µg· g^{-1}	3,108 µg· g^{-1}	Scallops fed with *P. multiseries* (4 - 6.7 pg DA· $cell^{-1}$) for 22 days.	Douglas *et al.* (1997)
	—	4.4 µg· g^{-1}	Fed with *P. multiseries* (4 – 8 ×10^6 cells L^{-1}) for 10 days.	Wohlgeschaffen *et al.* (1992)
Ruditapes philippinarum	35.9 µg· g^{-1}	—	Clams fed with cultured *P. multiseries* (700-3300 cells mL^{-1}) during 3 days.	Dusek Jennings *et al.* (2020)
Nuttallia obscurata	27.5 µg· g^{-1}	—		
Mya arenaria	4.3 µg· g^{-1}	—		
Siliqua patula	3.3 µg· g^{-1}	—		
Cancer magister	nd	65.9 µg· g^{-1}	Crabs fed with razor clams *S. patula* contaminated with DA (4,220 µg DA g^{-1}) during 4 and 6 days.	Lund *et al.* (1997)
	nd	2850 µg· g^{-1}		
Acartia clausi	~1250 fmol DA $copepod^{-1}$		Copepods feeded with single and mixed cultures of the toxic *P. multiseries* (3.6 × 10^3 cells L^{-1}).	Maneiro *et al.,* 2005
Acartia tonsa	8.46 ng DA $copepod^{-1}$ d^{-1}		Copepods grazed in laboratory conditions with the toxic *P. multiseries* (5 × 10^6 cells L^{-1}, 0.28 pg DA $cell^{-1}$, 13.6 ng DA mL^{-1}, 16^9 cells $copepod^{-1}$ h^{-1}).	Lincoln *et al.,* 2001
Temora longicornis	0.76 ng DA $copepod^{-1}$ d^{-1}			
Calanus finmarchicus	23 µg DA g $copepod^{-1}$		Copepods grazed 12 h in laboratory conditions with the toxic *P. multiseries* (4^6 cells L^{-1}, 2.52 pg DA $cell^{-1}$, 14581 cells $copepod^{-1}$ h^{-1}).	Leandro *et al.,* 2010
Engraulis mordax	1.6 µg· g^{-1}	199 µg· g^{-1}	Oral gavage with 200 µl nanopure water containing 800 µg pf pure DA.	Lefebvre *et al.,* 2001; 2002a

Marine bivalves can be broadly classified as fast or slow DA detoxifiers. The former takes weeks to detoxify; the latter takes months to years. Several commercially important species, such as mussels (Novaczek *et al.,* 1992; Blanco *et al.,* 2002b; Bresnan *et al.,* 2017), oysters (Jones *et al.,* 1995; Mafra *et al.,* 2010b), clams (Blanco *et al.,* 2010; Álvarez *et al.,* 2015; Dusek Jennings *et al.,* 2020), and some scallops (Álvarez *et al.,* 2020) have been classified as fast DA detoxifiers, since are capable of excrete almost total DA burdens within hours or a few days. Hence, they retain DA for a short time and the impact on their harvest and commercialization is low. Within the group of fast-DA depurators, *M. edulis* is the bivalve exhibiting the fastest detoxification rates, with ~ 2 µg day^{-1} in the whole body, and up to 60 day^{-1} in digestive tissues, that accumulate more than 80% of the total DA content. Nonetheless, in other species with high market value, DA can be accumulated in large amounts and retained for a long time, even months or years. Detoxification rates in slow DA depurators range from < 2 µg DA day^{-1} in the whole body to < 0.3 µg DA day^{-1} in the DG, as reported for the clams *Siliqua patula* (Drum *et al.,* 1993; Horner *et al.,* 1993; Dusek Jennings *et al.,* 2020), and *Spondylus cruentus* (Ha *et al.,* 2006). Yet, *Pecten maximus* (Blanco *et al.,* 2002a 2006; Mauríz & Blanco, 2010; Bresnan *et al.,* 2017; García-Corona *et al.,* in prep a) show the slowest DA-decontamination kinetics, with rates as slow as 0.005 day^{-1} in the DG. The information on DA depuration rates in all invertebrate species reported in the literature is concentrated in Table III.

Table III. Detoxification rates of ASP toxin domoic acid (DA) attained by several shellfish species (adults unless indicated), naturally or experimentally decontaminated from DA produced by Pseudo-nitzschia spp. The species are classified as fast (A) and slow (B) detoxifiers according to the total DA burden – body size relationship reported in each reference. DA depuration rates are expressed in µg DA d-1 except when indicated. FW = fresh weight.

Species	Detoxification rate (µg DA day^{-1} FW)		Detoxification conditions	Reference
	Whole tissues	Digestive tissues		
(A) Fast detoxifiers				
Perna canaliculus	2 day^{-1}	—	Mussels experimentally depurated in laboratory conditions.	MacKenzie *et al.,* 1993
Mytilus galloprovincialis	—	0.58 day^{-1}	Experimentally placed at 19 and 22 °C, and salinities of 12.5 and 31 UPS.	Blanco *et al.,* 2002b
Mytilus edulis	2.2 day^{-1}	10.59 day^{-1}	DA-free diet *Cylindrotheca fusiformis* 291 × 10^{6} cells L^{-1} during 15 days	Wohlgeschaffen *et al.* (1992)
	2.01 day^{-1}	10.59 day^{-1}	Experimentally fed with spray-dried yeast (4 mg h^{-1}) at 11 and 6 °C; 18 and 28 UPS.	Novaczek *et al.* (1991)
	0.49 day^{-1}	0.99 day^{-1}		Novaczek *et al.* (1992)
	2 day^{-1}	—	Mussels experimentally depurated in laboratory conditions	Krogstad *et al.* (2009)
	—	19.11 day^{-1}	Mussels flushed with uncontaminated seawater during 18 days in laboratory.	Grimmelt *et al.* (1990)
	—	60 day^{-1}	Monitoring of wild population after *P. multiseries* blooming in Cardigan Bay, Canada.	Silvert and Subba, 1992
	0.15 day^{-1}	1.6 day^{-1}	Mussels maintained at 12 °C and fed with the non-toxic *I. galbana* and *P. pinguis* (30,000 cells ml^{-1}) for 21days.	Mafra *et al.,* 2010b
	1 day^{-1}	—	Continuous monitoring after a *P. australis* blooms (6 × 10^{5} cells L^{-1}) in Scotland.	Bresnan *et al.,* 2017
Mytilus californianus	0.5 day^{-1}	—	Mussels experimentally depurated in laboratory conditions.	Whyte *et al.,* 1995
	2.1 day^{-1}	—	DA contaminated animals placed at 16 °C; 28 UPS with a continuous flow of filtered seawater for 120 h.	Jones *et al.,* 1995
Crassostrea gigas	—	6.9 day^{-1}		
Argopecten purpuratus	0.91 day^{-1}	0.9 day^{-1}	Naturally DA contaminated scallops maintained in filtered seawater at 16 °C and	Álvarez *et al.* (2020)

			fed twice a day with *Isochrysis galbana* at 6×10^5 cells mL^{-1} during 12 days.	
	0.27 day^{-1}	0.33 day^{-1}	Naturally DA contaminated scallops maintained during 12 days in suspended lanterns in a ocean farm in Tongoy Bay, Chile, with populations of *P. australis* significantly reduced but still present.	
Placopecten magellanicus	1.9 day^{-1}	0.17 day^{-1}	Fed with a blend of *Chaetoceros muelleriand* and *Thalassiosira pseudonana* during 14 days.	Douglas *et al.,* 1997
	—	0.25 day^{-1}	DA-free diet *Cylindrotheca fusiformis* 291 × 10^6 cells L^{-1} during 15 days	Wohlgeschaffen *et al.,* 1992
Mesodesma donacium	1.27 day^{-1}	—	Surf clams placed in 15 L containers (18 °C) and fed twice a day with Isochrysis galbana (6 ×10^6 cells ml^{-1}) and daily total filtered (1 µm) water changes.	Álvarez *et al.,* 2015
Crassostrea virginica	0.11 day^{-1}	0.88 day^{-1}	Oysters maintained at 12 °C and fed with the non-toxic *I. galbana* and *P. pinguis* (3×10^4 cells mL^{-1}) for 21 days.	Mafra *et al.,* 2010b
Ruditapes philippinarum	0.44 day^{-1}	—	Clams fed with cultured *P. multiseries* (700-3300 cells mL^{-1}) for 3 days and then purged in filtered seawater during 1, 2, 4, 8 and 15 days.	Dusek Jennings *et al.* (2020)
Nuttallia obscurata	0.1 day^{-1}	—		
Mya arenaria	0.37 day^{-1}	—		
Calanus finmarchicus	~0.08 pg DA h^{-1} 0.22 pg DA h^{-1}		Copepods starved 38 h in filtered seawater or feeded 16 h with the non-toxic *P. pungens* (4^6 cells L^{-1}) respectively.	Leandro *et al.,* 2010
(B) Slow detoxifiers				
Pecten maximus	0.025 day^{-1}	0.008 day^{-1}	Placed in two aquaculture locations at three depths with different temperatures, salinities and food concentrations.	Blanco *et al.,* 2006
	0.11 day^{-1}	—	Continuous monitoring of DA contaminated wild scallops in the Bay of Seine, Normandy France.	Amzil *et al.,* 2007
	0.57 day^{-1}	—	Continuous monitoring after a *P. australis* blooms (6×10^5 cells L^{-1}) in Scotland.	Bresnan *et al.,* 2017
	2.9 day^{-1}	—	Contaminated scallops starved during 4 days and then fed once every other day with a non-	Lui *et al.,* 2007b

			DA formulated blend of *Isochrysis sp.* and *Pavlova lutheri* (1:1, 5 × 10^6 cells L^{-1}).	
	0.008 day^{-1}	0.007 day^{-1}	Naturally DA contaminated scallops placed in 1000 L tanks with running raw seawater (12-19 °C) without additional food maintained there during 295 days.	Blanco *et al.,* 2002a
	—	0.005 day^{-1}	Naturally DA contaminated scallops placed in 800 L tanks with running raw seawater (15.9 °C, 34 UPS) fed with *Tisochrysis lutea* (10×10^9 cells.$scallop^{-1}$ day^{-1}) during 60 days.	García-Corona *et al.* (in prep)
Siliqua patula	0.04 day^{-1}	0.05 day^{-1}	Maintained at 11 °C, 28 UPS and fed with a concentrated algal diet (*Thalassiosira pseudonana*) for 86 days.	Horner and Postel, 1993
	0.6 day^{-1}	—	Monthly sampling between 1991 and 1992, after a *Pseudo-nitzschia sp.* outbreak in Washington, USA.	Wekell *et al.,* 1994a
	0.02 day^{-1}	—	Clams fed with cultured *P. multiseries* (700-3300 cells mL^{-1}) for 3 days and then purged in filtered seawater during 1, 2, 4, 8 and 15 days.	Dusek Jennings *et al.* (2020)
Spondylus cruentus	0 day^{-1}	—	Naturally DA-contaminated clams reared in plankton-free conditions in laboratory (30 °C) during 45 days.	Dao *et al.,* 2006

Among the nearly 40 scientific papers published to date dealing with DA detoxification capabilities in bivalves, all the studied species have been arbitrarily classified as fast or slow detoxifiers based only on the time it takes them to excrete almost total DA burdens accumulated in their tissues. In this work, a correspondence analysis was computed using the data available in the literature corresponding to the accumulation (Table II) and depuration (Table III) of DA in the whole body of the bivalve species for which both values were available. The objective of this analysis was to provide a layout of the risk degree for the extraction of biomasses of these bivalve species during or after ASP outbreaks as a function of their capabilities to accumulate and depurate DA. As shown in Fig. 2, the plot was divided into four sections, the lower right green-shaded section encompasses the species whose exploitation represents a minor concern after toxic blooms of *Pseudo-nitzschia spp*., since these bivalves exhibit low accumulation rates and accelerated toxin depuration. The sections shaded in yellow include species whose populations represent a moderate sanitary risk for human health, since on the one hand this bivalves accumulate large DA amounts, whith quick depuration rates (upper right), as is the case of mussels *M. edulis* and *Perna canaliculus*, as well as the scallop *P. magellanicus*. While the species contained in the lower left section accumulate feeble amounts of DA whith a risk of retention of toxin burdens. Finally, the upper left section, shaded in red, represents an undesirable fishing scenario, since it harbors species such as *P. maximus* and *S. patula*, that accumulate the highest DA concentrations in their tissues and exhibit the slowest depuration rates within bivalves (Fig. 2), then its exploitation during or after blooms of DA-producing *Pseudo-nitzschia* represents a major concern of risk for seafood consumers.

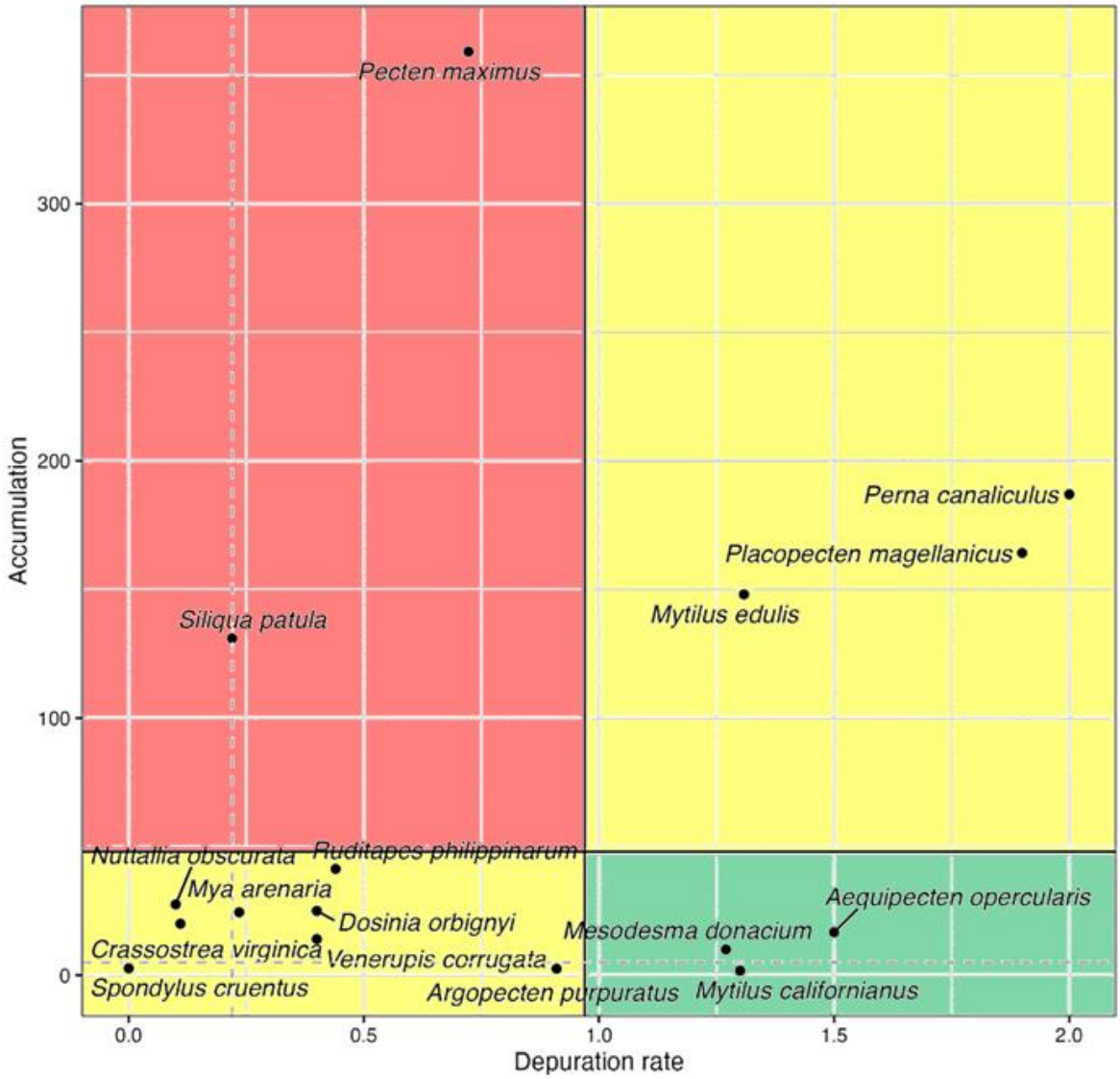

Figure 2. Kobe plot with accumulation as a function of depuration rates of DA in the whole body of several bivalve species commonly affected by blooms of toxic *Pseudo-nitzschia spp*. The Kobe plot is divided into four panels, where the decision lines on both axes represent the 33.33% (dotted) and 66.66% (solid) of the depuration and accumulation data reported in the literature, respectively. The red panel (upper left) corresponds to the species of "major concern", with slow DA depuration rates and high toxin accumulation. The green panel (lower right) is the "minor concern" area that shelters species that tend to accumulate low amounts of DA with high depuration capabilities. The two yellow panels of "moderate concern" characterize intermediate situations. Black dots represent the position of the species on the plot.

The final concentrations of DA accumulated in the tissues of affected animals after toxic *Pseudo-nitzschia* blooms is highly species-specific and depend on the allocation, distribution, and on the balance between absorption and detoxification kinetics (Blanco

et al., 2020; Álvarez *et al.,* 2020). Moreover, differences in DA amounts measured in the organisms during monitoring are strongly dependent on the toxicity of the *Pseudo-nitzschia* cells, the duration of the ASP-outbreaks, the time through the animals were exposed to toxic microalgae, and the moment at which the organisms were sampled during the bloom (García-Corona *et al.,* in prep b).

On the other hand, there is no enough evidence to date that DA biotransformation or translocation to any tissue for storage in fish and shellfish organs leads to changes in net DA burden (Vale and Sampayo, 2001; Costa *et al.,* 2005a; Álvarez *et al.,* 2020; Zheng *et al.,* 2022). The above mentioned greatly hinders the study of the kinetics of DA ingestion and excretion, and therefore, the ability to make predictions of ASP episodes, as well as to propose solutions to soften the economic impact of this natural phenomenon.

5. Effects of DA on marine invertebrates

Knowledge relating effects of *Pseudo-nitzschia spp*. or DA on invertebrates is very scarce. Benthic and filter-feeding bivalves are the most important vectors of DA in the environment (Bejarano *et al.,* 2008). Although literature indicates that DA uptake could potentially disrupt behavioral and complex metabolic, molecular, and physiological processes in bivalves, no lethal effects resulting from exposure to DA have been reported in species, suggesting either a low sensitivity to the toxin or yet unnoticed negative effects. Therefore, no mass mortality events have been reported in bivalves related to DA exposure up to date. After some transcriptomic analysis of the mussel *Mytilus galloprovincialis* (Pazos *et al.,* 2017) and the scallop *Aequipecten opercularis* (Ventoso *et al.,* 2019) *in vivo* exposed to toxic *Pseudo-nitzschia* cells, it was concluded that DA accumulation in these species could impair the antioxidant/detoxification

enzyme pathways, oxidative stress, and non-specific immune responses, making them more vulnerable to environmental stress-inducing agents after ASP blooms. In another RNA-seq analysis, Ventoso *et al.* (2021) found that the intramuscular injection of DA in *Pecten maximus* led to differential regulation of some processes such as autophagy, solute transport mediated by membrane transporters, and the antioxidant response in the digestive gland.

One study also found evidence that DA accumulation compromises the onset development (embryo-larval growth and survival) of *P. maximus* (Liu *et al.* 2007a), which suggests that ASP blooms could potentially impair the natural recruitment and aquaculture of this species. However, after feeding *P. maximus* scallops with DA, no negative effects were found on the survival and reproduction of adult individuals (Liu *et al.,* 2007b), nor the shell valve activity or the feeding rate of juveniles (Liu *et al.,* 2008). Notwithstanding, increases in the lysosomal enzymatic activity of the scallop *Argopecten irradians* (Chi *et al.,* 2019), as well as an augmentation in the total hemocyte counts and their phagocytic activity in the oyster *Crassostrea gigas* (Jones *et al.,* 1995) and the mussel *M. edulis* (Dizer *et al.,* 2001) were found after DA exposure, which could be considered as an indicator of potential physiological stress linked to DA exposure in these species.

Concerning other marine invertebrates, Lopes *et al.* (2013) found that the consumption of DA-contaminated mussels does not alter food intake in *Octopus vulgaris*. Nonetheless, an electrophysiological study demonstrated the potent neurotransmitter effect of DA on AMPA-kainate type GR (glutamate receptors) after *in vitro* exposure of slices of the vertical lobe from *O. vulgaris* to five different neurotransmitters, where DA was the most potent agonist of all (Langella, 2005). Given the evidence of the presence of GR (both AMPA-KA and NMDA type) in cephalopod central and peripheral neural

tissue (Lima *et al.,* 2003; Lee *et al.,* 2013; Zarrella *et al.,* 2019), and since DA is widely distributed in visceral tissues such as the digestive gland, posterior salivary glands, kidney, gills, systemic heart, and the brain of octopus and sepia (Costa *et al.,* 2004, 2005a,b; Ben Haddouch *et al.,* 2016; Lopes *et al.,* 2018), the potential neurotoxicological effects linked to DA ingestion cannot be excluded in cephalopods (Sykes *et al.,* 2020). Finally, Lincoln *et al.* (2001) evaluated the effect of diets of the DA-producing *P. multiseries* and the non-toxic *P. pungens* on the grazing rate, reproductive performance, and egg hatching successes of the copepods *Acartia tonsa* and *Temora longicornis*, without finding significant differences in any of the variables measured in the study. Thus, it was concluded that there are no adverse effects on copepods feeding on the toxic diatom compared to the non-toxic ones.

So far, there is not enough evidence to demonstrate that exposure to toxic *Pseudo-nitzschia*, or to DA, has highly detrimental or lethal effects on marine invertebrates. Nevertheless, the latent risk of pathologies linked to prolonged exposure to low-moderate concentrations of DA cannot be excluded, as has been demonstrated in marine mammals.

6. The effect of *Pseudo-nitzschia* and domoic acid on coastal ecosystem functioning

Since the late 1990s, DA production by toxigenic *Pseudo-nitzschia* has been linked to massive marine mammal and seabird mortalities (Lefebvre *et al.,* 2016; Anderson *et al.,* 2022). DA is one of the most potent excitatory compounds that could be found in seafood, and is of concern for food safety in marine coastal areas since it has been shown to be intricately associated with the food web, thus posing serious health risk to many top predators (Bejarano *et al.,* 2008). Despite awareness of the effects of DA in

marine ecosystems, little is known about the impact of toxic *Pseudo-nitszchia* blooms on the health and stability of the ecosystem in the affected areas (Trainer *et al.,* 2012; Lelong *et al.,* 2012; Bates *et al.,* 2018). The large body of existing literature focuses mainly on the toxicological effects of DA in vertebrates (mostly mammals), and the toxicokinetics of accumulation and depuration of the toxin in invertebrates (primarily bivalves). Nonetheless, to date no studies have attempted to forecast the population risk of recurrent exposure to DA on the food web and affected wildlife species.

A paramount issue and one of the most difficult to answer is whether there will be long-term consequences for wild populations. According to Bejarano *et al.* (2008) characterizing potential DA ecological impacts is immensely difficult mainly because of 1) the complex spatial and temporal dynamics of *Pseudo-nitzschia* blooms, 2) ASP events that occurs offshore where capabilities to detect effects on wildlife are limited, 3) the intricate relationship between DA-outbreaks and the food web, 4) population dynamics of prey-predator species, and 5) the spatiotemporal variability of prey, their abundance, and the fact that certain species are indicated as more potent vectors of DA than others.

Top predator populations have been cataloged as the most adversely affected by DA, but particularly those species with narrow geographical distribution or those that are already in decline as a result of other environmental or anthropic stressors, such as seabirds and dolphins (Work *et al.,* 1993; Sierra-Beltrán *et al.,* 1997), sea lions (Silvagni *et al.,* 2005; Brodie *et al.,* 2006; Lefebvre *et al.,* 2018), seals and sea elephants (Torres de la Riva *et al.,* 2006; McHuron *et al.,* 2013), baleen whales and walruses (Lefebvre *et al.,* 2002a, 2016; Anderson *et al.,* 2022), and sea otters (Kreuder *et al.,* 2005; Miller *et al.,* 2021). Moreover, there is evidence that toxic *Pseudo-nitzschia* blooms not only overlap the geographical distribution of these species, but also

temporally coincide with their breeding seasons (McHuron *et al.,* 2013; Lefebvre *et al.,* 2018). If top predators are effectively the most affected species by DA, this may lead to changes in the structure of marine communities by shifting the arrangement of the food web (Bejarano *et al.,* 2008; Anderson *et al.,* 2022). Thus, evaluating potential effects on populations of top predator species is a crucial first step towards assessing ecosystem impacts.

The forecast of DA impacts on wild populations requires also information on biotoxin-induced mortality rates and compromised survival skills coupled with population dynamics. Yet, only a few studies have attempted to assess the population level effects of recurrent exposures to DA by some species (Lefebvre *et al.,* 2018; Anderson *et al.,* 2022). Particularly for seabirds and sea lions populations, intense and repeated DA exposures have shown devastating consequences given their reproductive strategy (*i.e.,* low reproductive rate and delayed sexual maturity; (Shumway *et al.,* 2003). The large-scale blooms that have occurred prior to the pupping season of California sea lions *Z. californianus* have caused fatalities primarily of adult females, and was associated with rising of reproductive failures and problems during pregnancy and lactation (Silvagni *et al.,* 2005; Lefebvre *et al.,* 2018). Hence, these effects could be extrapolated to other populations of marine mammals commonly impacted by DA. Given repeated ASP events over time, the potential long-term risk for wild populations is also worth investigating. This raises concerns regarding the health of high trophic level fauna and the potential long-term implications on populations, which are the primary reason for conducting formal ecological risk assessments.

DA is well known to have deleterious effects on human health, causing up to human death (Lefebvre & Robertson, 2010). Monitoring networks developed in many countries ensure regular monitoring of the concentrations of toxic microalgae and the level of DA

in the shellfish species consumed and avoid human contaminations. Recurring blooms of DA-producing diatoms and toxin accumulation in commercially important shellfish species thus frequently leads to the closure of fishery and aquaculture activities, which represents severe economic impacts in large affected coastal areas (Chinabut *et al.,* 2006; Zabaglo *et al.,* 2016; Hallegraeff, 2017). The economic impact of ASP on fisheries and aquaculture largely depends on the target species capabilities to accumulate, and more than anything, to detoxify DA. Although non-lethal effects have been reported on invertebrates after DA exposure, studies on the toxicological effects of DA on these organisms are essential given its importance in marine food web, as well as research on their role as bioindicators and as vectors to upper level consumers.

Furthermore, as mentioned previously, DA can also affect marine organisms, which can result in massive mortality events of marine wildlife, thus seriously affecting marine environments and coastal ecosystem structure (Bates & Trainer, 2006; Bejarano *et al.,* 2008; Trainer *et al.,* 2012; La Barre *et al.,* 2014). Predicting ecological risks from *Pseudo-nitzschia* toxic blooms is essential to identify DA impairments on wildlife; nonetheless, meaningful assessments require the integration of a multidisciplinary research approach on the spatial and temporal occurrence of ASP-events, the trophic interactions of DA vectors species with top predators, toxicity, and effects on wildlife. All this knowledge is often not available to conduct such studies, hence, determining short-and long-term effects on marine populations is rather challenging.

CHAPTER 2

SUBCELLULAR LOCALIZATION OF THE AMNESIC SHELLFISH TOXIN, DOMOIC ACID, IN BIVALVE TISSUES

PREAMBLE

The lack of data concerning the precise anatomical localization of DA in the tissues of non-mammal organisms has made it extremely difficult to explain the causes underlying the contamination and decontamination of DA in these species. We consider that the best way to advance in understanding the long retention of DA in *P. maximus* was to visualize whether the toxin was bound to any cellular-tissue component of the contaminated animals by localizing it *in situ* at the subcellular level. In this chapter the results of an innovative immunohistochemical method of DA-labeling to localize the phycotoxin in the tissues of contaminated king scallops *P. maximus* are presented. This protocol is based on the use of a polyclonal anti-DA primary antibody that was proved to recognize the toxin on histological sections of the hippocampal-brain tissues of intoxicated rats (Vieira *et al.,* 2015a,b; 2016). Subsequently, this primary antibody is recognized by a specific secondary antibody conjugated to a peroxidase, which, in the presence of diaminobenzidine as substrate, produces a brown chromogenic compound that indicates the presence of DA on the contaminated tissue samples (Fig. 5).

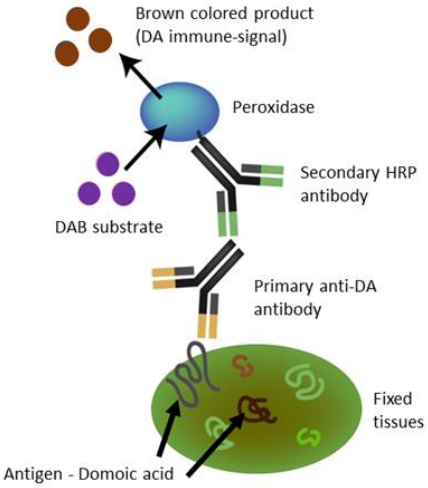

Figure 5: Anti-DA detection antibody system

This chapter was the subject of a research paper published in 2022 in the journal *Harmful Algae.*

Harmful Algae 116 (2022) 102251

Contents lists available at ScienceDirect

Harmful Algae

journal homepage: www.elsevier.com/locate/hal

Original Article

First subcellular localization of the amnesic shellfish toxin, domoic acid, in bivalve tissues: Deciphering the physiological mechanisms involved in its long-retention in the king scallop *Pecten maximus*

José Luis García-Corona [a], Hélène Hégaret [a], Margot Deléglise [a], Adeline Marzari [a], Carmen Rodríguez-Jaramillo [b], Valentin Foulon [c], Caroline Fabioux [a,*]

[a] Institut Universitaire Européen de la Mer, Laboratoire des Sciences de l'Environnement Marin (UMR6539 CNRS/UBO/IFREMER/IRD) Technopôle Brest-Iroise, Plouzané 29280, France
[b] Centro de Investigaciones Biológicas del Noroeste (CIBNOR), Mar Bermejo 195, Col. Playa Palo de Santa Rita, La Paz, B.C.S. 23090, Mexico
[c] Université Bretagne Loire, ENIB, UMR CNRS 6285 LabSTICC, Brest 29238, France

ABSTRACT

Domoic acid (DA), the phycotoxin responsible for amnesic shellfish poisoning (ASP), is an excitatory amino acid naturally produced by at least twenty-nine species of the bloom-forming marine diatoms *Pseudo-nitzschia spp.* Suspension feeders, such as bivalve mollusks, can accumulate and lengthy retain high amounts of DA in their tissues, threatening human health and leading to extensive-prolonged fishery closures, and severe economic losses. This is particularly problematic for the king scallop *Pecten maximus,* which retains high burdens of DA from months to years compared to other fast-depurator bivalves. Nonetheless, the physiological and cellular processes responsible for this retention are still unknown. In this work, for the first time, a novel immunohistochemical techniques based on the use of an anti-DA antibody was successfully developed and applied for DA-detection in bivalve tissues at a subcellular level. Our results show that in naturally contaminated *P. maximus* following a *Pseudo-nitzschia australis* outbreak, DA is visualized mainly within small membrane-bounded vesicles (1 – 2.5 µm) within the digestive gland cells, identified as autophagosomic structures by means of immune-electron microscopy, as well as in the mucus-producing cells, particularly those from gonad ducts and digestive tract. Trapping of DA in autophagososomes may be a key mechanism in the long retention of DA in scallops. These results and the development of DA-immunodetection are essential to provide a better understanding of the fate of DA, and further characterize DA contamination-decontamination kinetics in marine bivalves, as well as the main mechanisms involved in the long retention of this toxin in *P. maximus*.

Keywords: Amnesic Shellfish Poisoning, domoic acid, immunodetection, toxicokinetics, scallops, autophagosomes.

INTRODUCTION

Up to date, fifty-nine bloom-forming species of diatoms of the genus *Pseudo-nitzschia* have been identified in all the oceans around the world (Lelong *et al.,* 2012; Bates *et al.,* 2018), and at least twenty-eight of these are capable of synthesizing domoic acid (DA), an extremely dangerous amnesic phycotoxin responsible for amnesic shellfish poisoning (ASP) in humans (Lundholm *et al.,* 2009; Trainer *et al.,* 2012; Zabaglo *et al.,* 2016; Basti *et al.,* 2018). This toxin is a water-soluble amino acid, which acts as a potent neurotransmitter binding to the N-methyl-D-aspartate receptors in neurons of the hippocampus. DA is a structural analog of glutamic acid, proline, and glycine, three neurotransmitters targeting the NMDA-receptors essential to memory and synaptic plasticity, exhibiting respectively a three-fold to 100 fold higher affinity (Zaman *et al.,* 1997; Lefebvre & Robertson, 2010; Zabaglo *et al.,* 2016).

In the last two decades, *Pseudo-nitzschia* blooms have become more intense and frequent worldwide (Lelong *et al.,* 2012; Delegrange *et al.,* 2018), affecting large exploitable populations of suspension-feeding fish and molluscs, which are the main vector of ASP toxin to higher levels of the food chain, since they can accumulate large amounts of DA in their tissues through their filter-feeding activity (Trainer *et al.,* 2012; Hallegraeff, 2017; Basti *et al.,* 2018). Given the toxicity of DA, and as its presence in seafood represents a potential risk for human health, several countries have successfully established monitoring programs in places where *Pseudo-nitzschia* blooms are recurrent and intense (Lelong *et al.,* 2012), and also an international sanitary threshold of 20 mg DA kg^{-1} to regulate the maximum allowable amount of this toxin in bivalves (EFSA, 2009).

The rates of accumulation and depuration of DA in bivalves are species-specific and highly variable (Blanco *et al.,* 2006; Bogan *et al.,* 2007). Therefore, the incidence of

toxigenic *Pseudo-nitzschia* blooms on the harvest of natural beds depends on the balance between the kinetics of assimilation and elimination of the toxin (Álvarez *et al.,* 2020; Blanco *et al.,* 2021a). In this sense, bivalves have been broadly classified into two wide categories, rapid and slow DA detoxifiers. The former depurate the toxin within days to weeks and includes some species of mussels as *Mytilus galloprovincialis* (Blanco *et al.,* 2002b), *M. edulis* (Novaczek *et al.,* 1992; Mafra *et al.,* 2010; Bresnan *et al.,* 2017), and *Perna canalicus* (MacKenzie *et al.,* 1993), oysters such as *Crassostrea virginica* (Mafra *et al.,* 2010) and *C. gigas* (Jones *et al.,* 1995), and pectinids like *Argopecten purpuratus* (Alvarez *et al.,* 2020). The slow depurators can take months to years to depurate the DA. The main examples are some commercially important bivalves like *Pecten maximus* (Blanco *et al.,* 2002; Blanco *et al.,* 2006; Bresnan *et al.,* 2017), *Placopecten magellanicus* (Wohlgeschaffen *et al.,* 1992; Douglas *et al.,* 1997), *Siliqua patula* (Horner *et al.,* 1993), and *Spondylus cruentus* (Ha *et al.,* 2006).

The king scallop *P. maximus* is a high-valuable resource in Europe, and the third most important fishery species in France, with annual catches above 60,000 tons yielding a total of 87 million euros in 2017 (FAO, 2020). Nonetheless, the exploitation of this species is particularly problematic since during blooms of toxigenic *Pseudo-nitzschia* species, scallops can accumulate amounts up to ~3,200 mg DA kg^{-1} in the digestive gland (Blanco *et al.,* 2006), and lengthy retain them, even for years, due to its extremely low depuration rates, from 0.025 to 0.007 d^{-1} (Blanco *et al.,* 2002a; Blanco *et al.,* 2006). Considering the slow depuration and the risk for human health, these contamination episodes lead to extensive-prolonged fishery closures, and consequently severe economic losses.

More than 90% of the DA burdens are accumulated in the non-edible tissues of the scallops (Blanco *et al.,* 2006). It has been proposed that DA is mainly in “free-soluble”

form in the cytoplasm of the digestive gland cells (Mauriz & Blanco, 2010), and especially in the large digestive (absorptive) cells, responsible of the intracellular digestion of the pinocytized particulate matter using a complex enzymatic equipment in *P. maximus* (Beninger & Le Pennec, 2016). Hence, the digestive cells could have a particular contribution to the high accumulation of DA in the digestive gland (Blanco *et al.,* 2020). The long retention time of the toxin has been hypothesized to be due to the lack of some efficient membrane transporters in *P. maximus* (Mauriz & Blanco, 2010), or the presence of some high and low-affinity glutamate receptor as the present in the razor clam *Siliqua patula* (Trainer & Bill, 2004). Nevertheless, these hypotheses has not been confirmed yet. Despite the ecological and economic consequences associated with high accumulation of DA in scallops, the mechanisms underlying such a long retention of DA in *P. maximus* are still poorly understood. Hence, the aim of this work was to develop an immunohistochemical method to detect DA at the sub-cellular level in contaminated *P. maximus* tissues and thus decipher the subcellular mechanisms involved in its accumulation and long-retention.

1. MATERIALS AND METHODS

1.1. Biological material and sampling

Twenty adult *Pecten maximus* scallops (9.8 ± 0.1 cm shell length; 171.5 ± 5 g total weight) were collected by dredging from natural beds at three different sites in the west coast of Brittany, France. Six animals were obtained from the Bay of Concarneau (CN) in November 2019 (47° 52' 30.07'' N, 3° 55' 20.82'' W), and seven more from Camaret-sur-Mer (CM; 48° 26' 33.0096'' N, 4° 35' 49.6104'' W) in May 2021, after toxigenic *Pseudo-nitzschia* blooms. Additionally, seven scallops were collected from the Bay of

Brest (BB) in December 2020 (48° 19' 11" N, 4° 26' 33" W) and used as negative controls since no ASP outbreaks had recently been documented in this area.

Whole soft-bodies were carefully excised from the shells. The organs were then dissected in two groups: a) digestive gland (DG), and b) rest of tissues (RT) which included the gonad, the muscle, the heart, the kidney, the foot, gills and the mantle. As mentioned above, the digestive gland accumulates up to 90% of total domoic acid (DA) burdens (Blanco *et al.,* 2020); for this reason, this organ was first carefully dissected and separated from the RT to avoid any transfer of toxin between organs. Consequently, the DG was separated into three pieces for subsequent histology, toxin quantification, and transmission electron microscopy analysis, as described below. The RT section was used for histology.

1.2. Toxin extraction and quantification by High Performance Liquid Chromatography (HPLC)

Since the digestive gland accumulates most of DA, only this tissue was used for DA quantification in this work. For all 20 individuals, DA was extracted from scallop digestive gland following the procedure described by Quilliam *et al.* (1995). Frozen samples (-20 °C) were homogenised from 200 ± 5 mg of tissue in 1 mL of MeOH:MQ water (1:1, v/v) using a Laboratory Mixer Mill MM 400 system (Retsch® Fisher Scientific, Illkirch-Graffenstaden, FR) at 30 Hz/s for 10 min maintaining them in an ice bath. The extract was clarified by centrifugation at 15,000 × g for 10 min at 4 °C (eppendorf 5427 R, Thermo Scientific, West Sussex, UK) and the supernatant was isolated. An aliquot of 200 µL was filtered through a 0.2 µm nylon centrifugal filter (VWR International, Radnor, PA, USA) at 10,000 g for 5 min, at 4 °C. Since there may be substantial DA degradation in aqueous solutions stored in regular freezer (Thomas *et*

al., 1998), the filtered extracts were stored in amber-glass autosampler vials (Thermo Scientific, Rockwood, TN, USA) at -20 ºC for two days and analysed all at the same time.

All fractions obtained were analysed using a Thermo Scientific (Sunnyvale, CA, USA) HPLC System with an UV spectrophotometer Waters 996 PDA-UV detector, using a C18 reverse phase column (5 µm, 250 × 4.6 mm, Phenomenex). The separation was carried out using a mobile phase consisting of eluent A (Distilled water + 0.1 % TFA) and eluent B (ACN + 0.1 % TFA) whit gradient conditions from 5 to 20% ACN in 20 min at a flow rate of 1 mL min^{-1}, with an injection volume of 20 µL. The column temperature was maintained at 40 °C. A calibration curve was generated by serial dilutions in MeOH:H_2O (1:1, v/v) until concentrations of 0.2, 0.5, 1.0, 2.0, 4.0 and 8 µg DA mL^{-1} (r = 0.99) of certified DACS-1C DA standards obtained from National Research Council (Halifax, Canada). Thereupon, DA concentration was computed by comparing the absorbance at 242 nm of the chromatographic peaks of the samples with those of the reference solutions once it was checked that the retention time and the absorbance spectrum were the same. The LODs of this HPLC-UV method ranged from 0.2 to 1 mg DA kg^{-1} tissue.

1.3. Histology and Immunohistochemical staining of domoic acid

For all 20 scallops, the piece of digestive gland dedicated to histology (DG) and the rest of the tissues (RT) were separately fixed in Davidson solution for 24 hrs (Kim *et al.,* 2006), and preserved in Ethanol 70 % at 4 °C until processing. Then, tissue samples were dehydrated in ethanol series, cleared in claral, embedded in paraffin (Paraplast Plus, Leica Biosystems, Richmond, IL, USA), thin-sectioned (4 µm), mounted in polysine coated glass-slides (Sigma-Aldrich, St. Louis, MO, USA) and dried

overnight at 37 °C (Costa & Costa, 2012), as detailed in Table I. A series of 4 consecutive sections was performed for each samples, which were used for i) immunohistochemical detection of DA (test and negative control), ii) multichromic staining and iii) Hematoxyline/eosin staining.

Sections were deparaffinized and rehydrated in regressive series of ethanol before immunohistochemical staining (Table I). Following preliminary trials, the final procedure employed for immunostaining was performed as described below. An antigen retrieval step was applied in order to break potential methylene bridges formed during formalin-fixation and expose antigenic sites to allow the antibodies epitope to bind. For this, sections were placed in the Universal HIER Antigen Retrieval Reagent (abcam®, Cambridge, UK) diluted in MQ water in a ratio 1:10 (v/v), heated using a pressure cooker until full pressure for 3 min, and subsequently rinsed in washing buffer (TBS 20 mM, NaCl 150 mM, pH 7.6, with 0.025% Triton™ X-100). In order to quench endogenous peroxidase activity, samples were treated with a Hydrogen Peroxide Blocking Solution (abcam®, Cambridge, UK) at room temperature, and washed in washing buffer.

A polyclonal primary antibody anti-DA (abcam®, Cambridge, UK) was diluted (1: 1,000) in TBS 1× with 1% BSA, applied on slides, and incubated in the dark overnight. Sections were rinsed in washing buffer and then incubated in the dark for 1h with the HRP sharped IgG Goat anti-Rabbit secondary antibody (abcam®, Cambridge, UK) diluted (1:10,000) in TBS 1× with 1% BSA. Immunohistochemistry experimental conditions, as well as antibody optimization-dilutions are detailed in Table I.

Table I. Antibody (Ab) optimization and immunohistochemical experimental conditions.

Conditions	Concentrations		Antigen retrieval[a]	Peroxidase Quenching[b]
	Primary Ab Anti-DA	*Secondary Ab* HRP/nanogold conjugated		
	IHC			
Negative control	Without	1: 10,000	Yes	Yes
Treated	1:1,000	1: 10,000	Yes	Yes
	Immunogold			
Negative control	Without	1: 500	No	No
Treated	1:200	1: 500	No	No

[a]Antigen retrieval allows to break potential methylene bridges formed during formalin-fixation and expose antigenic sites to allow the antibodies epitope to bind.

[b]Endogenous peroxidase blocking is necessary to avoid non-specific staining.

Samples were then washed and revealed with diaminobenzidine (DAB+ Chromogen Substrate Kit, abcam®, Cambridge, UK) for 10 min in the dark. Finally, slides were rinsed in washing buffer, counterstained with hematoxylin, and mounted in Faramount Aqueous Medium (Dako®, Carpinteria, CA, USA). The complete version of the suggested immunohistochemical procedure is presented in Table II.

Table II. Full stepwise sequence of the immunohistochemical staining method.

Step	Reagent/Solution	Duration	Temperature
Tissue processing			
Fixation	Davidson solution	24 to 48 h	~ 4 °C
Preservation	Ethanol 70%	Weeks	~ 4 °C
Dehydration	Ethanol 80% to100%	8 × 1 h	~ 20 °C
Clarifying	Claral	2 × 1 h	~ 20 °C
Impregnation	Paraffin	Overnight	~ 60 °C
Staining			
Deparaffinization	Claral	2 × 3 min	~ 20 °C
Hydration	Ethanol 100%, 95% and 80%	5 × 3 min	~ 20 °C
Antigen retrieval	Universal HIER reagent 1×	3 min	~ 120 °C
Wash	Washing buffer[a]	3 × 5 min	~ 20 °C
Peroxidase quenching	Blocking peroxidase solution	2 h	~ 20 °C
Wash	Washing buffer	2 × 5 min	~ 20 °C
1st immune-staining	Primary Ab anti-DA	Overnight	~ 4 °C
Wash	Washing buffer	2 × 5 min	~ 20 °C
2nd immune-staining	Secondary Ab HRP conjugated	1 h	~ 37 °C
Wash	Washing buffer	2 × 5 min	~ 20 °C
Revelation	DAB+ substrate	10 min	~ 20 °C
Wash	Washing buffer	2 × 5 min	~ 20 °C
Counterstaining	Hematoxylin	1 min	~ 20 °C
Rinse	Tap water	A few dips	~ 20 °C

[a]TBS is recommended over PBS in washing buffer to get a cleaner background. 0.025% Triton X-100 in the TBS reduces surface tension, allowing reagents to cover the tissue section easily. Ab = antibody

Additionally, a series of slides from the same samples were stained with a multichromic procedure according to Costa & Costa (2012). This technique consists in a combination of Alcian Blue and Periodic Acid–Schiff's for the demonstration of acid mucopolysaccharides and neutral glycoconjugates, in blue and magenta tones, respectively, Hematoxylin blueing for nuclear materials, and Picric Acid to identify proteins in yellow hues.

A last set of sections for both DG and RT was stained with Hematoxylin–Eosin as reference (Kim *et al.,* 2006), and mounted in DPX resin. The slides were examined under a Zeiss Axio Observer Z1 light-microscope. The digestive stages of the diverticula in the DG were classified as holding, absorptive, digestion, advanced digestion, and undergoing breakdown or regeneration, according to Mathers (1976) and Beninger & Le Pennec (2016).

A six-level semi-quantitative scale from 0 (absent) to 2.5 (very high) was established to assess the intensity of the chromogenic anti-DA signal present in the mucus/globose cells of different tissues, the digestive gland, and the small inclusion bodies (IBs) in the digestive cells of the scallops (Table III).

Table III. Semi-quantitative scale categorizing the intensity of chromogenic anti-DA signal observed on the IHC slides.

Level intensity	Occurrence of the chromogenic anti-DA staining in the examined tissue area
0	Absence
0.5	Very low (<5 occurrence/presence in all fields at magnification 10×)
1	Low (>5 occurrence/presence in all fields at magnification 10×)
1.5	Moderate (presence in all fields at magnification 20×/ covering about one tenth of the tissue area)
2	High (presence in all fields at magnification 40×/ covering about one fifth of the tissue area)
2.5	Very high (presence in all fields at magnification 60×/ covering about one-third or above of the tissue area)

1.4. Transmission electron microscopy and Immunogold labeling

Transmission electron microscopy (TEM) studies were necessary in order to identify the small IBs with chromogenic anti-DA signal within the cells of the digestive gland. For this purposes, three small pieces of DG (~ 1 mm^3) were carefully dissected from some of the non-contaminated scallops collected in the Bay of Brest (n = 5), used as negative controls, and some of the contaminated-scallops from Camaret-sur-Mer (n = 5) with strongest IHC signal in the IBs within the digestive cells. Samples from scallops collected at Concarneau in 2019 were not considered for these analyses since the digestive glands were not processed for TEM purposes.

Samples were pre-fixed in glutaraldehyde 3 % (v/v) with 0.2 M cacodylate buffer (pH 7.4) supplemented with NaCl (21 mg mL^{-1}) for 3 h at 4 °C, rinsed in the same buffer (3 × 5 min), and subsequently post-fixed in 1% (w/v) osmium tetroxide in 0.2 M

cacodylate buffer (pH 7.4) for 1 h in an ice bath in the dark. Fixed specimens were rinsed in Milli-Q water (3 × 5 min) and dehydrated through successive baths of ethanol. Finally, samples were embedded into Spurr's resin (Science Services, Munich, Germany). After polymerization at 60 °C for 24h, semi-thin sections were cut to 800 nm thickness for quality control and then ultra-thin (ca. 70-80 nm) sections were cut for examination on a Leica EM UC6 ultramicrotome (Leica Microsystems, Germany) equipped with a 45º DiATOME diamond knife and floated on nickel grids (200 mesh).

Immunogold labeling was performed according to Skepper & Powell (2008) with minor modifications. Briefly, the grids were etched with drops of 4% sodium metaperiodate for 10 min to unmask antigenic sites on the surface of the section, rinsed three times on successive drops of MQ water, and placed on drops of 1% aqueous periodic acid for 10 min to remove eventual osmium tetroxide residue. Sections were then placed on a drop of blocking solution consisting of PBS 0.01 M, 0.01% Triton X-100, Glycine 20 mM, and 1% BSA for 10 min to reduce nonspecific binding of antibodies. The anti-DA antibody (abcam) was diluted 1:200 in blocking solution, and the sections were incubated with the primary antibody solution overnight at 4 °C in a moist chamber. After washing with blocking solution (6 × 5 min), the sections were incubated with the Goat anti-Rabbit IgG secondary antibody conjugated with 6-nm gold particles (abcam/ab41498) diluted 1:500 in blocking solution for 2 h at 28 °C, and consecutively rinsed in blocking solution and MQ water. Contrast reagents (e.g. uranyl acetate and lead citrate) were not applied to avoid masking the nanogold particles. Immunogold labeling experimental conditions, as well as antibody optimization-dilutions are shown in Table II. Finally, the samples were examined under a transmission electron microscope JEOL JEM 1400 operated at 120 kV on the imaging platform of Brest University. The autophagosomal structures identified in this work by means of MET

were classified according to their morphology and stage of development in marine bivalve cells (Owen, 1972; Yurchenko & Kalachev, 2019; Picot *et al.,* 2019).

1.5. Statistical analysis

To determine significant differences in toxin burdens in the digestive gland of scallops collected in the different sampling sites, *a priori* Fligner-Killeen's and Shapiro–Wilk test were used to evaluate the heterogeneity of variances and normality of frequencies of the data, respectively (Hector, 2015); the assumptions were not met. Values of DA concentrations were analyzed using a Kruskal-Wallis Test, where "the sampling site" was fixed as factor. In case of significant differences, a *post hoc* pairwise Wilcoxon rank test with Benjamini & Hochberg (BH) p-value adjustment was used to detect differences among means. For IHC results, Chi-square test (χ^2) were applied to assess statistically significant differences in the chromogenic anti-DA signal present in each tissue of the scallops. When needed, *a posteriori* Tukey HSD test were used to identify differences between means. All the statistical analyses were performed using command lines in the R language (R v. 4.0.2, R Core Team, 2017), and graphics were generated with the R package ggplot2 on the Rstudio programming interface. All values are expressed as mean ± standard error (SE). Differences were considered statistically significant at $\alpha = 0.05$ for all analyses (Hector, 2015).

2. RESULTS

2.1. Domoic acid (DA) quantification

Significant differences in the amount of DA accumulated in the digestive gland (DG) of the scallops from the three sampling sites were found after toxin quantification analysis by HPLC-UV (Fig. 1). Highest burdens (P <0.05) of toxin were recorded in animals from Concarneau (CN) (446.6 ± 101.3 mg DA kg^{-1}) followed by those from Camaret-sur-Mer (CM) (82.5 ± 4.9 mg DA kg^{-1}), while the significant lowest values were detected in the scallops from the Bay of Brest (BB) (1.6 ± 0.4 mg DA kg^{-1}).

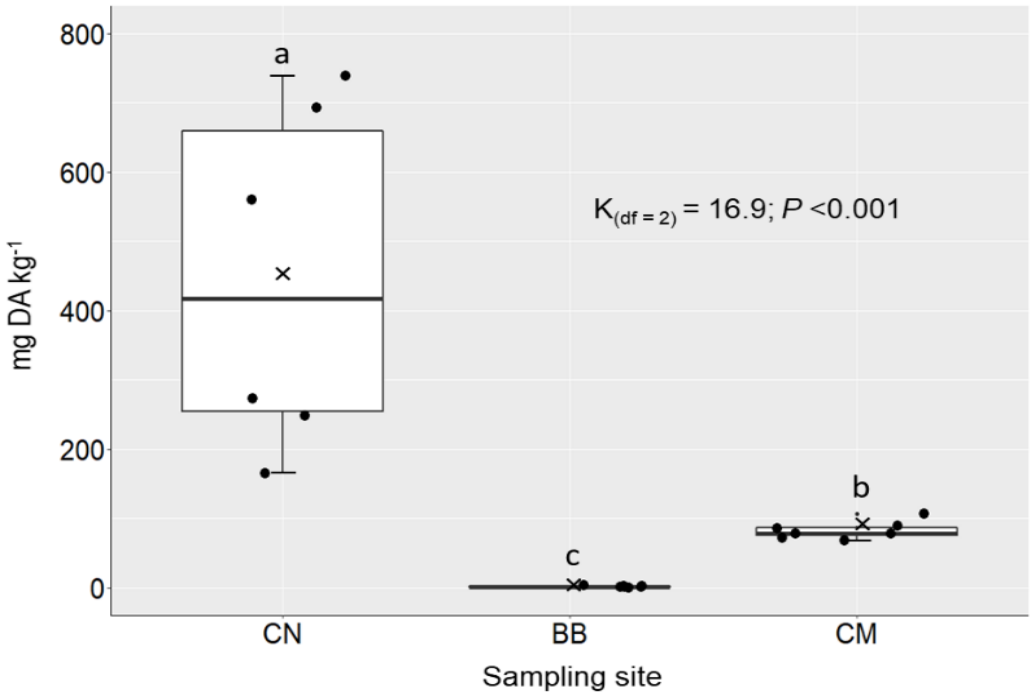

Figure 1. DA concentrations in the digestive gland of the scallops *P. maximus* naturally contaminated during outbreaks of the toxic *Pseudo-nitzschia* spp. and collected at three sites (CN = Concarneau [n = 6], BB = Bay of Brest [n = 7], and CM = Camaret-sur-mer [n = 7]) of the northwest coast of France between 2019 and 2021. The upper and lower limits of the boxes are the quartiles, the middle horizontal line is the median, the extremes of the vertical lines are the upper and lower limits of the observations, the dots are the individual observations, and the crosses are the means. Data were analyzed using the sampling sites (three levels) as independent variables in a Kruskal-Wallis Test. The K-test statistic and degrees of freedom (df) are reported. Different superscript letters denote statistically significant differences between groups of scallops. The level of statistical significance was set at α = 0.05.

2.2. Histology and immunohistochemistry (IHC)

The presence of DA was detected by IHC, as brown chromogenic signal, within the tissues of all contaminated scallops (Fig. 2, 3 and 4). The absence of non-specific background staining during IHC process was confirmed in control slides incubated with the secondary antibody but without the primary anti-DA antibody (Fig. 2 A-C, Fig. 3 C, D and Fig. 4 E-H). The DA brown chromogenic signal was observed mainly throughout the DG, and readily detected in highly contaminated scallops from CN and CM. The typical DA immuno-staining observed in the DG of scallops sampled at CN and CM is illustrated in Figures 2D-F. As shown in Fig. 2D, within the DG, the strongest immunoreactivity was observed in small (~1-2.5 µm) spherical inclusion bodies (IBs) distributed exclusively throughout the cytoplasm of the digestive (absorptive) cells of the digestive diverticula, which trapped an intense chromogenic staining (Fig. 2E, F). The anti-DA chromogenic signal detected in the DG of scallops from CN and CM has the same sub-cellular localization although DA burdens were significantly different between scallops from the two locations.

The multichromic staining allowed to clearly identifying these IBs within the cytoplasm of the digestive cells (Fig. 2G). As observed in Fig. 2H and 2I, the IBs had a dark violet-magenta dye, indicating the presence of neutral carbohydrates and neutral glycoconjugates on their surface. The IBs did not acquire any coloration with the conventional H&E staining (Fig. 2L). No histopathological patterns were observed in the DG of the scallops, even for the highest toxin burdens (Fig. 2J, K). The overall histological evidence allowed to observe that the IBs with DA-immunoreactivity were found mainly in the digestive cells of the diverticula in stages of active digestion (Fig. 2F, H, I, K, L).

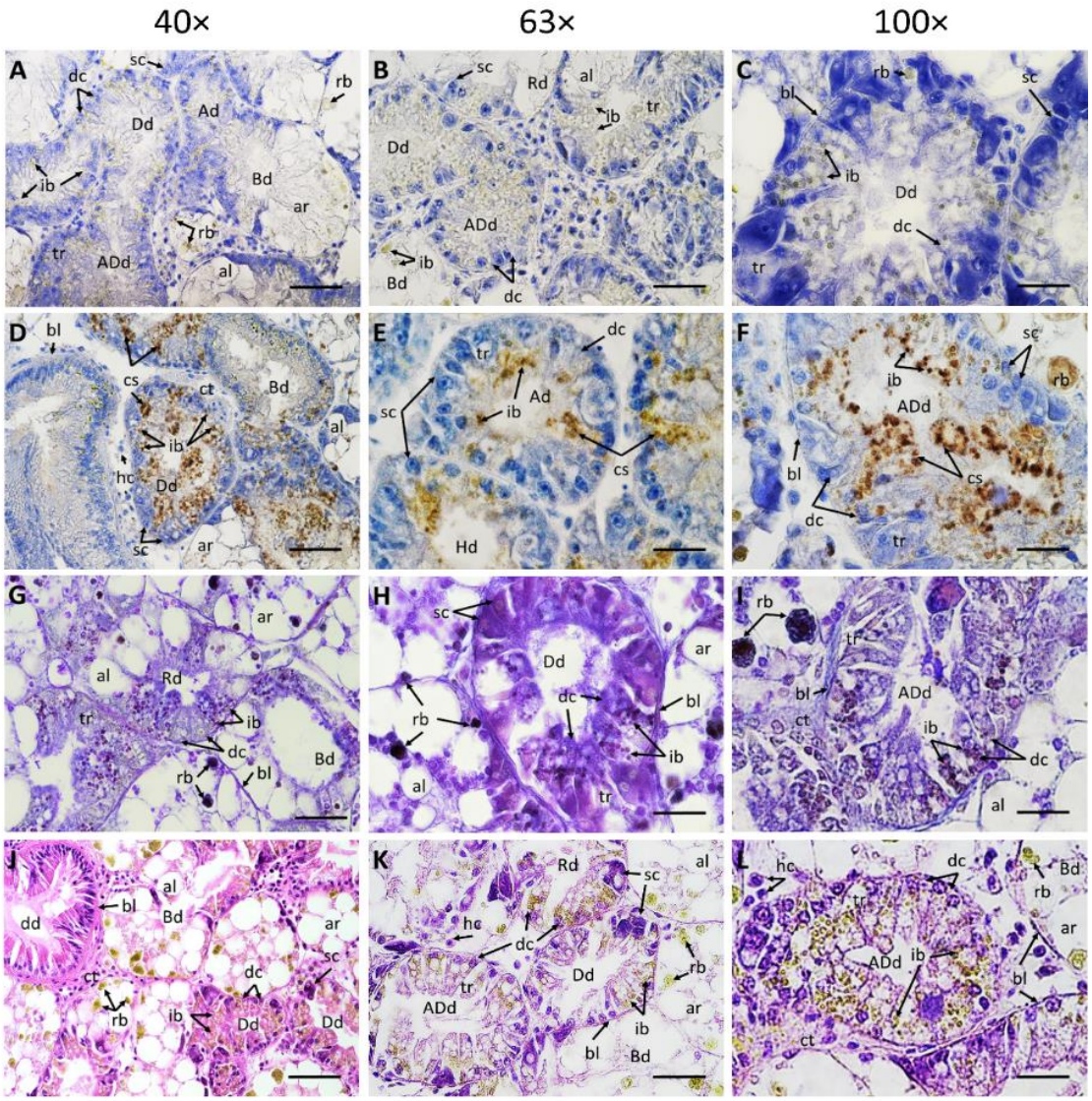

Figure 2. Microphotographs of digestive glands of scallops *P. maximus* naturally highly contaminated (~60 to 750 mg DA kg^{-1}) collected at Camaret-sur-mer (n = 7) and Concarneau (n = 6) in the northwest coast of France between 2019 and 2021during outbreaks of the toxic *Pseudo-nitzschia* spp. (A-C) negative controls of the IHC staining incubated with the secondary antibody but without the primary anti-DA antibody (1: 10,000 and 1: 0, respectively); (D-F) specific anti-DA immunohistochemical (IHC) staining incubated with the primary and secondary antibodies (1: 1,000 and 1: 10,000, respectively); (G-I) multichromic histochemical staining for the demonstration of neutral carbohydrates (violet-magenta dyes), acid glycoconjugates (blue hues), and proteins (yellowish tones); (J-L) conventional histological Hematoxylin-Eosin staining. Ad = digestive diverticulum in absorptive condition, ADd = digestive diverticulum in advanced digestive condition, al = adipocyte-like digestive cell, ar = acinar region, Bd = digestive diverticulum undergoing breakdown, bl = basal lamina, cs = positive anti-DA chromogenic signal, ct = connective tissue, dc = digestive cells, Dd = digestive diverticulum in digestive condition, dd = digestive duct, hc = hemocytes, Hd = digestive diverticulum in holding condition, ib = inclusion bodies, rb = residual bodies, Rd = diverticulum showing regeneration, sc = secretory cells, tr = tubular region. Scale bar: 40× = 50 µm, 63× = 30 µm, 100× = 10 µm.

In the samples from significantly weakly-contaminated scallops from BB, a slight-blurred and not well-located DA-chromogenic signal was observed in the “breakdown” and “regenerating” digestive diverticula of the DG (Fig. 3A-B). Nonetheless, it was possible to localize a few IBs with immunoreactivity in the cytoplasm of the remaining digestive cells (Fig. 3B). The H&E staining also allowed corroborating the absence of histopathologies in the DG due to DA accumulation (Fig. 3E, F).

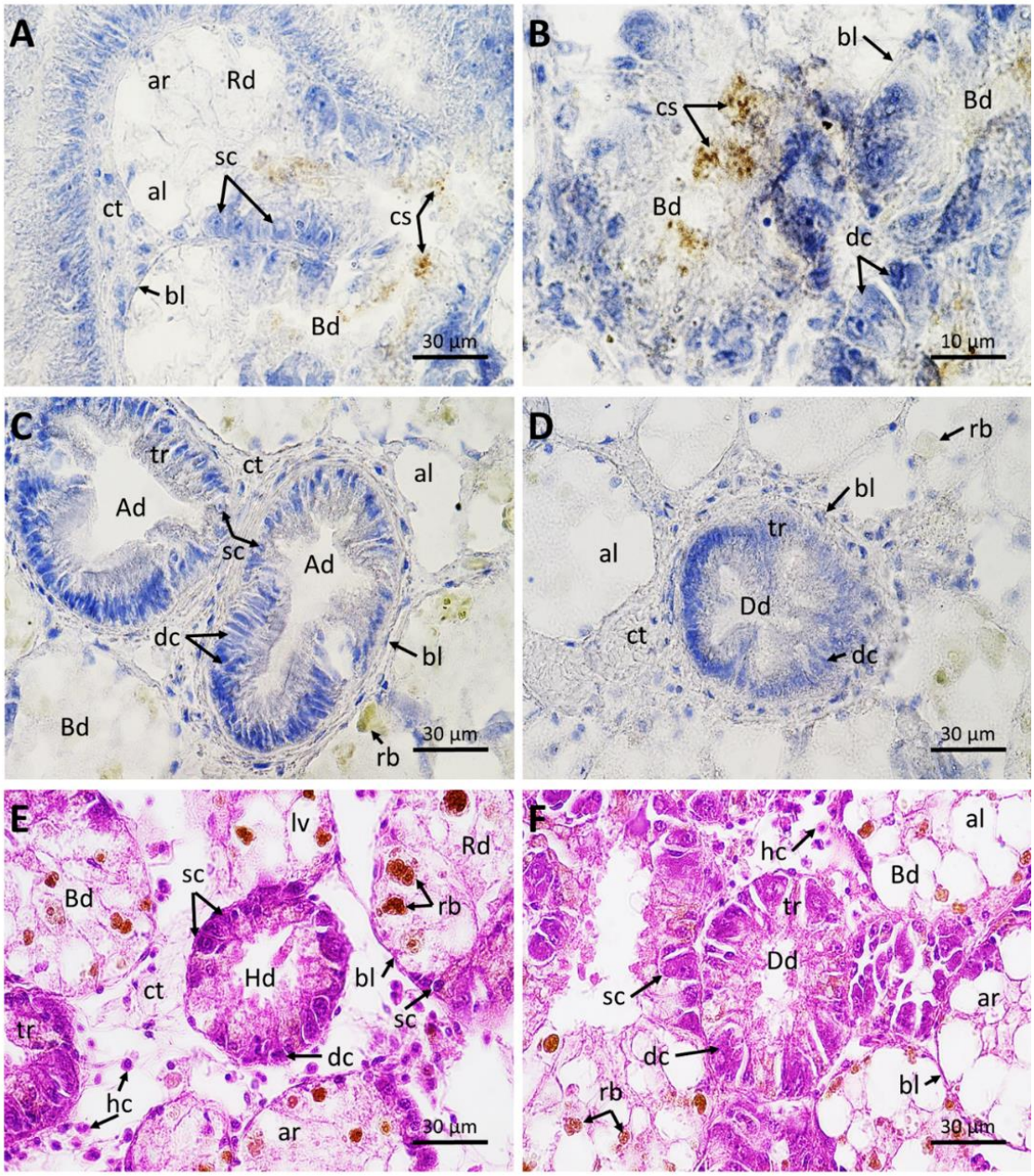

Figure 3. Microphotographs of digestive glands of scallops *P. maximus* naturally low contaminated with ~2 mg DA kg^{-1} collected at the Bay of Brest (n = 7) on the northwest coast of France in December 2020. (A-B) specific anti-DA immunohistochemical (IHC) staining incubated with the primary and secondary antibodies (1: 1,000 and 1: 10,000, respectively); (C-D) negative controls of the IHC staining incubated with the secondary antibody but without the primary anti-DA antibody (1: 10,000 and 1: 0, respectively); (E-F) conventional histological Hematoxylin-Eosin staining. Ad = digestive diverticulum in absorptive condition, al = adipocyte-like digestive cell, ar = ascinar region, Bd = digestive diverticulum undergoing breakdown, bl = basal lamina, cs = positive anti-DA chromogenic signal, ct = connective tissue, dc = digestive cells, Dd = digestive diverticulum in digestive condition, hc = hemocytes, Hd = digestive diverticulum in holding condition, rb = residual bodies, Rd = diverticulum showing regeneration, sc = secretory cells, tb = tubular region.

The DA-localization in the rest of the tissues was similar in all the scallops contaminated from ~2 up to ~750 mg DA kg^{-1} (Fig. 4). The DA-labeling was detected only in the mucus of the epithelia that lines the outer part of the stomach (Fig. 4A), in the globose cells embedded in the epithelium of the intestine (Fig. 4B), and in the globose cells of the spawning channels or gonadic ducts in the female (Fig. 4C) and male (Fig. 4D) gonads. No DA signal was found in any other tissues such as gills, mantle, labial palps, kidneys or adductor muscle. With the multichromic staining, it was possible to corroborate the presence of a light-blue coloration corresponding to acid glycoconjugates in the globose cells with immunolabeling (Fig. 4I-L). As seen in Fig. 4M-P, no histopathologies were observed in any of the additional tissues analyzed in this work.

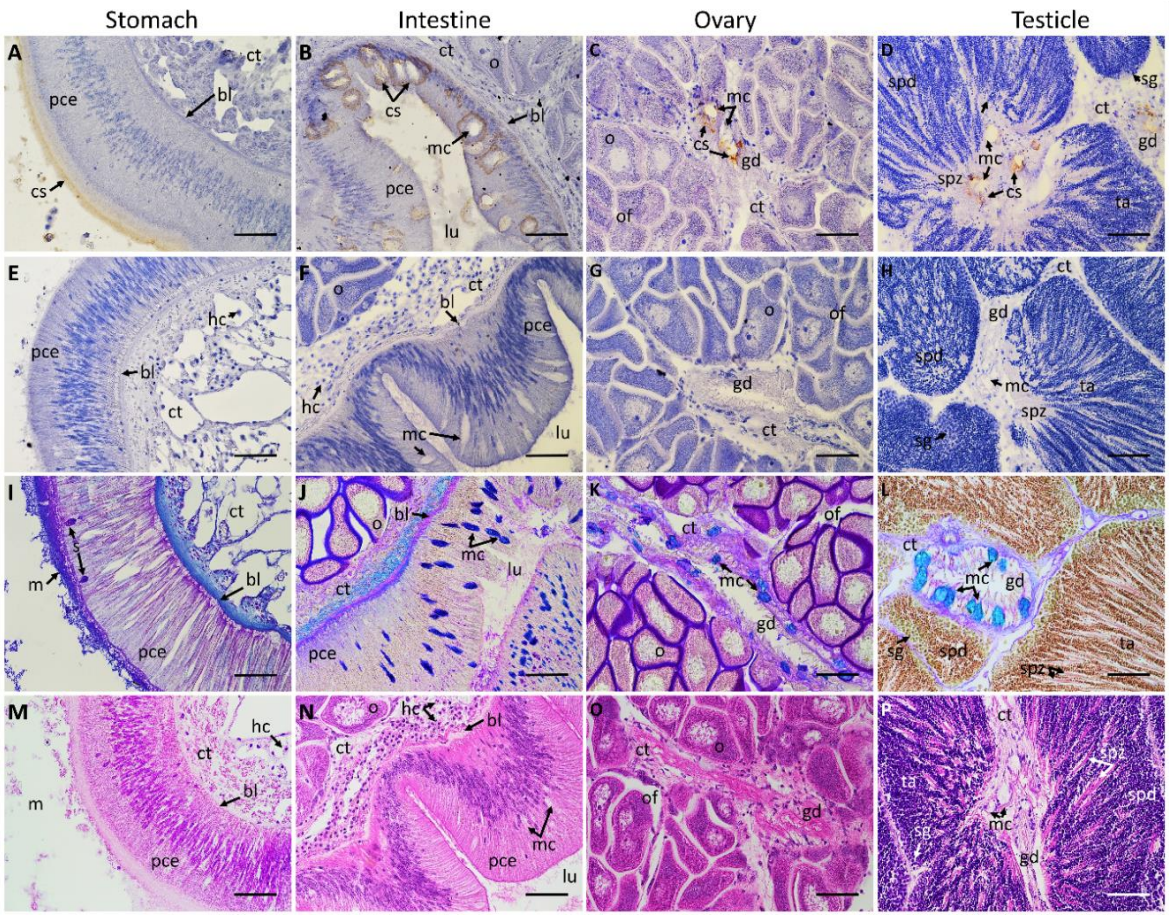

Figure 4. Microphotographs of the rest of the tissues of scallops *P. maximus* naturally contaminated between ~2 and 750 mg DA kg^{-1} collected at three sites (Concarneau [n = 6], Bay of Brest [n = 7], and Camaret-sur-mer [n = 7]) of the northwest coast of France between 2019 and 2021. (A-D) Specific anti-DA immunohistochemical (IHC) staining incubated with the primary and secondary antibodies (1: 1,000 and 1: 10,000, respectively); (E-H) negative controls of the IHC staining incubated with the secondary antibody but without the primary anti-DA antibody (1: 10,000 and 1: 0, respectively); (I-L) multichromic histochemical staining for the demonstration of neutral carbohydrates (violet-magenta dyes), acid glycoconjugates (blue hues), and proteins (yellowish tones); (M-P) conventional histological Hematoxylin-Eosin staining. bl = basal lamina, cs = positive anti-DA chromogenic signal, ct = connective tissue, gd = gonadic duct, hc = hemocytes, lu = lumen, m = mucus, mc = mucocyte, o = oocyte, of = ovarian follicle, pce = pseudostratified columnar epithelium, sg = spermatogonia, spd = spermatids, spz = spermatozoa, ta = testicular acinus. Scale bar: 40× = 50 µm.

As shown in Table IV, DA staining coverage in the DG was the same ($P > 0.05$) for scallops from CN and CM, while the anti-DA chromogenic signal detected in the DG of the scallops collected at BB was significantly lower. On the other hand, the chromogenic signal detected in the rest of the tissues (stomach, intestine, ovary, and testicle) was not different ($P > 0.05$) between the strongly (CN and CM) and weakly (BB) contaminated scallops.

Table IV. Comparison of IHC staining intensity of DA in the tissues of the scallops *P. maximus* naturally contaminated and collected at three sites (CN = Concarneau [n = 6], BB = Bay of Brest [n = 7], and CM = Camaret-sur-mer [n = 7]) of the northwest coast of France between 2019 and 2021. NA: not available (not enough data), "—": no chromogenic anti-DA staining.

Tissue	Sampling site			Statistical analysis	
	CN	BB	CM	χ^2, *n*	*P*
Digestive gland	2.4 ± 0.08[a]	0.57 ± 0.13[b]	2.4 ± 0.09[a]	20.4, 20	<0.05
Stomach	1.2 ± 0.11[a]	0.93 ± 0.14[a]	1.3 ± 0.1[a]	5.9, 20	>0.05
Intestine	1.3 ± 0.1[a]	1.07 ± 0.17[a]	1.3 ± 0.1[a]	4.3, 20	>0.05
Ovary	1.2 ± 0.1[a]	0.93 ± 0.13[a]	1.3 ± 0.1[a]	5.8, 20	>0.05
Testicle	1.1 ± 0.09[a]	1 ± 0.15[a]	1.4 ± 0.09[a]	4.2, 20	>0.05
Gills	—	—	—	NA	
Adductor muscle	—	—	—	NA	
Mantle	—	—	—	NA	
Labial palps	—	—	—	NA	

Data (mean ± SE) were analyzed according to the sampling sites (three levels) in a Chi-square test (χ^2). The χ^2 test statistic and sample size (*n*) are reported. Different superscript letters denote statistically significant differences at $p < 0.05$.

2.3. Immunoelectron microscopy

The IBs observed in the cytoplasm of the digestive cells in the diverticula of scallops with a dark-violet coloration by means of multichromic staining, and presenting a strong DA-immunostaining were analyzed by transmission electron microscopy (TEM) in order to decipher their cellular nature (Fig. 5). The diameter of these IBs ranged between 1-2.5 µm. Early single-membrane-bound IBs structures (Fig. 5A) were observed frequently in the apical and sub-apical regions of the digestive cells. Meanwhile late-developed structures with a double-membrane-bound and a halo (Fig. 5B) were observed mainly in the mid-basal region of the cytoplasm, and often clustered into groups of 3-6 vesicles that may be or not surrounded by a single-membrane (Fig. 5C) and fusing with the lysosomes of the cell (Fig 5D). The morphological observations by TEM described above allowed identifying these IBs as autophagic vesicles.

On a second hand, we coupled the use of the specific anti-DA antibody and a secondary antibody conjugated with gold nanoparticles to the TEM analyzes (immunogold labeling). As seen in Fig. 5A-D, no anti-DA signal was observed in any subcellular structure of the GD in the slide incubated without anti-DA primary antibody. By means of the immunogold labeling, DA-signal was found mostly in the undigested material attached to the inner side of the membranes within early (Fig. 5E-F) and late-autophagosomes (Fig. 5G-H), while a slight signal of gold-nanoparticles corresponding to the toxin was observed in the halo of autophagosomes and in the cytoplasm of the digestive cells (Fig. 5E-H).

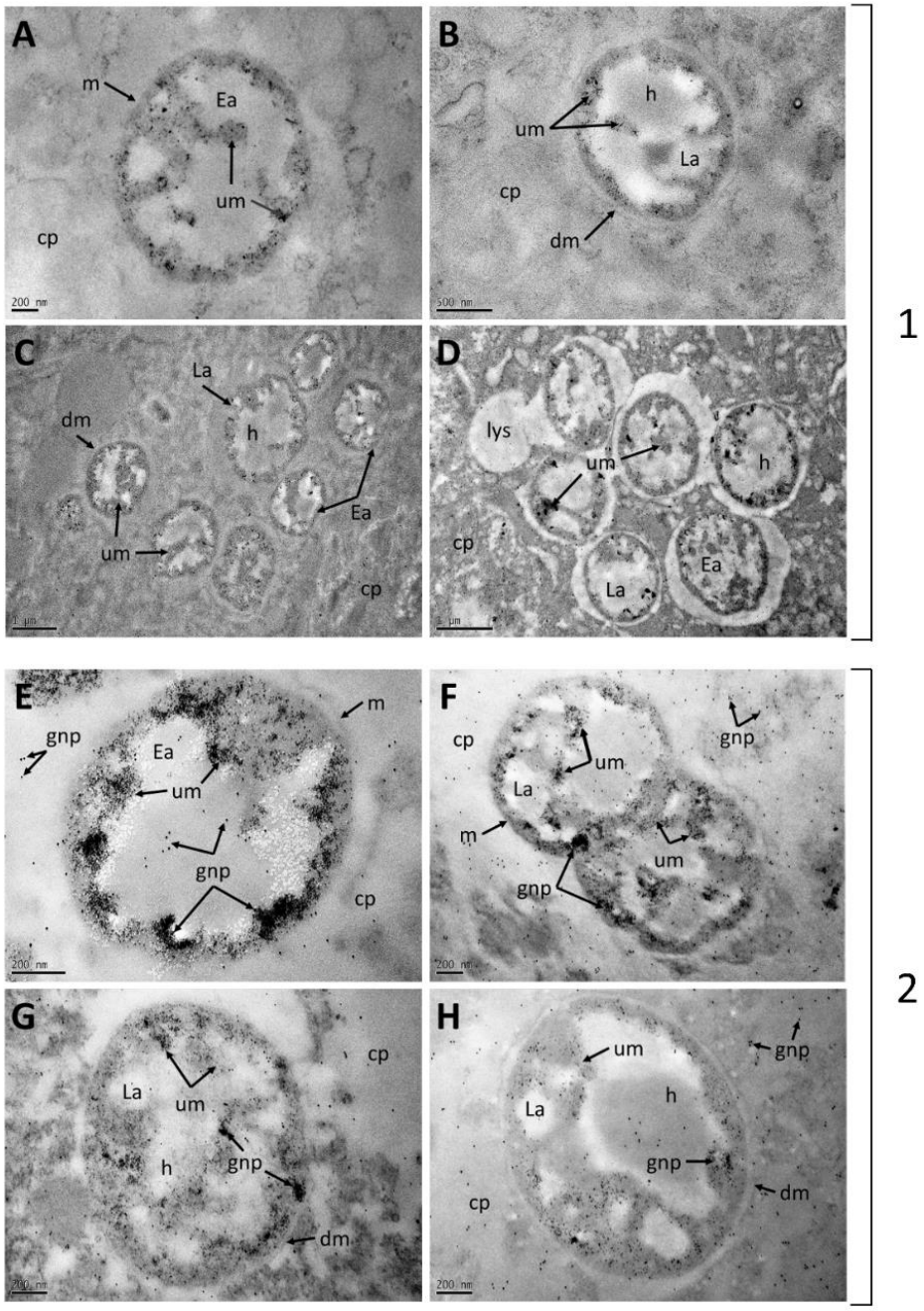

Figure 5. Electronmicrographs of ultrathin sections (70-80 nm) across the digestive glands of scallops *P. maximus* naturally contaminated (~75 mg DA kg^{-1}) during outbreaks of the toxic *Pseudo-nitzschia* spp. and collected in Camaret-sur-mer (n = 7) on the northwest coast of France in 2021. Detection of autophagic structures with positive DA immune-signal within digestive cells was possible by means of transmission electron microscopy (TEM). (1A-D) Negative controls of the immunogold labeling incubated with the secondary antibody but without the primary anti-DA antibody (1: 200 and 1: 0, respectively); (2E-H) Specific anti-DA immunogold labeling incubated with the primary anti-DA antibody and the secondary antibodies conjugated with 6-nm gold nanoparticles (1: 200 and 1: 500, respectively). cp = cytoplasm, dm = double-membrane-bound, Ea = early autophagosomes, gnp = gold nanoparticles, h = halo, La = late autophagosomes, lys = lysosomes, m = single-membrane-bound, um = undigested material.

3. DISCUSSION

In this work, for the first time, immunolabeling by IHC using photonic microscopy and immunogold using TEM has been successfully used for the localization of DA at the subcellular level in naturally contaminated marine mollusc tissues. The technique set up in the present paper has been shown to work for the immunostaining of DA with high precision, either in heavily contaminated (up to 750 mg DA kg^{-1} GD) or in weakly-contaminated scallops (~1 mg DA kg^{-1} DG) without nonspecific labeling. Although other methods, such as HPLC-UV/MS (Quilliam *et al.,* 1989) and ELISA (Litaker *et al.,* 2008), have been widely used to quantify DA content in contaminated shellfish with a high-resolution power (0.1 – 1 µg DA g^{-1}), they do not allow the subcellular visualization of DA in the tissues, as opposed to the immunolabeling methods developed in this study. Furthermore, this immunostaining method has proven to be suitable to be coupled with TEM, allowing to pinpoint DA localization.

Using a subcellular fractionation analysis on homogenized DA-contaminated digestive glands of *P. maximus* , Mauriz & Blanco (2010) found that almost 90% of the toxin accumulated in this organ was in soluble form in the cytoplasm of the cells, with a mostly homogeneous distribution within the DG (Blanco *et al.* 2020). One mechanism that could influence high accumulation and long retention of DA in this species could be its binding to high affinity receptors, as those found in the razor clam *S. patula* (Trainer & Bill, 2004). Moreover, Mauriz & Blanco (2010) concluded that the cause of the long DA-retention was not the binding of the toxin to some cellular component, but the lack of some efficient membrane transporters in the scallops. Our results cope with these findings, since most of the DA immune-signal was localized in the cytoplasm of the digestive cells of the digestive diverticula. Several digestive stages (holding, absorptive, digestion, advanced digestion, breakdown, and regeneration) have been

described for the digestive diverticula of *P. maximus* (Mathers, 1976). In this work, the inclusion bodies (IBs) with anti-DA signal were observed mostly in the digestive cells of the diverticula in states of active digestion (absorption, digestion and advanced digestion). This is probably due to digestive cells predominate in these digestion stages and are responsible for the intracellular enzymatic digestion of the material ingested by pinocytosis (Beninger & Le Pennec, 2016). Free domoic acid in the cytoplasm was visualized by immunogold. Nonetheless, the evidence of this work suggests that a significant proportion of the toxin is not simply "free-dissolved" in the cytoplasm, but is enclosed in small (1-2.5 µm) membrane-bound vesicles, identified as autophagosomal structures by means of TEM, distributed throughout the cytoplasm of digestive cells in digestive condition.

Autophagy is a well-developed, highly regulated, and complex-dynamic system related to ingestion, storage and catabolic processes of intracellular digestion (Balbi *et al.,* 2018; Wang *et al.,* 2019; Zhao *et al.,* 2021). In bivalves, autophagy plays a key role in maintaining cell homeostasis (Carella *et al.,* 2015). This mechanism has been used as an indicator of cell injury in response to different stressors (Moore, 2004; Picot *et al.,* 2019), such as environmental changes (Moore, 2008), and the innate-immune response to pathogens (Canesi *et al.,* 2002; Moreau *et al.,* 2015; Canesi *et al.,* 2016; Balbi *et al.,* 2018) However, nothing is still known on the role of autophagy in ingestion, mobilization and excretion of phycotoxins in these organisms.

During autophagy, cytoplasmic components, either of exogenous (e.g. contaminants, and pathogens), or endogenous (macromolecules and organelles) origin are sequestered into spherical-shaped vesicles with double membrane layers called autophagosomes. Subsequently, they are delivered to lysosomes for degradation, where the outer membrane of the autophagosome fuses with a lysosome to form an

autolysosome (Cuervo, 2004; Wang *et al.,* 2019). Finally, the hydrolases of the lysosome degrade the autophagosome-delivered contents and its inner membrane (Zhao *et al.,* 2021).

In samples of DA-contaminated scallops, mostly two types of membrane-bound autophagosomic vesicles were identified by transmission electron microscopy as part of this dynamic system. Early autophagosomes, which are usually involved in the ingestion and accumulation of exogenous materials, were present mainly in the apical region of the digestive cells; whereas in the mid- and basal regions of the cytoplasm we observed late-autophagosomes. These autophagosomes are involved in digestion and accumulation of undigested and indigestible residues, which may then be stored within the cell or eliminated (Owen, 1972; Zhao *et al.,* 2021). The transformation rate from early to late-autophagosomes is presumably dependent on the nature of the ingested material, and variations of this basic but highly-complex cycle probably depends on feeding rates, nature of the ingested food/substances, and the mode of release/excretion of the autophagosomic vesicles (Owen, 1972; Cuervo, 2004). The processing of autophagosomes by intracellular digestion could be a key to explain the long retention time of DA in the digestive cells of *P. maximus*. The toxin is probably normally ingested and accumulated in early autophagosomes, but cannot then be digested by the lysosomal machinery, thus remaining stored within autophagosomes as indigestible material in the cytoplasm of the cells. Moreover, it is difficult to know exactly how long it may take for the material present within autophagosomes to be excreted; since some experiments suggest that it can go from a few minutes to indefinite periods of time (Owen, 1972; Cuervo, 2004).

After DA injection in the adductor muscle, and subsequent transcriptomic analysis of the digestive gland of *P. maximus*, Ventoso *et al.* (2021) found as well as an

upregulation of genes related to autophagy and vesicle-mediated transport. Even though these results were not obtained under conditions of ingestion of the toxin through the filtration of toxic *Pseudo-nitzschia* cells, these findings could also indicate that the formation of autophagosomic structures could be part of explanation for DA long retention, blocking its digestion and excretion.

In order to corroborate whether autophagy is the subcellular mechanism involved in the long retention of DA in the DG of *P. maximus,* the next step would be to follow, by means of digital image analysis, the evolution of the anti-DA chromogenic signal in the tissues in parallel to the formation of autophagosomes with strong DA-immunoreactivity within the digestive cells during the contamination and decontamination processes.

There is evidence of the profound interspecific differences in the retention and depuration of DA in bivalves, even between pectinid species, like for example *P. maximus* and *A. purpuratus*. While the former is capable of accumulating up to 3,000 mg DA kg^{-1} and retain it for months or even years (Blanco *et al.,* 2006), *A. purpuratus* transfers almost all the DA accumulated in the digestive gland to other organs (mainly the intestine and the gonad) within a few days and then excrete the toxin into the environment (Álvarez *et al.,* 2020). Although the physiological mechanisms enabling *A. purpuratus* to quickly depurate the DA are unknown, Alvarez *et al.* (2020) hypothesized a two-compartment model, where the toxin acquired by the DG is quickly transported to other organs. In *P. maximus,* we could hypothesized that a significant part of DA accumulated stay in DG due to the absence of specific transporter as proposed by Mauriz and Blanco (2020), and that, secondly, its its detoxification be slower due to the formation of autophagosomes that retain the DA. Further analyses, comparing these species, using histological, immunohistochemistry, as well as

molecular biology techniques appear necessary to confirm this hypothesis and to determine whether autophagy appears in other slow-depurator shellfish species.

In the rest of the tissues of *P. maximus,* the IHC technique developed in this work revealed specific toxin-immunoreactivity and thus DA-localization within the mucus, particularly in the mucocytes of some epithelia such as the stomach and intestine, and in the mucocytes of the gonad spawning-ducts. Mucus is composed of water, glycoproteins and mineral salts (Davies & Hawkins, 1998), and is produced by almost all the epithelia of mollusks, playing an essential role in several functions such as lubrication, nutrition, the first barrier against environmental stress, and as an innate-immune barrier against pathogenic infections (Allam & Pales Espinosa, 2015). Hence, complementary studies are necessary to determine if DA has an affinity or is chemically-bounded to any of the components of mucus, and if the latter may be involved in DA-depuration or retention in the scallops. This hypothesis is totally new, since DA detection techniques in contaminated bivalve tissues had never allowed to localize the toxin at the level of mucus or mucus-producing cells during a contamination and decontamination scenario.

4. CONCLUSIONS

The DA-immunodetection methods proposed in this work by immunohistochemistry and immunogold are innovative ways to visualize the phycotoxin DA in the tissues of the king scallop *P. maximus*, and to decipher the subcellular mechanism involved in the retention of this toxin in a marine bivalve. The results of this work show that, most of the DA is found in the cytoplasm of digestive cells of *P. maximus*, as previously mentioned by Mauriz & Blanco (2010). Notwithstanding, most part of DA-signal does not appear free in the cytoplasm, but mainly within autophagic structures as revealed

by DA-immunostaining, suggesting that autophagic subcellular mechanisms could play a crucial role in the retention of the ASP toxin in the digestive cells of scallops. Furthermore, the role of mucus in the retention-depuration of DA in *P. maximus* must be investigated, since the toxin was only immunolocalized in the mucus of specific remaining tissues.

DA-immunodetection also provides a great tool to compare DA-localisation within species depurating at different speed over a contamination and decontamination period. The findings of this work constitute an important step forward in explaining the slow depuration of DA in *P. maximus*, and provide basic knowledge for the proposal of procedures to accelerate the depuration of the toxin in this species.

Acknowledgments

The authors are grateful to Aouregan Terre-Terrillon and Erwan Amice for the scallop sampling. We thank Nelly Le Goïc and Adeline Bidault (from IUEM-LEMAR, Brest) for their technical support. We also thank Amélie Derrien and Malwenn Lassudrie (Ifremer, Concarneau) for their valuable help with HPLC technique, as well as Philippe Elies (PIMM platform, UBO, Brest) for his assistance with transmission electron microscopy.

Conflict of interest

All authors approved the final version of this manuscript and declare no conflict of interest.

Funding

This work received financial support from the research project “MaSCoET” (Maintien du Stock de Coquillages en lien avec la problématique des Efflorescences Toxiques) financed by France Filière Pêche and Brest Métropole, and the project “CoDDA” (Contamination and Decontamination of Domoic Acid in marine bivalves) funded by

ISblue under the academic responsibility of JLGC, CF and HH. JLGC is recipient of a doctorate fellowship from CONACyT, Mexico (REF: 2019-000025-01EXTF-00067).

Data availability statement

The evidence and data that support the findings of this study are available from the corresponding author upon reasonable request.

Ethics statements

The adult scallops (*Pecten maximus*) were transported and handled according to the International Standards for the Care and Use of Laboratory Animals. The number of sampled organisms contemplated "the rule of maximizing information published and minimizing unnecessary studies". In this sense, 20 scallops were considered as the minimum number of organisms needed for this work.

TO RETAIN

- For the first time, DA was *in situ* detected in the tissues of the king scallop *P. maximus,*
- IHC appeared very sensitive allowing visualizing DA into the scallop tissues.
- DA is visualized mainly within autophagosomes from the digestive gland cells.
- Trapping of DA within autophagososomes may be a key mechanism of its long retention in the scallops.
- This work constitutes an important step forward in explaining the slow depuration of DA in *P. maximus,*

CHAPTER 3

COMPARISON OF THE SUBCELLULAR LOCALIZATION OF DOMOIC ACID AMONG MARINE INVERTEBRATE SPECIES

PREAMBLE

The immunohistochemistry technique using anti-domoic acid antibodies appeared effective in localizing domoic acid in scallop tissues (chapter 2; García-Corona *et al.,* 2022).

As our aim was to identify the physiological mechanisms that might explain the difference in domoic acid accumulation and depuration rates between scallops and rapid depurators such as other bivalves species. It seemed important to extend our IHC analysis to other bivalve species contaminated by domoic acid. To be able to compare results between species, it was essential to sample animals that had been subjected to the same exposure conditions. We took advantage of the occurrence of a toxic *Pseudo-nitzschia* bloom in Brittany in 2021, detected by the REPHY network, to sample several marine invertebrate species on the same site or in nearby areas.

This enabled us to compare the amount of domoic acid present in the digestive glands of different species subjected to the same *Pseudo-nitzschia* bloom, and to compare the subcellular distribution of DA by immunohistochemistry.

The results are presented in this chapter 3.

Comparative study of domoic acid accumulation, isomer content and associated digestive subcellular processes in five marine invertebrate species

José Luis García-Corona[1], Caroline Fabioux[1], Malwenn Lassudrie-Duchesne[2], Amélie Derrien[2], Aouregan Terre-Terrillon[2], Tomé Delaire[1], Hélène Hegaret[1]*

[1]Institut Universitaire Européen de la Mer, Laboratoire des Sciences de l'Environnement Marin (UMR6539 CNRS/UBO/IFREMER/IRD) Technopôle Brest-Iroise 29280, Plouzané, France.

[2]Ifremer, LITTORAL LER BO, Station de Biologie Marine, Place de la Croix, BP40537, 29900 Concarneau Cedex, France.

*Corresponding author: Hélène Hegaret

Institut Universitaire Européen de la Mer, Laboratoire des Sciences de l'Environnement Marin (UMR6539 CNRS/UBO/IFREMER/IRD) Technopôle Brest-Iroise 29280, Plouzané, France.

e-mail: helene.hegaret@univ-brest.fr

ABSTRACT

Despite the deleterious effects of the phycotoxin domoic acid on human health, and the permanent threat of blooms of the toxic *Pseudo-nitzschia sp*. over commercially important fishery-resources, knowledge regarding the physiological mechanisms behind the profound differences in accumulation and depuration of this toxin in contaminated invertebrates remain very scarce. In this work, a comparative analysis of accumulation, biotransformation, and subcellular localization of DA in different shellfish species was performed. Samples of scallops *Pecten maximus* and *Aequipecten opercularis*, clams *Donax trunculus*, slippersnails *Crepidula fornicata*, and seasquirts *Asterocarpa sp*. were collected after blooms of the toxic *P. australis.* Differences (P <0.05) in DA accumulation were found, wherein *P. maximus* showed up to 20-fold more DA in the digestive gland than the rest of the species. Similar profiles of DA isomers were found between *P. maximus* and *A. opercularis*, whereas *C. fornicata* was the species with the highest biotransformation rate (~10%) and *D. trunculus* the lowest (~4%). The immunohistochemical analysis revealed differences (P <0.05) in DA localization between species. In *P. maximus* the anti-DA chromogenic signal was detected mainly within autophagosomic-vesicles in the cytoplasm of digestive cells, while in *A. opercularis* and *C. fornicata* significant DA immunoreactivity was found in post-autophagy residual bodies. A slight DA staining was found free within the cytoplasm of the digestive cells of *D. trunculus* and *Asterocarpa sp*. The PCA analysis allowed distinguishing the species based on their capacities to accumulate, biotransform, and distribute the toxin within their tissues. These findings contribute to improve the understanding of the fate of DA between shellfish species, and the further

Keywords: domoic acid, shellfish, biotransformation, autophagy, interspecific differences.

1. INTRODUCTION

Domoic acid (DA) is an extremely dangerous phycotoxin responsible of the illness referred as amnesic shellfish poisoning (ASP) syndrome in humans (Perl *et al.,* 1990, Pulido, 2008; La Barre *et al.,* 2014). This highly potent neuroexitatory amino acid is naturally produced by some diatoms of the genus *Pseudo-nitzschia* (Bates *et al.,* 1998, 2018), wherein the species *Pseudo-nitzschia australis* seems to be one of the most toxigenic (Lelong *et al.,* 2012; La Barre *et al.,* 2014). The recurrent presence of toxic blooms of *Pseudo-nitzschia sp.,* and the subsequent production of DA, frequently affect shellfish resources on the North Atlantic coasts of France. Indeed, suspension-feeding invertebrates are capable of ingesting toxic *Pseudo-nitzschia* cells leading to high amounts of DA accumulated in their tissues (Basti *et al.,* 2018; Dusek Jennings *et al.,* 2020). Contaminated shellfish are key potential vectors of DA, strongly modifying the structure of marine ecosystems (Lefebvre *et al.,* 2002; Bejarano *et al.,* 2008; Trainer *et al.,* 2012), and seriously threatening human health through contaminated seafood consumption (Pulido, 2008; La Barre *et al.,* 2014). Over the last two decades, these blooms have caused numerous and persistent harvest closures for some economically important contaminated species (Amzil *et al.,* 2001; Husson *et al.,* 2016).

Notwithstanding, profound inter and intra-specific variability in the toxicokinetics of accumulation and depuration rates of DA burdens have been reported between several shellfish species in the same affected area (Bogan *et al.,* 2007a,b,c; Dusek Jennings *et al.,* 2020; Blanco *et al.,* 2021; Kvrgić *et al.,* 2022). Thus, invertebrates have been broadly classified as “fast” or “slow” DA-depurators (Blanco *et al.,* 2002a,b; Basti *et al.,* 2018). Larger scallops, such as King scallops *Pecten maximus* (Blanco *et al.,* 2002a; García-Corona *et al.,* 2022) and giant scallops *Placopecten magellanicus* (Gilgan, 1990; Haya *et al.,* 1991), and some big-clams, such as razor clams *Siliqua patula*

(Horner *et al.,* 1993; Dusek Jennings *et al.,* 2020) are capable of accumulating the highest registered amounts of DA in the digestive gland, and require from many months to a couple of years to depurate the toxin from their tissues. Therefore, these species have been considered as slow DA-depurators. Moreover, during ASP outbreaks, the king scallop *P. maximus*, is usually amongst the most contaminated species (James *et al.,* 2005; Blanco *et al.,* 2002a, 2021). Levels of DA exceeding up to 5-fold the european regulatory limit of 20 mg kg^{-1} are not unusual in this species (Blanco *et al.,*2006; Bogan *et al.,* 2007a,b; García-Corona *et al.,* 2022). Conversely, mussels (Novaczek *et al.,* 1992; Blanco *et al.,* 2002b; Mafra *et al.,* 2010), and even smaller scallops, such as *Argopecten purpuratus* (Álvarez *et al.,* 2020) are known as fast DA-depurators since they can depurate up to 90 % of total DA burdens over hours to days. These species-specific differences in DA accumulation-depuration represent a real issue for fishery economy and management after ASP-blooms. Thus, understanding the physiological mechanisms behind this phenomenon is of high interest.

It has been hypothesized that the high DA accumulation and its slow depuration in species like *P. maximus* could be due to the absence of efficient membrane transporters to excrete the toxin (Mauriz and Blanco, 2010). In other species such as *S. patula*, the presence of some high and low-affinity glutamate receptor has been identified, suggesting that the differential activation of these receptors in precise tissues could explain that razor clams retain DA for long periods of time without significant toxigenic effects (Trainer and Bill, 2004). Nevertheless, none of these hypotheses have been fully confirmed yet. Mauriz and Blanco (2010) found that nearly 90% of total DA accumulated in *P. maximus* was free in a soluble form in the cytoplasm of the digestive cells. Likewise, the immunohistochemical subcellular localization of DA in *P. maximus* (García-Corona *et al.* 2022) corroborated that most of the signal

corresponding to the toxin was present in the cytoplasm of digestive cells, but trapped into small-spherical autophagosomic-vesicles. These results suggested that autophagy could be one of the potential physiological mechanisms behind the long retention of DA in this species. Nevertheless, to date, the immunohistochemical (IHC) localization of DA has not been applied to any other invertebrate species contaminated with DA, which greatly hinders the comparison of the subcellular mechanisms involved in the accumulation and long retention of this toxin between affected species. Autophagy is a highly regulated and dynamic "self-eating" catabolic system related to the intracellular ingestion and digestion (Cuervo, 2004; Wang *et al.,* 2019; Zhao *et al.,* 2021). Through autophagy the lysosomes receive phagosomic vesicles (phagosomes) containing cytoplasmic cellular components, such as macromolecules, damaged or misfolded proteins, and entire organelles, as well as extracellular-derived molecular cargo from endocytosis and phagocytosis for degradation, digestion, recycling, or excretion (McMillan, 2018; Wang *et al.,* 2019). Once the intracellular digestion of worn-out cellular organelles and compounds taken into the cell has finished, the autophagic-vesicles can fuse with the plasmatic membrane of the cell to secrete their content by exocytosis (Cuervo, 2004; Zhao *et al.,* 2021). These distinctive capabilities establish an essential role of autophagy in maintaining metabolic homeostasis and cellular health in bivalves (Balbi *et al.,* 2018; Picot *et al.,* 2019; Rodríguez-Jaramillo *et al.,* 2022).

Not only untransformed DA, but also some structural isomers of the toxin (*i.e.* isoA, isoD, isoE, and epi-DA) are frequently detected in seafood during ASP-monitoring. The concentrations of DA-isomers commonly ranges from 0.5 to ~20% of total DA burdens (Wright *et al.,* 1990a; Costa *et al.,* 2005; Takata *et al.,* 2009; Zheng *et al.,* 2022). Despite some studies pointing out some degree of species-specific biotransformation

of DA (Wright *et al.,* 1990b; Vale and Sampayo, 2001; Costa *et al.,* 2005; Blanco *et al.,* 2010), no work has ever compared the biotransformation profiles of DA against the subcellular localization of this toxin in contaminated shellfish. This information could be useful to elucidate differences in DA uptake and allocation, as well as the potential implication of subcellular mechanisms on depuration of this toxin between species.

The hypotheses on DA accumulation, biotransformation, depuration and subcellular localization among contaminated invertebrates described above raise the question: How do shellfish species differ in their ability to accumulate, process, and allocate DA in their tissues? This study compared biotransformation and subcellular localization of DA in five shellfish species simultaneously exposed to natural toxigenic *P. australis* blooms.

2. MATERIALS AND METHODS

2.1. Sample collection and *Pseudo-nitzschia australis* environmental data

A total of 38 shellfish samples were collected in 2021 in the northwest coast of Brittany, France. The samples consisted in clams *Donax trunculus* (n =11) collected on the 30th of March in the Bay of Douarnenez, and scallops *P. maximus* (n =5), *A. opercularis* (n =10), slippersnail *Crepidula fornicata* (n =7), and sea squirt *Asterocarpa sp.* (n =5) collected on the 8th of April in Camaret-sur-Mer (Fig. 1). The animals were collected eight days after blooms of similar intensity of the DA-producing *P. australis* according to the REPHY monitoring network in both sampling sites (2.6×10^5 cell.L^{-1} on March 23, 2021, and 1.1×10^5 cell.L^{-1} on March 30, 2021, respectively, REseau de surveillance du PHYtoplancton et des phycotoxines, https://envlit-alerte.ifremer.fr/) (Fig 1). Once at the laboratory, the meat was excised from the shells of the organisms. The digestive gland (DG) of the scallops (*P. maximus* and *A. opercularis*) was carefully dissected

from the rest of the tissues, and subsequently sectioned in two halves. For the rest of the species with diffuse visceral mass (*C. fornicata, D. trunculus*, and *Asterocarpa sp.*) the soft body (*i.e.* total flesh) was divided into two equal portions at the mid visceral level, including a section of the DG on each. For each individual, one of these DG/visceral sections was fixed in Davidson's solution (Kim *et al.,* 2006) for histology, and the second DG/visceral sections section was stored at -20 °C for toxin analysis.

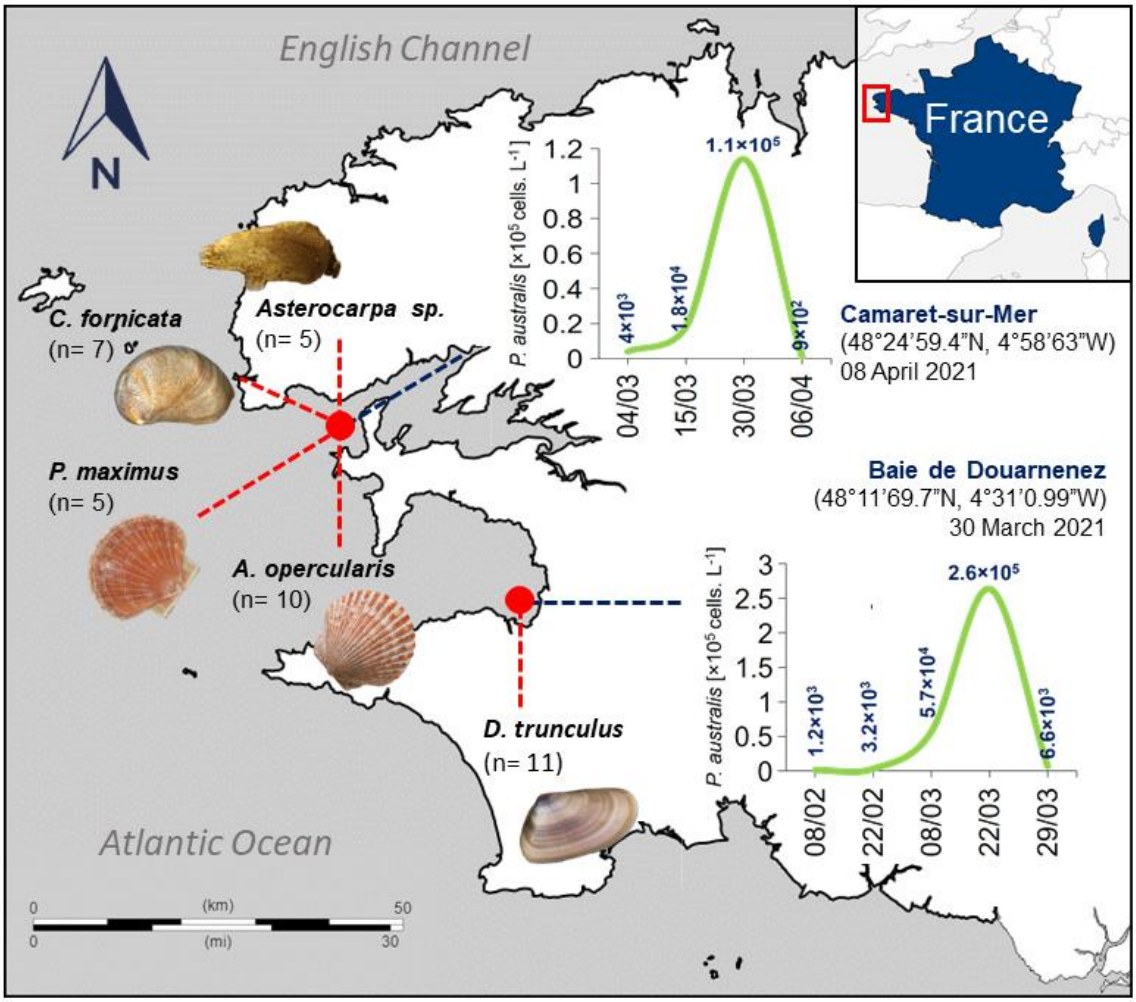

Figure 1. Sampling sites of the scallops *P. maximus* (n =5) and *A. opercularis* (n = 10), the clam *D. trunculus* (n =11), the slippersnail *C. fornicata* (n =7), and the sea squirt *Asterocarpa sp.* (n =5) and cell densities (cells. L^{-1}) of *P. australis* during toxic blooms in the northwest coast of Brittany, France between February and-April 2021.

2.2. Toxin quantification and DA-isomer analysis by liquid chromatography-tandem mass spectrometry (LC-MS/MS)

Since the DG accumulates most of DA (Mauriz and Blanco, 2010), only this tissue was considered for toxin analysis in this work. For the non-pectinid species, the DG was separated from the rest of the visceral mass once the tissues were frozen. DA was extracted from the DG following the procedure described by Quilliam *et al.,* (1989). Samples were homogenized from 200 ± 10 mg of frozen DG in 1 mL of 50% MeOH/H_2O using a Fastprep-24 5G system (MP Biomedicals, Sta. Ana, CA, USA). The extract was clarified by centrifugation at 19,000 × g at 4 °C for 10 min and the supernatant was isolated, filtered through a 0.2 µm nylon centrifugal filter (VWR International, Radnor, PA, USA), and stored at -20 °C until analysis.

The quantification of total DA (tDA) and its isomers in the DG was carried out by LC-MS/MS according to Ayache *et al.* (2019) with modifications, using a Shimadzu UFLCxr system coupled to a quadruple hybrid mass spectrometer API400Q-Trap (Sciex, Concord, ON, Canada) equipped with a heated electrospray ionization (ESI) source. Chromatographic separation was carried out on a reversed-phase column Phenomenex Luna Omega C18 (150 × 2.1 mm, 3 µm, Phenomenex, Torrance, CA, USA). The separation was carried out using a mobile phase consisting of aqueous eluent A (100% H_2O + 0.1% H-COOH) and organic eluent B (95% CH_3CN/ 5% H_2O + 0.1% H-COOH). The run started following a gradient from A to B as follows: 5% at min 0, 18.6% at 17 min, 95% at 17.5 min, 95% at 19.5 min, 5% at 20 min, and 5% at 25 min. The flow rate was 200 µL.min^{-1} and the injection volume was 5 µL. The column temperature was maintained at 30 °C.

The ESI interface was operated with a curtain gas of 20 psi, temperature of 550 °C, gas1 55 psi, gas2 60psi, and an ion spray voltage of 5500 V. The detection of DA was achieved by multiple reaction monitoring (MRM) in positive ion mode. The transition 312.1 > 266.1 (collision energy = 22 V) was used for quantification and 312.1 > 161.1 (collision energy = 33 V) for confirmation. The quantification was performed relative to the DA standard (National Research Council Canada, NRCC) with a 6-point calibration curve. The Limit of Quantification (LOQ) (S/N = 10) and the Limit of Detection (LOD) (S/N = 3) of the method were 0.25 and 0.08 ng.mL^{-1}, respectively.

2.3. Immunodetection of DA and quantitative histology

Tissue samples fixed in Davidson's solution were dehydrated in ethanol series of progressive concentrations (70%, 80%, 95%, and 100%), cleared in xylene, and embedded in paraffin (Paraplast Plus, Leica Bio-systems, Richmond, IL, USA). Paraffin blocks were cut in 4-µm-thick sections using a rotary microtome (Leica RM 2155, Leica Microsystems) and sections mounted on polylysine-coated glass slides (Sigma-Aldrich, St. Louis, MO, USA). A series of three consecutive sections was performed for each sample, which were used for (i) immunohistochemical detection of DA, (ii) multichromic staining, and (iii) hematoxyline/eosin staining, as described below. Sections were deparaffinized in xylene and rehydrated in ethanol series of regressive concentrations before staining.

In order to detect the presence of DA at the subcellular level in the tissue sections, an immunohistochemical anti-DA labeling technique was applied according the procedure described in García-Corona *et al.* (2022) on the first slide from each sample. Briefly, tissue sections were incubated overnight with a Goat polyclonal anti-DA primary antibody (0.01 mg.mL^{-1}, Eurofins Abraxis®, Warminster, PA, USA) at 4°C, and the next

day the slides were incubated at 37 °C for 2h with an HRP sharped IgG Rabbit anti-Goat secondary antibody (0.001 mg.mL^{-1}, abcam®, Cambridge, UK). Then, samples were washed and revealed with diaminobenzidine (DAB+ Chromogen Substrate Kit, abcam®, Cambridge, UK) for 1 h in darkness at room temperature and counterstained with Harry's hematoxylin.

The second slide from each sample was stained with a multichromic procedure (Costa and Costa, 2012). This technique consists of a combination of Alcian Blue and Periodic Acid–Schiff's for the demonstration of acid mucopolysaccharides and neutral glycoconjugates, in blue and magenta tones, respectively, Hematoxylin blueing for nuclear materials, and Picric Acid to identify proteins in yellow hues.

The last set of tissue sections was stained with Hematoxylin–Eosin as reference (Kim *et al.,* 2006). The slides were examined under a Zeiss Axio Observer Z1 light microscope.

For quantitative histological analysis, five randomly selected regions (63×; ~1.3 mm^2) from each DG section stained with the anti-DA immunohistochemical technique, multichromic, and hematoxylin-eosin staining were digitized at high resolution (600 dpi). A total of 570 images were used to obtain the following data: (a) DA chromogenic signal (DAcs) corresponds to the coverage area, in pixels, occupied by the positive anti-DA staining. It was was automatically calculated using a digital image analysis system (Image Pro Plus software v. 4.5, Media Cybernetics, Silver Spring, MD, USA) (Gómez-Robles *et al.,* 2005). The area reported as the DA chromogenic signal was calculated as DAcs = (DA chromogenic signal area/ total area occupied by the DG) × 100. Since almost all the DA chromogenic signal detected in DG is trapped in autophagosomal vesicles present in the cytoplasm of digestive cells (García-Corona

et al., 2022), the (b) Total autophagy (Ta) and total DA autophagy (DAa) were calculated by counting the total number of autophagosomic vesicles, and the number of autophagosomic vesicles with DA chromogenic signal, respectively, on each digitized image. A fraction of the anti-DA chromogenic signal is also observed in post-autophagic residual bodies within the digestive cells (García-Corona *et al.,* 2022), thus the frequencies of (c) Total residual bodies (Trb) and DA residual bodies (DArb) were assessed as the total number of residual bodies and the total number of residual bodies with DA chromogenic signal, respectively, on each digitized image. Finally, (d) Cell vacuolization (Vac), measured as an indicator of potential histopathologies related to DA accumulation in the DG, represents the total number of vacuoles within the digestive cells of each invertebrate species on each digitized image.

2.4. Statistical analysis

All statistical analyses were performed using command lines in the R computing environment (R v. 4.2.2, R Core Team, 2022). A priori Lilliefors (Kolmogorov-Smirnov) and Bartlett tests were applied to confirm the normality of frequencies and homogeneity of variances of the residuals of the data, respectively (Hector, 2015). All data were transformed (log, $1/\chi$, or $\sqrt{\chi}$) prior to analysis to meet a priori, assumptions. The percentage-expressed values were also arcsine (arcsine $\sqrt{P}$) transformed (Zar, 2010), but all data are reported untransformed as the means ± standard errors (SE). Separate one-way analyses of variance (ANOVA, type II Sum of Squares) were applied to assess statistically significant differences of toxin accumulation in the DG, proportion of DA isomers, and quantitative histological features between species. As neededpost hoc comparisons of means with Tukey's honest significance test (HSD) were performed to identify differences between means (Hector, 2015; Zar, 2010). Principal component analysis (PCA) was performed using the FactoMineR package with the

factoextra package for data visualization into smaller factorial clusters within a 95% confidence interval. All data matrices were auto-scaled before PCA analysis. The corrplot package was run to calculate the correlation coefficients and their significance between variables within their given PCs. All graphics were generated using the package ggplot2. The level of statistical significance was set at $\alpha = 0.05$ for all analyses (Zar, 2010).

3. RESULTS

3.1. Toxin accumulation and biotransformation

Significant differences in the amounts of total DA (tDA) accumulated in the digestive glands (DG) were found between the different shellfish species sampled after blooms of the toxic *P. australis* (Fig. 2). The significantly higher burdens of tDA were observed in the scallop *P. maximus* , with 638.6 ± 35.5 mg.kg^{-1}, followed by those of the snail *C. fornicata*, with 48.5 ± 13.1 mg.kg^{-1}, the scallop *A. opercularis* (22.7 ± 2.6 mg kg^{-1}), and the clam *D. trunculus* (12 ± 1.7 mg kg^{-1}). Whereas the lowest values (P <0.05) of tDA were found in the ascidian *Asterocarpa sp.* (4.2 ± 1.2 mg kg^{-1}). Moreover, as shown in Fig. 2, an important intraspecific variability in tDA accumulation was also reported in *P. maximus* and *C. fornicata*, with values that ranged from 530 to 731 mg kg^{-1}, and 0.2 to 93.8 mg kg^{-1}, respectively.

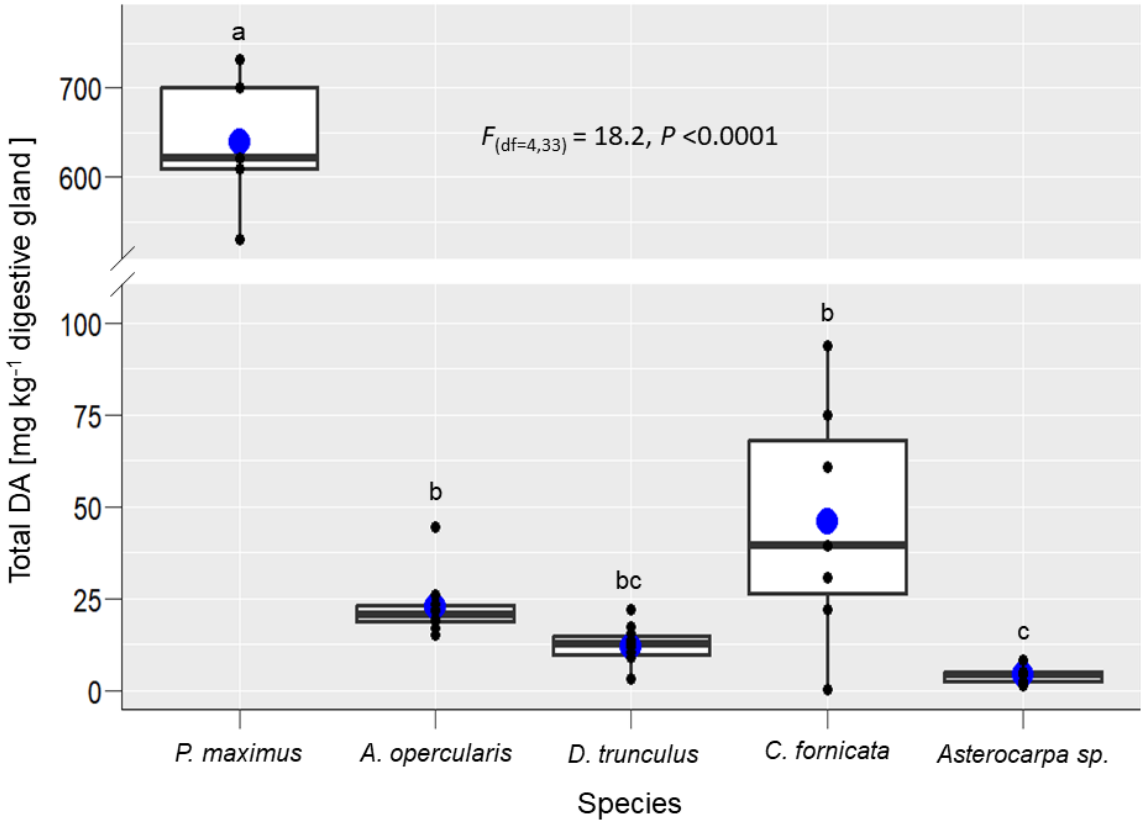

Figure 2. total domoic acid (tDA) concentration in the digestive glands of the scallops *P. maximus* (n =5) and *A. opercularis* (n = 10), the clam *D. trunculus* (n =11), the slippersnail *C. fornicata* (n =7), and the sea squirt *Asterocarpa sp.* (n =5) contaminated during *P. australis* blooms in the northwest coast of Brittany, France between the 30th of March and 8th of April, 2021. The upper and lower limits of the boxes are the quartiles, the middle horizontal line is the median, the extremes of the vertical lines are the upper and lower limits of the observations, black dots are the individual observations. The blue dots are the means for each species. Data were analyzed using species (five levels) as factor using a one-way ANOVA (*P* <0.05). The F-test statistic and degrees of freedom (df) are reported. Different superscript letters indicate significant differences between species. The level of statistical significance was set at α =0.05.

The toxin analysis carried out by LC-MS/MS revealed differences in digestive gland DA biotransformation among the different invertebrate species (Table I). For all species, biotransformation rates were <10 % of the tDA burdens. Nonetheless, *C. fornicata* was the species with the highest (P <0.05) DA biotransformation rate (9.3 ± 1.1 %), while *D. trunculus* showed significantly low biotransformation amounts (4.2 ± 0.3 %). Concerning the analysis of DA isomers proportion, *P. maximus* and *A. opercularis* showed similar biotransformation profiles of the toxin since similar amounts of each DA isomer were reported in both species. Furthermore, as seen in Table I, among the five species, the lowest ratio (P <0.05) of isoE was measured in *Asterocarpa sp.,* and a significantly higher proportion of isoD was recorded in *C. fornicata*, while the smallest amounts (P <0.05) of isoA and epi-DA were quantified for *D. trunculus*.

Table 1. Relative abundance of DA and its isomers in the digestive glands of the scallops *P. maximus* (n =5) and *A. opercularis* (n =10), the clam *D. trunculus* (n =11), the slippersnail *C. fornicata* (n =7), and the sea squirt *Asterocarpa sp.* (n =5) contaminated during *P. australis* blooms in the northwest coast of Brittany, France between March-April 2021.

	Species					Statistical analysis	
	P. maximus	*A. opercularis*	*D. trunculus*	*C. fornicata*	*Asterocarpa sp.*		
DA (%)	93.3 ± 0.6^{b}	93.6 ± 0.3^{b}	95.8 ± 0.3^{a}	90.7 ± 1.1^{c}	94.5 ± 0.1^{ab}	$F_{(df=4,33)} = 11.8$,	$P = 0.00$
isoE (%)	4.3 ± 0.3^{a}	4.3 ± 0.3^{a}	3.5 ± 0.3^{a}	3.2 ± 0.4^{a}	1.6 ± 0.1^{b}	$F_{(df=4,33)} = 10.9$,	$P = 0.00$
isoD (%)	1.5 ± 0.3^{bc}	1 ± 0.1^{bc}	0.5 ± 0.1^{c}	4 ± 0.8^{a}	2.1 ± 0^{b}	$F_{(df=4,33)} = 17.3$,	$P = 0.00$
isoA (%)	0.4 ± 0^{ab}	0.7 ± 0^{a}	0.2 ± 0^{b}	0.6 ± 0.1^{a}	0.5 ± 0^{a}	$F_{(df=4,33)} = 10.4$,	$P = 0.00$
epi-DA (%)	0.4 ± 0.1^{b}	0.4 ± 0^{b}	0 ± 0^{c}	1.5 ± 0.1^{a}	1.3 ± 0^{a}	$F_{(df=4,33)} = 156.4$,	$P = 0.00$

Results are expressed as mean ± SE. Data were analyzed using species (five levels) as factor in separate one-way ANOVA's ($P < 0.05$). The F-test statistic and degrees of freedom (df) are reported. Different superscript letters indicate significant differences between species. The level of statistical significance was set at $\alpha = 0.05$.

3.2. DA subcellular localization and histological measurements

The microanatomical observations of histological sections evidenced qualitative differences in the localization of DA and the subcellular features linked to the accumulation of the toxin among the invertebrate species analyzed in this study (Fig. 3). DA detected by IHC appeared as a brown chromogenic signal (cs) on slides (Fig 3A, 3D, 3G, 3J, 3M). In the digestive gland of *P. maximus* DA was detected mainly trapped within small (~1-2.5 µm diameter) autophagosomic-vesicles (a) distributed throughout the cytoplasm of the digestive cells (dc). A narrow fraction of DA-immunoreactivity was also observed in residual bodies (rb) distributed in the acinar region (ar) of the digestive diverticula (dd) (Fig. 3A). The identity of autophagosomes (a) with positive DA-signal (cs) in the tubular region (tr) of the digestive diverticula (dd) was confirmed by means of the multichromic staining (MC), which produces a dark violet/blue hueing in membrane-bounded structures (Fig. 3B). Hemotosylin-Eosin (H&E) staining (Fig. 3C) highlighted a moderate vacuolization (v) within the cytoplasm of the digestive cells of *P. maximus*. Neither the autophagosomes (a) nor the residual bodies (rb) acquired any coloration with the H&E staining but residual bodies appeared yellow-green.

In the queen scallop *A. opercularis*, a strong DA-chromogenic signal (cs) was found in the residual bodies (rb) of the digestive diverticula (dd) (Fig. 3D). No DA chromogenic signal was observed in the autophagosomes (a) present in the cytoplasm of the digestive cells of the digestive diverticula (dd) (Fig. 3E-F). An intense process of vacuolization (v) of the digestive cells of *A. opercularis* was found (Fig. 3E-F), while H&E staining (Fig. 3F) showed that the autophagosomes seem to gather giving rise to

the residual bodies (rb) in the cytoplasm of the adipocyte-like digestive cells (al) of the digestive diverticula (dd).

A similar result was found for *C. fornicata,* since most of the brown DA-chromogenic staining (cs) was found in small residual bodies (rb) present in the basal cytoplasmic region (bl) of the digestive cells (dc) (Fig. 3G), while autophagosomes (a) distributed in the apical region of the digestive cells (dc) (Fig. 3H-I) did not show any DA-immunoreactivity.

A slight-blurred DA-chromogenic signal (cs) was also observed only free in the cytoplasm of the digestive cells of *D. trunculus* (Fig 3J). The presence of autophagosomes (a, small blue colored vesicles distributed in the cytoplasm, Fig 3K) and residual bodies (rb, larger round non-colored structures present within adipocyte-like cells, Fig 3L) was confirmed in the digestive cells (dc) of clams (Fig. 3K-L).

Meanwhile, in sea squirts (*Asterocarpa sp.*) DA-chromogenic signal (cs) was rarely located as small brown points (Fig. 3M) distributed through the digestive epithelium (pse) of the blind ampulla (ba) (Fig. 3N-O).

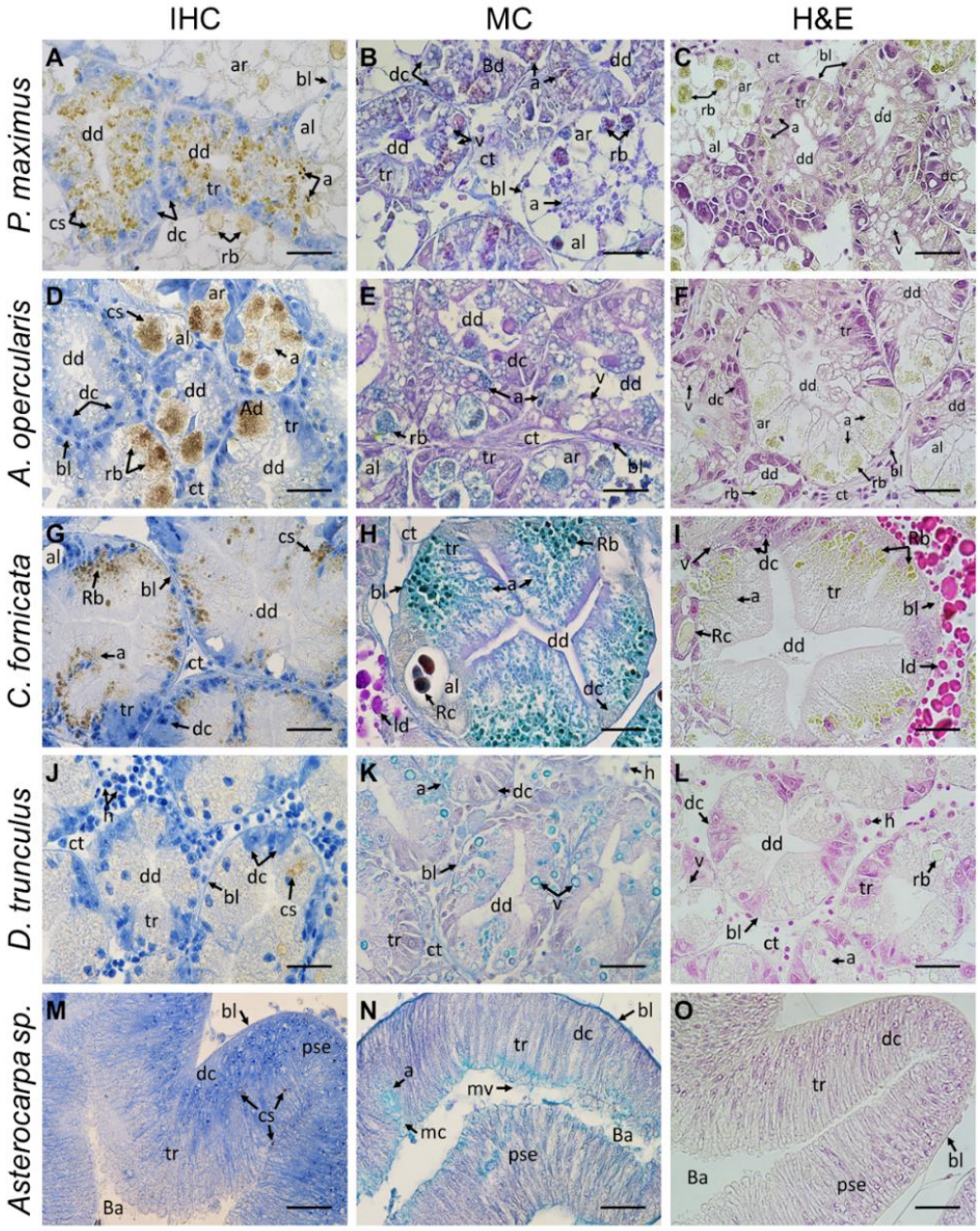

Figure 3. Microphotographs of digestive glands of the scallops *P. maximus* (A, B, C) and *A. opercularis* (D, E, F), the slippersnail *C. fornicata* (G, H, I), the clam *D. trunculus* (J, K, L), and the sea squirt *Asterocarpa sp.* (M, N, O) contaminated whit domoic acid (DA) during *P. australis* blooms in the northwest coast of Brittany, France in March-April, 2021. IHC (A, D, G, J, M) = Immunohistochemical detection of DA using specific anti-DA antibody (0.08 mg. mL^{-1}); MC (B, E, H, K, N) = multichromic histochemical staining of neutral carbohydrates (violet-magenta dyes), acid glycoconjugates (blue hues), and proteins (yellowish tones); H&E (C, F, I, L, O) = conventional histological Hematoxylin-Eosin staining. a = autophagosomes, al = adipocyte-like cell, ar = acinar region, Ba = blind ampulla, bl = basal lamina, cs = DA chromogenic signal, ct = connective tissue, dc = digestive cells, dd = digestive diverticulum, hc = hemocytes, ld = lipid droplets, mc = mucus, mv = microvilli, pse = pseudostratified epithelium, Rb = residual bodies, Rc = residual concretions, tr = tubular region, v = vacuoles. Scale bar: 63 × = 30 µm.

The results of the quantitative analysis of histological parameters are shown in Fig. 4. The coverage area of the DA chromogenic signal (%DAcs, Fig. 4A) was significantly higher in the most contaminated shellfish species (*P. maximus* = 4.8 ± 0.4 %, and *C. fornicata* = 5.3 ± 0.4 %). In addition, differences (P <0.05) were found in the amount of DA chromogenic signal in *A. opercularis* (3.2 ± 0.2 %) compared to the species contaminated with the lowest DA burdens (*D. trunculus* = 0.2 %, and *Asterocarpa sp.* = 0%).

On the other hand, as seen in Fig. 4B, total autophagy (Ta) reached its highest values (P <0.05) in the bivalve species, with frequencies of 185.4 ± 18 autophagosomes. area^{-1} in *P. maximus* , 123.2 ± 12.6 autophagosomes. area^{-1} in *D. trunculus*, and 102.9 ± 9.7 autophagosomes. area^{-1} in *A. opercularis*. The proportion of total autophagy (Ta) was significantly lower in *C. fornicata* (60.9 ± 5.8 autophagosomes. area^{-1}) and *Asterocarpa sp.* (18.3 ± 2.9 autophagosomes. area^{-1}). Nevertheless, the frequency of autophagosomes with positive DA-chromogenic signal (DAa) significantly peaked in *P. maximus* (99.7 ± 9.7 autophagosomes. area^{-1}, corresponding to 53.8% of the Ta), followed by *C. fornicata* (39.8 ± 4.6 autophagosomes. area^{-1}, corresponding to 65.3% of the Ta). The lowest proportions (P <0.05) of autophagosomes with positive DA-chromogenic signal (DAa) were observed in *A. opercularis*, *D. trunculus,* and *Asterocarpa sp,* with ≤7 autophagosomes. area^{-1}, which corresponded to 8.4, 1.2, and 0% of the total autophagy (Ta), respectively (Fig. 4B). In contrast, the frequencies of total residual bodies (Trb) and residual bodies with DA chromogenic signal (DArb) significantly peaked in *C. fornicata* (92.4 ± 5.2 rb. area^{-1}, and 51.9 ± 4.1 rb. area^{-1}, respectively), while the frequencies of both subcellular parameters showed their lowest values (P <0.05) in the rest of the species (Fig. 4C). It is important to highlight that the

percentage of residual bodies with DA chromogenic signal (%DArb) compared to total residual bodies (Trb) was significantly higher in *A. opercularis*, with a 67.1 ± 3%, followed by *C. fornicata* and *P. maximus* , with rates of 58 ± 3.8% and 35.4 ± 3.3%, respectively. The lowest % DArb (P <0.05) was reported for *D. trunculus* (2.2 ± 1.3%) and *Asterocarpa sp.* (0%). Finally, the highest frequency of cell vacuolization (Vac) of the digestive cells was measured in *A. opercularis* (67.4 ± 6.7 vacuoles. area^{-1}, P <0.05), followed by *P. maximus* (31.6 ± 2.4 vacuoles. area^{-1}). Significantly lower vacuolization (Vac) rates were reported for the rest of the species (<8 vacuoles. area^{-1}, Fig. 4D).

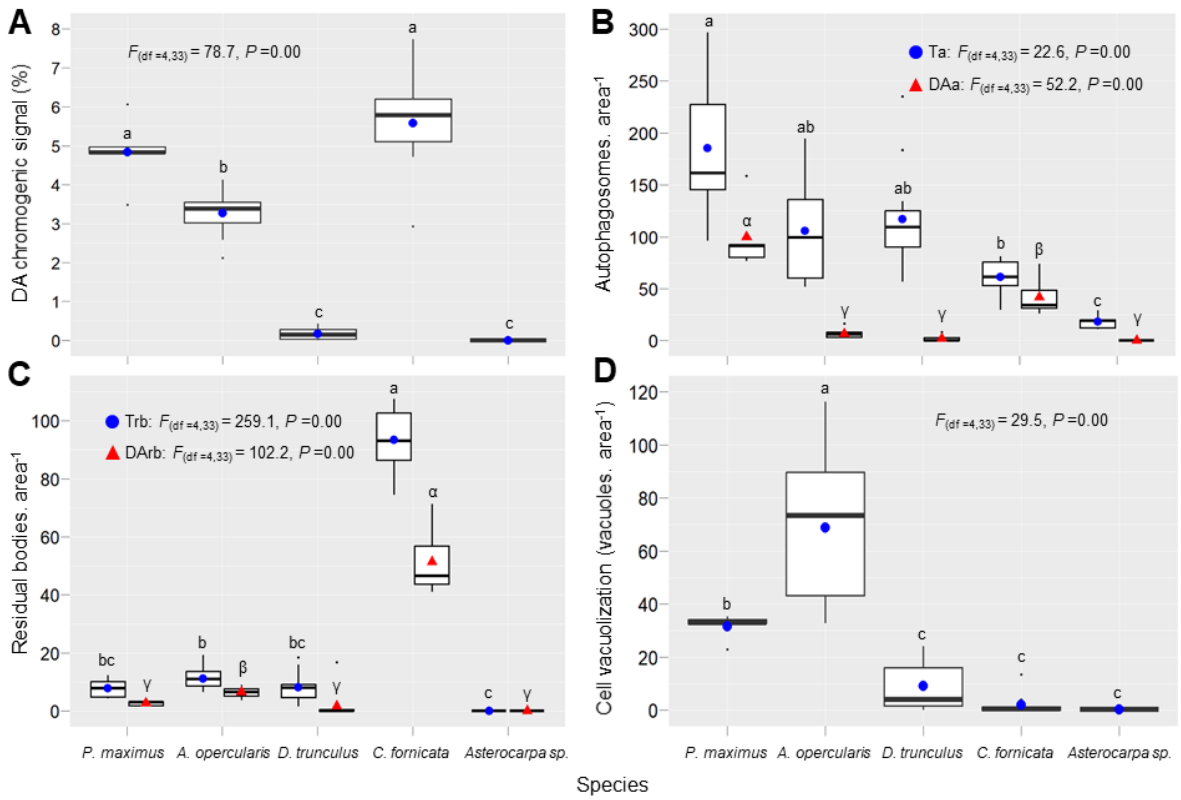

Figure 4. Quantitative analysis of DA localization and subcellular features in the digestive glands of the scallops *P. maximus* (n =5) and *A. opercularis* (n =10), the clam *D. trunculus* (n =11), the slippersnail *C. fornicata* (n =7) and the sea squirt *Asterocarpa sp.* (n =5) contaminated with DA during *P. australis* blooms in the northwest coast of Brittany, France in March-April, 2021. (A) DA chromogenic signal (%); (B) Autophagy (autophagosomes. 1.3 mm^2, Ta = total autophagy, DAa = DA autophagy); (C) Residual bodies (residual bodies. 1.3 mm^2, Trb = total residual bodies, DArb = DA in the residual bodies); (D) Cell vacuolization (vacuoles. 1.3 mm^2). The upper and lower limits of the boxes are the quartiles, the middle horizontal line is the median, the extremes of the vertical lines are the upper and lower limits of the observations, and black dots are the outliers (values that deviate from the median more than 1.5 times the interquartile range). The blue dots and red triangles are the means of each variable. Data were analyzed using species (five levels) as factor in separate one-way ANOVA's (P <0.05). The F-test statistic and degrees of freedom (df) are reported. Different superscript letters indicate significant differences between species. The level of statistical significance was set at α =0.05.

3.3. Integrative analysis compiling DA accumulation/biotransformation and subcellular features

A principal component analysis (PCA) was computed to summarize all variables measured in this study on the five invertebrate species studied: DA accumulation, biotransformation, and subcellular parameters (Fig. 5). The PCA described two-thirds

(66.6 %) of the total variance of the data along the first two principal dimensions. For the whole data set, the clustering-PCA provided a clear distinction between species, except for the two pectinid species, which slightly overlapped (Fig. 5A). In the scatter plot, *P. maximus* and *A. opercularis* showed similar scores on the principal components and were different from the rest of the species. Meanwhile, *D. trunculus*, *C. fornicata,* and *Asterocarpa sp.,* were grouped separately from each other (Fig. 5A). As shown in Fig. 5B, the dimension/principal component 1 (PC1, 42.3 % of the total variance) mainly explained the accumulated untransformed DA, isoD and isoA, as well as the histological parameters such as domoic acid chromogenic signal (%DAcs), domoic acid autophagy (DAa), total residual bodies (Trb), and residual bodies with DA signal (DArb). In this PC1, the fraction of isoA was strongly and positively correlated to the %DAcs and DArb (r = 0.5 and 0.6, P <0.05, respectively). Likewise, a strong and significant correlation was found between the untransformed DA and DAa (r = 0.8), and between DArb and %DAcs (r = 0.8) in this dimension. The amounts of isoE and epi-DA, as well as total autophagy (Ta) and vacuolization (Vac), were the strongest correlated variables to dimension/principal component 2 (24.3 % of the explained variance). A positive correlation (r = 0.5, P <0.05) between total DA (tDA) and isoE was found with Ta within the PC2. As observed in Fig. 5, *P. maximus* and *A. opercularis* were associated with higher tDA and isoE, as well as the maximum frequencies of Ta and Vac. Meanwhile, *C. fornicata* was related to higher amounts of isoD, epi-DA, Trb, and *D. trunculus* with the highest fraction of untransformed DA.

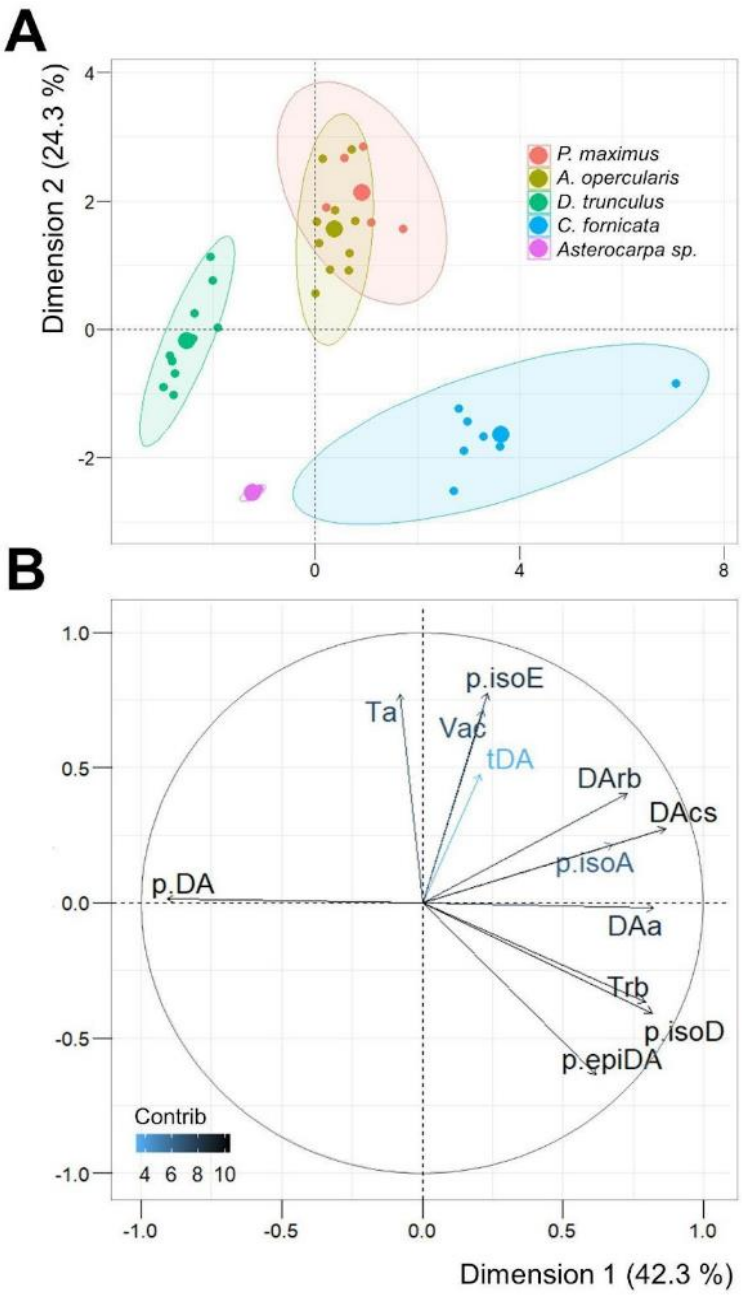

Figure 5. Principal component analysis (PCA) summarizing data from the scallops *P. maximus* (n =5) and *A. opercularis* (n =10), the clam *D. trunculus* (n =11), the slippersnail *C. fornicata* (n =7), and the sea squirt *Asterocarpa sp.* (n =5) contaminated whit domoic acid (DA) during *P. australis* blooms in the northwest coast of Brittany, France between March-April 2021. Dimension 1 and dimension 2 together describe 66.6 % of the total variance. (A) Scatter plot of individuals from each species. Larger symbols are the barycenter of each group, confidence ellipses level was fixed at α =0.05. (B) Variable contribution plot. The direction of the arrows shows the correlations of variables (tDA = total DA, DAscs = DA chromogenic signal, Ta = total autophagy, DAa = DA autophagy (%), Trb = total residual bodies, DArb = DA in the residual bodies (%), Vac = cell vacuolization, and the percentages (p) of DA isomers, p.DA = untransformed DA, p.isoE = isoE, p.isoD = isoD, p.isoA = isoA, p.epiDA = epiDA) with given PCs, and its color intensity shows their contribution (Contrib %) to the explained variance.

4. DISCUSSION

In this study, we compared domoic acid (DA) accumulation and isomer profiles with the subcellular localization of this toxin among naturally contaminated invertebrates to progress in the understanding of interspecific differences in DA fate in marine invertebrates. The DA contents measured in this study, and in all of other published studies, are the result of the accumulated and the subsequently depurated toxin. Moreover, differences in the DA accumulation in the organisms are strongly dependent on the toxicity of the *Pseudo-nitzschia* cells, the duration of the ASP-outbreaks, the time through the animals were exposed to toxic microalgae, and the moment at which the organisms were sampled during the bloom. In this work, DA contaminated animals were collected 8 days after maximum cell densities of *P. australis* bloom of similar intensity, duration and origin.

Since DA is a highly water-soluble molecule, it is expected to be easily accumulated in the majority of forager species (Trainer *et al.,* 2012; La Barre *et al.,* 2014). Nonetheless, the scallops, but notably *P. maximus*, as well as *C. fornicata,* remained significantly more contaminated than the rest of the species in this study. These important differences in DA accumulation in the digestive gland at the interspecific level are in accordance with considerably high variability in DA amounts frequently detected in these species (Bogan *et al.,* 2007a,b,c; Basti *et al.,* 2018, Blanco *et al.,* 2021) resulting from differences in the accumulation but also in the depuration rates of DA reported mostly for bivalve species (Vale and Sampayo, 2001; Blanco *et al.,* 2010; Dusek Jennings *et al.,* 2020). Notably, within the pectinidae family, some large scallops like *P. maximus* can accumulate up to 3,200 mg DA.kg^{-1} in their DG (James *et al.,* 2005; Blanco *et al.,* 2006), which is 5-fold more DA than the accumulated in the DG of the same species in this work. In contrast, smaller scallops, such as *A.*

opercularis (Ventoso *et al.,* 2019), *A. purpuratus* (Álvarez *et al.,* 2020) and *A. irradians* (O'Dea *et al.,* 2012) accumulate lower DA burdens (~7-30 mg DA kg^{-1}) similar to those recorded in *A. opercularis* in this work, in the same organs. Depuration kinetics of the toxin differ also between these species. Whereas *P. maximus* exhibits depuration rates as slow as 0.007-0.005 day^{-1} in the DG, remaining highly contaminated for months or even a few years (Blanco *et al.,* 2002a, 2006; García-Corona *et al.,* in prep a), other scallops such as *A. purpuratus* show decontamination debits near to 10 day^{-1} in the DG, allowing to depurate ~90% of total DA burdens within hours or a couple of days (Álvarez *et al.,* 2020). Thus, after all the differences in accumulation and depuration rates of DA between invertebrate species discussed above, a possible event of rapid depuration of DA in *A. opercularis*, *D. trunculus,* and *Asterocarpa sp.* before sampling can be part of the interspecific differences of DA concentrations measured in this study. Several factors could explain variability in DA decontamination: the transfer of DA in others tissues than DG, its biotransformation and its depuration.

Differential tissue distribution of DA may not explain more than 20% of the interspecific variability observed in this study since the digestive gland accumulates more than 80% of total DA burdens in most invertebrates (Blanco *et al.,* 2002a; Costa *et al.,* 2005). For all the five species of this study, 3 bivalve molluscs *(P. maximus*, *A. opercularis* and *D. trunculus*), 1 gasteropod mollusc (*C. fornicata*) and 1 ascidian (*Asterocarpa sp.*) DA isomers were observed in digestive gland with significant interspecific differences between the proportions of isomers E, D, A and epi-DA, iso-E being more represented in molluscs compared to ascidian. Although it is known that DA isomerization can occur within toxic *Pseudo-nitzschia* cells (Amzil *et al.,* 2001; Bates *et al.,* 2018; Quilliam *et al.,* 1989; Wright *et al.,* 1990a), in the present study all invertebrate species were exposed to the same *Pseudo-nitzschia* toxic bloom. These two set of information

demonstrate that metabolic conversion of DA occurs in marine invertebrates as hypothesized first by Vale and Sampayo (2001) and is species-specific. The integrative analysis revealed a close and significant relationship between some subcellular features (vacuolization, autophagy, presence of residual bodies) and the isomer profile of the toxin. Understanding DA compositional changes is important not only as a means of predicting toxicity, but also because biotransformation could participate for the prolonged retention of this toxin in shellfish species by means of some of the subcellular mechanisms analyzed here. Notwithstanding, biotransformation does not appear to be the main route of DA elimination in these species since it represents less than 10% of total DA of the digestive gland measured in these five species, as well as in previous studies (Costa *et al.,* 2005; Blanco *et al.,* 2010; Zheng *et al.,* 2022). There is only one study showing some insights of DA biotransformation linked to apparent augmentation of the overall DA detoxification rate in the cuttlefish *Sepia officinalis*, wherein DA isomers comprise a relevant percentage of the toxin profile in the branchial hearts, suggesting that this organ has an important function in system detoxification of DA (Costa *et al.,* 2005).

Despite the enormous differences in DA concentrations between the marine invertebrates analyzed in this work, the physiological mechanisms behind this phenomenon remain poorly understood. To date, only a few hypotheses about the biological processes potentially involved in the large accumulation and long retention of DA in some bivalve species have been proposed. On the one hand, Trainer and Bill (2004) characterized tissue-specific expression of high and low affinity glutamate receptors *in S. patula*, inferring that this species might selectively express low affinity glutamate receptors in all tissues, and high affinity sites in specific tissues that retained DA for long periods of time. On another hand, Mauriz and Blanco (2010) hypothesized

that one of the causes of the long retention of DA in the DG of *P. maximus* was not the binding of the toxin to some cellular component as previously discussed, but the lack of efficient membrane transporters in the scallops to excrete the toxin. Recently, using immunostaining of DA, García-Corona *et al.* (2022) revealed that in *P. maximus* most of DA-signal was localized in the cytoplasm of digestive cells of the digestive diverticula, trapped within autophagosomal vesicles. Moreover, transcriptomic analyses revealed the upregulation of genes related to autophagy and vesicle-mediated transport in the DG of *P. maximus* injected with DA in the adductor muscle (Ventoso *et al.,* 2021), as well as in the DG of *A. opercularis* after exposure to DA-producing *Pseudo-nitzschia* (Ventoso *et al.,* 2019). Taken together, these data suggest that the formation of autophagosomal structures could be part of the explanation for the long retention of DA, blocking its excretion in *P. maximus*. The results obtained in this work cope with these findings, since most of the DA-labeling was found within a large number of autophagosomes distributed throughout the cytoplasm of the digestive cells in *P. maximus,* Additionally, a strong DA-chromogenic signal was found within the post-autophagic residual bodies present in the adipocyte-like cells in *A. opercularis*, and in the basal region of the digestive diverticula in *C. fornicata*. During autophagy the lysosomes in the digestive cells of these species receive DA trapped within phagosomic-vesicles. Nonetheless, the evidence of this work indicates that the enzymatic battery of the lysosomes is unable to digest the toxin, leading to the accumulation of DA within the autophagosomes, and consequently blocking its excretion outside the cell by exocytosis (Cuervo, 2004; Zhao *et al.,* 2021). This eventually triggers the aggregation of autophagosomes with sequestered DA to form residual bodies that can remain in the cytoplasm of the digestive cells indefinitely.

There is evidence of the long retention of exogenous compounds through specialized cellular mechanisms in animals. A concrete example is the dynamics of phagocytosis displayed by dermal macrophages, explaining both persistence and strenuous removal of tattoo ink in mammalian skin. Baranska *et al.* (2018) demonstrated that upon tattooing, pigment particles are captured by dermal macrophages. Eventually, macrophages laden with tattoo ink die and release the pigment particles, which remain in an extracellular form at the site of tattooing where they are recaptured by neighboring or incoming macrophages. During the adult life, several cycles of ink capture-release-recapture can occur, accounting for long-term tattoo persistence (Baranska *et al.* 2018). Macrophagy and autophagy are analogous processes. During macrophagy specialized cells called macrophages use their cytoplasmic membranes to engulf large extracellular particles (≥ 0.5 µm, *i.e.* bacteria and debris) via endocytosis, giving rise to internal vesicular compartments called phagosomes. Phagosomes with cargo materials fuse with lysosomes, forming phagolysosomes, leading to enzymatic degradation (Flannagan *et al.,* 2012; Gordon, 2016). Like autophagy, macrophagy is a major mechanism used to remove pathogens and cellular debris for detoxification or nutrient recycling purposes, in which macrophages can have lifespans of months to a few years (Baranska *et al.,* 2018). The discussed above rises a new hypothesis suggesting that DA may undergo successive cycles of capture–release–recapture by autophagosomes through the regenerative cycle of digestive cells in some invertebrates, without any toxin vanishing from months to years. Therefore, long-term DA persistence could relies on autophagosome renewal or on potential longevity of residual bodies. A close relationship between early autophagy and DA sequestration can be established in *P. maximus*, whereas in *A. opercularis* and *C. fornicata* toxin accumulation seems to be closely linked to late autophagy and the formation of

residual bodies in the DG. This evidence strengthens the hypothesis stated by García-Corona *et al.* (2022), where autophagy was proposed as one of the possible causes of the prolonged retention of part of DA initially accumulated, now not only in *P. maximus*, but also in other marine invertebrates. The next step is to decipher the fate of autophagosomes and residual bodies with anti-DA immunolabelling within a scenario of contamination and decontamination.

Although the IHC method for the *in situ* detection of DA in contaminated shellfish used in this work has a high-sensitivity (~1 mg DA.kg^{-1}, García-Corona *et al.,* 2022) only a slight-blurred DA chromogenic signal was found in the cytoplasm of the digestive cells of *D. trunculus*, and *Asterocarpa sp*. This would suggest that in these species, intracellular DA is not bounded to any subcellular structure or component; thence, the feeble amounts of toxin free in the cytoplasm of the digestive cells of these species could be quickly depurated after ASP outbreaks. Further analyzes will be necessary to corroborate this idea.

Scallops, *P. maximus* but even more so *A. opercularis* contaminated by DA in this study have significantly higher digestive cell vacuolization rates in their digestive gland compared to other species. Cell vacuolization is a common histopathological lesion in bivalves under stressful environmental conditions (Rodríguez-Jaramillo *et al.,* 2022). According to Shubin *et al.* (2016) this is a well-known subcellular phenomenon observed in animal cells which often accompanies cell death after exposure to artificial or natural low-molecular-weight compounds, such as DA. The scarce literature related to the effects of *Pseudo-nitzschia spp*. or DA on invertebrates indicates that DA could potentially disrupt behavioral, metabolic, molecular, and physiological processes in some bivalves such as *P. maximus* (Ventoso *et al.,* 2021; Liu *et al.,* 2007a,b), *A. opercularis* (Ventoso *et al.,* 2019), *A. irradians* (Chi *et al.,* 2019), and some mussels,

like *M. edulis* (Dizer *et al.,* 2001) and *M. galloprovincialis* (Pazos *et al.,* 2017). Nevertheless, no lethal effects resulting from exposure to DA have been reported in any of these species, suggesting either a low sensitivity to the toxin or yet unnoticed negative effects. Further research is needed in order to decipher how DA exposure and its biotransformation modulate cell vacuolization, as well as its potential detrimental effects on the digestive cells of pectinids, and possibly, over other invertebrates, as reported for other phycotoxins in other bivalve species (Hegaret *et al.,* 2010; Lassudrie *et al.,* 2014).

Furthermore, as discussed above, the highest proportions of total autophagy, and production of residual bodies reported in *P. maximus* , *A. opercularis,* and *C. fornicata*, seems to directly correspond to the sequestration of DA within these subcellular structures, which indicates that autophagy could be also considered as a sign of homeostatic impairment, as reported in other marine bivalve species when activated as an auxiliary mechanism for recycling internal energy to cope with detrimental environmental conditions (Moore, 2008; Rodríguez-Jaramillo *et al.,* 2022), or to depurate toxicological agents (Moore, 2004; Picot *et al.,* 2019). The particularly highest proportions of DA-autophagy in *P. maximus* analyzed here stress out the need to carry out the measurement of the frequency of these subcellular features in a DA contamination and decontamination scenario. This basic knowledge is necessary to confirm these physiological processes are the actual reasons of the long retention of this toxin in this species.

The findings presented in this work put in evidence DA biotransformation in invertebrate species, and strongly suggest the role of subcellular mechanisms such as early and late autophagy, in the accumulation, localization and long retention of DA in some marine invertebrates.

5. CONCLUSIONS

The evidence presented in this work corroborates the profound interspecific differences in the accumulation of DA between different species of marine invertebrates, as well as species-specific profiles of toxin biotransformation among the analyzed shellfish. Similar profiles of DA isomers were found between *P. maximus* and *A. opercularis*, whereas *C. fornicata* was the species with the highest biotransformation rate, and *D. trunculus* the lowest. In *P. maximus, A. opercularis* and *C. fornicata* the DA chromogenic signal was detected mainly within autophagosomic-structures in the cytoplasm of digestive cells, while in *D. trunculus* and *Asterocarpa sp.* DA signail was found free in the cytoplasm of the digestive cells. This evidence indicates that localization of DA and its effects at the subcellular level appear to be species-specific, and the integrative analysis revealed that these parameters could be potentially influenced by the biotransformation profiles of the toxin. All this new information is highly valuable to strengthen ASP-monitoring systems since most of the invertebrate species analyzed in this work could be used as sentinels of DA contamination in affected areas. Furthermore, this study provides a set of innovative histological parameters developed to assess quantitatively some subcellular mechanisms potentially involved in the accumulation and long-retention of DA among contaminated invertebrates. This quantitative information may be integrated into numerical models that allow estimating and predicting toxicokinetics of contamination and depuration in fishery-stocks frequently affected during blooms of toxic *Pseudo-nitzschia sp.*

Acknowledgments

The authors are extremely grateful to Sylvain Enguehard (Novakits, Nantes) for providing the non-commercial primary antibodies necessary to carry out this study, as well as Nicolas Chomerat (from Ifremer, Concarneau) for sample transporting, and

Adeline Bidault and Morgan Perennou (from LEMAR, Brest) for their support during sampling and dissections. We also thank Marie Calvez and Nelly Le Goïc (LEMAR, Brest) for their assistance with tissue sectioning, and Carmen Rodríguez-Jaramillo (CIBNOR, La Paz) for her advices to optimize non-commercial antibodies for the IHC analysis.

Funding

This work received financial support from the research project “MaSCoET” (Maintien du Stock de Coquillages en lien avec la problématique des Efflorescences Toxiques) financed by France Filière Pêche and Brest Métropole. JLGC is recipient of a doctorate fellowship from CONACyT, Mexico (REF: 2019- 000025-01EXTF-00067).

Ethics statements

The organisms used in this work were transported and handled according to the International Standards for the Care and Use of Laboratory Animals. The number of sampled organisms contemplated "the rule of maximizing information published and minimizing unnecessary studies". In this sense, 38 individuals were considered the minimum number of organisms needed for this work.

Author contributions

Conceived the study: CF, HH, JLGC. Sampling: JLGC, HH, CF, ML, TD, AT. Processed the samples: JLGC, TD, AD, AT. Analyzed the data: JLGC, AD. Interpretation of data: JLGC, CF, HH, AD. Contributed reagents/materials/analysis tools: CF, HH, AD, AT, ML. Wrote the first draft of the manuscript: JLGC. Writing – review & editing: CF, HH, JLGC.

TO RETAIN

- There are profound differences in the accumulation rates of DA between shellfish species.
- DA biotransformation profiles were similar between pectinids and different for the rest of species.
- The subcellular localization of the toxin appears to be species specific.
- Autophagy seems to be behind the long retention of this toxin.

CHAPTER 4

KINETICS OF THE SUBCELLULAR LOCALIZATION OF THE AMNESIC SHELLFISH POISONING TOXIN, DOMOIC ACID, IN THE KING SCALLOP *Pecten maximus*

PREAMBLE

The application of the immunohistochemical method developed in chapter 2 to compare the subcellular localization of DA in different species of naturally contaminated invertebrates revealed that implications of autophagy in DA-sequestration are not exclusive of king scallops. In *P. maximus, A. opercularis* and *C. fornicata* the DA chromogenic signal was detected mainly within autophagosomic-structures in the cytoplasm of digestive cells, while in *D. trunculus* and *Asterocarpa sp.* DA signail was found free in the cytoplasm of the digestive cells. These results strengthened the hypothesis that autophagy could be one of the physiological mechanisms behind the long retention of DA in species with lower toxin depuration capabilities, such as king scallops.

Nonetheless, the mentioned above also rised the question: for how long DA is trapped within these autophagosomic structures in slow DA-depurators? Up to this point of the thesis we had only localized of the toxin in tissues of afected organisms after contamination. To confirm that autophagy is involved in DA retention, we performed an immunohistochemical time-tracking of DA at the subcellular level in tissues of scallops *P. maximus* during natural contamination, and laboratory decontamination phases, this in order to follow the succession of events that lead to autophagy in both scenarios (Fig. 6).

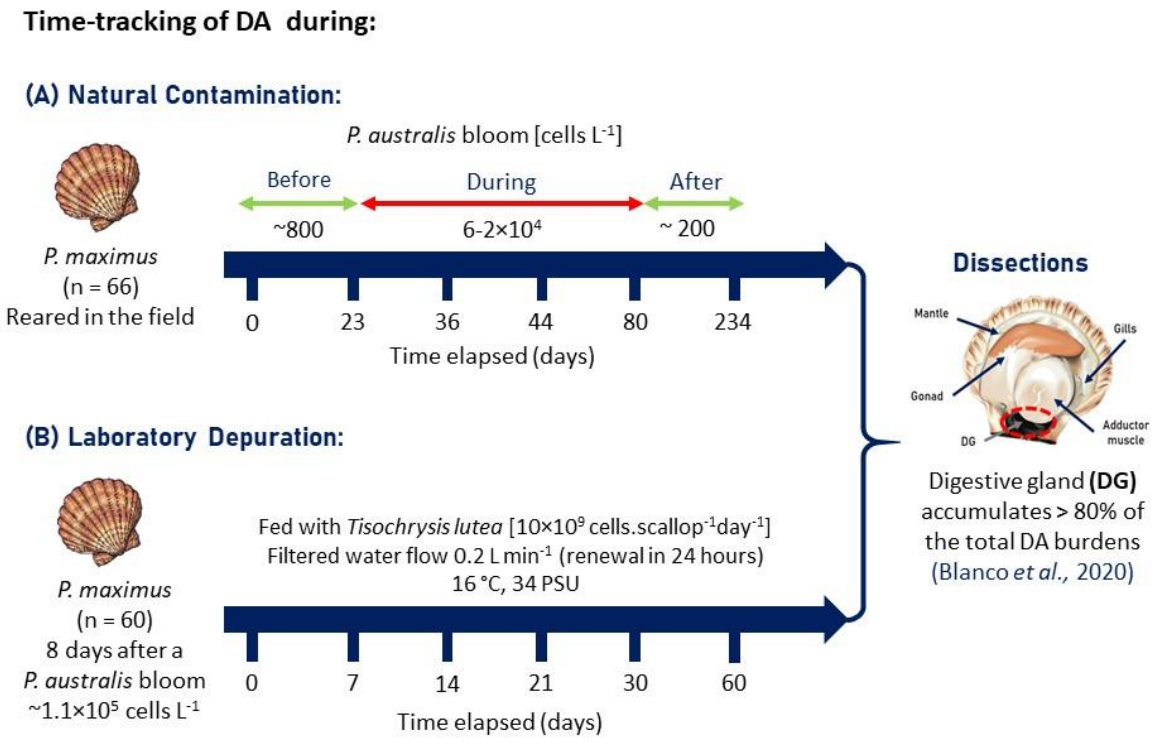

Figure 6: Experimental design set up to follow domoïc acid contamination and decontamination in scallop *Pecten maximus*

Kinetics of the subcellular localization of the Amnesic Shellfish Poisoning toxin, domoic acid, in the king scallop *Pecten maximus* in a contamination and decontamination scenario.

José Luis García-Corona[1], Margot Deléglise[1], Jean Vanmaldergem[1], Sylvain Petek[1], Aouregan Terre-Terrillon[2], Laura Bressolier[1,] Caroline Fabioux[1] & Hélène Hegaret[1*]

[1]Institut Universitaire Européen de la Mer, Laboratoire des Sciences de l'Environnement Marin (UMR6539 CNRS/UBO/IFREMER/IRD) Technopôle Brest-Iroise 29280, Plouzané, France.

[2]Ifremer, LITTORAL LER BO, Station de Biologie Marine, Place de la Croix, BP40537, 29900 Concarneau Cedex, France.

*Corresponding author: Hélène Hegaret

Institut Universitaire Européen de la Mer, Laboratoire des Sciences de l'Environnement Marin (UMR6539 CNRS/UBO/IFREMER/IRD) Technopôle Brest-Iroise 29280, Plouzané, France.

e-mail: helene.hegaret@univ-brest.fr

ABSTRACT

Domoic acid (DA) is a potent neurotoxin produced by diatoms of the genus *Pseudo-nitzschia* and is responsible for Amnesic Shellfish Poisoning (ASP) in humans. Some fishery resources of high commercial value, such as the king scallop *Pecten maximus*, are frequently exposed to ASP blooms and are capable of accumulating high amounts of DA, retaining it for months or even a few years. This poses a serious threat to public health and a continuous economical risk due to fishing closures of this resource in the affected areas. Recently, it was hypothesized that trapping of DA within autophagosomic-vesicles could be one reason explaining the long retention of the remaining toxin in *P. maximus* digestive gland. To test this idea, we follow the kinetics of the subcellular localization of DA in the digestive glands of *P. maximus* during (a) the contamination process— with sequential samplings of scallops reared in the field during 234 days and naturally exposed to blooms of DA-producing *Pseudo-nitzschia australis*, and (b) the decontamination process — where highly contaminated scallops were collected after a natural bloom of toxic *P. australis* and subjected to DA-depuration in the laboratory for 60 days. In the digestive gland, DA-depuration rate (0.005 day^{-1}) was much slower than contamination kinetics. The subcellular analyses revealed a direct implication of early autophagy in DA sequestration throughout contamination (r = 0.8, P <0.05), while the presence of residual bodies (late autophagy) appeared to be strongly and significantly related to slow DA-depuration (r = 0.7). This work provides new evidence about physiological mechanisms involved in the long retention of DA in *P. maximus* and represents the baseline to explore procedures to accelerate decontamination in this species.

Keywords: domoic acid, *Pecten maximus*, toxicokinetics, rapid accumulation, slow depuration, autophagy.

1. INTRODUCTION

Over the last three decades, natural stocks of important fishery resources have been subjected to intense and frequent blooms of toxic diatoms of the genus *Pseudo-nitzschia,* widely distributed throughout all oceans of the world (Hallegraeff 1993; Lelong *et al.,* 2012; Trainer *et al.,* 2012). To date, about 29 species of this genus have been reported to be capable of producing domoic acid (DA), an extremely dangerous amino acid responsible for Amnesic Shellfish Poisoning (ASP) in mammals (Pulido, 2008; La Barre *et al.,* 2014; Bates *et al.,* 2018). The species *P. australis* is frequently reported as one of the most toxigenic of all (Basti *et al.,* 2018; Ayache *et al.,* 2020) and in recent years, its presence has been detected in several countries around the world (Lelong *et al.,* 2012; Bates *et al.,* 2018) including on the northwest coast of France (Amzil *et al.,* 2001; Husson *et al.,* 2016).

The European Union 2002/226/EC has banned shellfish harvesting when DA concentrations exceed the sanitary limit of 20 $mg.kg^{-1}$ of flesh on the whole or individual parts of shellfish (Mc Kenzie *et al.,* 2002; Wekel *et al.,* 2004) to avoid public health issues. This represents a threat to the fishing-aquaculture industry due to the numerous persistent harvest closures of shellfish beds (Amzil *et al.,* 2001; Husson *et al.,* 2016; Ayache *et al.,* 2020). Many bivalves depurate the toxin quickly, showing decontamination rates of up to 10 day^{-1} in digestive tissues, like some mussels (Wohlgeschaffen *et al.,* 1992; Novaczek *et al.,* 1992; Blanco *et al.,* 2002b; Mafra *et al.,* 2010; Bresnan *et al.,* 2017), clams (Gilgan *et al.,* 1990; Blanco *et al.,* 2010; Álvarez *et al.,* 2015; Dusek Jennings *et al.,* 2020), and oysters (Jones *et al.,* 1995; Mafra *et al.,* 2010). Some scallops such as *Argopecten purpuratus* are also capable of excreting up to ≥ 80% of total DA-burdens in a few hours, and ~ 90% in a couple of days (Alvarez

et al., 2020). On the contrary, other bivalves exhibit toxin excretion rates ≤ 0.3 day^{-1} in the digestive gland, as reported for the clams *Siliqua patula* (Drum *et al.,* 1993; Horner *et al.,* 1993; Dusek Jennings *et al.,* 2020). Yet, larger scallops such as *Placopecten magellanicus* (Wohlgeschaffen *et al.,* 1992; Douglas *et al.,* 1997), and *Pecten maximus* (Blanco *et al.,* 2002a 2006; Mauríz & Blanco, 2010; Bresnan *et al.,* 2017) show the slowest DA-decontamination kinetics, with rates as slow as 0.05 to 0.007 day^{-1}, respectively, in the digestive gland. Furthermore, king scallop *P. maximus* has been reported to accumulate DA amounts as high as 3,200 mg kg^{-1} in the digestive gland, retaining it from several months to even a few years (Husson *et al.,* 2016; Blanco *et al.,* 2002a, 2006). Furthermore, the recurrent proliferations of DA-producing *Pseudo-nitzschia* and the subsequent reintoxication episodes of the natural stocks of these resources worsen the scenario (Blanco *et al.,* 2006; Ayache *et al.,* 2020), hindering the proposal of alternatives or a solution to this problem. King scallop *P. maximus* is a very valuable fishery resource in France and in the western coast of Europe, with an important economic and commercial value. It thus appears necessary to better understand the mechanisms associated with this long retention.

Physiological mechanisms behind the broad interspecific differences in accumulation and depuration dynamics of DA are still not fully understood. Mauriz and Blanco (2010) suggested that, in *P. maximus*, the absence of efficient membrane transporters to excrete the toxin could be the answer for the high accumulation and/or the slow depuration of DA in this species. Meanwhile, in *A. purpuratus*, the key to the accelerated depuration rates of the toxin could rely on the rapid transfer of most of DA burdens accumulated in the digestive gland to other organs capable to excrete it with greater efficacy (Álvarez *et al.,* 2020). Other mechanisms such as the differential

activation of some high and low-affinity glutamate receptors in specific tissues have been proposed as a possible explanation for the long retention of DA in species like the razor clam *S. patula* (Trainer and Bill, 2004). Recently, Garcia-Corona *et al.* (2022; in prep b) observe, thanks to an immunostaining of DA, that in species like *P. maximus*, queen scallop *Aequipecten opercularis*, and slipper-limpet *Crepidula fornicata*, most of the DA staining was trapped within small (~ 1-2.5 µm) autophagic vesicles in the cytoplasm of the digestive cells, as well as in remaining post-digestion residual bodies in the digestive cells (García-Corona *et al.,* 2022, in prep b). Nevertheless, none of these hypotheses has been fully elucidated so far. Autophagy is a highly organized and complex intracellular catabolic degradation system well conserved in eukaryotic cells (Owen, 1972, Wang *et al.,* 2019; Zhao *et al.,* 2021). Through this process the own (*e.g.,* abnormal proteins, excess or damaged organelles) or foreign (*e.g.,* pathogenic microorganisms, chemical compounds) cytoplasmic contents of the cell are digested to recycle energy usable by the cell, or processed for its cell excretion, respectively (Cuervo, 2004; Zheng *et al.,* 2022). The key structure in autophagy are autophagosomes, spherical vesicles from 500 nm to 2.5 µm in diameter with a double phospholipid membrane (Mizushima *et al.,* 2002). The essential role of autophagy is a key piece in the maintenance of homeostasis and cellular health of bivalves when exposed to potentially toxicological compounds (Moore, 2004; Picot *et al.,* 2019), including harmful algae-derived phycotoxins, as recently demonstrated in different species of marine invertebrates, but particularly in *P. maximus* contaminated with DA (García-Corona *et al.,* in prep b). Hence, we hypothesized that autophagy could be one reason explaining the long retention of remaining DA in these species, but particularly in *P. maximus* (García-Corona *et al.,* 2022). But for how long DA is trapped within these autophagosomic structures? So far, the localization of the toxin has only

been performed at a specific time after scallop contamination. To confirm that autophagy is involved in DA retention, it would be necessary to follow the succession of events that lead to autophagy during the contamination and decontamination process. In this study, the localisation of DA within tissues of *P. maximus* during the contamination and decontamination phases, as well as its toxicokinetics and the implication of autophagy was followed thanks to an immunohistochemical time-tracking at the subcellular level.

2. MATERIALS AND METHODS

2.1. Source of scallops and *P. australis* environmental data

A total of 66 scallops *P. maximus* (5.1 ± 0.3 cm shell length, 42.8 ± 8.2 g total weight) were reared in the field within culture-suspended cages at the Lanvéoc cove (48°29'56.3"N, 4°46'29.6"W; Bay of Brest, France) between February and October 2021. The information on the cellular densities of all phytoplankton species, including the DA-producing *Pseudo-nitzschia australis* in the area along the rearing period was obtained from the online database REPHY (REseau de surveillance du PHYtoplancton et des phycotoxines, https://envlit-alerte.ifremer.fr/) at the site called "Lanvéoc large". On March 30, 2021, a bloom of *P. australis* was recorded with densities reaching up to 6×10^4 cells L^{-1} and lasted for ~20 days. To study the contamination process, sequential sampling of 7-13 scallops were carried out before (corresponding to days 0 and 23 of the sampling), during (corresponding to days 36 and 44 of the sampling), and after (corresponding to days 80 and 234 of the sampling) the bloom of the toxic *P. australis* mentioned above.

To study the decontamination process, 60 wild scallops (9.7 ± 0.1 cm shell length, 168 ± 6.6 g total weight) were collected by dredging a natural bed in Camaret-sur-Mer, France (48° 26' 33.1"N, 4° 35' 49.6" W) in early April 2021, eight days after a bloom of *P. australis* (~1.1×10^5 cells L^{-1}, REseau de surveillance du PHYtoplancton et des phycotoxines, https://envlit-alerte.ifremer.fr/) to follow depuration of DA at laboratory.

2.2. Depuration of DA in the laboratory and scallop dissection

Scallops naturally contaminated with DA were transported to the Tinduff hatchery (Plougastel-Daoulas, France) within a few hours after collection. Upon arrival at the aquaculture facilities, the organisms were washed and scrubbed of epibionts, and immediately distributed in two 800L fiberglass tanks (30 scallops. $tank^{-1}$) with a sandy bottom. Filtered seawater (1 µm) was supplied and renewed in the thanks at 0.2 L min^{-1} (complete renewal in 24 hours to minimize re-ingestion of feces) through a continuous upstream-flow system with water pumped from the Bay of Brest. Animals were fed daily with a diet consisting of 10×10^9 cells.$scallop^{-1}day^{-1}$ of the flagellate *Tisochrysis lutea*. These food intakes were provided continuously by mixing the phytoplankton with the filtered water supply. Each tank was covered with a canvas and illuminated separately by a LED spotlight bar (NICREW Classic LED Plus 120-150 cm, 1150 lm) placed 1 m above the water surface with a photoperiod set at 12h:12h (light: darkness). During the experiment, the water was maintained fully oxygenated (100% O_2 saturated) and at a constant temperature of 15.9 °C, and salinity of the pomped seawater within the Bay (*i.e.* between 32.5 and 34 PSU over the 2 months of experiment). The scallops were maintained under these experimental conditions for 60 days, with sequential sampling of 10 animals after 0, 7, 14, 21, 30, and 60 days of depuration in the laboratory.

All sampled scallops were placed on a freezed plate to avoid suffering during sacrifice. The meat was carefully excised from the shells, and since the digestive gland (DG) accumulates ≥ 80% of the total DA burdens (Blanco *et al.,* 2002a) this tissue was carefully dissected and separated from the rest of the tissues (RT = gills, adductor muscle, and gonad) to avoid contamination of the other organs by DA of the DG during dissections (García-Corona *et al.,* 2022). The DG as well as the RT of each animal were sliced into two halves, one stored at -20 °C to determine the toxin concentration in each individual, and the other fixed in Davidson solution (Kim *et al.,* 2006) for anti-DA immunohistochemical purposes.

2.3. Toxin quantification by HPLC-UV analysis

Toxin was extracted from frozen tissues (DG and RT) of each scallop following the procedure described by Quilliam *et al.* (1989). Extractions were performed from approximately 200 mg of tissue homogenate with 1 mL of MeOH/H_2O (1:1, *v/v*) using a Laboratory Mixer Mill MM 400 system (Retsch® Fisher Scientific, Illkirch-Graffenstaden, FR) at 30 Hz for 10 min. The extract was clarified by centrifugation at 15,000 × *g* for 10 min at 4°C (Eppendorf 5427 R, Thermo Scientific, West Sussex, UK). Then, a 200-µL aliquot was filtered through a 0.2 µm nylon centrifugal filter (VWR International, Radnor, PA, USA) at 10,000 *g* for 5 min, at 4 °C, and stored in amber-autosampler vials at -20 °C until analysis.

DA quantification was performed by HPLC-UV according to García-Corona *et al.* (2022). The instrumental analysis was developed using a Thermo Scientific (Sunnyvale, CA, USA) HPLC System coupled to a UV spectrophotometer Waters 996 PDA-UV detector and a reversed-phase HPLC column Phenomenex C18 (250 × 4.6 mm; 5 µm). The flow rate was set to 1 mL min^{-1}, and the injection volume was 20 µL.

The separation was carried out using a mobile phase consisting of eluent A (H_2O + 0.1 % CF_3CO_2H) and eluent B (CH_3CN + 0.1 % CF_3CO_2H) with gradient conditions from 5 to 20% CH_3CN. The total analysis run time was 20 min. The column temperature was maintained at 40 °C. A six-point calibration curve was generated by serial dilutions in MeOH:H_2O (1:1, *v/v*) of certified DACS-1C DA standards obtained from the National Research Council (Halifax, Canada). Subsequently, DA concentrations were computed by comparing the absorbance at 242 nm of the chromatographic peaks of the samples with those of the reference solutions. The LODs of this HPLC-UV method ranged from 0.2 to 1 mg DA kg^{-1} tissue.

2.4. Quantitative anti-DA immunohistochemistry

In order to follow the *in situ* localization of the toxin at the subcellular level in the tissues of the scallops in both contamination and decontamination scenarios, a specific anti-DA immunohistochemical protocol recently developed by García-Corona *et al.* (2022) was applied in this work with minor modifications. Paraffin tissue sections (4-µm thickness) were rehydrated and incubated overnight with a dilution (0.01 mg. mL^{-1}) of a Goat polyclonal anti-DA primary antibody (Eurofins Abraxis®, Warminster, PA, USA) at 4°C. The next day, the slides were incubated at 37 °C for 2 h with a dilution (0.001 mg. mL^{-1}) of an HRP sharped IgG Rabbit anti-Goat secondary antibody (abcam®, Cambridge, UK). Finally, samples were revealed with diaminobenzidine (DAB+ Chromogen Substrate Kit, abcam®, Cambridge, UK) for 1 h in darkness at room temperature. The qualitative description of DA localization in the digestive gland was made considering the development stages of the digestive diverticula of the DG of *P. maximus* according to Mathers (1976) (Fig. 1) as: digestive diverticula in holding, absorptive, active, and advanced digestion, undergoing breakdown, or showing regeneration.

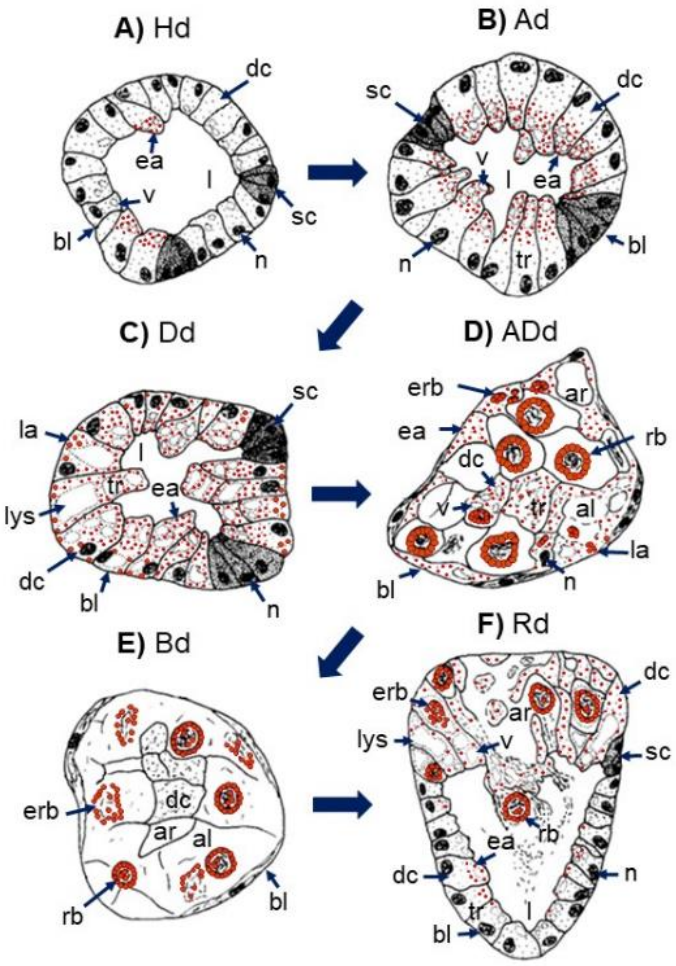

Figure 1. Transversal diagrammatic illustrations of the digestive diverticula (dd) in the digestive gland (DG) of *P. maximus* during a digestive cycle. (A) digestive diverticulum in a holding condition (Hd); cubical digestive cells (dc) with few vacuoles (v) and almost no autophagosomes line a large lumen (l) and secretory cells (sc) are easily identified. (B) diverticulum in absorptive condition (Ad); vacuoles and small early autophagosomes are present in the apical region of the digestive cells. (C) diverticulum in digestive condition (Dd); early autophagosomes (ea) are widely distributed throughout the digestive cells in the tubular region; basal vacuoles or lysosomes (lys) are identified, few bigger late autophagosomes (la) are present in the basal region of the cytoplasm. (D) diverticulum in advance digestive condition (ADd); secretory cells are absent, digestive cells in the tubular region are filled with early autophagosomes in the apical region and late autophagosomes in the basal region of the cytoplasm, and early residual bodies (erb) are visualized in the adipocyte-like cells (al) and residual bodies (rb) in the adipocyte-like cells as well. (E) diverticulum undergoing breakdown; digestive cells show loss of structure and form, high presence of residual bodies (rb) in the ascinar region (ar) within abundant adipocyte-like cells. (F) diverticulum showing regeneration; the secretory cells are again visible at the junctions between the old (ascinar region) and new (tubular region) diverticulum, early autophagosomes present in the apical region, and late autophagosomes in the basal region of digestive cells, presence of residual bodies in adipocyte-like cells. bl = basal lamina, n = nucleus. Modified from Mathers (1976).

Three regions from each section of the digestive glands treated with the anti-DA immunohistochemical protocol were randomly selected and digitized at 63×. In García-Corona *et al.* (2022), DA was mainly localized in structures identified as autophagosomes and residual bodies in the cytoplasm of digestive cells. Therefore, a total of 378 micrographs were used to count the number of total and positive DA-immunostained autophagosomes, as well as the number of total and anti-DA stained residual bodies present in a predetermined area of ~1.33 mm^2 (García-Corona *et al., in prep*). Then, calculations of the occurrence of early and late DA-autophagy in the DG through contamination and depuration processes were performed according to the following formulas, respectively:

DA early autophagy (%) = anti-DA stained autophagosomes/ total number of autophagosomes ×100

DA late autophagy (%) = anti-DA stained residual bodies/ total number of residual bodies ×100

2.5. Statistical analysis

Separate one-way analyses of variance (ANOVA, type II Sum of Squares) were applied to determine statistically significant differences in toxin concentrations in the tissues, as well as in the frequencies of early and late autophagy of DA in the DG of the scallops. *A priori* Anderson-Darling and Fligner-killeen tests were applied to confirm the normality of frequencies and homogeneity of variances of the residuals of the data, respectively (Hector, 2015). When needed, data were transformed (log, $1/\chi$, or $\sqrt{\chi}$) prior to analysis to meet a priori assumptions. The percentage-expressed values were also arcsine (arcsine $\sqrt{P}$) transformed (Zar, 2010), but all data are reported untransformed as the mean ± standard error (SE) except when indicated. As needed, *post hoc*

comparisons of means with Tukey's honest significance test (HSD) were performed to identify differences between means (Hector, 2015; Zar, 2010). Pearson's correlation coefficients were run to assess the relationship between DA burdens and the formation of autophagosomes and residual bodies in the DG of the animals during contamination and decontamination process (Zar, 2010). The rate of DA depuration in the DG of the scallops at the end of decontamination experiment was calculated according to Dusek-Jennings *et al.* (2020) using the one-compartment exponential decay model, $DA_t = DA_0 \cdot e^{-rt}$, where DA_t is the DA concentration after *t* days, DA_0 represents DA concentration at the end of the depuration, *t* is days elapsed, and the slope of the equation (*r*) is the daily depuration rate. DA_0 and the slope were estimated using linear regression after ln-transformation of DA burdens (Álvarez *et al.,* 2020), but untransformed data are presented. All data were analyzed with a level of statistical significance set at $\alpha = 0.05$ using command lines in the R language (R v. 4.2.2, R Core Team, 2022).

3. RESULTS

3.1. Toxin accumulation and depuration

Changes in DA concentrations in the DG of scallops through the natural contamination process are shown in Fig. 2A. The significantly lower toxin burdens in this organ were recorded at the beginning of our monitoring (day 0), with 11.3 ± 1.3 mg DA. kg^{-1}; this value slightly increased (51.2 ± 3.9 mg DA. kg^{-1}, $P < 0.05$) after 23 days of monitoring and following an exposure to a concentration of 800 cells L^{-1} of the toxic *P. australis*. Nonetheless, the contamination rate of scallops peaked abruptly and significantly between 36 and 44 days after our first sampling during a *P. australis* bloom (6×10^4 and 2.1×10^4 cells $L^{-1,}$ respectively recorded from March 30 to April 07, 2021) with average burdens of ~700 mg DA. kg^{-1} in the DG of the scallops. Moreover, the highest interindividual variability in DA accumulation was also observed through this period,

with values ranging from 86.5 up to 1,806.8 mg DA. kg^{-1}. Although *P. australis* populations drastically decreased until disappearing after 80 days, scallops remained strongly contaminated (290.2 ± 83.5 mg DA. kg^{-1}). At the last sampling point, 234 days after the first sampling, *i.e.* 198 days after the first bloom, the concentrations of DA in the DG of the animals were close to the sanitary threshold (32.3 ± 4.5 mg DA. kg^{-1}, Fig. 2A).

The depuration experiment in the laboratory started with heavily contaminated scallops, with DA concentrations of 812.9 ± 36.8 mg DA. kg^{-1} in the DG. These amounts significantly decreased to values of 259.5 ± 36 mg DA. kg^{-1} after 7 days of conditioning. Toxin concentrations however did not significantly decrease throughout the following 23 days, DA burdens remaining at about 270 mg. kg^{-1} during this 3 week-period. Even with a slight reduction (P <0.05) of toxin amounts in the DG, between 30 and 60 days, the scallops were still contaminated nearly 5-fold above (107 ± 4.9 mg DA. kg^{-1}) the sanitary limit (Fig 2B). As seen in Fig. 2B, DA depuration rate in the DG of the scallops was estimated at 0.005 day^{-1} from a one-compartment exponential decay model that explained 84% of the variance, with a good statistical fit (P <0.05) and without evidence of over-dispersion of the data.

The quantities of DA in the RT (gills, adductor muscle, and gonad) of the most contaminated scallops in both contamination and decontamination scenarios were below the HPLC detection limit (<1 mg DA kg^{-1}).

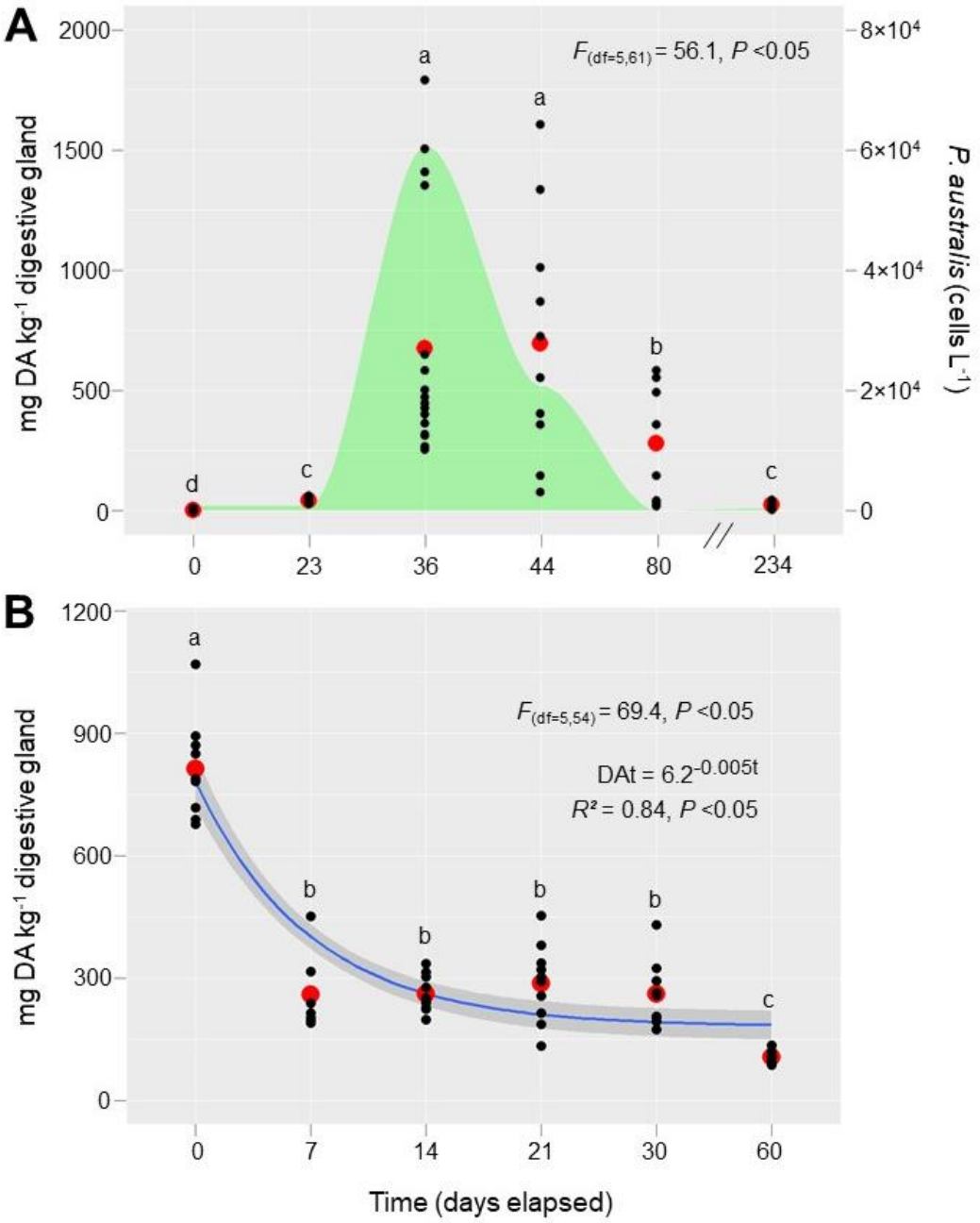

Figure 2. Concentrations of DA in the digestive glands of scallops *P. maximus* (A) during natural contamination process during outbreak of the toxic *Pseudonitzschia australis* in the northwest coast of France between February and October 2021, and (B) during the DA-depuration in the laboratory for 60 days after a natural DA-contamination event during toxic *Pseudo-nitzschia spp.* outbreak in the northwest coast of France in April 2021 . The black dots are the individual observations, and red dots are the means. The green shaded area (A) corresponds to the cell densities of *P. australis* in the field. The exponential daily DA depuration rate is the slope of the regression blue line (R^2 ± standard deviation). Data on DA concentrations were analyzed using the sampling time (six levels) as independent variable in separate one-way ANOVA's. The *F*-test statistic and degrees of freedom (*df*) are reported. Different superscript letters denote statistically significant differences between groups. The level of statistical significance was set at $\alpha = 0.05$.

3.2. Domoic acid *in situ* localization in a contamination and decontamination scenario

The presence of DA was readily detected in the DG of scallops through a natural contamination process (Fig. 2A and Fig. 3). As observed in Fig. 3A, the DA-chromogenic signal appeared since day 0 trapped within few early autophagosomes (ea) of small size (~1-2.5 µm) distributed in the apical region of the cytoplasm of the digestive cells (dc), particularly in the digestive diverticula (dd) in absorptive (Ad) condition, while the bigger residual bodies (rb) of ~5-10 µm and present only in the adipocyte-like cells (al) in the ascinar region (ar) of the digestive diverticula undergoing breakdown (Bd) acquired a slight anti-DA staining. Along the period of steady contamination (days 23 to 80, Fig. 3B-E), an intense process of early autophagy of the toxin was observed with the appearance of numerous early autophagosomes with a positive anti-DA signal in the apical zone of the digestive cells in the tubular region (tr) within the digestive diverticula in active (Dd) and advanced (ADd) digestion, as well as the digestive diverticula undergoing breakdown (Bd) or showing regeneration (Rd). The formation of late autophagosomes (la) of bigger size (~ 3-5 µm) than early autophagosomes with positive DA-labeling and present in the basal zone of digestive cells was also detected mainly in digestive diverticula in stages of active or advanced digestion, or in the diverticula showing regeneration. Through this period, the presence of some residual bodies with DA-chromogenic signal also occurred in the digestive diverticula undergoing breakdown or regeneration. Finally, at the end of the contamination surveillance (day 234, Fig. 3F), a low prevalence of early autophagosomes was observed in the digestive diverticula in absorption condition, while a high number of residual bodies with an intense anti-DA signal were found widely distributed in the DG of scallops.

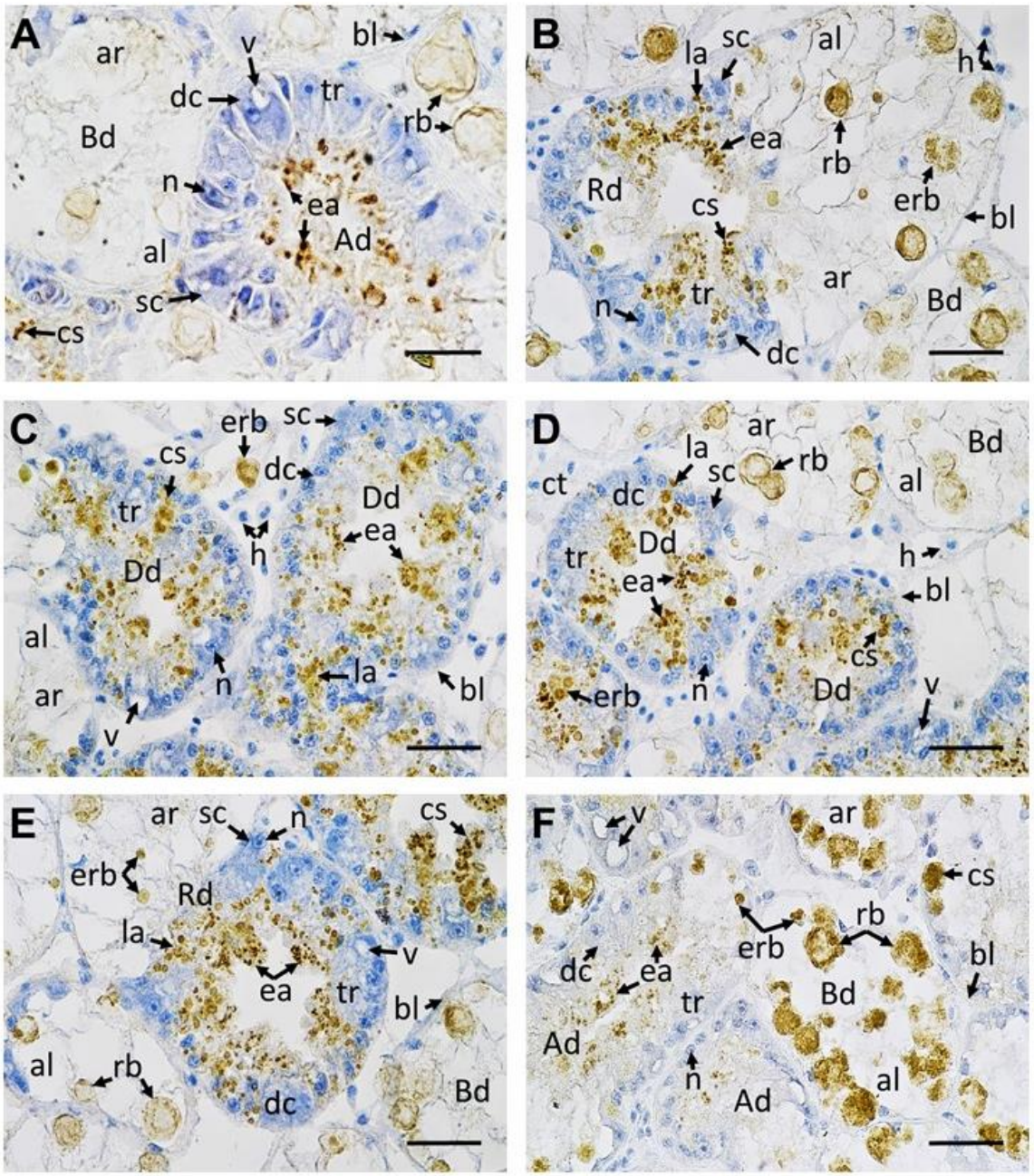

Figure 3. Microphotographs of digestive glands of scallops *P. maximus* during a natural process of DA-contamination during outbreaks of the toxic *P. australis*in the northwest coast of France between February and October 2021. A) Day 0, B) Day 23, C) Day 36, D) Day 44, E) Day 80, F) Day 234. Specific anti-DA immunohistochemical (IHC) staining appeared in brown. Ad = digestive diverticulum in absorptive condition, ADd = digestive diverticulum in advanced digestive condition, al = adipocyte-like digestive cell, ar = acinar region, Bd = digestive diverticulum undergoing breakdown, bl = basal lamina, cs = positive anti-DA chromogenic signal, ct = connective tissue, dc = digestive cells, Dd = digestive diverticulum in digestive condition, ea = early-autophagosomes, erb = early- residual bodies, h = hemocytes, la = late-autophagosomes, n = nucleus, rb = residual bodies, Rd = diverticulum showing regeneration, tr = tubular region. Scale bar: 63 × = 30 µm.

On the other hand, in the laboratory DA-depuration scenario, a strong process of early (ea) and late autophagy (la) of the toxin was already activated in highly contaminated scallops since day 0, mainly in digestive diverticula in advanced digestion (ADd), with only few-dyed residual bodies (rb) in the DG (Fig. 4A). As shown in Figs. 4B-C, over the following 7 to 14 days of DA-depuration, a similar amount of early and late autophagy of the toxin was observed in the DG of the animals, with the presence of autophagosomes and residual bodies with chromogenic signal mostly in the digestive diverticula showing regeneration (Rd). Notwithstanding, between days 21 and 30 of scallop conditioning, the early autophagy of the toxin was negligible, and it was observed how the labeled late autophagosomes gathered in the digestive diverticula undergoing breakdown to gave rise to residual bodies with intense anti-DA signal, that were distributed throughout the DG (Fig. 4D-E). At the end of the toxin depuration period (day 60, Fig. 4F), almost any traces of DA autophagy were observed in the digestive diverticula in absorption stages either, with a high prevalence and intensity of DA-labeling in the residual bodies widely distributed in the DG.

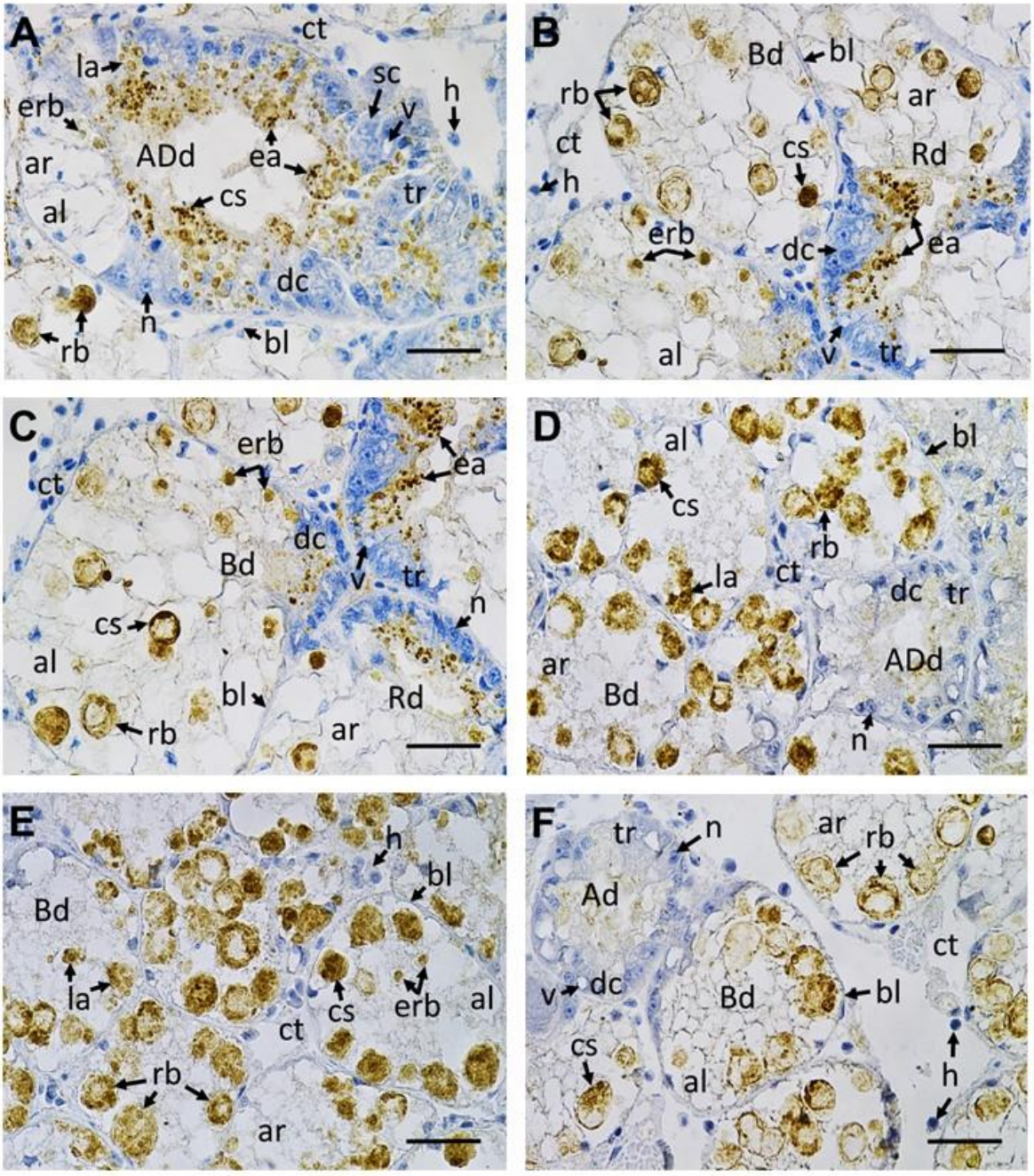

Figure 4. Microphotographs of digestive glands of naturally DA-contaminated scallops *P. maximus* collected after outbreaks of toxic *Pseudo-nitzschia spp.* in the northwest coast of France in early April 2021 and subjected to DA-depuration in the laboratory for 60 days. A) Day 0, B) Day 7, C) Day 14, D) Day 21, E) Day 30, F) Day 60.Specific anti-DA immunohistochemical (IHC) staining incubated with the primary and secondary antibodies (0.01 mg. mL^{-1} and 0.001 mg mL^{-1}, respectively). Ad = digestive diverticulum in absorptive condition, ADd = digestive diverticulum in advanced digestive condition, al = adipocyte-like digestive cell, ar = acinar region, Bd = digestive diverticulum undergoing breakdown, bl = basal lamina, cs = positive anti-DA chromogenic signal, ct = connective tissue, dc = digestive cells, Dd = digestive diverticulum in digestive condition, ea = early-autophagosomes, erb = early- residual bodies, h = hemocytes, la = late-autophagosomes, n = nucleus, rb = residual bodies, Rd = diverticulum showing regeneration, tr = tubular region. Scale bar: 63 × = 30 µm.

The quantitative IHC analyzes allowed to corroborate the overall microanatomical observations described above (Fig. 5). Across natural contamination of scallops during ASP bloom, early DA-autophagy (autophagosomes with DA-chromogenic signal) in the GD increased steadily and significantly from day 0 (36.6 ± 7.6 %) to its highest values on day 44 (74 ± 3 %), then, this frequencies decreased to its lowest values (P <0.05) at the end of the surveillance (25.9 ± 3.2 %) after 234 days (Fig. 5A). Whereas late DA-autophagy frequencies (Fig. 5A) showed slight increases (P <0.05) of stained-residual bodies between 0 days (3.6 ± 2 %) and 44-80 days (28.9 ± 6 %, and 19.5 ± 4.6 %, respectively). However, the amount of stained residual bodies significantly peaked up to its highest frequency (92.8 ± 1.5 %) at the end of the field monitoring. Under this scenario, early DA-autophagy was strongly and directly correlated (r = 0.8, P <0.05) with DA accumulation in the DG, while the relationship between the proliferation of anti-DA autophagosomes and residual bodies was negative and significant but not strong (r = -0.46). The correlation between toxin burdens and DA-stained residual bodies in the DG was low (r = -0.21) and non-significant.

Conversely, as shown in Fig. 5B, an inverse pattern between early and late autophagy was found along DA-depuration process (r = -0.8, P <0.05). The frequencies of IHC-labeled autophagosomes decreased (P <0.05) from 76.2 ± 2.6 % at the beginning of the experiment, to ~ 49.2 % between days 7 and 14, to then continue dropping to the minimum values (P <0.05) of ~ 12.3 % at the end of the experiment. While the amount of residual bodies significantly rose from the start (21.9 ± 3.7 %) to days 7 and 14 (~ 44.5 %) and subsequently peaked at its highest frequencies (~ 88.1 %, P <0.05) at the end of the laboratory depuration. Furthermore, a positive and significant relationship (r = 0.7) was found between DA amounts and late autophagy (anti-DA residual bodies) in the DG of the scallops.

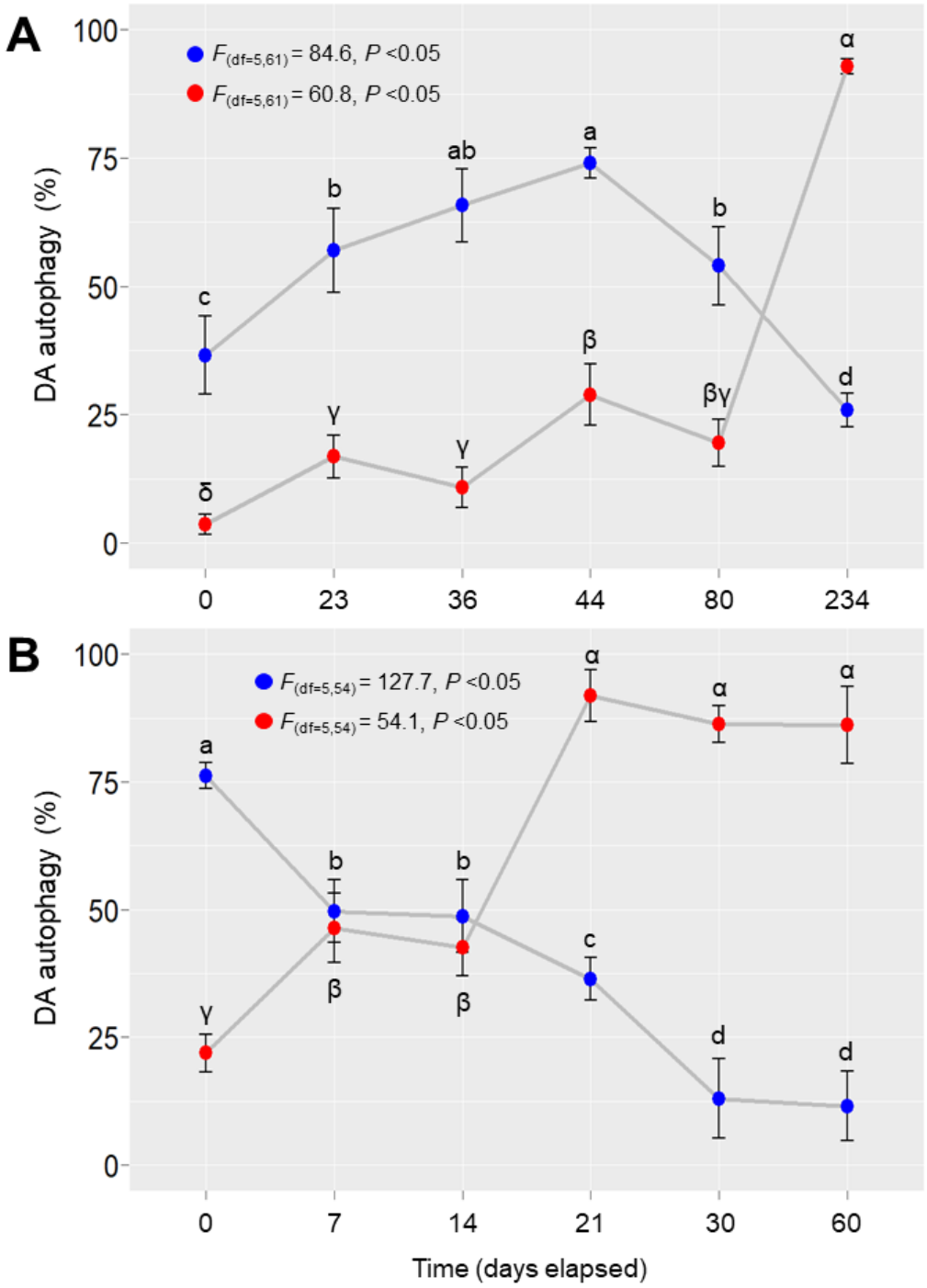

Figure 5. DA autophagy (%) in the digestive gland of scallops *P. maximus* (A) naturally contaminated during outbreaks of the toxic *P. australis* in the northwest coast of France between February and October 2021, and (B) naturally contaminated scallops *P. maximus* collected after outbreaks of toxic *Pseudo-nitzschia spp.* in the northwest coast of France in April 2021 and subjected to DA-depuration in the laboratory for 60 days. The blue dots (early-autophagy = autophagosomes) and red dots (late-autophagy = residual bodies) are the means. Results are expressed as mean ± SE. Data were analyzed using the sampling time (six levels) as independent variable in separate one-way ANOVA's. The *F*-test statistic and degrees of freedom (*df*) are reported. Different superscript letters denote statistically significant differences between groups. The level of statistical significance was set at $\alpha = 0.05$.

Even though the amounts of DA in the rest of the tissues (RT), except for the digestive gland, were under the instrumental quantification capabilities, through the application of the specific IHC technique it was possible to detect a positive anti-DA chromogenic dying only in highly contaminated scallops with 700 to 1,800 mg DA. kg^{-1} in the DG during both contamination (13% of the individuals) and decontamination (14% of the individuals) processes (Fig. 6). Toxin labeling was observed mainly in the microvilli of the branchial filaments (Fig. 6A), as well as in the axons and the somal body of the neurons embedded between the bundles of the adductor muscle (Fig. 6B). Moreover, anti-DA hues were also localized in the globose cells of the gonad ducts embedded in the male and female parts of the gonads of the scallops (Fig. 6C and D, respectively).

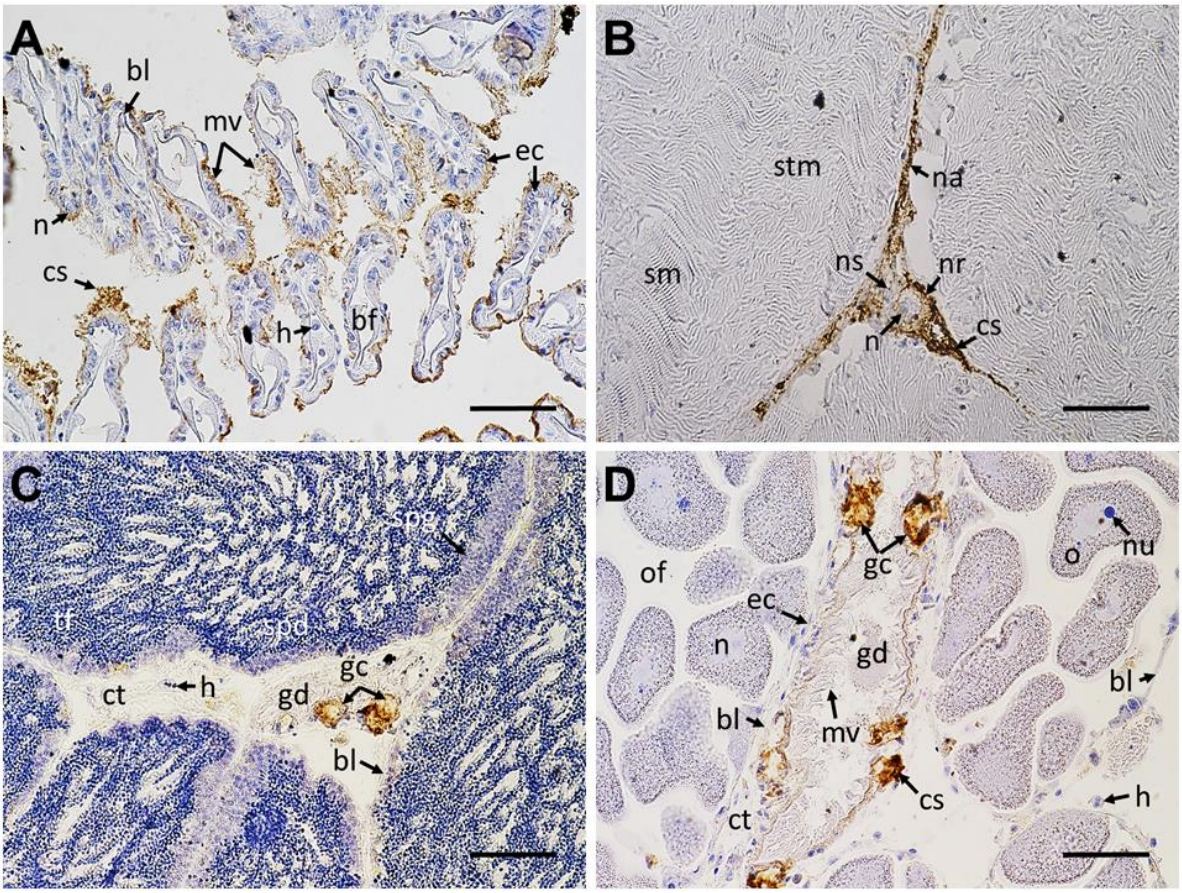

Figure 6. Microphotographs of the rest of tissues (A, gills; B, adductor muscle; C, male gonad; D, female gonad) of highly DA-contaminated (~ 679-1,806 mg DA kg^{-1}) scallops *P. maximus*. Specific anti-DA immunohistochemical (IHC) staining appeared in brown on the images. . bf = branchial filament, bl = basal lamina, cs = positive anti-DA chromogenic signal, ct = connective tissue, ec = epithelial cell, gc = globose cell, gd = gonadal duct, h = hemocytes, mv = microvilli, n = nucleus, na = neuronal axon, nr = neuron, ns = neuronal soma, nu = nucleolus, o = oocyte, of = ovarian follicle, sm = striated muscle, spd = spermatids, spg = spermatogonia, stm = smooth muscle, tf = testicular follicle. Scale bar: 40 × = 50 µm.

4. DISCUSSION

A clear gap exists in knowledge about the physiological causes of the long retention of DA in scallops, leading to long periods of fishery closures with important economical repercussions. The understanding of the biological mechanisms involved in both DA accumulation and depuration processes is of the utmost importance since the toxicity of shellfish stocks during and after *Pseudo-nitzschia* blooms, and the consequent exploitation capacity of these resources is determined by the kinetics of contamination and depuration of DA. In this work, for the first time, the kinetics of the localization of DA was monitored at the subcellular level in scallops during contamination and depuration thanks to a specific DA staining by immunohistochemistry recently developed by García-Corona *et al.* (2022).

The ability to accumulate, retain and redistribute DA burdens between different organs differs greatly between bivalve species (Blanco *et al.,* 2002b; Basti *et al.,* 2018). Furthermore, there is vast evidence that, in bivalves, DA depuration time is species-specific and has a wide range of variability. Most fast DA-depurators like mussels *M. edulis* (Silvert and Subba, 1991; Wohlgeschaffen *et al.* 1992; Novaczek *et al.,* 1992; Mafra *et al.,* 2010; Bresnan *et al.,* 2017), *M. californianus* (Whyte *et al.* 1995), *Perna canaliculus* (MacKenzie *et al.,* 1993), and *M. galloprovincialis* (Blanco *et al.* 2002b), many clams as *Mya arenaria* (Gilgan *et al.* 1990; Dusek Jennings *et al.,* 2020), *Mesodesma donacim* (Álvarez *et al.,* 2015), *Callista chione* (Fernández *et al.* 2003), *Ruditapes phillippinarum* and *Nuttallia obscurata* (Dusek Jennings *et al.,* 2020), and *Dosinia obirgny* and *Venerupis corrugata* (Blanco *et al.,* 2010), some oysters such as *Crassostrea gigas* (Jones *et al.,* 1995) and *C. virginica* (Mafra *et al.,* 2010b), and even scallops such as *A. purpuratus* (Álvarez *et al.,* 2020) are capable of detoxifying DA

burdens up to 900 mg. kg^{-1} within hours or a few days, with detoxification rates ranging from 0.1 to ~ 2 day^{-1} in the whole body, and up to 10 day^{-1} in digestive tissues. Hence, retaining DA for a short time with a low impact on their harvest and commercialization.

Nonetheless, *P. maximus* is a particular case, since, as found in this work, the DA depuration rate calculated for the scallops in the digestive gland in this work was very low (0.005 day^{-1}) when compared to those of the bivalves mentioned above, but very similar to that reported for the same species in the same organ by Blanco *et al.* (2002a, 2006) of about 0.003 and 0.007 day^{-1}, respectively. Notwithstanding, these depuration rates are too low even against those found in the digestive gland of other bivalves classified as slow DA-depurators as well, like *P. magellanicus* (~ 0.2 day^{-1}, Wohlgeschaffen *et al.,* 1992; Douglas *et al.,* 1997) and *S. patula* (0.05 and 0.02 day^{-1}, Horner *et al.,* 1993; Dusek Jennings *et al.,* 2020, respectively). Thus demonstrating that *P. maximus* has the slowest DA-depuration kinetics among bivalves studied until now. In fact, using the depuration rate estimated in this study, it would take around one year (350 days) for the scallops of our experiment to almost depurate the total burdens of DA in the digestive gland. This duration is calculated under an environment virtually free of toxic *Pseudo-nitzschia*, which is practically impossible with the repeated seasonal blooms of *P. australis* registered several times a year on the northwest coast of France (Amzil *et al.,* 2001; Husson *et al.,* 2016; Ayache *et al.,* 2020; REPHY-ifremer). To date, the only alternative for the profession to accelerate DA depuration of king scallop would be keeping contaminated animals in aquaculture facilities during several months such as those used in this work for DA depuration. Nevertheless, this solution would not be economically feasible considering the space required for the conditioning of scallops and the cost of such a procedure.

Moreover, there is a high inter-individual variability in the toxin burdens in the scallops. These large variations in DA contents, particularly in the DG, seem to be a characteristic of this species, as it was detected in several other studies (Blanco *et al.,* 2002a, 2006; Bogan *et al.,* 2007; García-Corona *et al.,* 2022). This has a strong repercussion on the precision of the measurements of DA concentrations and therefore it has to be taken into account during ASP-monitoring programs, either to avoid unnecessary fishery closures or to ensure public safety. The actual reasons for these profound differences in DA accumulation/depuration rates between bivalves are still unclear. Recently, Alvarez *et al.* (2020) designed a multi-compartment model that suggests DA accumulated by *A. pupuratus* is rapidly transferred from the digestive gland to other organs such as the gonad, muscle, mantle, and gills, which depurate the toxin independently and with much more efficiency following a first-order exponential decay. The same strategy was proposed to explain the rapid detoxification of visceral DA in *M. edulis* and *C. virginica* (Mafra *et al.,* 2010), as well as in *M. donacium* (Álvarez *et al.,* 2015) during early toxin uptake phase. Nonetheless, there is evidence that in the king scallop, DA redistribution from the digestive gland to other tissues does not seem to occur since throughout our monitoring of contamination and decontamination of the scallops, DA concentrations in the rest of the tissues (pool of the gonad, muscle, mantle, gills, foot, and kidneys) were below the quantification limit of the HPLC-instrument. Moreover, DA-staining in the rest of the tissues was only observed in specific structures of the most contaminated scallops (~ 700-1,800 mg DA kg^{-1}) in the entire study, and disappeared as soon as the depuration of the toxin began, whereby no toxin transfer from the digestive gland to the rest of the tissues may be inferred in this case either. These results cope with previous findings (Blanco *et al.,* 2002a, 2006) demonstrating the small fraction (≤ 5%) of total DA stored in the rest of

the tissues, which is excreted at a rate 2.5-fold faster than in the digestive gland (Blanco *et al.,* 2002a, 2006). The DA-signal was visualized in the microvilli of the gills and the globose cells embedded in the spawning ducts of the gonads. A similar result was reported by García-Corona *et al.* (2022) in strongly DA-contaminated scallops *P. maximus*, where immunoreactivity occurred in mucus-producing structures. So far, it has not been confirmed whether DA has a simple chemical affinity, or if it is chemically bound to some component of the mucus. Nevertheless, as discussed above, since the amount of toxin in the rest of the tissues is negligible, it can be inferred that mucus production does not play an important role in toxin depuration in this species. Interestingly, DA IHC-staining was also found in the peripheral neural tissue of the scallops, particularly in the axon extensions and the soma body of some neurons embedded in the adductor muscle. The presence of high DA-affinity and low-sensitivity receptors has been identified in tissues of other bivalve species like *S. patula* (Trainer and Bill, 2004), which could indicate the presence of this type of receptors in *P. maximus*. Further studies are necessary to corroborate all these ideas.

As digestive gland appeared as the key organ for storage and depuration of DA in *P. maximus*, we focused on this organ to go deeper into the cause of the long retention of DA in *P. maximus,* We observed a rapid depuration of around 70% of total DA accumulated in the digestive gland of scallops within the first 7 days of conditioning in the laboratory. This fraction likely corresponds to the toxin dissolved in the cytoplasm of the digestive cells, as stated by Mauriz and Blanco (2010), while the remaining ~30% of the DA burdens appear to keep trapped within autophagic structures for a long time as observed in García-Corona *et al.* (2022). This work constitutes the evidence of the importance of autophagy in the toxicokinetics of DA in *P. maximus*. Our results put in

evidence that during the period of active contamination, an intense process of early DA-autophagy was triggered, with the formation of autophagosomes in the apical region of the digestive cells cytoplasm, mainly within the digestive diverticula in absorptive and active digestion stages. According to Owen (1972) and Mathers (1976), this suggests an early and active assimilation of recently ingested food-particles into the cells for digestion. Whereas the appearance of bigger autophagosomes in the distal cytoplasmic zone of digestive cells, such as those observed in the digestive diverticula in stages of advanced digestion, indicates the end of intracellular digestion or the early formation of residual bodies (Mathers, 1976; Yurchenko and Kalachev, 2019). On the other hand, the high intensity and prevalence of residual bodies with strong anti-DA signal widely distributed in digestive diverticula under breakdown or showing regeneration until the end of the depuration process reveal that DA is not completely excreted from the cells, remaining in the digestive gland for an indefinite time, as described in the literature (Owen, 1972; Cuervo, 2004; McMillan, 2018).

The long retention of exogenous compounds does not appear to be a phenomenon exclusively related to autophagy, it also occurs in other types of cells under analogous cellular processes. Through macrophagy, specialized cells called macrophages use their cytoplasmic membranes to phagocytose large extracellular particles (≥ 0.5 µm, *e.g.* bacteria and metabolic debris) via endocytosis, creating internal vesicular compartments called phagosomes. Phagosomes with cargo materials fuse with lysosomes, forming phagolysosomes, leading to enzymatic degradation (Flannagan *et al.,* 2012; Gordon, 2016). There is evidence that, upon tattooing, mouse and human dermal macrophages are capable of: 1) phagocytosing pigment particles through several capture-release-recapture cycles across cell regeneration, or 2) exhibiting lifespans as long as the adult life of tattooed animals, accounting for both long-term

persistence and strenuous removal of tattoo ink on the skin. Even when the macrophages laden with tattoo ink die and release the pigments, the staining-particles remain in the extracellular space at the site of tattooing where they are recaptured by new macrophages (Baranska *et al.,* 2018). Like autophagy, macrophagy is a catabolic mechanism used to remove pathogens and cellular waste for detoxification or nutrient recycling purposes, in which macrophages can exhibit lifespans of months to years (Flannagan *et al.,* 2012; Gordon, 2016; Baranska *et al.,* 2018).

The results of this work and the discussed above suggest two new hypothesis: 1) DA may undergo successive cycles of capture–release–recapture by autophagosomic structures through the regenerative cycle of digestive cells of the scallops, or 2) autophagosomes and residual bodies with DA exihibit long lifespans without any toxin vanishing from months to years, thus triggering an analogous long-term DA-tattooing in the digestive glands of *P. maximus*. The direct and strong relationship found between early autophagy and DA accumulation, as well as the formation of residual bodies with depuration of the toxin denote that, at the subcellular level, autophagy could modulate the long-retention of DA in the digestive cells of *P. maximus* , by trapping the toxin and making it inaccessible to the detoxification system. The findings of this work are also reinforced by those of Ventoso *et al.* (2021) since the intramuscular injection of DA in *P. maximus* led to the overexpression of some genes related to autophagy and vesicle-mediated transport. Another question to be answered is the fate of the residual bodies with DA labeling after regeneration of digestive cells. Mathers (1976) demonstrated that the digestion cycle in the DG of *P. maximus* is closely correlated with feeding tidal-rhythm, where the intracellular digestion process of phagocytosed food-materials is accomplished within a biphasic 12-h tidal cycle (24h total), including the formation of autophagosomes in cells showing active digestion, to

the disintegration of residual bodies in the diverticula undergoing breakdown or showing regeneration. This strengthens the DA-tattooing hypothesis proposed in this study, given the long persistence (up to several months) of DA-labeled autophagosomes and residual bodies observed in the digestive diverticula of *P. maximus* through the entire process of contamination and depuration of the toxin.

5. CONCLUSIONS

The *in situ* DA-immunodetection method applied in this work is a powerful tool to perform a subcellular time-tracking of domoic acid in tissues of king scallops during contamination and depuration phases. Early autophagy, with the formation of autophagosomes, appeared actively involved in the accumulation of the toxin in the digestive gland. This study also provides strong presumption that long retention of a portion of DA initially accumulated in king scallop is due to late autophagy, with the occurrence and persistence of residual bodies. The quantitative immunohistochemical information developed in this work could be valuable for the development of numeric models that allow predicting the dynamics of contamination and decontamination with DA in natural fishery stocks. Moreover, our findings represent a cornerstone in the proposal of strategies to accelerate the depuration kinetics of ASP-toxin in this species.

Acknowledgments

The authors are deeply grateful to Sylvain Enguehard (Novakits, Nantes) for providing the non-commercial primary antibodies necessary to carry out this study, as well as Valentin Siebert, Erwan Amince, and Julien Thebault (LEMAR, Brest) for help with scallop collection. We also thank Florian Breton (Ecloserie du Tinduff, Brest) for technical assistance with laboratory conditioning of scallops, Marie Calvez, and Sébastien Artigaud (LEMAR, Brest) for assistance with tissue sectioning, and

antibodies quantification, respectively, as well as Carmen Rodríguez-Jaramillo and Raúl Martínez-Rincón (CIBNOR, La Paz) for advices to optimize non-commercial antibodies for the IHC analysis, and for help improving R-scripts, respectively.

Funding

This work received financial support from the research project “MaSCoET” (Maintien du Stock de Coquillages en lien avec la problématique des Efflorescences Toxiques) financed by France Filière Pêche and Brest Métropole. JLGC is recipient of a doctorate fellowship from CONACyT, Mexico (REF: 2019- 000025-01EXTF-00067). MD is recipient of a doctorate fellowship from Region Bretagne ARED.

Data availability statement

The evidence and data that support the findings of this study are available from the corresponding author upon reasonable request.

Ethics statements

The organisms used in this work were transported and handled according to the International Standards for the Care and Use of Laboratory Animals. The number of sampled animals contemplated "the rule of maximizing information published and minimizing unnecessary studies". In this sense, 126 scallops were considered the minimum number of organisms needed for this work.

Author contributions

Conceived the study: HH, CF, JLGC. Provided environmental data: AT, Performed the experiments: MD, JV. Sampling: JLGC, MD, JV, CF, HH. Processed the samples: JLGC, MD, JV, SP, LB. Analyzed the data: JLGC. Interpretation of data: JLGC, CF, HH. Contributed reagents/materials/analysis tools: CF, HH, SP. Wrote the first draft of the manuscript: JLGC. Writing – review & editing: CF, HH, JLGC.

TO RETAIN

- DA IHC is a powerful tool to perform a subcellular time-tracking of DA during contamination and depuration phases.
- Early autophagy is actively involved in DA-accumulation through contamination.
- Long retention of a portion of DA initially accumulated is due to late autophagy.
- Autophagy seems to be one of the reasons behind the long retention of DA in *P. maximus,*
- These results provide a better understanding of the fate of DA, and its contamination-decontamination process in king scallops.

CHAPTER 5

DIFFERENCIAL ACTIVATION OF MOLECULAR ET CELLULAR MECHANISMS IN *P. maximus* AND *M. edulis* EXPOSED TO DOMOIC ACID

PREAMBLE

The physiological differences in the way that domoic acid is accumulated, processed, and depurated among the invertebrate species at the different organizational levels (cellular, tissular, individual, interspecific) analyzed in the past chapters of this work led us to hypothesize that this variations would necessarily have molecular bases differentially regulated between fast and slow toxin depurators, which could explain the fundamental reasons for the long retention of DA in *P. maximus*.

The detailed review of the scarce literature existing on the effects of DA at the transcriptomic level point to differential activation of some mecanisms implicated in the recognition (glutamate receptors), transport (autophagy and vesicle-mediated transport), and metabolism (antioxidant and detoxification system) of DA in the digestive glands of the slow DA depurator *P. maximus* (Ventoso *et al.,* 2021) and the fast depurators *M. galloprovincialis* and *A. opercularis* (Pazos *et al.,* 2017, 2019). Therefore, in this chapter we attempt to compare the expression levels of some genes related to biological processes mentioned above and potentially involved in the differential retention of DA between the slow depurator *P. maximus* andthe fast *M. edulis.*

The ideal would have been to study the gene expression levels during an episode of natural contamination of scallops by DA-producing *Pseudo-nitzschia* cells in the laboratory. Unfortunately, it was not possible to obtain sufficient toxic *Pseudo-nitzschia* culture volumes to perform these experiments. Hence, we decided to perform exposures of slices of digestive glands in vitro to dissolved AD, following the procedure developed by Blanco *et al.* (2021a). Due to the nature of the experiment, the number of mRNA copies for each gene evaluated in both species was very low (beyond 35

cycles of qPCR). Thus, we opted for a digital droplet PCR (ddPCR) strategy to perform the gene expression analysis. This method is based on the sample-fractionationing into 20,000 water-oil emulsion droplets, where target and background DNA are randomly distributed the droplets. Afterwards, end-point PCR amplification of the template occurs in each individual droplet, and counting the positive droplets gives highly precise absolute target quantification. (Whale *et al.,* 2013) (Fig. 7).

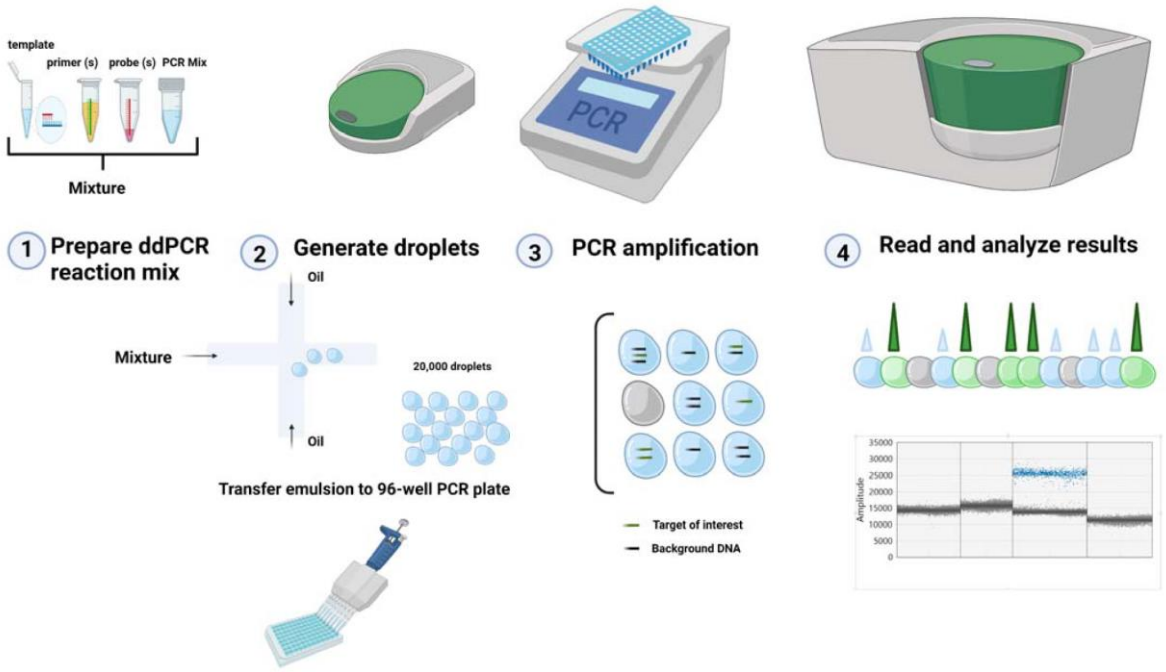

Figure 7 : ddPCR logistic strategy for absolute quantification of mRNA targets

Differential activation of molecular and cellular mechanisms in digestive gland of *Pecten maximus* and *Mytilus edulis* after *in vitro* exposure to domoic acid

José Luis García-Corona[1], Hélène Hegaret[1], Juan Blanco[2], Adeline Bidault[1], Elodie Fleury[1], Araceli E. Rossignoli[2], Eva Calvo[1], Caroline Fabioux[1]*

[1]Institut Universitaire Européen de la Mer, Laboratoire des Sciences de l'Environnement Marin (UMR6539 CNRS/UBO/IFREMER/IRD) Technopôle Brest-Iroise 29280, Plouzané, France.

[2]Centro de Investigacións Mariñas (CIMA), Xunta de Galicia, Pedras de Coron s/n, 36620 Vilanova de Arousa, Spain.

*Corresponding author: Caroline Fabioux

Institut Universitaire Européen de la Mer, Laboratoire des Sciences de l'Environnement Marin (UMR6539 CNRS/UBO/IFREMER/IRD) Technopôle Brest-Iroise 29280, Plouzané, France.

e-mail: caroline.fabioux@univ-brest.fr

ABSTRACT

Domoic acid (DA), the phycotoxin responsible for Amnesic Shellfish Poisoning, impacts economically important bivalves, such as scallops *Pecten maximus*, and mussels *Mytilus edulis.* These two species can accumulate large amounts of DA, with profound differences in their toxin decontamination kinetics; while the former takes months to years, the latter can depurate up to 90% of total DA in a few hours or days. Notwithstanding, physiological reasons for these differences are still unknown. In this work, subcellular and molecular mechanisms potentially involved in these differences were investigated by *in vitro* DA exposition of digestive gland (DG) from both bivalves for two different times (40, and 120 min). The incorporation of DA in the DG of *P. maximus* was nearly 15-fold higher than in *M. edulis*. Using immunohistochemistry, DA was visualized within autophagosome-vesicles dispersed throughout the cytoplasm of digestive cells only in exposed scallops. Absolute transcripts quantification by digital PCR revealed a strong upregulation (P <0.05) of autophagy-related genes in the DA-exposed *P. maximus,* whereas a significant overexpression of genes encoding for membrane solute-carriers (SLC) and glutamate receptors (GR) was found in DA-exposed *M. edulis*. The differential regulation of GR and SLC genes between *P. maximus* and *M. edulis* during DA-exposure could support differences in DA recognizing, as well as entry and/or exit of DA in these two species, while autophagy seems to be involved in the long retention of this toxin.

Key words: Domoic acid, toxicokinetics, autophagy, glutamate receptors, membrane transporters.

1. INTRODUCTION

The Amnesic Shellfish Poisoning (ASP) syndrome is a dangerous neurotoxic illness in mammals provoked by the phycotoxin domoic acid (DA), which is a highly water-soluble tricarboxylic amino acid produced by at least 29 diatom species of the genus *Pseudo-nitzschia* (Bates *et al.,* 1998; 2018). The potent toxicity of DA relies on the fact that this toxin is a structural analogue of glutamic acid, functioning as a strong agonist of glutamate receptors in the nervous system of vertebrates (Baden and Trainer, 1993; Pulido *et al.,* 2008; La Barre *et al.,* 2014). Populations of toxigenic *Pseudo-nitzschia* spp., and the subsequent presence of DA in seafood have been reported worldwide (Lelong *et al.,* 2012; Basti *et al.,* 2018; Bates *et al.,* 2018), thus becoming a problem of major concern, particularly in the North Atlantic coast of Europe where ASP outbreaks have occur more frequently and intensely during the last three decades (Amzil *et al.,* 2001; Husson *et al.,* 2016; Blanco *et al.,* 2021b).

Bivalve mollucs, as filter-feeders, are prone to accumulate large amounts of DA during blooms of toxic *Pseudo-nitzschia*, leading to extensive and prolonged closures of the fishing and aquaculture activities when concentrations exceed 20 mg DA kg^{-1} of total wet weight, established as the maximum level of contamination allowed in the whole body for marketing (Wekell *et al.,* 2004). These events are associated with major economic losses, as well as a serious threat to public health (Blanco *et al.,* 2002; Trainer *et al.,* 2012; Basti *et al.,* 2018). Notwithstanding, DA concentrations measured in bivalves tissues during monitoring programs varies substantially between species, mostly due to important differences in depuration velocity of the toxin (Blanco *et al.,* 2002, 2021b). These differences in toxin excretion rates have led bivalves to be classified as "fast" or "slow" DA depurators. While mussels and oysters (Novaczek *et al.,* 1992; Blanco *et al.,* 2002a; Mafra *et al.,* 2010), several species of clams (Blanco *et*

al., 2010; Álvarez *et al.,* 2015; Dusek Jennings *et al.,* 2020), and some scallops (Wohlgeschaffen *et al.,* 1992; Álvarez *et al.,* 2020) rapidly eliminate DA, other species, such as *Pecten maximus* (Blanco *et al.,* 2002a; 2006; García-Corona *et al.,* in prep) and the razor clam *Siliqua patula* (Horner *et al.,* 1993; Dusek Jennings *et al.,* 2020) are very slow DA depurators.

For example, P. maximusis capable of accumulating amounts as high as 2,900 mg DA kg^{-1} in the whole body, and up to 3,200 mg DA kg^{-1} in the digestive gland (Blanco *et al.,* 2002a, 2006). The digestive gland in *P. maximus* accumulates ≥80% of total DA burdens (Mauriz and Blanco, 2010) and exhibits the slowest DA-depuration rates among all bivalves (0.008-0.005 d^{-1}), scallops thus remaining highly contaminated and unsuitable for human consumption from several months to a few years (Blanco *et al.,* 2002a, 2006; García-Corona *et al.,* in prep). Meanwhile, *M. edulis*, despite being a species also capable to accumulate large amounts of DA in its visceral mass (700-900 mg kg^{-1}, Quilliam *et al.,* 1989; Bates *et al.,* 1998) exhibits the most accelerated DA depuration rates (11-60 day^{-1}), being able to depurate ~90% of total DA burdens within hours or a few days (Silvert and Subba, 1991; Wohlgeschaffen *et al.,* 1992).

In *P. maximus*, Mauriz and Blanco (2010) suggested that one of the potential causes of slow DA-depuration could be the absence of efficient membrane transporters to excrete the toxin. While in another slow DA-depurator, *S. patula*, the activation of high affinity and low sensitivity glutamate receptors in some tissues could explain DA retention for long periods of time (Trainer and Bill, 2004). Recently, García-Corona *et al.* (2022) proposed, thanks to a subcellular tracking of DA by immunohistochemistry technique, that autophagy could be one of the physiological mechanisms behind the long retention of this toxin in the digestive gland of *P. maximus* (García-Corona *et al.,* 2022 and in prep a). The same technique used in the digestive gland of five species of

contaminated marine invertebrates, revealed that subcellular sequestration of DA through autophagy is also observed in the pectinid*Aequipecten opercularis* and in the gastropod *Crepidula fornicata*, while in other species, such as the clam *Donax trunculus*, and the sea squirt *Asterocarpa sp.,* the anti-DA signal was found free in the cytoplasm of digestive cells (García-Corona *et al.,* in prep b).

Nonetheless, none of these hypotheses have been fully confirmed yet, and information about the molecular mechanisms implicated in DA recognition, assimilation and excretion in affected invertebrate species is still almost unknown.

The characterization of DA uptake mechanisms in *M. galloprovincialis* digestive glands performed by Blanco *et al.* (2021a) pointed to the presence of Cl^- (or anion-) dependent membrane transporters responsible for the entry of DA into the digestive cells, suggesting that DA transport mechanism in this species is not Na+, H+, or ATP-dependent. Similar results were reported by Madhyastha *et al.* (1991), indicating that the absorption of DA in the digestive glands of *M. edulis* seems to take place by a cellular membrane transporter with a negligible ATP-requirements, but also by the competitive inhibition of DA intake by some structural analogs of the toxin, like kanaic acid, glutamic acid, and proline. After some transcriptomic analysis of the mussel *M. galloprovincialis* (Pazos *et al.,* 2017) and the scallop *A. opercularis* (Ventoso *et al.,* 2019) exposed *in vivo* to toxic *Pseudo-nitzschia* cells, differential regulation of some glutamate receptors, as well as some membrane-proteins encoding for transporters of the solute carrier family (*SLC*) and enzymes implicated in the antioxidant/detoxification system were observed. In another RNA-seq analysis, Ventoso *et al.* (2021) found that the intramuscular injection of DA in *P. maximus* led to the identification of several glutamate receptors, as well as the overexpression of some genes related to

autophagy, vesicle-mediated transport, the antioxidant response, and some *SLC* transporters in the digestive cells of the scallops.

To go deeper into the understanding of differential regulation of molecular pathways proposed to be involved in the uptake and elimination of DA, we compare DA concentration, DA localization and transcripts levels of candidate genes regarding literature and our previous studies, between the slow depurator *P. maximus* and the fast depurator *M. edulis*, after *in vitro* exposure of digestive gland to dissolved DA. .

2. MATERIALS AND METHODS

2.1. Biological material

A total of 20 adult bivalves were collected in the Bay of Brest, France early 2022. Ten king scallops *Pecten maximus* (9.9 ± 0.2 cm shell length; 202.2 ± 10.6 g total weight) were dredged from a natural bed on the 28th of January, and ten mussels *Mytilus edulis* (4.2 ± 0.1 cm shell length; 6.9 ± 0.3 g total weight) collected on the 08th February. Animals were washed and scrubbed to remove epibionts, placed in two separate 100-L tanks supplied with running filtered (1 µm) seawater, and fed with a daily ration of *T.iso* at a density of 5×10^{8} cells ind^{-1} day^{-1}. After a minimum period of 48h of acclimatization, two specimens from each batch of sampled organisms were dissected and analyzed to verify the amounts of domoic acid (DA) in their digestive glands (DG) before the experiments. Other ones were used for the *in vitro* experiment.

2.2. *In vitro* exposure of digestive glands to domoic acid

The experiment of *in vitro* exposure of the DG to dissolved DA was conceived according to Blanco *et al.* (2021a) with modifications. First, the DA-supplemented incubation media was prepared by dissolving 4 mg of powdered DA (abcam®,

Cambridge, UK) in 20 mL of sterile-filtered (0.22 µm) seawater (34 UPS) to a final concentration of 200µg DA mL^{-1}. This solution was stored in the dark at 4 °C until use, and an aliquot of 500 µL was analyzed to check the DA concentration of the media prior to the experiment.

Both scallops (n=8) and mussels (n=8) were opened and the meat was excised from the shells, then the DG from each organism was carefully dissected on chilled plates, and 5 thin (~1 mm^3) slices of approximately 100-120 mg were obtained from the inner part of the DG by mean of transversal cuts. The slices from each individual were weighed. Two slices per individual were placed into one well of a 24-well cell culture plate (Greiner bio-one Cellstar®, Frickenhausen, DE) filled with 2 mL of filter-sterilized (0.22 µm) seawater (control condition), and the other two slices were placed into one well containing 2 mL of the DA-supplemented incubation media. Additionally, one slice from each individual was immediately sampled to assess the initial (T=0min) DA concentration of the DG, gene expression levels, and autophagy (sections below). Finally, the slices were incubated in both experimental conditions in the dark, at room temperature (~25 °C), while subjected to gentle agitation (30 RPM) using an orbital shaker. After 40 min and 120 min of incubation, slices of DG from each species (*P. maximus* and *M. edulis*) and each condition (control and DA exposed) were sampled. The tissues were placed in Eppendorf tubes and rinsed with filtered seawater (0.22 µm) and centrifuged at 900× *g* at 4 °C for 5 min, discarding the supernatant, twice, to remove the remaining incubation medium. Afterwards, each slice was dissected into three portions (30-40 mg) for DA quantification, gene expression, and immunohistochemical purposes (sections below).

2.3. Toxin quantification by LC-MS/MS

The DA extractions from the samples of DG, and the subsequent quantification analyses were performed according to Blanco *et al.* (2021) with minor modifications. DA was extracted from the tissues by adding 0.2 mL of a mixture of H_2O:MeOH in a proportion of 1:2 *w:v* (Quilliam *et al.,* 1989) and frozen at -80 °C. After 30 days, the samples were thawed and homogenized in an ultrasonic iced bath. Homogenates were clarified by centrifugation at 19,000× g at 4 °C, filtered through 0.22 µm syringe filters, and frozen at -80 °C until analysis.

The analysis of DA concentrations was carried out by LC-MS/MS using a chromatographic system ExionLC AD coupled, through an electrospray interface Turbo V, to a Qtrap 6500+ triple quadrupole mass spectrometer (Sciex, Framingham, MA, USA). The chromatographic method used a reversed-phase chromatographic column Kinetex C18 (50 × 2.5 mm, 2.6 µm) (Phenomenex, Torrance, CA, USA), 0.2% formic acid as phase A, and 50% MeOH as phase B. The run started at 100% A, changing linearly to 45% A / 55% B from min 2 to min 4, maintaining this proportion for 2 min, and then returning in 1 min to the initial conditions, which were maintained for 1.6 min to re-equilibrate the column before the next injection. The flow rate was 280 µL min^{-1} and the injection volume 5 µL.

The mass spectrometer was operated in positive ionization mode, with 5,500 V of ionization voltage, 60 nominal units of Gas1 and Gas2, 30 units of curtain gas, 400 °C of source temperature, nitrogen as collision gas with a “Medium” pressure, and a declustering potential of 80. The transition 312.1 > 266.1 was used for quantification and 312.1 > 248.1 for confirmation, both obtained using a collision energy of 35. The quantification was made by external standards using as a certified reference solution

provided by CIFGA (Lugo, Spain). The LOQ (s/n = 10) and LOD (s/n = 3) of the method are 3.6 and 1.1 ng mL^{-1}, respectively.

2.4. Total RNA extraction and cDNA synthesis

Individual samples (30-40 mg) of the DG from each organism were stored at 4 °C for 6 days in RNA*later*® solution (Sigma-Aldrich, St. Louis, MO, USA). Subsequently, DG were ground using a Fastprep-24 5G homogenizer (MP Biomedicals, Sta. Ana, CA, USA) and total RNA was isolated using the E.Z.N.A total RNA kit II (Omega Biotech, Norcross, GA, USA) following the manufacturer's protocol. To remove genomic DNA contamination, total RNA was treated with RNAse-free DNAse RQ1 (1 U/µg total RNA, Promega, Madison, WI, USA). Then, RNA was precipitated with 0.1 volume of potassium acetate 5 M, and the pellet was dissolved in 20 µL of nuclease-free water (Gentrox, Claremont, CA, USA). RNA purity and concentration was measured with a spectrophotometer Nanodrop ND-8000 (NanoDrop Technologies, Wilmington, DE, USA), and the integrity of the RNA samples was assessed using 2% agarose-TAE gel electrophoresis, and Agilent 2100 Bioanalyzer (Agilent Technologies, Santa Clara, CA, USA). The final quantity of the total RNA was determined using Qubit 2.0 fluorometer (Invitrogen, Carlsbad, CA, USA).

Each RNA sample was PCR-tested as a non-amplification control to verify the absence of DNA contamination using the GoTaq® Green Master Mix (Promega), 1 µL of RNA preparation, and the 18S ribosomal specific primers (0.5 µM each) for both species (Table 1). Afterwards, from each verified RNA sample, 1 µg of total RNA was reverse transcribed using 2 µL M-MLV reverse transcriptase from the RevertAid H Minus First-Strand Synthesis System SuperMix® (ThermoFisher Scientific, Vilnius, LT) and oligo-

dT according to the manufacturer's protocol. cDNA was stored at 4 °C for immediate use.

2.5. Selection of target genes and primer design

Target gene sequences were selected from differentially expressed genes (DEGs) coding for proteins related to autophagy, glutamate receptors, solute carriers, and the detoxification system, identified in the transcriptomes of the DG from *Mytilus galloprovincialis* (NCBI BioProject PRJNA326100; Pazos, *et al.,* 2017) and *Aequipecten opecularis* (NCBI BioProject PRJNA508885; Ventoso *et al.,* 2019) *in vivo* exposed to DA-producing *Pseudo-nitzschia* cells, and in the transcriptome of the DG of *P. maximus* (NCBI BioProject ID PRJNA704533) after an intramuscular injection of DA (Ventoso *et al.,* 2021). The selected transcripts related to the biological processes of each of the three species mentioned above were used to find highly homologous sequences in the genomes of *M. edulis* (NCBI BioProject PRJEB38403), and *P. maximus* (NCBI BioProject PRJEB35330), using the NCBI nucleotide Basic Local Aligmnent Search Tool (BLASTn). Only the sequences with >70 % of identity between both species were considered to obtain the whole coding DNA sequence (CDS) for each gene. Thereupon, the CDS of each gene from both species were aligned using a hierarchical clustering algorithm in the Multialin online software (Copert, 1988).

Species-specific primers for each target gene were designed in the conserved nucleotide regions between the CDS from both scallops and mussels using the NCBI primer-BLAST design tool (https://www.ncbi.nlm.nih.gov/tools/primer-blast/), taking into account an amplification product size ranged from 150 to 200 bp. The primer pairs (Suppl. Table. S1) were tested by Real-Time qPCR to verify their specificity (a single amplification product), the absence of primer dimers, and their target transcript amplification efficiency (Andersen *et al.,* 2004). The qPCR analyses were performed

on the LightCycler® 480 System (Roche Diagnostics, Indianapolis, IN, USA). The reaction cocktail-mix consisted of 7.5 µL of the SYBR® Green I Master Mix (Roche Diagnostics), 0.5 µM of forward and reverse primers, 5-µL nuclease-free water, and 1 µL of a 1:5-diluted pool of template cDNA dilution (*n* = 10 by species, non DA contaminated animals) in a total volume of 15 µL. Cycling conditions were a preincubation of 5 min at 95 °C, followed by 45 cycles of denaturation for 30 s at 95 °C and extension at 58 °C for 1 min, with ramp rate of 2 °C s^{-1}, followed by 1 min at 72 °C, a final cooling step of 1 min at 40 °C, and a hold at 4 °C. To verify that the selected primer pairs produced only a single product, a dissociation protocol was added after thermocycling, determining dissociation of the PCR products from 65 °C to 95 °C. The assay included a no-template control, a standard curve of four serial dilution points (in steps of 5-fold) of a cDNA pool, and each of the tested primer pairs. Only primer pairs with a single amplicon and no dimer formation were kept for further transcriptomic analysis (Table I). Nevertheless, in both species, most of the primers amplified after 35 cycles of the qPCR; therefore, a droplet digital PCR (ddPCR) strategy was applied to quantify the gene expression on low copy cDNA samples (Whale *et al.,* 2013).

2.6. Droplet digital PCR analysis

Digital droplet PCR was conducted using the Bio-Rad QX200 ddPCR system (Bio-Rad Laboratories, Hercules, CA, USA). Each cDNA sample of both species was amplified for each target gene. One No Template Control (*i.e.*, nuclease-free water) were additionally included for each gene. Each PCR reaction, of a total volume of 22 µL contained 11-µL QX200 ddPCR™ EvaGreen® Supermix, 0.1 µM of each primer, 5-µL nuclease-free water, and 5.5 µL of a 1:10 aqueous template cDNA dilution from each sample. Thereafter, emulsions were generated in the QX200 Droplet Generator (Bio-Rad, Munich, Germany), according to manufacturer's instructions, by mixing for each

sample 20 µL of the PCR mix and 70 µL of Droplet Generation Oil for probes (Bio-Rad, Cat No. 186-4006) . Then, 42.5 µL of the water-oil emulsion were carefully transferred to a ddPCR 96-well plate (Bio-Rad, Cat No. 12001925) and sealed with pierceable foil (Bio-Rad, Cat No. 181-4040). PCRs were performed using a C1000 Touch^{TM} Thermal Cycler with a 96-well Deep Reaction Module (Bio-Rad, Munich, Germany). PCR conditions were exactly the same as those used in the Real-Time qPCR tests described above. Positive fluorescent droplets (containing one amplicon) were then read on a QX200 droplet reader (Bio-Rad, Munich, Germany). On average ddPCR yielded a number of 18,021 accepted droplets, with a standard deviation of 1,225 droplets.Thresholds for positive signals wasere determined manually at 10,000 according to QuantaSoft software instructions. All droplets abovebeyond the fluorescence threshold (10,000) were counted as positive events, and those below as negative events.

Results were analyzed using the Bio-Rad's QuantaSoft software version 1.7.4.0917, where Poisson statistics were applied to determine the target cDNA absolute quantity, expressed as copies of cDNA. μL^{-1} and, calculated according to published formulas (Hindson *et al.,* 2013, Whale *et al.,* 2013).

Table I. Data on genes selected for ddPCR absolute quantification analysis: gene family/symbols, name/description, GenBank ID, forward and reverse sequences, and amplicon length (bp) of each primer pair. *Pm = P. maximus*, *Me = M. edulis*.

Family/Symbol	Gene name/description	GenBank ID	Sense primer (5' -3')	Antisense primer (5' -3')	bp
Autophagy					
Pm-A13	*Autophagy related protein 13-like*	XM_033886103.1	CAGACCGCCAAGGTAGGAAC	GGGGGTCGTTGATCGTTTTG	171
Me-A13		CAJPWZ010000560.1	GGTTGGATCTGTCCCTACACC	AGGAACAAGGTTTGGGGGTT	176
Pm-A16	*Autophagy related protein 16-like*	XM_033904285.1	TCGGCTGTGACTGGTCTAGA	TCCCCGCTGAGTACGTATGA	178
Me-A16		CAJPWZ010001792.1	GCAACAGGGGGTTCAGACAG	TGTAAGAGACCAAACACGGCT	170
Pm-A101	*Autophagy related protein 10-like*	XM_033886478.1	GGGAGATAGGCGTGTTCAGG	CCTGCCGCTCATTCTCATT	178
Me-A101		CAJPWZ010001586.1	CCATGGGAAGTGTGGACCAT	AGTTCGGACTGGTTTGGCAT	170
Glutamate receptors					
Pm-IGR25α	*Ionotropic glutamate receptor 25α*	XM_033900741.1	CCTGGTGGCTGTTTGGGTTT	ACCATAGCAGCACTTCCGTT	160
Me-IGR25α		CAJPWZ010002033.1	TTGGGATGGACAAGGACCAG	AAACCGTCAGGAATGCAGCTA	200
Pm-NMDA1	*Glutamate [NMDA] ionotropic receptor subunit 1-like*	XM_033885630.1	GATCGCTGGAGGGGTAACATC	GAGTCTGCTACCTGTGGCCT	195
Me-NMDA1		CAJPWZ010001507.1	ACCATTAACCCGGAGAGAGC	TAGTGCCACCACATGGACAG	174
Pm-NMDA2	*Glutamate [NMDA] ionotropic receptor subunit 2A-like*	XM_033883213.1	TGCCTAATGGGAGCACAGAG	GTTGTTTGGTGCAGCCGTTT	150
Me-NMDA2		CAJPWZ010002780.1	GTGGCGTGGCATCGTAAATG	TCGCCAGTCTTGTATCCCTG	175
Pm-GRU1	*Glutamate ionotropic kainate receptor U1-like*	XM_033886849.1	ATCGCTCTTGCACCATTCCA	AGCACTAAGGCTGTCGTCAC	197
Me-GRU1		CAJPWZ010002768.1	TCCAGACGGAAAATTCGGCA	CTTCGTTCAGGCTTTCGCAC	189
Solute carriers/ membrane transporters					
Pm-SLC5	*Sodium/glucose vesicular solute carrier/cotransporter 5-like*	XM_033876532.1	TCAGATGACGCTCGGATGG	TAAGCCGCCCACTTTGTTG	182
Me-SLC5		CAJPWZ010000380.1	TCTCTGTGCAGTGTACATCC	AGTCAGCTTGTTCCCCAG	150
Pm-SLC5A1	*Sodium-dependent glucose vesicular carrier/transporter 5A1-like*	XM_033906500.1	TTGCGAAAGGCCAGATTGG	TGAGCTAACAGGAGAGACCG	169
Me-SLC5A1		CAJPWZ010002902.1	GGGACAATGCTGATCTCCG	GCATGTCCTCTCCTAGCCAAG	199
Pm-SLC17	*Vesicular glutamate/sialin-like transporter*	XM_033871282.1	GCCATGAGTGCTATGTGGG	CACCCAAGGACACCGAATATG	184
Me-SLC17		CAJPWZ010002227.1	GGAAACAGTCAAAGGAGGACC	CTCTCATGTCATCGCCACC	182
Pm- SLC16A10	*Monocarboxylate transporter 10-like*	XM_033885380.1	GACAATCTTGCGGCGATGG	CCGATTAGCGCAACACCAAG	152
Me- SLC16A10		CAJPWZ010000369.1	TGCACATAACGCATTGGGAG	CATACCCGCTGAGATAGGC	184
Pm- SLC6A9	*Sodium and chloride-dependent glycine transporter 1-like*	XM_033895916.1	CGTTTACTTGACCCCCGTG	GATGACGAGACCAGCGAAC	183
Me- SLC6A9		CAJPWZ010002160.1	TGGTCAAGTCACGAATGG	AACGGAGTAACGCATGGC	151
Pm- SLC22A8	*Organic anion solute carrier/transporter 5-like*	XM_033904264.1	CTTTTGGGCGTAGGATGGTTG	GCAATAAGGCAAACGCTGTCT	187
Me- SLC22A8		CAJPWZ010002518.1	ACAGACATAGCTGACCACCTG	ACATCCGGGTATTCTCCGTG	186
Pm- AVT1J-like	*Proton-coupled amino acid transporter*	XM_033884846.1	CACCCTCTTCGGAGTTGG	GCGGTTGCTATGGTAGCTC	195
Me- AVT1J-like		CAJPWZ010001622.1	CCTCCGAATACGTGTGTCC	CTGGGTAGTGTGCCTTCC	191

Antioxidant/detoxification system					
Pm- P5CR2	*Pyrroline-5-carboxylate reductase 2-like*	XP_033727520.1	CATAAGTGCCCCTCGGAACC	CGAGGGACATGGCTGTGAAAC	173
Me- P5CR2		CAJPWZ010003088.1	GATGGTGGTGGATGGATCG	CTTCGCCATCTCTCGTTTCC	200
Pm-GStAlike	*Glutathione S-transferase A-like*	XM_033870699.1	CTTAACCCCAGAGGCCAG	GTTGTTATGCGCCTCATGC	180
Me-GStAlike		CAJPWZ010002200.1	CGAAACCAGATGAACCAGGC	CACTCCCCTTCTCCTTGTG	151
Pm- ST1A2	*Sulfotransferase 1A2-like*	XM_033891178.1	GGATAACGTGAGGAGGGAGC	GCGTAAACGTCTTTGTGGC	198
Me- ST1A2		CAJPWZ010001685.1	CGAAAAACGTCGAAATGGCG	GCGACAGGAATCATTGGTC	199
Pm- GCL	*Glutamate--cysteine ligase*	XM_033907205.1	GGAGGAGTTGGACACATCG	CGCCCAGTTAAACAGCTCC	196
Pm- GCL		CAJPWZ010002359.1	CTGAACAAGAAGACCAAGAGG	GCGAGAAGCAGAAGTACGAC	192
Constitutive/Housekeping					
Pm-18S	*18S ribosomal RNA*	XM_033892113.1	GAAGCCGTGCTGTGTTTCAG	ACCACCAGCAAACAGACACA	158
Me-18S		CAJPWZ010001237.1	CATGGGAGCAGTGAAGACCC	TACCCGGACTGCTTACAACG	188

2.7. Domoic acid *in situ* detection and autophagy analysis by immunohistochemistry

In order to localize DA in the digestive glands of *P. maximus* and *M. edulis*, an immunohistochemical (IHC) staining of DA was applied. For this purposes, a third of each sampled slice of DG (30-40 mg) pre-fixed in RNA*later*® solution was dehydrated in ethanol series, cleared in xylene, and embedded in paraffin (Paraplast X-Tra, McCormick Scientific, San Diego, CA, USA). Slides were prepared in 4-µm thick sections using a rotary microtome (Leica RM 2155, Leica Microsystems, Wetzlar, DE) and mounted on polysine-coated glass slides (Sigma-Aldrich, St. Louis, MO, USA).

The IHCtreatment was performed according to the protocol described in García-Corona *et al.* (2022) with minor modifications. Briefly, the slides were deparaffinized in claral and rehydrated in ethanol. Afterwards, tissue sections were incubated overnight with a Goat polyclonal anti-DA primary antibody (0.01 mg mL^{-1}, Eurofins Abraxis®, Warminster, PA, USA) at 4°C. The next day, the slides were incubated at 37 °C for 90 min with a HRP sharped IgG Rabbit anti-Goat secondary antibody (0.001 mg mL^{-1}, abcam®, Cambridge, UK). Finally, samples were revealed with diaminobenzidine (DAB+ Chromogen Substrate Kit, abcam®, Cambridge, UK) for 1 h in darkness at room temperature, counterstained with Harry's hematoxylin, and mounted in Faramount Aqueous Medium (Dako®, Carpinteria, CA, USA).

Three regions from each section of the DG treated by IHC were randomly selected and digitized at high resolution (600 dpi; 63×). Then, counting of total autophagosomes, and autophagosomes with positive DA-immunostaining present in a predetermined area of ~1.33 mm^2 were performed as an estimation of the occurrence of total autophagy and DA-autophagy in the DG of both species (García-Corona *et al.,* in prep a).

2.8. Statistical analysis

All statistical analysis were performed using the computing environment R (R v. 4.0.2, R Core Team, 2020). When needed, data were transformed (log, $1/\chi$, or $\sqrt{\chi}$) prior to analysis to meet *a priori* homoscedasticity (Fligner- Killeen's test) and normality (Lilliefors Kolmogorov-Smirnov test) assumptions (Zar, 2010). To assess the effect of DA exposure (2 levels, control *vs* DA-exposed), the exposure time (3 levels, 0, 40 and 120 min), and their interaction, on DA assimilation, gene expression, and the formation of autophagosomes in the DG, two-way ANOVAs (type II Sum of Squares) were used, in which the above factors were fixed as independent variables, and separately analyzed for each species. When the effect of at least one factor was significant ($P < 0.05$), the Duncan's *post-hoc* multiple range test was used to identify differences between treatment means (Zar, 2010). Gene expression data were transformed to their mean-centered $\log_2$ fold change (mean gene expression value in DA condition versus mean expression value in the control, according to their respective point of exposure time) and plotted in heatmaps.

A Pearson's correlation coefficient was run to calculate the relationship between DA incorporation (iDA) by the DG of both species and the response parameters (autophagy and gene expression). The significance of each correlation was estimated after separate *t*-tests (Hector, 2015). Principal component analysis (PCA) was performed using the FactoMineR package with the factoextra package for data visualization into smaller factorial clusters with a 95% confidence interval. All data matrices were auto-scaled before PCA analysis. The corrplot package was run to calculate the correlation coefficients and their significance between variables and their given PCs. All graphics were generated using the package ggplot2. All values are

expressed as mean ± standard error (SE) except where indicated. Differences were considered statistically significant at α = 0.05 (Hector, 2015).

3. RESULTS

3.1. Domoic acid *in vitro* assimilation

Domoic acid (DA) concentrations in the digestive glands (DG) of scallops *P. maximus* were significantly low at the start of the experiment (4 ± 1.4 mg DA kg^{-1}) and remained negligible in the controls incubated in seawater throughout the experiment (~ 0.02 ± 0.01 mg DA kg^{-1} at both 40 and 120 min) (Fig. 1A). DA uptake sharply increased to 103.9 ± 7.2 mg DA kg^{-1} (P <0.05) after 40 min of incubation in the DA-supplemented medium, and peaked to its significantly higher values of 132.3 ± 9.4 mg DA kg^{-1} after 120 min (Fig. 1A). On the other hand, the amounts of DA in the DG of mussels *M. edulis* were significantly lower compared to those measured in *P. maximus* at the beginning of the experiment (1.3 ± 0.1 mg DA kg^{-1}) and remained negligible after 40 and 120 min of incubation in the control media (~ 2 mg DA kg^{-1}). The amounts of toxin assimilated by the DG increased significantly to 6.7 ± 0.6 mg DA kg^{-1} after 40 min of incubation in the medium supplemented with DA. Thereafter, a slight but not significant decrease in the quantities of DA assimilated by the DG was observed after 120 min (6 ± 0.4 mg DA kg^{-1}) of incubation in the toxin solution (Fig. 1B). As observed in Fig. 1, the DG of the scallops incorporated nearly 20-fold more DA than the DG of the mussels after at both 40 and 120 min of exposure.

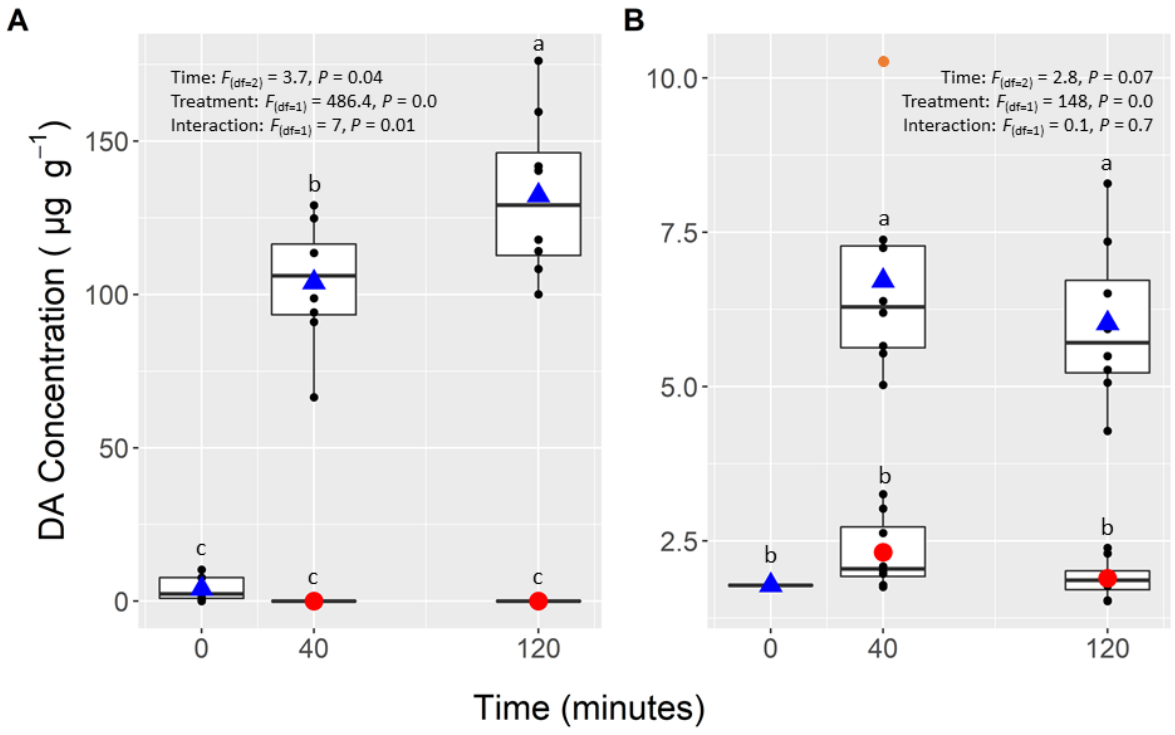

Figure 1. Domoic acid (DA) assimilation by the digestive glands of (A) the scallop *P. maximus* (n = 8), and (B) the mussel *M. edulis* (n = 8) after 0, 40 and 120 min of incubation in a DA-supplemented media (200-µg DA mL^{-1}) and seawater (control). The upper and lower limits of the boxes are the quartiles, the middle horizontal line is the median, the extremes of the vertical lines are the upper and lower limits of the observations, black dots are the individual observations and orange dots are the outliers (values that deviate from the median more than 1.5 times the interquartile range). The blue triangles are the mean of the DA-treated conditions, and the red circles are the mean of the controls. Data were analyzed using the time (three levels) and the treatments (two levels) as independent variables in separate two-way ANOVAs for each species. The *F*-test statistic and degrees of freedom (df) are reported. Different superscript letters denote statistically significant differences between treatments. The level of statistical significance was set at α = 0.05.

3.2. Gene expression analysis

The gene expression analysis using ddPCR revealed differences in the activation of molecular processes supposed to be related to the recognition, transport and metabolism of DA in the digestive glands between both *P. maximus* and *M. edulis* (Fig. 2). In the DG of scallops, all transcripts related to autophagy (A) were strongly and significantly overexpressed after exposure to dissolved DA. Concerning ionotropic glutamate receptors (iGR), only the transcript *NMDA1* had an overexpression (P <0.05) in DG exposed to the toxin, while the receptor *GRU1* showed a significant upregulation with time of incubation but not by treatment. Only the transcripts *SLC17* and *SLC22A8* encoding solute carrier type membrane transporters (SLC/MT) showed high overexpression (P <0.05) due to the exposure of the DG to DA solution in *P. maximus*. Most of these membrane transporters (*e.g. SLC5*, *SLC5A1,* and *SLC6A9*) were regulated (P <0.05) by effect of the time of incubation, but not by effect of the DA exposure. No significant effects were found in the antioxidant or detoxification system (AX/DTX) in the DG of scallops (Fig. 2A).

Conversely, as shown in Fig. 2B, any effect (P >0.05), neither caused by DA exposition nor the incubation time, was found on the genes related to autophagy in the DG of the mussels. Notwithstanding, a high and significant upregulation of all the genes coding for the iGRs (except for the transcript *NMDA1*), as well as all the genes coding for the solute carrier membrane transporters (except *SLC22A8* and *AVT1Jlike*) took place in the DG of *M. edulis* due to DA exposure. Finally, no significant effects (P >0.05) of the exposure to the toxin was observed in the antioxidant or detoxification system on the DG of the mussels (Fig. 2B).

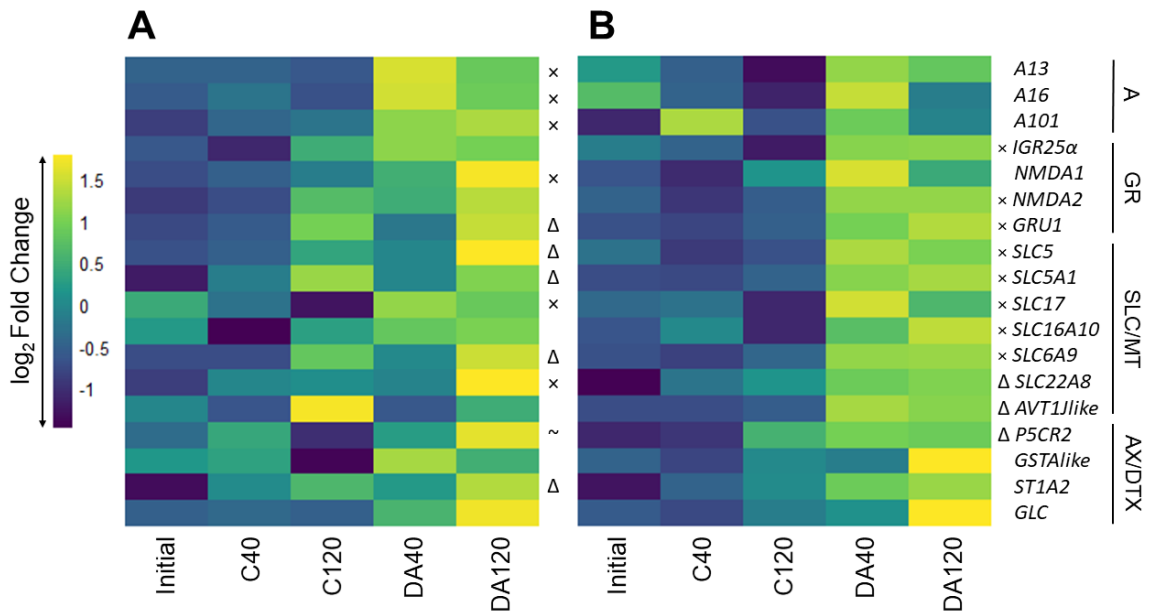

Figure 2. Heat map summarizing differential gene expression (DGE) data for 18 transcripts in the digestive glands of (A) scallops *P. maximus* (n = 8) and (B) mussels *M. edulis* (n = 8) after 0 (initial), 40 and 120 min of *in vitro* incubation in a DA-supplemented media (200-µg DA mL^{-1} = DA) and seawater (controls = C). Gene names are grouped by families according to their biological function along the vertical axis: A= autophagy, GR = glutamate receptors, SLC/MT = solute carriers/membrane transporters, AX/DTX = antioxidant/detoxification system. Color intensity represents the mean-centered log_2 fold change (mean gene expression value in DA condition versus mean expression value in the control, according to their respective point of exposure time) within each row. DGE analysis were performed using the time (three levels) and the treatments (two levels) as independent variables in separate two-way ANOVAs for each transcript by species. Statistically significant differences ($P < 0.05$) in gene expression by effect of the treatment (×), time (Δ), or the interaction of factors (~) are indicated.

3.3. Immunohistochemical detection of domoic acid

Histological sections of the DG of *P. maximus* and *M. edulis* were treated with a specific immunohistochemical (IHC) protocol for the detection of DA as a brown chromogenic staining on the tissues (Fig. 3). As shown in Fig. 3A-C, no anti-DA staining was found in the DG of *P. maximus* at the beginning of the experiment nor in the control conditions. Nevertheless, an intense anti-DA chromogenic staining was localized trapped within small (~ 1-1.5 µm diameter) autophagosomic vesicles (a) in the apical region of the digestive cells (dc) in the digestive diverticula (dd) of the DG of scallops incubated in DA-solution after 40 and 120 min (Fig. 3D-E). Contrariwise, in the DG of *M. edulis* only few autophagosomes (a) were observed in the cytoplasm of the digestive cells (dc), and no brown anti-DA staining was found in the DG of the mussels under any of the experimental conditions of this study (Fig. 3F-J).

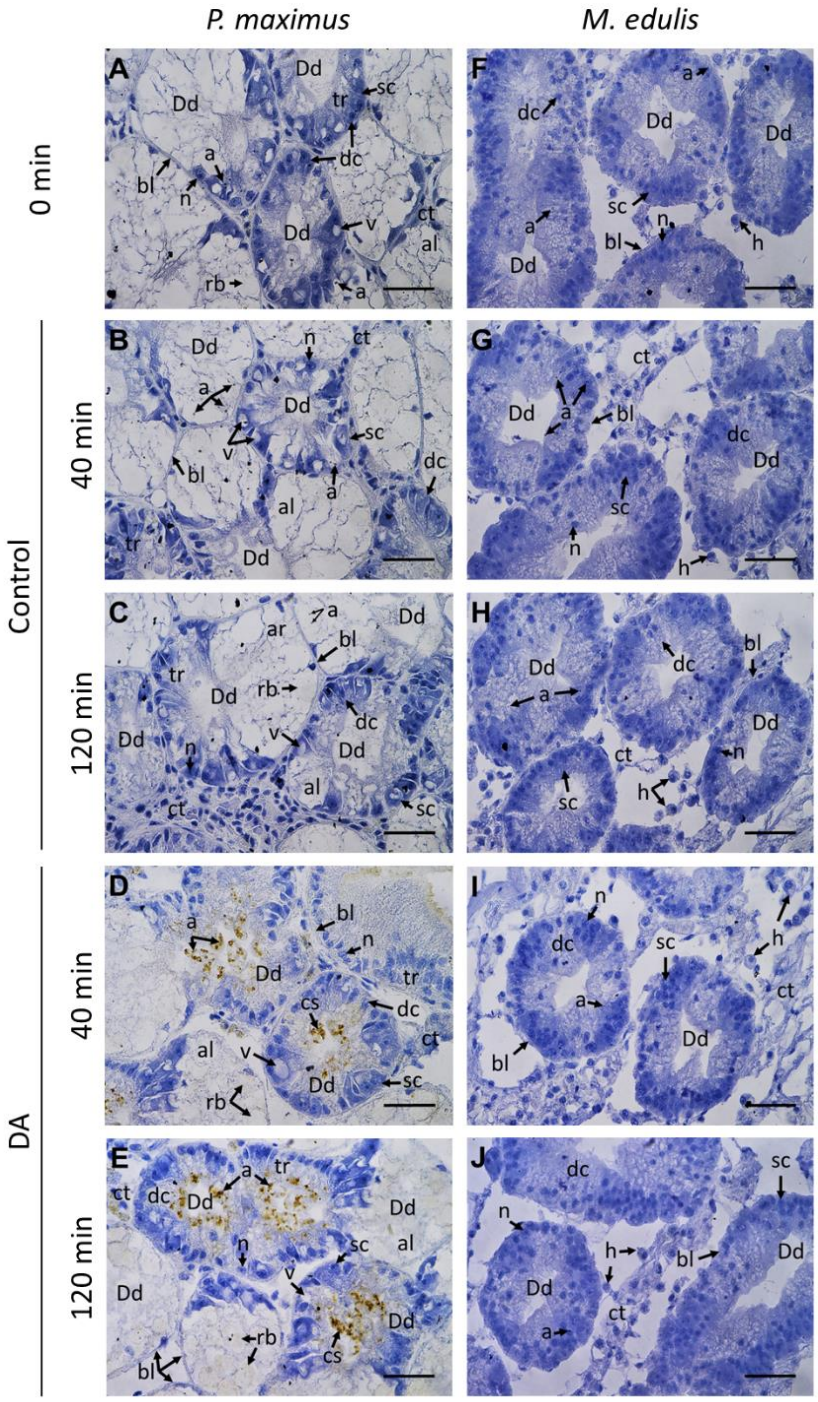

Figure 3. Microphotographs of digestive glands of scallops *P. maximus* (n = 8, A-E) and mussels *M. edulis* (n = 8, F-J) after 0 (A, F), 40 (B-G, D-I) and 120 (C-H, E-J) min of incubation in a DA-supplemented media (200-µg DA mL^{-1} = DA) and seawater (control). Tissue sections were stained with a specific anti-DA immunohistochemical (IHC) technique using a primary anti-DA antibody (0.01 mg mL^{-1}) and a HRP-conjugated secondary antibody (0.001 mg mL^{-1}). a = autophagosomes, Dd = digestive diverticulum, al = adipocyte-like digestive cell, bl = basal lamina, cs = positive anti-DA chromogenic signal, ct = connective tissue, dc = digestive cells, hc = hemocytes, rb = residual bodies, sc = secretory cells, tr = tubular region. Scale bar: 63× = 30 µm.

Quantitative analysis of histological slides showed maximum frequencies (P <0.05) of total autophagy in the DG of *P. maximus* incubated in DA-supplemented media, while the significantly lowest were registered at the beginning of the experiment, as well as in the controls (Table II). The total number of autophagosomes in the DG of *M. edulis* were not different (P >0.05) in any of the treatments tested in this work. Since anti-DA staining was only observed in the DG of scallops incubated in DA solution, the frequencies of autophagosomes labeled with brown staining corresponding to the toxin were only obtained in the DG of *P. maximus* incubated in DA solution at 40 and 120 min (Table II).

Table II. Total autophagy and immune-positive DA autophagy (autophagosomes. area^{-1}) in the digestive glands of the scallop *P. maximus* (n = 8), and the mussel *M. edulis* (n = 8) after 0, 40 and 120 min of incubation in a DA-supplemented media (= DA, 200-µg DA mL^{-1}) and seawater (Control). NA: not available (not enough data), "—": no chromogenic anti-DA staining.

	Exposure time/ treatment					Statistical analysis		
	0 min	40 min		120 min				
		DA	Control	DA	Control			
Total autophagy								
P. maximus	33.5 ± 2.9^{b}	68.8 ± 4.1^{a}	32.7 ± 2.9^{b}	69.7 ± 4.4^{a}	33.4 ± 2.7^{b}	Time: Treatment: Interaction:	$F_{(df = 2)}$ = 10.4, $F_{(df = 1)}$ = 109.7, $F_{(df = 1)}$ = 0.002,	$P < 0.0001$ $P < 0.0001$ $P > 0.05$
M. edulis	8.5 ± 1^{a}	8.1 ± 0.9^{a}	9 ± 0.8^{a}	9.2 ± 1.1^{a}	7.5 ± 1^{a}	Time: Treatment: Interaction:	$F_{(df = 2)}$ = 0.024, $F_{(df = 1)}$ = 0.2, $F_{(df = 1)}$ = 1.8,	$P > 0.05$ $P > 0.05$ $P > 0.05$
DA autophagy								
P. maximus	—	51.8 ± 3.7^{a}	—	51.5 ± 3.6^{a}	—	Time: Treatment: Interaction:	$F_{(df = 2)}$ = 49.9, $F_{(df = 1)}$ = 499.1, $F_{(df = 1)}$ = 0.004,	$P < 0.0001$ $P < 0.0001$ $P > 0.05$
M. edulis	—	—	—	—	—	NA		

Results are expressed as mean ± SE. Data were analyzed using the exposure time (three levels) and the experimental condition (two levels) as factors in separate two-way ANOVA's ($P < 0.05$). The F-test statistic and degrees of freedom (df) are reported. Different superscript letters indicate significant differences between treatments. The level of statistical significance was set at $\alpha = 0.05$.

3.4. Integrative analysis compiling DA assimilation, gene expression, and subcellular features

The correlation coefficients between DA uptake with subcellular and gene expression parameters in the DG of *P. maximus* and *M. edulis* after DA exposure. A strong and significant correlation was found between the incorporation of DA and the activation of autophagy at the subcellular (r = ~0.9) and molecular (r = ~0.5) level in *P. maximus*. In scallops the expression of only one iGR (NMDA1) and the SLC (SLC5) were correlated with DA concentrations in digestive cells. Conversely, in the DG of mussels exposed to the toxin, it was observed that the expression of all iGRs and most of the SLCs (except the *SLC22A8* and *AVT1Jlike*) were correlated ($P < 0.05$) with the uptake of DA in the GDs. No relationship was found between the DA assimilation and the activation of the antioxidant system of both species (Table III).

Table III. Pearson's correlation coefficient (*r*) between domoic acid (DA) assimilation by the digestive glands of the scallops *P. maximus* and the mussels *M. edulis* after 40 and 120 min of incubation in a DA-supplemented media (200-µg DA mL^{-1}), and autophagy and gene expression parameters. NA: not available (not enough data).

	P. maximus	*M. edulis*
Autophagy		
Total autophagy	0.83*	0.03
DA autophagy	0.96*	NA
Gene expression		
Autophagy		
A13	0.49*	0.11
A16	0.45*	0.47
A101	0.52*	0.27
Glutamate Receptor		
IGR25A	0.31	0.51*
NMDA1	0.41*	0.42*
NMDA2	0.32	0.48*
GRU1	0.33	0.48*
Solute carriers		
SLC5	0.65*	0.44*
SLC5A1	0.19	0.37*
SLC17	0.31	0.41*
SLC16A10	0.15	0.42*
SLC6A9	0.26	0.49*
SLC22A8	0.28	0.26
AVT1Jlike	0.17	0.28
Detoxification/ antioxidant system		
P5CR2	0.27	0.25
GSTAlike	0.12	0.11
ST1A2	0.32	0.06
GLC	0.21	0.28

*Significant correlation after separate *t*-test at $P < 0.05$.

A principal component analysis (PCA) was computed to summarize all variables measured in the DG on the two bivalve species compared in this work: DA assimilation, gene expression, and subcellular parameters (Fig. 4). For the whole data set of *P. maximus* (Fig. 4A), the PCA described 43.4 % of the total variance of the data along the first two dimensions. The clustering-PCA provided a clear distinction between controls and DA-exposed conditions. The incorporated DA (iDA), the histological parameters of total autophagy (Ta) and DA-autoutophagy (DAa), as wells as the expression of all the transcripts related to autophagy (*A16*, *A13,* and *A101*), and the solute carrier membrane transporter *SLC17* were significantly correlated (r = ~ 0.5) within the dimension/principal component 1 (PC1, 28% of the total variance). Whereas the dimension/principal component 2 (PC2, 15.4% of the total variance) mainly explained the expression of the genes *GLC* and *GSTAlike*, related to the antioxidant/detoxification system, as well as the solute carriers *SLC5* and *SLC22A8* (Fig. 4A).

On the other hand, the PCA performed for the data of *M. edulis* explained 40.4% of the total variance within the first two dimensions (Fig. 4B). The scatter plot revealed a clear distinction between the DG incubated in DA solution during 40 min and the controls, which were grouped separately. Nonetheless, as observed on Fig. 4B, the group of the DG exposed to DA for 120 min showed similar scores on the principal components to those of the controls and the DG exposed to DA during 40 min, slightly overlapping with all the groups.The expression levels of the glutamate receptors *NMDA2* and *GRU1,* as well as most of solute carriers (except the *SLC5*) were highly correlated (r = 0.6-0.8, P <0.05 P <0.05) within the dimension/PC1, that explained 28.8% of the total variance. The dimension/PC2 (11.6 % of the total variance) explained the expression of the genes *IGR25A*, *SLC5*, *A16*, and *GSTAlike.*

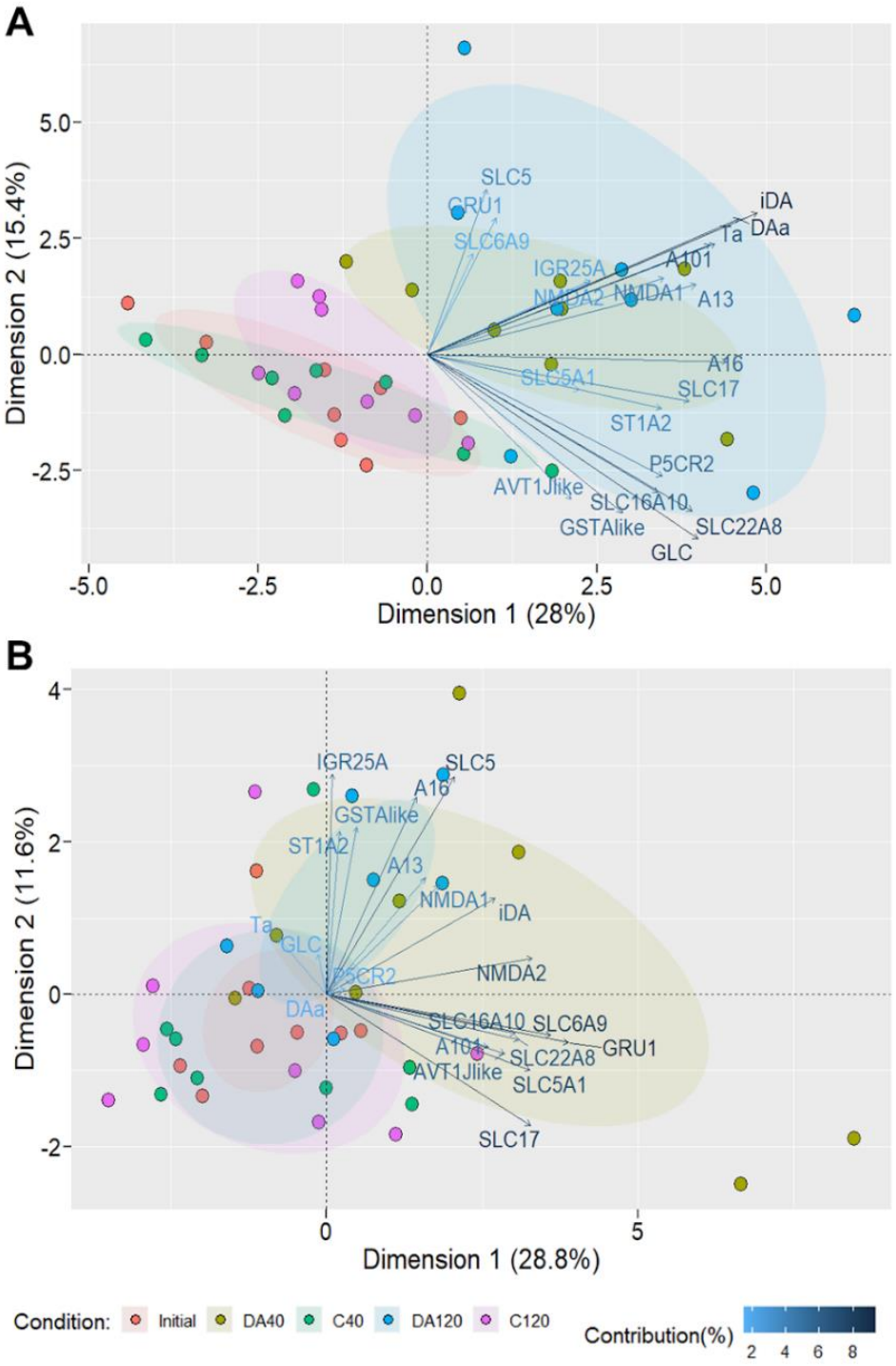

Figure 4. Results of principal component analysis (PCA) of digestive glands of (A) scallops *P. maximus* (n = 8) and (B) mussels *M. edulis* (n = 8) after 0 (initial), 40 and 120 min of incubation in a DA-supplemented media (200-µg DA mL^{-1} = DA) and seawater (controls = C). The direction of the arrows shows the correlations of variables (incorporated DA = iDA, total autophagy = Ta, DA autophagy = DAa, and expression of the several genes) with given principal components, and its color intensity shows their contribution (%) to the explained variance. Each point corresponds to an individual observation and the confidence ellipses shows how the individual observations from each experimental conditions are related to the others using factor scores.

4. DISCUSSION

The aim of this study was to carry out an integrative physiological study on two bivalve species with different capabilities to depurate DA in order to fill the gaps in the comprehension of the physiological mechanisms involved in uptake and elimination of this toxin in bivalves. All data in this study pointed to autophagy as the likely mechanism explaining DA retention in the scallop *P. maximus* compared to fast depurators, such as *M. edulis,* as proposed by Corona *et al.* (2022 and in prep a and b). In fact, an up-regulation of genes coding for proteins related to autophagy as well as sequestration of DA into autophagosomes were observed following *in vitro* DA incorporation in the DG of *P. maximus,* while these mechanisms did not appear activated in *M. edulis* in presence of DA. . A similar pattern was reported by García-Corona *et al.* (in prep b) after comparing the subcellular localization of DA in several contaminated invertebrates after *P. australis* blooms, where DA-autophagy appeared to be a species-specific mechanism triggered mainly in the species that beared the highest amounts of toxin in the DG, such as the scallops *P. maximus* and *A. opercularis*, but also the snail *C. fornicata*, while species like the clam *D. trunculus,* and the seasquirt *Asterocarpa spp.,* that retained the lowest DA-burdens, also exhibited the lowest frequencies of DA-autophagy. Furthermore, the overexpression of the three autophagy-related proteins evaluated in this work was also found by Ventoso *et al.* (2021) in the DG of *P. maximus* after intramuscular injection of a DA solution. Through autophagy cells are capable of incorporating exogenous compounds, such as DA, by endocytosis or pinocytosis, forming vesicles that deliver their cargo-contents to the lysosomal enzymatic degradation system for the subsequent excretion of waste products by exocytosis (Cuervo, 2004; Kruppa *et al.,* 2016; Zhao *et al.,* 2021). Notwithstanding, for autophagy to occur, extracellular compounds have to be forcibly

recognized by specific membrane receptors (McMillan, 2018; Zhao *et al.,* 2021). Therefore, the study and characterization of membrane receptors orchestrating the signaling cascade for DA autophagy in the digestive cells of some marine invertebrates, and particularly in *P. maximus* deserve further research.

Concerning the recognition of DA by the cells, it is well known that DA is a potent agonist of a high variety of ionotropic glutamate receptors (iGRs) divided into large families classified as kainateα-amino-5-methyl-3-hydroxyisoxazolone-4-propionate (AMPA), kainate (KA), and N-methyl-D-aspartate (NMDA), widely distributed in vertebrates central nervous system of vertebrates (Perl *et al.,* 1990; Lefebvre and Robertson, 2010; La Barre *et al.,* 2014). DA exhibits a 3 to 100-fold higher affinity for this type of iGR's than for its structural analogs, glutamate and kanaic acid being the major excitatory neurotransmitters, particularly in the brain of mammals (Todd, 1993; Zaman *et al.,* 1997; McCabe *et al.,* 2016; Zabaglo *et al.,* 2016). The fixation of DA on NMDA or AMPA, ligand-gated ion channels selective to Na^{+}, K^{+}, and Ca^{2+}, explains its excitotoxicity (Hampson & Manalo, 1998; Ramsdell, 2007; Pulido, 2008) through the depolarization and release of glutamate into the synapse, causing an uncontrolled influx of Ca^{+2} into the cell followed by degeneration and permanent neural damage (Perl *et al.,* 1990; Miller *et al.,* 2021). Although the vast existing knowledge on the involvement of iGRs in DA neurotoxicity in mammals, the activation pathways of these receptors, and their influence on DA-toxicokinetics in bivalves remain poorly understood. In this work, only one of the four iGRs evaluated, NMDA1, showed overexpression in the digestive glands of *P. maximus* incubated in DA solution, while all the four iGRs (NMDA1, NMDA2, IGR25a and GRU1) were overexpressed in *M. edulis*. These results partially meet with those of Ventoso *et al.* (2021) since none of the ten genes coding for iGRs identified in the transcriptome of digestive glands of *P.*

maximus was differentially expressed after intramuscular injection with DA. Our findings also coincide with Ventoso *et al.* (2019) who observed a downregulation of two transcripts encoding for NMDA receptors and five for KA receptors in the digestive gland of *A. opercularis* after blooms of toxic *Pseudo-nitzschia spp*. Adversely, the three non-activated iGRs by the effect of the toxin in *P. maximus* were overexpressed in the digestive glands of *M. edulis* after DA exposure, thus suggesting that mussels could have high-affinity DA receptors, conferring it a better toxin recognition, but lower DA-binding capabilities than scallops. Indeed, Trainer and Bill (2004) found that the slow DA-depurator *S. patula* is capable to express low-affinity glutamate receptors in all tissues, and selectively expressing both high-affinity but low DA-binding capacity receptors, and low-affinity but high DA-binding capacity receptors in the siphon, hypothesizing that it may be via these low-affinity but high toxin-capacity sites that razor clams retain DA for long periods of time. This is likely to happen in the digestive gland of *P. maximus* when exposed to DA, thereby allowing slow DA-depurators to prevent toxification. Through integrated genomic, evolutionary and transcriptomic analyses, it has been demonstrated that iGRs are well conserved in bivalves, where this particular family of genes have experienced a rapid expansion of variants. The scallop *P. maximus* exhibits ubiquitously high expression and altered high-ligand selectivity, which may contribute to the remarkable tolerance to DA in this species (Zeng *et al.,* 2021). The evidence discussed above, and the unparallel expression of iGR between both scallops and mussels found in this study rises a new inquiry: could the differential activation of the iGRs be involved in specific DA-recognition, and the consequent activation of a complex membrane transporting system linked to the entry or exit of the toxin in the digestive cells of bivalves?

This work highlights the profound differences in the activation and regulation of several membrane transporter proteins between *P. maximus* and *M. edulis* at the molecular level. Membrane transporters are specialized proteins that translocate hydrosoluble substances across the lipid cellular membranes, often playing key roles in determining accumulation of exogenous compounds within cells (Lin *et al.,* 2015; Song *et al.,* 2020). Generally membrane transporters can be molecularly and mechanistically classified within two major super-families: the ATP-binding cassette (ABC) family, and the solute carrier (SLC) family. ABC transporters are primary active transporters that require ATP hydrolysis for substrate transport against a concentration gradient and they are mainly efflux transporters, mediating the transfer of compounds out of the cells; while the SLC family members utilize an electrochemical potential difference or an ion gradient generated by primary active transporters to facilitate the mobilization of small molecules through passive diffusion into the cell and are thus categorized as facilitated transporters or secondary active transporters (You & Morris, 2007; Hong, 2017). Nonetheless, there is evidence that some SLC transporters function as bidirectional influx-efflux transporters (Song *et al.,* 2020). DA is a zwitterionic compound, therefore needing transport proteins to cross the cell membrane, as demonstrated in mytilids (Madhyastha *et al.,* 1991; Pazos *et al.,* 2017; Blanco *et al.,* 2021a) and as in the case of glutamic acid in mammals (Smith *et al.,* 2000; Kimura *et al.,* 2011). Taking this into account, it could be expected that some proteins related to membrane transporters, and potentially some belonging to the SLC family could be involved in the absorption or excretion of DA in bivalves.

In this work, the expression profiles of seven SLC-type transporter proteins were compared in digestive glands of *P. maximus* and *M. edulis* exposed to DA to infer whether this mechanism of passive transport is involved in the differences in the

toxicokinetics of the toxin between both species. In scallops, only the *SLC17* transporter was overexpressed when the digestive glands were exposed to DA, while in mussels, five (*SLC5, SLC5A1, SLC17, SLC16A10,* and *SLC6A9*) of the seven membrane transporters were upregulated by effect of the toxin. Furthermore, the expression of these transporters was strongly correlated with traffic of DA in the digestive cells of both species, thus inferring the paramount involvement of these proteins in the transport (entry or exit) of this toxin.

The SLC gene series include 52 families and 395 transporter transcripts in the human genome (Hediger *et al.,* 2013; César-Razquin *et al.,* 2015; Lin, *et al.,* 2015), and some of them are responsible for the transmembrane transport of DA in the intestinal barrier of mammals (Kimura *et al.,* 2011). Most studies on SLCs have been performed on model organisms, with 392 SLCs identified in *Mus musculus*, 344 in *Drosophila melanogaster*, and 348 in *Caenorhabditis elegans*. Yet, the total number, copy amounts, and SLC sub-families vary greatly among species (Höglound *et al.,* 2010; Xun *et al.,* 2020). By far, in the course of the last decade, and thanks to the advancement of genomic-functional tools, knowledge related to the involvement of these proteins in the accumulation, translocation and detoxification in mussels (Pazos *et al.,* 2017), oysters (Matt *et al.,* 2018), scallops (Xun *et al.,* 2020; Ventoso *et al.,* 2019; Wang *et al.,* 2022), and fish (Zhang *et al.,* 2022) has increased.

The significant upregulation of the *SLC17* transporter in the digestive glands of *P. maximus* was strongly correlated with the expression of the three proteins related to autophagy due to the effect of DA exposure. Among the top upregulated genes in the digestive gland of *M. galloprovincialis* after exposure to DA-producing *Pseudo-nitzschia spp.*, Pazos *et al.* (2017) found that the *SLC17A5* protein and three other transcripts from the same family were involved in sialin transport. Globally, this family

mediates the transmembrane transport of organic anions (Reimer, 2013) with a dominance in the trafficking of sialin (*SLC17A5*) and glutamate through vesicular transport. In mammals, sialin transports sialic acid to lysosomes for enzymatic processing through autophagy, but may also function as a vesicular transporter for aspartic acid and glutamic acid, regulating the neurotransmitter concentrations in the synaptic cleft to affect proper signaling between neurons (Gether *et al.,* 2006; Miyaji *et al.,* 2008, 2011; Reimer, 2013). This evidence points to the vesicular sialin and glutamate transporters of the *SLC17* family might be involved in the transport and processing of DA throught autophagy, since this toxin shares structural characteristics with glutamic acid. This turns this family of transporters into interesting candidates for future characterization and functionality of DA toxicokinetics analyses.

The expression of the *SLC5* transporter was closely correlated with the incorporation of DA in the DG of *P. maximus*, while the two genes of this family (*SLC5* and *SLC5A1*) were significantly upregulated in *M. edulis* by effect of DA exposure. Even though relatively little is known about the role of the *SLC5* family in DA transport, members of *SLC5* have been designated as diverse functional and highly expanded transporters in scallops (Xun *et al.,* 2020). These sodium dependent-glucose vesicular carriers participate actively in the absorption of paralytic shellfish toxins (PSTs) produced by dinoflagellates in the digestive glands DG of the scallops *Patinopecten yessoensis* (Xun *et al.,* 2020) and in the gills of *Chlamys farreri* (Li *et al.,* 2017; Wang *et al.,* 2022). Moreover, six protein carriers of this type showed high affinity for the loading of PSTs in *C. gigas* (Mat *et al.,* 2018). Hence, a strong implication of this family in the accumulation of DA in both *P. maximus* and *M. edulis* cannot be discarded.

There was a gene belonging to the *SLC6* sodium-and chloride-dependent neurotransmitter family (the *SLC6A9*) only upregulated in the DG of *M. edulis*

incubated in DA. Indeed, some members of the *SLC6* family are also glutamate transporters (Gether *et al.,* 2006). Moreover, the *SLC6A8* was overexpressed in zebrafish brain after DA exposure (Lefebvre *et al.,* 2009), while the *SLC6A14* was found among the SLCs responsible for the translocation, depuration and high tolerance to tetrodoxin in the liver of the pufferfish *Takifugu rubripes* (Zhang *et al.,* 2022). This allowed us to assume that the transporter *SLC6A9* would be likely involved in a rapid eflux than in an influx transport of DA in *M. edulis.* Another interesting result in this study was the opposite pattern of overexpression between the transporters *SLC22A8* (organic-anion transporter) and *SLC16A10* (monocarboxylate transporter) by effect of the toxin in scallops and mussels. The large differences in the final concentrations of DA in the digestive glands of both species lead to hypothesize that the *SLC22A8* would be involved in the entry of the toxin into the digestive cells of *P. maximus*; conversely, the *SLC16A10* transporter would be implicated in the excretion of the toxin in *M. edulis*. A high number of differentially expressed transcripts belonging to these three families (*SLC6, SLC22* and *SLC16*) was found in the digestive glands of *M. galloprovinciallis* (Pazos *et al.,* 2017) and *A. opercularis* (Ventoso *et al.,* 2019) exposed to DA-producing *Pseudo-nitzschia spp*. The family *SLC22* comprises organic cation/anion/zwitterion transporters, which mediate the absorption (in the small intestine) and excretion (in the liver and kidney) of variety of smaller and highly hydrophilic substrates such as various drugs and toxins in mammals (Roth *et al.,* 2012; Koepsell *et al.,* 2013; Nigam, 2015). On the other hand, the *SLC16* family comprises a total of 14 members that share highly conserved motifs, exhibiting a broad substrate specificity (Halestrap, 2013; Song *et al.,* 2020). The *SLC16* family includes efficient lactate exporters, and has shown responsibility in the traffic through the plasma membrane of monocarboxylated compounds, as well as weak organic acids in the human intestine (Meredith and

Christian, 2008; Steffansen *et al.,* 2004), where the transport direction is determined by the concentration gradients of the substrates (Song *et al.,* 2020). Hence, the unequivocal identification of the specificity and flux-direction of DA through these SLCs in bivalves will require further study.

All the families of SLCs that showed differential expression between *P. maximus* and *M. edulis* in this work (*SLC5, SLC17, SLC6, SLC16* and *SLC22*) have also shown a high expansion and diversification in the genomes of the scallops *P. yessoensis* (Xun *et al.,* 2020) and *C. farreri* (Li *et al.,* 2017; Wang *et al.,* 2022), being highly correlated with toxin accumulation after exposure to PST-producing *Alexandrium spp*. Particularly the DG of bivalves harbor the significant expansion of these transporters which might contribute to the adaptive evolution of bivalves to tolerate and survive in environments with toxic microalgae (Xun *et al.,* 2020). The rapid expansion and functional novelty of SLCs in bivalves genome has led to alterations at important recognition sites of the proteins (Hong, 2017; Xun *et al.,* 2020), explaining the vast diversity of trafficked substances across the membrane or the ability of the transporters to interact with different substrates.

Although the evidence in the literature is strongly biased towards the involvement of *SLC* transporters in the entry of phycotoxins, the rapid depuration of DA initially assimilated by the digestive cells through this type of transporters in rapid-depurators cannot be excluded, which could also explain the enormous differences in DA final concentrations found between scallops and mussels in this work. This evidence also reinforces the idea of Mauriz and Blanco (2010) since probably some of the *SLC* transporters found upregulated in *M. edulis* are much more efficient to excrete the toxin from the cells than those of *P. maximus*. Moreover, after the characterization of the DA uptake process in the digestive glands of *M. galloprovinciallis*, Blanco *et al.* (2021a)

stated that even if the transporters involved in the uptake of the toxin have similar characteristics among slow and fast-DA depurators, toxin accumulation would be expected to be substantially higher in the formers, as occurred in this work in the DG of *P. maximus*, whit a DA uptake nearly 20-fold higher than in *M. edulis*.

The integrative analysis combining the DA uptake, subcellular features, and the activation of specific genes revealed that, in the digestive gland of *P. maximus,* a higher DA-incorporation was strongly associated with autophagy at the subcellular and molecular level strengthening the idea suggesting this physiological mechanism is behind the long retention of DA in this species (Fig. 5A). Furthermore, differences in DA accumulation, and the gene expression analyses point to a poor-recognition capacity of the toxin on the digestive cells and a less efficient excretion of DA trought the *SLC*s in *P. maximus* (Fig. 5A). Meanwhile, the scarce DA-accumulation in the DG of mussels showed an intricate relationship with the activation of the iGRs and with the expression of almost all *SLCs* proteins in the DG of *M. edulis*, which could indicate a potential implication of glutamate receptors in recognizing the toxin on the outer side of the cell membrane, thus triggering its influx, but a much more efficient efflux transport of this toxin across the digestive cells in the mussels (Fig. 5B).

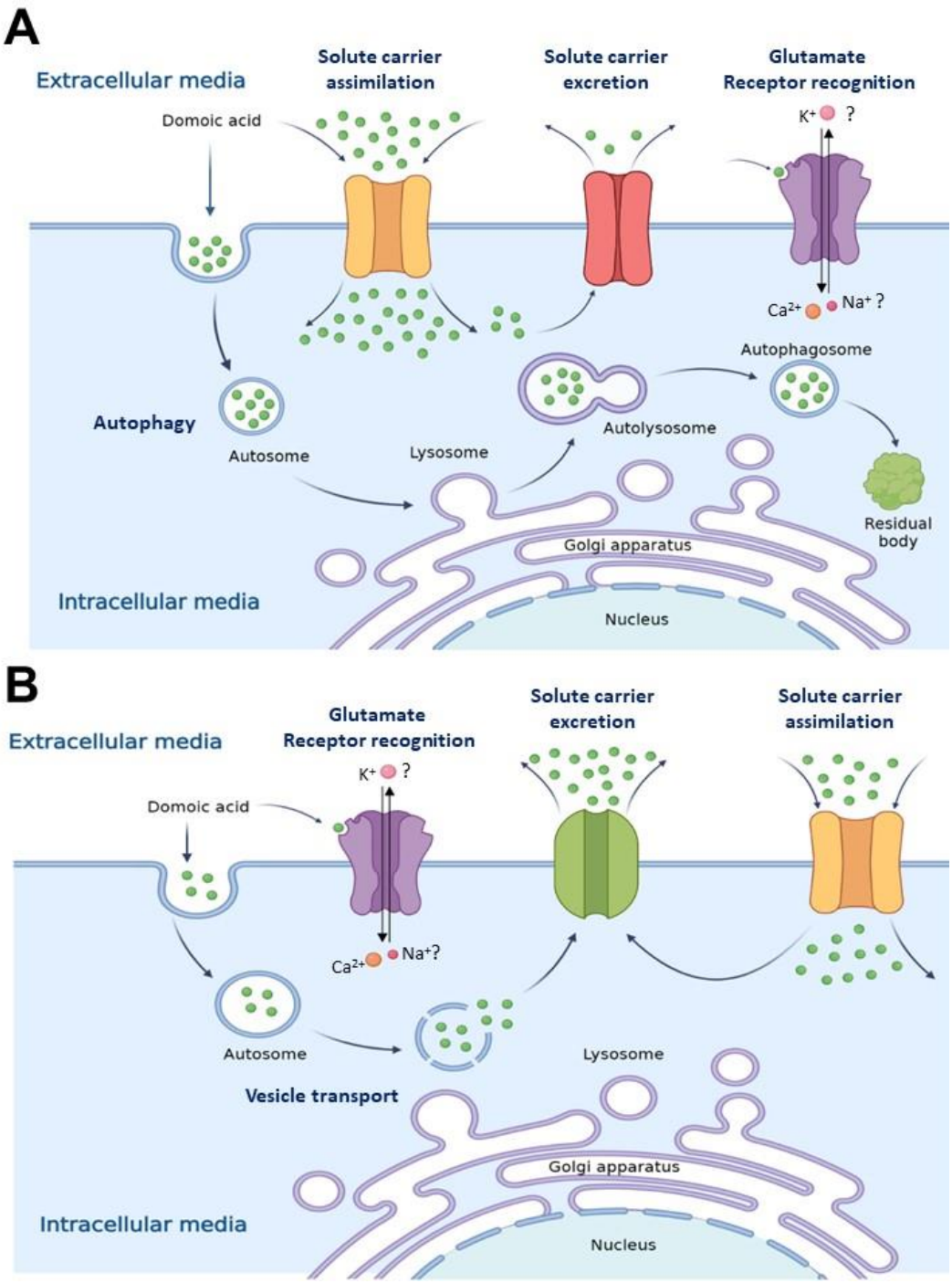

Figure 5. Conceptual summary of the potential physiological mechanisms implicated in the recognition, assimilation, and excretion of DA in the digestive cells of marine bivalves classified as (A) slow DA-depurators and (B) fast DA-depurators. Schematic illustrations were constructed using the BioRender (https://biorender.io) online tool based on the results of gene expression analysis by ddPCR and the microanatomical observations by anti-DA immunohistochemical (IHC) analysis of the digestive glands of *P. maximus* and *M. edulis* exposed *in vitro* to dissolved DA in this study, as well as from the subcellular and transcriptomic results published in the literature for these and other species of marine bivalves exposed to toxic *Pseudo-nitzschia spp*., or directly exposed to DA. IGR = ionotropic glutamate receptors, MGR = metabotropic glutamate receptors.

Despite the expression of ABC-type membrane transporters was not measured in this work, its further study comparing fast and slow DA-depurators is strongly recommended. In aquatic organisms, ABC proteins have shown effective protection against deleterious effects caused by exposure to a variety of toxic compounds (Jeong *et al.,* 2017), including their potential implication on phycotoxin excretion in bivalves (Huang *et al.,* 2014; Lozano *et al.,* 2015; Xu *et al.,* 2014). Previous RNA-seq studies have revealed that a wide variety of upregulated ABC transporters behind the translocation and detoxification process of accumulated PSTs in *C. gigas* (Matt *et al.,* 2018), *P. yessoensis* (Xun *et al.,* 2020), and *C. farreri* (Wang *et al.,* 2022), as well as okadaic acid in the scallop *Argopecten irradians* (Chi *et al.,* 2018), and tetrodotoxin (TTX) in the fish *T. rubripes* (Zhang *et al.,* 2022). Other transcriptomic studies have only identified the differential regulation of member numbers of this group of transporters after exposure to DA-producing *Pseudo-nitzschia*, as in the case of *M. galloprovinciallis* (Pazos *et al.,* 2017) and *A. opercularis* (Ventoso *et al.,* 2019) suggesting its involvement in the uptake or excretion of DA in the DG of this organisms. Schultz *et al.* (2013) hypothesized that DA-absorption from the foregut and transfer into the hepatopancreas and hemolymph was regulated by unidirectional ABC transporters in Dungeness crabs *Metacarcinus magister.* However, this contradicts the findings of Blanco *et al.* (2021a) since in the DG of *M. galloprovincialis* the mechanism of DA uptake seems to be independent of ATP, H+ or Na+, but it is dependent on Cl- or other anions. Most of the *SLCs* evaluated in this study, despite being Na+ dependent, are also Cl- dependent, which reinforces the findings of Blanco *et al.* (2021a) pointing to the involvement of these transporters in DA traffic in the DG of bivalves.

A significant activation of some candidate proteins related to xenobiotic metabolism was expected in this work after DA-exposure of the DG of *P. maximus* and *M. edulis*. Nevertheless, any of the enzymes involved in antioxidant defense/detoxification showed differential expression due to the effect of the toxin in either of both species. A great number of genes or proteins involved in detoxification and antioxidant metabolism have been identified when several bivalve species were exposed to harmful microalgae or their respective toxins. Among the most commonly reported families of detoxification enzymes are the cytochromes P450, aldo-keto reductases, glutathione S-transferases (GST), sulfotransferases (ST), glutathione peroxidase (GPx), superoxide dismutase (SOD), and 70-kDa heat shock protein (HSP70). Most of these enzymes have been identified in tissues of scallops (Lou *et al.,* 2020; Wang *et al.,* 2022) and oysters (Fabioux *et al.,* 2015; Matt *et al.,* 2018) exposed to PST-producing algae, implying their antioxidant/detoxification role in toxin resistance. Notably, the GST and ST, have shown strong upregulation in the transcriptomes of *M. galloprovinciallis* (Pazos *et al.,* 2017) and *A. opercularis* (Ventoso *et al.,* 2019) in response to the accumulation of DA in the DG, which indicates their potential effects on the mediation of harmful effects linked to ASP-toxin absoption. Even when the evidence of this work indicates that biotransformation is not the main route of DA elimination in both scallops and mussels, the evidence discussed above stress that some effects of enzymes involved in DA-biotransofrmation cannot be discarded under a natural DA-contamination scenario.

Adaptative evolution probably couples with combination of acquisition of new genes and modification of existing genes driven by positive selection under the environment with DA, implying the diverse role of physiological mechanisms in regulating DA accumulation in bivalves. Studies at the transcriptomic and proteomic level are

essential to elucidate which SLCs may be prone to be under positive selection, and possibly involved in species/lineage-specific adaptation to cope with DA-producing *Pseudo-nitzschia*. The findings of this work provide unprecedented insights to go further in the proposal of procedures to accelerate the depuration of DA in highly affected bivalves.

5. CONCLUSIONS

The present work underscores that untangling the interaction of implied physiological processes is key to decipher interspecific variability in DA-accumulation among affected shellfish species. Investigation of associations linking DA uptake and differential physiological traits at the subcellular and molecular level offers a new approach for functional analyses of candidate genes/proteins that can lead to a more comprehensive understanding of bivalve-ASP outbreak interactions. This work is also transformative in the field, emphasizing that intertwining of complex metabolic pathways is a cornerstone in bivalves response to DA exposure that cannot be ignored in future studies about ASP blooms effects on marine invertebrates. Associations among DA assimilation, subcellular features, and mRNA levels revealed in this work opened new doors for further studies identifying physiologically-based differences in toxin accumulation between slow and fast DA depurators. The results of this work also emphasize taking into account all the potential biological processes involved in toxin load in providing stakeholders with necessary information to limit the cost of ASP outbreaks in the context of a changing marine environment and aquatic pollution legacy.

Ethics statement

Scallops (*Pecten maximus*) and mussels (*Mytilus edulis*) used in this work were transported and handled according to the International Standards for the Care and Use of Laboratory Animals. The number of sampled organisms contemplated "the rule of maximizing information published and minimizing unnecessary studies". In this sense, 10 scallops and 10 mussels were considered as the minimum number of organisms needed for this work.

Funding

This work received financial support from the research project “MaSCoET” (Maintien du Stock de Coquillages en lien avec la problématique des Efflorescences Toxiques) financed by France Filière Pêche and Brest Métropole. JLGC received a mobility grant funded by the Interdisciplinary graduate School for the blue planet (ISblue) to develop a part of the experiments of this work at the CIMA, Spain, and he is recipient of a doctorate fellowship from CONACyT, Mexico (REF: 2019- 000025-01EXTF-00067).

Acknowledgments

The authors are deeply grateful to Sylvain Enguehard (Novakits, Nantes) for providing the non-commercial primary antibodies necessary to carry out this study, as well as Malwenn Lassudrie, Aouregan Terre-Terrillon, and Amélie Derrien (from Ifremer, Concarneau) for scallop collection and preliminary toxin analysis. We also thank Carmen Mariño and Helena Martín (from CIMA, Vilanova de Arousa), and Tomé Delaire (IUEM-LEMAR, Brest) for their support during experiments, sampling, and domoic acid extractions. Special thanks to Christine Dubreuil (Ifremer, Brest) for her technical assistance with ddPCR analyses, Carmen Rodríguez-Jaramillo and Raúl Martínez (CIBNOR, La Paz) for their help with non-commercial antibodies optimization

and with polishing the code-scripts in R, respectively, as well as Guillaume Riviere (UCN-BOREA, Caen) for his valuable ideas to carry out the experiments of this work.

Author contributions

Conceived the study and designed the experiments: CF, HH, JB, JC. Performed the experiments: JC, JB, AER, CF, EF, EC. Processed the samples: JC, EC, JB, AER, AB, CF. Analyzed the data: JC, JB, EF. Contributed reagents/materials/analysis tools: CF, HH, JB, AER AB, EF. Wrote the first draft of the manuscript: JC, CF, HH. Interpretation of data: JC, CF, HH, JB, EF.

TO RETAIN

- Profound differences in DA assimilation between bivalve species.
- The subcellular localization of the toxin appears to be species specific.
- Differential expression of iGR and SLC could support differences in DA recognizing, entry and/or exit of DA.
- Autophagy seems to be one mechanism behind the long retention of this toxin.
- These results provide a better understanding of the fate of DA, and its contamination-decontamination process in marine bivalves.

SUPPLEMENTARY MATERIALS

Suppl. Table S1. Whole data set on genes selected for qPCR test: gene family/symbols, name/description, forward and reverse sequences, and amplicon length (bp) of each primer pair. *Pm = P. maximus*, *Me = M. edulis*.

Primer	GenBank ID	Sequence 5' – 3'	Gen	Amplicon (bp)	Function
Pm-A13like-Fw	XM_033886103.1	CAGACCGCCAAGGTAGGAAC	*Autophagy related protein 13-like*	171	Autophagy
Pm-A13like-Rv		GGGGGTCGTTGATCGTTTTG			
Me-A13like-Fw	CAJPWZ010000560.1	GGTTGGATCTGTCCCTACACC		176	
Me-A13like-Rv		AGGAACAAGGTTTGGGGGTT			
Pm-A101like-Fw	XM_033886478.1	GGGAGATAGGCGTGTTCAGG	*Autophagy related protein 101-like*	178	
Pm-A101like-Rv		CCTGCCGCTCATTCTCATT			
Me-A101like-Fw	CAJPWZ010001586.1	CCATGGGAAGTGTGGACCAT		170	
Me-A101like-Rv		AGTTCGGACTGGTTTGGCAT			
Pm-A16like-Fw	XM_033904285.1	TCGGCTGTGACTGGTCTAGA	*Autophagy related protein 16-like*	187	
Pm-A16like-Rv		TCCCCGCTGAGTACGTATGA			
Me-A16like-Fw	CAJPWZ010001792.1	GCAACAGGGGGTTCAGACAG		177	
Me-A16like-Rv		TGTAAGAGACCAAACACGGCT			
Pm-A5like-Fw	XM_033885104.1	GCAACTCTGGTCTGGTCTCC	*Autophagy protein 5-like*	196	
Pm-A5like-Rv		GAGGAGGTCACGGAGAGTCT			
Me-A5like-Fw	CAJPWZ010001840.1	TGAACAACCGCTGAAATGGC		155	
Me-A5like-Rv		ACTGGGACTCTACTGCTTCCT			
Pm-MGR8like-Fw	XM_033889174.1	CGGGATGACGGAAGATACGA	*Metabotropic glutamate receptor 8-like*	174	Neurotransmission/ Induction of postsynaptic responses
Pm-MGR8like-Rv		CCAACAACAACTCTCGCCCT			
Me- MGR8like-Fw	CAJPWZ010001444.1	TATCAACGGACGGGTATGGC		178	
Me- MGR8like-Rv		CAAGCTGCGTGTTCCCTTTC			
Pm-MGRlike-Fw	XM_033904533.1	GCCGATCATCTTTCTCGCCT	*Metabotropic glutamate receptor-like*	163	
Pm-MGRlike-Rv		TGTTCTGTCCAGCGGAGATG			
Me- MGRlike-Fw	CAJPWZ010002503.1	GTGGCATACAAAAGGGCGTG		152	
Me- MGRlike-Rv		TTACAAACGGTGGCCATGGT			
Pm-IGR2like-Fw	XM_033887508.1	GTCTGCTGCTGGTCGGATAA	*Ionotropic Glutamate Receptor 2-like*	187	Excitatory synaptic transmission
Pm-IGR2like-Rv		CTGTGTTGACCCCGAATCCA			
Me-IGR2like-Fw	CAJPWZ010000765.1	AGCCAACGGGATTTGTCGAT		194	
Me-IGR2like-Rv		TAACCCAGAGCGTTTCCACG			
Pm-IGR25alike-Fw	XM_033900741.1	CCTGGTGGCTGTTTGGGTTT	*Ionotropic Glutamate Receptor 25a-like*	160	
Pm-IGR25alike-Rv		ACCATAGCAGCACTTCCGTT			
Me-IGR25alike-Fw	CAJPWZ010002033.1	TTGGGATGGACAAGGACCAG		200	

Me-IGR25alike-Rv		AAACCGTCAGGAATGCAGCTA			
Pm-NMDA3AlikeFw	XM_033883146.1	TCGTAATAAGGTGTGGCGGG	*Glutamate receptor ionotropic, NMDA 3A-like*	172	Excitatory synaptic transmission
Pm-NMDA3Alike-Rv		TGGATTCGGTTTCTGCTCCA			
Me-NMDA3Alike-Fw	CAJPWZ010001999.1	AGAGGGTGTGTCAGGTCCAA		165	
Me-NMDA3Alike-Rv		TCGTCCGGCCAAAGAATACC			
Pm-NMDA1like-Fw	XM_033885630.1	GATCGCTGGAGGGGTAACATC	*Glutamate [NMDA] receptor subunit 1-like*	195	
Pm-NMDA1like-Rv		GAGTCTGCTACCTGTGGCCT			
Me-NMDA1like-Fw	CAJPWZ010001507.1	ACCATTAACCCGGAGAGAGC		174	
Me-NMDA1like-Rv		TAGTGCCACCACATGGACAG			
Pm-IGRδ1like-Fw	XM_033904120.1	AGCTCTAACCCGGAAGTCCA	*Glutamate receptor ionotropic, delta-1-like*	163	
Pm-IGRδ1like-Rv		TCGGAAGTCCAACCGCATAC			
Me-IGRδ1like-Fw	CAJPWZ010000765.1	TGGTGACCGAACTCAGATGG		197	
Me-IGRδ1like-Rv		TCGGCCAGTGTTCTAACTTCC			
Pm-NMDA2AlikeFw	XM_033883213.1	TGCCTAATGGGAGCACAGAG	*Glutamate receptor ionotropic, NMDA 2A-like*	150	
Pm-NMDA2Alike-Rv		GTGGCGTGGCATCGTAAATG			
Me-NMDA2Alike-Fw	CAJPWZ010002780.1	GTTGTTTGGTGCAGCCGTTT		175	
Me-NMDA2Alike-Rv		TCGCCAGTCTTGTATCCCTG			
Pm-GRU1like-Fw	XM_033886849.1	ATCGCTCTTGCACCATTCCA	*Glutamate receptor U1-like*	197	
Pm-GRU1like-Rv		AGCACTAAGGCTGTCGTCAC			
Me-GRU1like-Fw	CAJPWZ010002768.1	TCCAGACGGAAAATTCGGCA		189	
Me-GRU1like-Rv		CTTCGTTCAGGCTTTCGCAC			
Pm-GAPDH-Fw	XM_033907751.1	ATTGGTTGGGGTGACTCTGG	*Glyceraldehyde 3-phosphate dehydrogenase*	160	Glycolytic enzyme/ uracil DNA glycosylase
Pm-GAPDH-Rv		TGTGGTTGACTCCCATGACA			
Me-GAPDH-Fw	CAJPWZ010001520.1	GCAGCTAAAGCCGTCGGTA		183	
Me-GAPDH-Rv		AACACCCTTCATTGGACCCT			
Pm-18S-Fw	XM_033892113.1	GAAGCCGTGCTGTGTTTCAG	*18S rRNA*	158	Protein synthesis
Pm-18S-Rv		ACCACCAGCAAACAGACACA			
Me-18S-Fw	CAJPWZ010001237.1	CATGGGAGCAGTGAAGACCC		188	
Me-18S-Rv		TACCCGGACTGCTTACAACG			
Pm-SLC5-Fw	XM_033876532.1	TCAGATGACGCTCGGATGG	*Sodium/glucose cotransporter 4-like*	182	Sodium/glucose cotransporter
Pm-SLC5-Rv		TAAGCCGCCCACTTTGTTG			
Me-SLC5-Fw	CAJPWZ010000380.1	TCTCTGTGCAGTGTACATCC		150	
Me-SLC5-Rv		AGTCAGCTTGTTCCCCAG			
Pm-SLC5A1-Fw	XM_033906500.1	TTGCGAAAGGCCAGATTGG	*Sodium-dependent glucose transporter 1A-like*	169	
Pm-SLC5A1-Rv		TGAGCTAACAGGAGAGACCG			
Me-SLC5A1-Fw	CAJPWZ010002902.1	GGGACAATGCTGATCTCCG		199	
Me-SLC5A1-Rv		GCATGTCCTCTCCTAGCCAAG			
Pm-SLC5A6-Fw	XM_033875678.1	TTGGCGTCCGTTGTCTATG		197	

Pm-SLC5A6-Rv		CTGGGAAGCCAGTCATTGC	*Sodium-coupled monocarboxylate transporter 1-like*	177	Sodium-dependent multivitamin transporter
Me-SLC5A6-Fw	CAJPWZ010002503.1	CAGGGACTGCCAACTTACC			
Me-SLC5A6-Rv		CGGTCTGGTTCAATATCGCC			
Pm-SLC6-Fw	XM_033870584.1	TATGGTGCTTGTTCCGGTCC	*Sodium-dependent transporter YocR-like*	170	Na^+/Cl^{-1} dependent neurotransmitter transporter
Pm-SLC6-Rv		CGGTGTCAAATGCGTTCTGG			
Me-SLC6A5-Fw	CAJPWZ010002044.1	GTGACGGAAAGGAACCAATG		156	
Me-SLC6A5-Rv		GGACTTCGTGAATGACGTGG			
Pm-SLC6A5-Fw	XM_033895341.1	CAACAAGTTGCTCGAGACCC	*Sodium- and chloride-dependent GABA transporter 1-like*	184	
Pm-SLC6A5-Rv		AACCATTCCGGCAAAGATGC			
Me-SLC6A5-Fw	CAJPWZ010002367.1	CTGGTGTCTTTTAGAACATGGC		155	
Me-SLC6A5-Rv		GTGATACCAGCACTAAAAGCTG			
Pm-SLC6A9-Fw	XM_033895916.1	CGTTTACTTGACCCCCGTG	*Sodium- and chloride-dependent glycine transporter 1-like*	183	
Pm-SLC6A9-Rv		GATGACGAGACCAGCGAAC			
Me-SLC6A9-Fw	CAJPWZ010002160.1	TGGTCAAGTCACGAATGG		151	
Me-SLC6A9-Rv		AACGGAGTAACGCATGGC			
Pm-SLC8-Fw	XM_033891235.1	CAAGGCCCCAATTATGTTCC	*Mitochondrial sodium/calcium exchanger protein-like*	163	Na^+/Ca^{2+} exchanger
Pm-SLC8-Rv		ATGTGCCGCCGATTGTTTC			
Me-SLC8-Fw	CAJPWZ010003087.1	TAACTGCACTCCGACGATC		177	
Me-SLC8-Rv		CGGTCCAACTACACTGCAC			
Pm-SLC10A2-Fw	XM_033898712.1	TTCATCACACTGGCGTTTGG	*Ileal sodium/bile acid cotransporter-like*	165	Ideal Na^+ bile acid cotransporter
Pm-SLC10A2-Rv		AGCCACAGAAGGTTGGTCAG			
Me-SLC10A2-Fw	CAJPWZ010003058.1	GTTTCACTTGTACCACCTCCG		197	
Me-SLC10A2-Rv		ACCAGAAACCCACACGAACG			
Pm-SLC16A10-Fw	XM_033885380.1	GACAATCTTGCGGCGATGG	*Monocarboxylate transporter 10-like*	152	Monocarboxylate transporter
Pm-SLC16A10-Rv		CCGATTAGCGCAACACCAAG			
Me-SLC16A10-Fw	CAJPWZ010000369.1	TGCACATAACGCATTGGGAG		184	
Me-SLC16A10-Rv		CATACCCGCTGAGATAGGC			
Pm-SLC16A12-Fw	XM_033906023.1	TTCGGTCTTTCCAGCGCA	*Monocarboxylate transporter 13-like*	196	
Pm-SLC16A12-Rv		GAATCACGATGGCGGCTGTC			
Me-SLC16A12-Fw	CAJPWZ010003296.1	TGGGTTCATCGCAGAGGTATC		166	
Me-SLC16A12-Rv		CACTTGCCGATGGCCTTATG			
Pm-SLC17-Fw	XM_033871282.1	GCCATGAGTGCTATGTGGG	*Sialin transporter-like*	184	Vesicular glutamate transporter
Pm-SLC17-Rv		CACCCAAGGACACCGAATATG			
Me-SLC17-Fw	CAJPWZ010002227.1	GGAAACAGTCAAAGGAGGACC		182	
Me-SLC17-Rv		CTCTCATGTCATCGCCACC			
Pm-SLC22A15-Fw	XM_033884029.1	GTGATGATGCCCTGAAGACG		193	Organic cation transporter
Pm-SLC22A15-Rv		CCAGGACGACGAAACTGACC			

Me-SLC22A15-Fw *Me-SLC22A15-Rv*	CAJPWZ010000700.1	GGGCGAAAGAATCCCACG GAGAGACCCTGAGTAAGC	*Organic cation transporter protein-like*	197	
Pm-SLC22A8-Fw *Pm-SLC22A8-Rv*	XM_033904264.1	CTTTTGGGCGTAGGATGGTTG GCAATAAGGCAAACGCTGTCT	*Solute carrier family 22 member 5-like*	187	Organic anion transporter
Me-SLC22A8-Fw *Me-SLC22A8-Rv*	CAJPWZ010002518.1	ACAGACATAGCTGACCACCTG ACATCCGGGTATTCTCCGTG		186	
Pm-SLC01C1-Fw *Pm-SLC01C1-Rv*	XM_033871590.1	GACGGGAAGTCAGGTTTTC GCCGGAATCTGGAACTGTG	*solute carrier organic anion transporter 3A1-like*	178	
Me-SLC01C1-Fw *Me-SLC01C1-Rv*	CAJPWZ010002326.1	CGTGGGAGAAACACTTCTGTC TGCATTCAGTGACCGGTGG		188	
Pm-SLC40-Fw *Pm-SLC40-Rv*	XM_033906434.1	CGCAAAATAGCAGTGGAGCG GCGGCTATAAAAAGAGCGCC	*Basolateral iron transporter 1-like*	182	Basolateral iron transporter
Me-SLC40-Fw *Me-SLC40-Rv*	CAJPWZ010000942.1	GCCAAAGCACCGAAGAACAG GGCTACGGCTTTTCGCTTTC		198	
Pm-SLC46A3-Fw *Pm-SLC46A3-Rv*	XM_033879289.1	CCGAGCAGGAAAGTCGAGAG CATAACTGCAACACAGGCGAC	*Solute carrier 3-like*	160	Proton-coupled amino acid transporter
Me-SLC46A3-Fw *Me-SLC46A3-Rv*	CAJPWZ010001460.1	CCTACAACGTGATCGGAGTG CCCAGGTCCCAGTACATCC		198	
Pm-AVT1Jlike-Fw *Pm-AVT1Jlike-Rv*	XM_033884846.1	CACCCTCTTCGGAGTTGG GCGGTTGCTATGGTAGCTC	*Amino acid transporter AVT1J-like*	195	
Me-AVT1Jlike-Fw *Me-AVT1Jlike-Rv*	CAJPWZ010001622.1	CCTCCGAATACGTGTGTCC CTGGGTAGTGTGCCTTCC		191	
Pm-P5CR2like-Fw *Pm-P5CR2like-Rv*	XP_033727520.1	CATAAGTGCCCCTCGGAACC CGAGGGACATGGCTGTGAAAC	*Pyrroline-5-carboxylate reductase 2-like*	173	Metabolism of proline
Me-P5CR2like-Fw *Me-P5CR2like-Rv*	CAJPWZ010003088.1	GATGGTGGTGGATGGATCG CTTCGCCATCTCTCGTTTCC		200	
Pm-GStAlike-Fw *Pm-GStAlike-Rv*	XM_033870699.1	CTTAACCCCAGAGGCCAG GTTGTTATGCGCCTCATGC	*Glutathione S-transferase A-like*	180	Glutathione detoxification metabolism
Me-GStAlike-Fw *Me-GStAlike-Rv*	CAJPWZ010002200.1	CGAAACCAGATGAACCAGGC CACTCCCCTTCTCCTTGTG		151	
Pm-GSTθ1like-Fw *Pm-GSTθ1like-Rv*	XP_033748808.1	GCAAGGGTGGACGAGTTCA GGCTGACGGTAATTCCAAC	*Glutathione S-transferase theta-1-like*	162	
Me-GSTθ1like-Fw *Me-GSTθ1like-Rv*	AY557404.1:19-639	CAGCTTGTGCAGTCTAACGC GAATGGCTCTTTTCCTGCTTC		174	
Pm-GSlike-Fw *Pm-GSlike-Rv*	XP_033729010.1	GCAACCTGTCGTGGAATACG CATGTCCGCCACATCAAGG	*Glutamine synthetase-like*	150	Metabolism of glutamine

Me-GSlike-Fw	CAJPWZ010002580.1	GAGAAGTGGCGGAAGTTGG		175	
Me-GSlike-Rv		GATAATTCTGGCGAGCGAGC			
Pm-ST1A2-Fw	XM_033872239.1	GGATAACGTGAGGAGGGAGC	*Sulfotransferase 1A2-like*	198	Detoxification metabolism/ sulfotransferase family
Pm-ST1A2-Rv		GCGTAAACGTCTTTGTGGC			
Me-ST1A2-Fw	CAJPWZ010002049.1	CGAAAAACGTCGAAATGGCG		199	
Me-ST1A2-Rv		GCGACAGGAATCATTGGTC			
Pm-ST1C4-Fw	XM_033891178.1	GTCACCAAGATGGCGTCG	*Sulfotransferase 1C4-like*	200	
Pm-ST1C4-Rv		CTTCCAATCCCCAACCTCTCC			
Me-ST1C4-Fw	CAJPWZ010001685.1	ACGGTAGAGGAATTGGGGTTAC		197	
Me-ST1C4-Rv		CGACAATGTGGTTGGTCC			
Pm-ST1B-Fw	XM_033908168.1	GTGATCGGCTGTTTCAGGG	*Sulfotransferase family cytosolic 1B member 1-like*	152	
Pm-ST1B-Rv		CACGCCATTCAAACCAGG			
Me-ST1B-Fw	CAJPWZ010002149.1	GTCACCAAATGAAAGCAAGG		197	
Me-ST1B-Rv		GTTAGCAACTTCTCTGTTTTGC			
Pm-DXS-Fw	XM_033904908.1	GTCACCCCGAATGGGAAGAG	*1-deoxyxylulose-5-phosphate synthase YajO-like*	190	Synthesis of steroids
Pm-DXS-Rv		CCATGCTGGACTGCTCTG			
Me-DXS-Fw	CAJPWZ010002684.1	GGACAGAATATCCACCAGATGC		196	
Me-DXS-Rv		CTGGTGTTGGCAGAGATACC			
Pm-AKR-Fw	XM_033896572.1	CGGTAACGAGAAGGCAGTG	*Aldo-keto reductase A1-like*	189	
Pm-AKR-Rv		GTGGACGAGGTACAGGTC			
Me-AKR-Fw	CAJPWZ010001791.1	GCCATCTTCCATCATCCACC		165	
Me-AKR-Rv		GATTCCGCCATCAGCAAACAAG			
Pm-GCL-Fw	XM_033907205.1	GGAGGAGTTGGACACATCG	*Glutamate--cysteine ligase*	196	Glutathione Antioxidant production
Pm-GCL-Rv		CGCCCAGTTAAACAGCTCC			
Me-GCL-Fw	CAJPWZ010002359.1	CTGAACAAGAAGACCAAGAGG		192	
Me-GCL-Rv		GCGAGAAGCAGAAGTACGAC			

DISCUSSION GENERALE & PERSPECTIVES

Malgré les effets délétères de la phycotoxine acide domoïque (DA) sur la santé humaine (Trainer *et al.,* 2012; Pulido, 2008), et la menace permanente d'efflorescences de *Pseudo-nitzschia spp*. toxique sur les ressources halieutiques commercialement importantes (Amzil *et al.,* 2001*;* Husson *et al.,* 2016*;* Blanco *et al.,* 2021b), les connaissances sur les mécanismes physiologiques à l'origine des profondes différences d'accumulation et de dépuration de cette toxine chez les organismes marins non-vertébrés contaminés sont restées rares au cours des dernières années. Les résultats présentés dans ce travail et obtenus grâce à une approche à différents niveaux d'organisations biologiques, constituent une pierre angulaire qui comble une lacune importante dans la compréhension des mécanismes physiologiques impliqués dans les différences profondes de la toxicocinétique de l'AD chez les non-vertébrés marins présentant des capacités différentes sur l'accumulation et la dépuration de cette toxine et en particulier concernant la très longue rétention de l'AD chez la coquille Saint-Jacques *Pecten maximus*.

Le manque de données concernant la localisation anatomique précise de l'AD dans les tissus des organismes non mammifères contaminés a rendu extrêmement difficile l'explication des causes à l'origine de la contamination et décontamination de l'AD chez ces espèces. La méthode immunohistochimique de marquage de l'AD développée dans ce travail (García-Corona *et al.,* 2022) a abouti à une manière innovante de localiser *in situ* la phycotoxine dans les tissus des invertébrés contaminés, en particulier dans les tissus de la coquille Saint-Jacques *P. maximus* . L'application de cette nouvelle méthode nous a permis de visualiser que la majeure partie de l'AD se trouve dans le cytoplasme des cellules digestives de *P. maximus*, comme mentionné précédemment par Mauriz & Blanco (2010) qui avaient utilisé une technique de fractionnement subcellulaire. Néanmoins, le signal de l'AD n'apparaît pas libre dans le

cytoplasme mais est principalement piégé dans des structures autophagiques, comme le révèle l'immunomarquage. Cette découverte nous a conduit à émettre l'hypothèse que l'autophagie pourrait être un mécanisme subcellulaire à l'origine de la dépuration lente de l'AD, jouant un rôle crucial dans sa rétention dans les cellules digestives des coquilles Saint-Jacques.

La découverte de l'implication de l'autophagie dans la séquestration de l'AD dans les cellules digestives de *P. maximus* a soulevé de nouvelles questions et hypothèses qui ont été abordées tout au long des chapitres de cette thèse. Tout d'abord : comment les espèces de coquillages diffèrent-elles dans leur capacité à accumuler, métaboliser et répartir l'AD dans leurs tissus au niveau subcellulaire? Pour répondre à cette question, nous avons effectué une analyse comparative de l'accumulation et de la localisation subcellulaire de l'AD chez différentes espèces d'invertébrés couramment affectés lors des efflorescences de *Pseudo-nitzschia*, telles que les pectinidés *P. maximus* et *A. opercularis*, les clams *D. trunculus*, les crépidules *C. fornicata* et le tunicié *Asterocarpa sp*. recueillies après les efflorescences du *P. australis* toxique (chap.3).

Nos résultats tendent à montrer que les différences interspécifiques dans les capacités d'accumulation et de dépuration de l'AD parmi les espèces d'invertébrés marins pourraient être liées à l'activation différentielle de plusieurs mécanismes physiologiques qui régissent la toxicocinétique de la toxine. Les pectinidés, mais surtout *P. maximus*, ainsi que *C. fornicata*, sont restés significativement plus contaminés que le reste des espèces comparées dans cette étude entre leur exposition et le moment du prélèvement. Ces différences importantes dans l'accumulation de l'AD dans la glande digestive au niveau interspécifique sont conformes à la forte variabilité des quantités de l'AD fréquemment détectées entre

ces espèces (Bogan *et al.,* 2007a,b,c; Basti *et al.,* 2018; Blanco *et al.,* 2021). La quantité d'AD mesurée dans les organismes résulte de différences dans l'accumulation mais aussi dans les taux de dépuration de l'AD signalés principalement pour les espèces de bivalves (Vale et Sampayo, 2001; Blanco *et al.,* 2010; Dusek Jennings *et al.,* 2020). Néanmoins, il est important de souligner que les teneurs en AD mesurées dans les tissus des animaux contaminés dans cette étude, et dans toutes les autres études publiées, sont également le résultat d'une interaction complexe entre les traits physiologiques impliqués dans l'accumulation et la dépuration de l'AD et la durée et la toxicité des efflorescences de *Pseudo-nitzschia spp*. toxique, le temps pendant lequel les animaux ont été exposés aux microalgues toxiques, et le moment auquel les organismes ont été prélevés pendant les efflorescences. Les résultats présentés dans cette thèse sont d'autant plus intéressants qu'ils ont comparé des taux de contamination entre espèces soumises à une même efflorescence de Pseudo-nitzschia, ce qu'il n'est pas le cas dans la plupart des études, permettant de comparer les mécanismes physiologiques en jeu dans l'entrée et le devenir de l'AD dans les organismes.

Nos résultats indiquent que la localisation de l'AD et ses effets au niveau subcellulaire sont spécifiques de l'espèce. Chez *P. maximus*, le signal chromogénique anti-AD a été détecté principalement dans les vésicules autophagosomiques du cytoplasme des cellules digestives. Cependant, l'autophagie de l'AD n'est pas un processus exclusif aux coquilles Saint-Jacques, car une immunoréactivité significative de l'AD a été trouvée dans les corps résiduels post-autophagie chez *A. opercularis* et *C. fornicata*. À l'inverse, un léger signal de l'AD a été trouvé libre dans le cytoplasme des cellules digestives de *D. trunculus* et d'*Asterocarpa sp*. Cela suggère que, chez ces espèces, l'AD intracellulaire n'est lié à aucune structure ou composant subcellulaire, ce qui

pourrait conduire à une dépuration rapide des faibles quantités de l'AD accumulé chez ces espèces après les efflorescences de *Pseudo-nitzschia*. D'autres analyses seront nécessaires pour confirmer cette hypothèse. Ces observations suggèrent des stratégies distinctes face à la présence d'AD dans les tissus des différentes espèces affectées, avec en particulier l'autophagie qui semble être l'une des raisons de la longue rétention de l'AD chez certaines espèces. En effet, l'autophagie joue un rôle essentiel dans le maintien de l'homéostasie métabolique et de la santé cellulaire chez les bivalves (Balbi *et al.*, 2018; Picot *et al.*, 2019). Néanmoins, ce processus peut également être considéré comme un signe d'altération physiologique dans des conditions environnementales néfastes (Moore *et al.*, 2008; Rodríguez-Jaramillo *et al.*, 2022). Des recherches futures sur les implications de l'autophagie dans la séquestration de l'AD devraient être menées pour déterminer si ce mécanisme peut déclencher des pathologies chez les espèces affectées.

Les péctinidés, *P. maximus* mais plus encore *A. opercularis*, contaminés par l'AD dans cette étude avaient des taux de vacuolisation des cellules digestives significativement plus élevés que les autres espèces. La vacuolisation cellulaire est une lésion histopathologique fréquente chez les bivalves soumis à des conditions environnementales stressantes (Rodríguez-Jaramillo *et al.*, 2022), notamment lorsqu'ils sont exposés à des phycotoxines (Hegaret *et al.*, 2010; Lassudrie *et al.*, 2014). Selon Shubin *et al.* (2016) il s'agit d'un phénomène subcellulaire bien connu observé dans les cellules animales qui accompagne souvent la mort cellulaire après exposition à des composés artificiels ou naturels de faible poids moléculaire, tels que l'AD. La rare littérature relative aux effets de *Pseudo-nitzschia spp*. ou de l'AD sur les non-vertébrés indique que cette toxine pourrait potentiellement perturber les processus comportementaux, métaboliques, moléculaires et physiologiques chez

certains bivalves tels que *P. maximus* (Ventoso *et al.*, 2021; Liu *et al.*, 2007a,b), *A. operculari*s (Ventoso *et al.*, 2019), *A. irradians* (Chi *et al.*, 2019) et certaines moules, comme *M. edulis* (Dizer *et al.*, 2001) et *M. galloprovincialis* (Pazos *et al.*, 2017). Néanmoins, aucun effet létal résultant d'une exposition à l'AD n'a été signalé chez aucune de ces espèces, ce qui suggère soit une faible sensibilité à la toxine, soit des effets sub-létaux encore inaperçus. Dans tous les travaux publiés, ainsi que dans ces travaux de thèse, les effets secondaires de l'AD n'ont été analysés qu'après une exposition ponctuelle soit à *Pseudo-nitzschia* toxique, soit directement à la toxine. Par conséquent, des pathologies potentielles liées à des expositions chroniques à de faibles concentrations en AD ne peuvent être exclues, comme cela a été rapporté dans le cas des mammifères marins (Miller *et al.*, 2021).

L'étendue des connaissances à ce jour sur les implications de l'autophagie dans la séquestration de l'AD au niveau interspécifique nous a amené à nous demander comment ces mécanismes se mettaient en place lors des épisodes de contamination et combien de temps l'AD pouvait rester piégé dans ces structures autophagosomiques ? Jusqu'à présent, la localisation de la toxine n'était effectuée qu'à un moment précis après les événements de contamination (García-Corona *et al.*, in prep a, b, Chap. 2 et 3). Pour confirmer que ce processus subcellulaire était impliqué dans la rétention de l'AD, il était nécessaire de suivre la succession des événements qui conduisent à l'autophagie au cours de la contamination et de la décontamination. Par conséquent, nous avons suivi la localisation de l'AD dans les tissus de *P. maximus* pendant les phases de contamination et de décontamination, ainsi que sa toxicocinétique et l'implication de l'autophagie a été analysée grâce à un suivi temporel immunohistochimique au niveau subcellulaire (Chap. 4). Nos résultats indiquent l'implication directe et forte de l'autophagie précoce dans l'accumulation de l'AD. De

même, il semble exister une relation directe entre la formation de corps résiduels et la dépuration lente de la toxine. Cela indiquerait qu'au niveau subcellulaire, l'autophagie module fortement la longue rétention de l'AD dans les cellules digestives de *P. maximus* en piégeant la toxine et en la rendant inaccessible au système de détoxification. Les raisons de ce blocage dans la dégradation/digestion de l'AD par la machinerie enzymatique lyosomale, ainsi que les raisons qui empêchent son excrétion ultérieure restent à élucider.

Cependant, la longue rétention de composés exogènes n'est pas un phénomène exclusivement lié à l'autophagie, elle se produit également dans d'autres types de cellules dans le cadre de processus analogues. Grâce à la macrophagie, des cellules spécialisées appelées macrophages utilisent leurs membranes cytoplasmiques pour phagocyter de grosses particules extracellulaires (≥ 0,5 µm, par exemple des bactéries et des débris métaboliques) via l'endocytose, créant des compartiments vésiculaires internes appelés phagosomes. Les phagosomes, après avoir phagocyté les matériaux présents dans le cytoplasme, fusionnent avec les lysosomes, formant des phagolysosomes, entraînant une dégradation enzymatique (Flannagan *et al.*, 2012*;* Gordon, 2016). Il est prouvé que, lors du tatouage, les macrophages dermiques de souris et d'humains sont capables de: 1) phagocyter les particules de pigment à travers plusieurs cycles de capture-libération-recapture à travers la régénération cellulaire, ou 2) présenter des durées de vie aussi longues que la vie adulte des animaux tatoués, ce qui explique la persistance et la difficulté d'élimination de l'encre de tatouage sur la peau. Même lorsque les macrophages chargés d'encre de tatouage meurent et libèrent les pigments, les particules de coloration restent dans l'espace extracellulaire au site de tatouage où elles sont re-capturées par de nouveaux macrophages (Baranska *et al.*, 2018). Comme l'autophagie, la macrophagie est un mécanisme catabolique utilisé

pour éliminer les agents pathogènes et les déchets cellulaires à des fins de détoxification ou de recyclage des nutriments, dans lequel les macrophages peuvent présenter des durées de vie de plusieurs mois à plusieurs années (Flannagan *et al.*, 2012; Gordon, 2016; Baranska *et al.*, 2018). Les résultats de ce travail et les résultats de cette thèse suggèrent deux nouvelles hypothèses: 1) l'AD pourrait subir des cycles successifs de capture–libération–recapture par des structures autophagosomiques à travers le cycle de régénération des cellules digestives des coquilles Saint-Jacques, ou 2) des autophagosomes et des corps résiduels avec l'AD présentent de longues durées de vie, conservant ainsi la toxine qui ne disparaît qu'après des mois voire des années, déclenchant ainsi un mécanisme que l'on pourrait qualifier de tatouage à l'AD dans les glandes digestives de *P. maximus.*

Comme la glande digestive est l'organe clé pour le stockage et la dépuration de l'AD chez *P. maximus*, nous nous sommes concentrés sur cet organe pour approfondir la cause de la longue rétention de cette toxine chez cette espèce. Nous avons observé une dépuration rapide d'environ 70% de l'AD total accumulé dans la glande digestive des coquilles Saint-Jacques au cours des 7 premiers jours de conditionnement en laboratoire (chapitre 4). En supposant que cette fraction correspond probablement à la toxine libre dans le cytoplasme des cellules digestives, comme indiqué par Mauriz et Blanco, (2010), tandis que les ~30% restants des charges de l'AD semblent rester piégée dans les structures autophagiques pendant longtemps comme observé dans García-Corona *et al.* (2022) (Fig. 1 chapter 2 et Fig. 8).

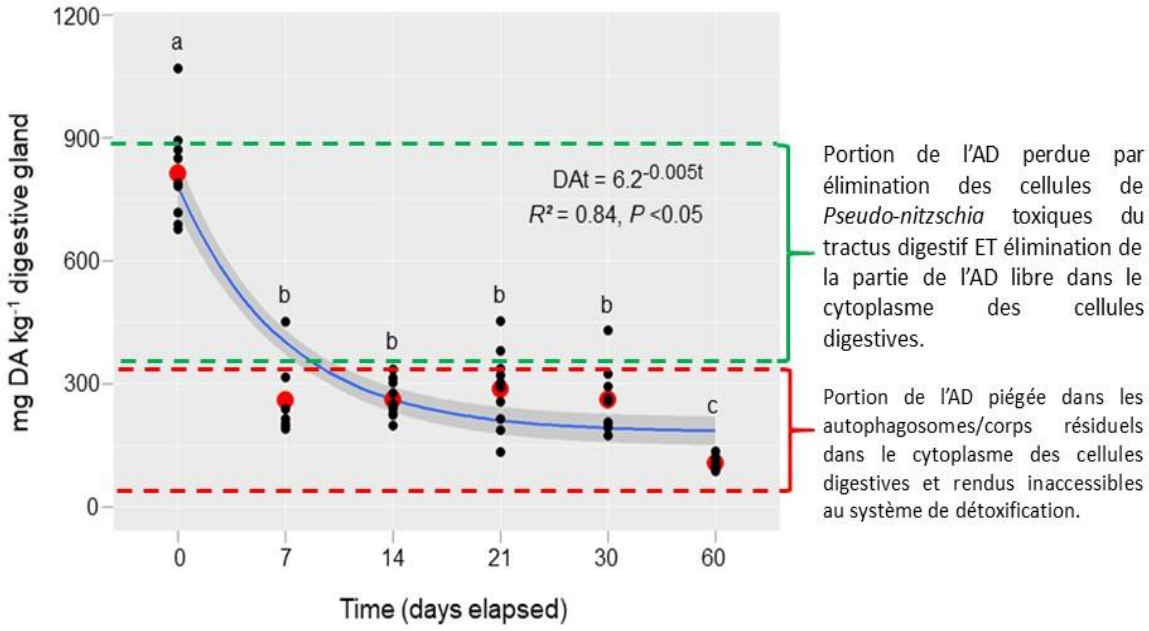

Figure 8 : Schéma présentant l'hypothèse expliquant le profil de décontamination de l'acide domoïque observé chez la coquille Saint-Jacques au cours de notre expérimentation de décontamination en laboratoire, en deux phases (chapitre 4). La partie en vert correspondrait à la partie rapidement dépurée alors que la partie en rouge correspondrait à la partie piégée dans les autophagosomes et mise en évidence par la technique d'immunohistochimie développée dans cette thèse (chapitre 2) .

Cette preuve renforce l'importance de l'autophagie dans la toxicocinétique de l'AD chez *P. maximus*. Álvarez *et al.* (2020) ont conçu un modèle à plusieurs compartiments qui suggère que l'AD accumulé par *A. pupuratus* est rapidement transféré de la glande digestive vers d'autres organes tels que la gonade, le muscle, le manteau et les branchies, qui dépurent la toxine de manière indépendante et avec beaucoup plus d'efficacité. La même stratégie a été proposée pour expliquer la détoxification rapide de l'AD viscérale chez *M. edulis* et *C. virginica* (Mafra *et al.*, 2010), ainsi que chez *M. donacium* (Álvarez *et al.*, 2015) au cours de la phase précoce d'absorption de la toxine. Il n'y a aucune preuve de redistribution tissulaire différentielle de l'AD dans les différents tissus chez *P. maximus*, et dans tous les cas, ce processus peut ne pas expliquer plus de 20% de la variabilité interspécifique observée dans cette étude puisque la glande digestive accumule plus de 80% des charges totales de l'AD chez la plupart des non-vertébrés (Blanco *et al.*, 2002a; Costa *et al.*, 2005).

La coloration AD-IHC a également été trouvée dans le tissu neural périphérique des coquilles St-Jacques, en particulier dans les extensions axonales et le corps soma de certains neurones intégrés dans le muscle adducteur (chapitre 4). La présence de récepteurs à forte affinité et à faible sensibilité à l'AD a été identifiée dans les tissus d'autres espèces de bivalves comme *S. patula* (Trainer et Bill, 2004), ce qui pourrait indiquer la présence de ce type de récepteurs chez *P. maximus*. L'activation de ces récepteurs par l'AD, et son implication potentielle dans la reconnaissance ou l'activation du transport des toxines à travers la membrane cellulaire méritent des investigations futures car elles restent peu étudiées. Nous avons également visualisé le signal de l'AD dans les microvillosités des branchies et les cellules globuleuses incrustées dans les canaux de ponte des gonades. Un résultat similaire a été rapporté par García-Corona *et al.* (2022), chapitre 2 chez *P. maximus* fortement contaminés par l'AD, où l'immunoréactivité a été détectée dans les structures productrices de mucus. D'autres analyses protéomiques sont nécessaires pour corroborer si l'AD a une simple affinité ou s'il est chimiquement lié à un composant du mucus. Néanmoins, comme la quantité de toxine dans le reste des tissus était négligeable, on peut en déduire que la production de mucus ne joue pas un rôle important dans la dépuration de la toxine chez cette espèce.

La façon dont l'AD est traité, accumulé et dépuré aux niveaux organisationnels tels que l'individu, les tissus et les cellules a nécessairement des bases moléculaires qui sont régulées différemment entre les dépurateurs rapides et lents de la toxine, ce qui expliquerait les raisons fondamentales de ces différences au niveau interspécifique. L'idéal aurait été d'étudier la cinétique de régulation de l'expression des gènes au cours d'un épisode de contamination de coquilles Saint-Jacques par des cellules de *Pseudo-nitzschia* productrices d'AD en laboratoire afin de pouvoir réaliser des pas de

temps serrés pour les prélèvements. Malheureusement, il n'a pas été possible d'obtenir des volumes de culture de *Pseudo-nitzschia* toxiques suffisants pour réaliser ces expériences. Par conséquent, dans le chapitre 5, nous avons décidé de réaliser, alternativement, des expositions de tranches de glandes digestives in vitro à de l'AD dissous, suivant le modèle développé par Blanco *et al.* (2021). Une régulation à la hausse de l'expression des gènes codant pour les protéines liées à l'autophagie ainsi que la séquestration de l'AD dans les autophagosomes ont été observées suite à cette exposition *in vitro* des glandes digestives de coquilles Saint-Jacques *P. maximus*. Cela corrobore l'implication de l'autophagie chez cette espèce. Au contraire, chez *M. edulis*, l'absence d'autophagosomes marqués à l'AD et la régulation à la hausse des gènes codant pour les protéines liées à l'autophagie ne semblaient pas activées en présence de l'AD. Ces résultats rejoignent et renforcent l'hypothèse que nous avons proposée suggérant que l'autophagie de l'AD est un mécanisme spécifique à l'espèce déclenché principalement chez les espèces qui retiennent la toxine dans la glande digestive pendant de plus longues périodes, comme les pétoncles *P. maximus* et *A. opercularis*, mais aussi la crépidule *C. fornicata*, tandis que des espèces comme le clam *D. trunculus* et le tunicate *Asterocarpa spp.,* qui présentaient les charges de l'AD les plus faibles au moment du prélèvement sur le terrain (chap. 3), présentaient également les fréquences les plus basses d'autophagie liée à l'AD. De plus, la surexpression des trois protéines liées à l'autophagie (A13, A16, and A101) évaluées dans ce travail a également été trouvée par Ventoso *et al.* (2021) dans la glande digestive de *P. maximus* après injection intramusculaire d'une solution d'AD.

Pour que l'autophagie se produise, les composés extracellulaires doivent être reconnus par des récepteurs membranaires spécifiques qui signalent à la membrane plasmique de déclencher le processus (McMillan, 2018; Zhao *et al.*, 2021). Cette

cascade de signalisation cellulaire complexe et bien organisée a été largement étudiée chez les mammifères pendant la privation de nutriments cellulaires, l'infection, le ciblage de médicaments, la réparation des organites et des protéines endommagés et la mort cellulaire programmée (Mizushima *et al.*, 2002; Wang *et al.*, 2019*;* Zheng *et al.*, 2022). Néanmoins, les connaissances sur les récepteurs membranaires qui orchestrent la cascade de signalisation pour que l'autophagie de l'AD soit déclenchée dans les cellules digestives de certains invertébrés marins, et en particulier chez *P. maximus,* sont encore loin d'être connues.

Certains récepteurs ionotropes du glutamate (iGR) se sont avérés être régulés de manière différentielle en présence d'AD dans les glandes digestives de *P. maximus*, mais surtout dans celles de *M. edulis* (Chapitre 5). Il est bien connu que l'AD est un puissant agoniste d'une grande variété d'iGR divisés en grandes familles classées comme kainateα-amino-5-méthyl-3-hydroxyisoxazolone-4-propionate (AMPA), kainate (KA) et N-méthyl-D-aspartate (NMDA), largement distribués dans le système nerveux central des vertébrés (Perl *et al.*, 1990; Lefebvre et Robertson, 2010; La Barre *et al.*, 2014). De plus, l'AD présente une affinité de 3 à 100 fois plus élevée pour ce type d'iGR que ses analogues structuraux, le glutamate et l'acide kainique (premier neurotransmetteur excitateur majeur), en particulier dans le cerveau des mammifères (Todd, 1993; Zaman *et al.*, 1997*;* McCabe *et al.*, 2016; Zabaglo *et al.*, 2016). Les récepteurs NMDA et AMPA sont des canaux ioniques ligand-dépendants sélectifs de Na^{+}, K^{+} et Ca^{2+} et tous deux sont activés par le glutamate et son agoniste l'AD, médiant une transmission synaptique excitatrice rapide (Ramsdell, 2007; Pulido, 2008). L'excitotoxicité de l'AD conduit à la dépolarisation et à la libération de glutamate dans la synapse, provoquant un afflux incontrôlé de Ca^{+2} dans la cellule. Cet excès de Ca^{+2} est hautement toxique pour les cellules neuronales entraînant une dégénérescence et

des lésions nerveuses permanentes (Katnelson *et al.*, 2016*;* Miller *et al.*, 2021). Bien que les vastes connaissances existantes sur l'implication des iGR dans la neurotoxicité de l'AD chez les mammifères, les voies d'activation de ces récepteurs et son influence sur la toxicocinétique de l'AD chez les bivalves restent mal connues et encore moins comprises.

Un seul des quatre iGR évalués dans cette étude (Chapitre 5), NMDA1, a montré une surexpression dans les glandes digestives de *P. maximus* incubées dans une solution d'AD. Ces résultats rejoignent partiellement ceux de Ventoso *et al.* (2021) car aucun des gènes codant pour les iGR identifiés dans le transcriptome des glandes digestives de *P. maximus* n'a été différentiellement exprimé après injection intramusculaire de l'AD. Nos résultats coïncident également avec Ventoso *et al.* (2019) qui ont trouvé une régulation à la baisse de deux transcrits codant pour les récepteurs NMDA et pour les cinq récepteurs KA dans la glande digestive d'*A. opercularis* après des efflorescences de *Pseudo-nitzschia spp*. A l'inverse, les trois iGR non activés chez *P. maximus* par l'effet de la toxine dans notre étude étaient surexprimés dans les glandes digestives de *M. edulis* après exposition à l'AD, suggérant ainsi que les moules pourraient avoir des récepteurs de haute affinité à la toxine, lui conférant une meilleure reconnaissance et des capacités de liaison inférieures à celles des *P. maximus*. En effet, Trainer et Bill (2004) ont découvert que le dépurateur lent de l'AD *S. patula* est capable d'exprimer sélectivement dans certains tissus comme le siphon, à la fois des récepteurs de haute affinité mais à faible capacité de liaison à l'AD et des récepteurs de faible affinité mais à haute capacité de liaison à l'AD, en supposant que c'est peut-être via ces sites de faible affinité mais à haute capacité de fixation de la toxine que les couteaux retiennent l'AD pendant de longues périodes. Cela pourrait également se produire dans la glande digestive de *P. maximus* lorsqu'elle est exposée à de l'AD, permettant ainsi aux

dépurateurs lents de limiter la toxicité. Grâce à des analyses génomiques et transcriptomiques il a été démontré que les iGR sont bien conservés chez les bivalves, où cette famille particulière de gènes a montré une expansion rapides des variants (Zeng *et al.*, 2021). Notamment, *P. maximus*, présente une expression et une sélectivité élevée aux ligands, ce qui peut contribuer à la remarquable tolérance a l'AD chez cette espèce (Zeng *et al.*, 2021). Les évidences discutées ci-dessus et l'expression inégalée d'iGR entre les coquilles Saint-Jacques et les moules trouvées dans cette étude soulèvent une nouvelle question: l'activation différentielle des iGR pourrait-elle être impliquée dans la reconnaissance spécifique de l'AD, et l'activation conséquente d'un système de transport membranaire complexe lié à l'entrée ou à la sortie de la toxine dans les cellules digestives des bivalves?

Ce travail a mis en évidence les différences profondes dans l'activation et la régulation de plusieurs protéines de transport membranaire entre *P. maximus* et *M. edulis* au niveau moléculaire. Les transporteurs membranaires sont des protéines spécialisées qui transportent des substances hydrosolubles à travers les membranes cellulaires lipidiques, jouant souvent un rôle clé dans la détermination de l'accumulation de composés exogènes dans les cellules (Lin *et al.*, 2015; Song *et al.*, 2020). Généralement, les transporteurs membranaires peuvent être classés moléculairement et mécaniquement dans deux grandes super-familles: la famille des "ATP binding-cassette" (ABC) et la famille des transporteurs de solutés (Solute Carrier = SLC). Les transporteurs ABC sont des transporteurs actifs primaires qui nécessitent l'hydrolyse de l'ATP pour le transport du substrat contre un gradient de concentration et ce sont principalement des transporteurs d'efflux, médiant le transfert de composés hors des cellules; tandis que les membres de la famille SLC utilisent une différence de potentiel électrochimique ou un gradient ionique généré par des transporteurs actifs primaires

pour faciliter la mobilisation de petites molécules par diffusion passive dans la cellule et sont donc classés comme transporteurs facilités ou transporteurs actifs secondaires (You, 2007; Hong, 2017). Néanmoins, il existe des preuves que certains transporteurs SLC fonctionnent comme des transporteurs bidirectionnels d'influx-efflux (Song *et al.*, 2020). L'AD est un zwitterion, il a donc besoin de protéines de transport pour traverser la membrane cellulaire, comme démontré chez les mytilidés (Madhyastha *et al.*, 1991; Pazos *et al.*, 2017; Blanco *et al.*, 2021) et comme dans le cas de l'acide glutamique chez les mammifères (Smith *et al.*, 2000; Kimura *et al.*, 2011). Compte tenu de cela, on pourrait s'attendre à ce que certaines protéines liées aux transporteurs membranaires, et potentiellement certaines appartenant à la famille SLC, soient impliquées dans l'absorption ou l'excrétion de l'AD chez les bivalves.

Dans ce travail de thèse, les profils d'expression transcriptionnel de sept protéines transporteuses de type SLC ont été comparés dans les glandes digestives de *P. maximus* et *M. edulis* exposées à l'AD afin d'identifier si ce mécanisme de transport passif est impliqué dans les différences de toxicocinétique de la toxine entre les deux espèces. Chez la coquille Saint-Jacques, seul le transporteur *SLC17* a été surexprimé lorsque les glandes digestives étaient exposées à l'AD, tandis que chez les moules, cinq (*SLC5, SLC5A1, SLC17, SLC16A10* et *SLC6A9*) des sept transporteurs membranaires ont été régulés positivement par l'effet de la toxine. De plus, l'expression de ces transporteurs apparait aussi fortement corrélée avec l'accumulation de l'AD dans les cellules digestives des deux espèces, inférant ainsi l'implication primordiale de ces protéines dans le transport (entrée ou sortie) de cette toxine.

La série de gènes SLC comprend 52 familles et 395 transcrits de transporteurs dans le génome humain (Hediger *et al.*, 2013*;* César-Razquin *et al.*, 2015*;* Lin, *et al.*, 2015),

et certains d'entre eux sont responsables de la transmission transmembranaire de l'AD dans la barrière intestinale des mammifères (Kimura *et al.*, 2011). La plupart des études sur les SLC ont été réalisées sur des organismes modèles, avec 392 SLC identifiés chez *Mus musculus*, 344 chez *Drosophila melanogaster*, et 348 chez *Caenorhabditis elegans*. Pourtant, le nombre total, le nombre de copies et les sous-familles SLC varient considérablement selon les espèces (Heglound *et al.*, 2010; Xun *et al.*, 2020). Au cours de la dernière décennie, et grâce à l'avancement des outils de génomique fonctionnelle, les connaissances liées à l'implication de ces protéines dans l'accumulation, la translocation et la détoxification chez les moules (Pazos *et al.*, 2017), les huîtres (Matt *et al.*, 2018), les pétoncles (Xun *et al.*, 2020; Ventoso *et al.*, 2019; Wang *et al.*, 2022) et les poissons (Zhang *et al.*, 2022) ont augmenté.

La régulation positive significative du transporteur *SLC17* dans les glandes digestives de *P. maximus* (capitre 5) apparait fortement corrélée à l'expression des trois protéines liées à l'autophagie en raison de l'effet de l'exposition à l'AD. Parmi les gènes les plus "sur-exprimés" dans la glande digestive de *M. galloprovincialis* après exposition à *Pseudo-nitzschia spp*. toxique, Pazos *et al.* (2017) ont trouvé que la protéine *SLC17A5* et trois autres transcrits de la même famille étaient impliqués dans le transport de la sialine. Globalement, cette famille assure la médiation du transport transmembranaire des anions organiques (Reimer, 2013) avec une dominance dans le trafic de la sialine (*SLC17A5*) et du glutamate par transport vésiculaire. Chez les mammifères, la sialine transporte l'acide sialique vers les lysosomes pour le traitement enzymatique via l'autophagie, mais peut également fonctionner comme un transporteur vésiculaire pour l'acide aspartique et l'acide glutamique, régulant les concentrations de neurotransmetteurs dans la fente synaptique pour affecter la signalisation appropriée entre les neurones (Gether *et al.*, 2006*;* Miyaji *et al.*, 2008,

2011*;* Reimer, 2013). Cette évidence indique que les transporteurs vésiculaires de la sialine et du glutamate de la famille *SLC17* pourraient être impliqués dans le transport de l'AD et la régulation de l'autophagie, puisque cette toxine partage des caractéristiques structurelles avec l'acide glutamique. Cette hypothèse fait de cette famille de transporteurs des candidats intéressants pour la caractérisation future et des analyses fonctionnelles de toxicocinétique de l'AD.

L'expression du transporteur *SLC5* était étroitement corrélée à l'incorporation de l'AD dans la glande digestive de *P. maximus*, tandis que les deux gènes de cette famille (*SLC5* et *SLC5A1*) étaient significativement régulés chez *M. edulis* par l'effet de l'exposition à l'AD. Même si l'on sait relativement peu de choses sur le rôle de la famille *SLC5* dans le transport de l'AD, les membres de *SLC5* ont été désignés comme divers transporteurs fonctionnels et très étendus chez les péctinidés (Xun *et al.*, 2020). Ces transporteurs vésiculaires sodium-dépendants du glucose participent activement à l'absorption des toxines paralysantes (PST) des mollusques produites par les dinoflagellés dans les glandes digestives des pétoncles *Patinopecten yessoensis* (Xun *et al.*, 2020) et dans les branchies de *Chlamys farreri* (Li *et al.*, 2017; Wang *et al.*, 2022). De plus, six transporteurs de protéines de ce type ont montré une forte corrélation avec la charge en PST chez *C. gigas* (Mat *et al.*, 2018). Par conséquent, une forte implication de cette famille dans l'accumulation d'AD chez *P. maximus* et *M. edulis* ne peut être écartée.

Le gène *SLC6A9*, appartenant à la famille des neurotransmetteurs dépendant du sodium et du chlorure *SLC6* est apparue uniquement régulé positivement dans la glande digestive de *M. edulis* incubé dans l'AD. Certains membres de la famille *SLC6* sont également des transporteurs de glutamate (Gether *et al.*, 2006). De plus, le SLC6A8 est apparu surexprimé dans le cerveau du poisson zèbre après exposition à

l'AD (Lefebvre *et al.*, 2009), tandis que le *SLC6A14* a été trouvé parmi les SLC responsables de la translocation, de la dépuration et de la haute tolérance à la tétrodoxine (TTX) dans le foie du poisson-globe Takifugu rubripes (Zhang *et al.*, 2022). Cela nous a permis de supposer que le transporteur *SLC6A9* serait plus susceptible d'être impliqué dans un efflux rapide que dans l'entrée de l'AD chez *M. edulis*. Un autre résultat intéressant de cette étude était le modèle opposé de surexpression entre les transporteurs *SLC22A8* (transporteur d'anions organiques) et *SLC16A10* (transporteur de monocarboxylates) suite à l'exposition à la toxine dans les coquilles Saint-Jacques et les moules. Les grandes différences dans les concentrations finales d'AD dans les glandes digestives des deux espèces conduisent à émettre l'hypothèse que le *SLC22A8* serait impliqué dans l'entrée de la toxine dans les cellules digestives de *P. maximus*; à l'inverse, le transporteur *SLC16A10* serait impliqué dans l'excrétion de la toxine chez *M. edulis*. Un nombre élevé de transcrits différentiellement exprimés appartenant à ces trois familles (*SLC6, SLC22* et *SLC16*) a été trouvé dans les glandes digestives de *M. galloprovincialis* (Pazos *et al.*, 2017) et *A. opercularis* (Ventoso *et al.*, 2019) exposés à *Pseudo-nitzschia spp.* productrice d'AD. La famille *SLC22* comprend des transporteurs organiques de cations/anions/zwitterions, qui interviennent dans l'absorption (dans l'intestin) et l'excrétion (dans le foie et les reins) d'une variété de substrats plus petits et hautement hydrophiles, tels que divers médicaments et toxines chez les mammifères (Roth *et al.*, 2012*;* Koepsell *et al.*, 2013*;* Nigam, 2015). D'autre part, la famille SLC16 comprend un total de 14 membres qui partagent des motifs hautement conservés, présentant une large spécificité de substrat (Halestrap, 2013*;* Song *et al.*, 2020). La famille *SLC16* comprend des exportateurs de lactate efficaces et est impliquée dans le transport à travers la membrane plasmique des composés monocarboxylés, ainsi que des acides organiques faibles dans l'intestin humain

(Meredith et Christian, 2008*;* Steffansen *et al.*, 2004), où la direction du transport est déterminée par les gradients de concentration des substrats (Song *et al.*, 2020). Par conséquent, l'identification sans équivoque de la spécificité et de la direction du flux de l'AD à travers ces SLC chez les bivalves nécessitera une étude plus approfondie.

Toutes les familles de SLC qui ont montré une expression différentielle entre *P. maximus* et *M. edulis* dans ce travail de thèse (*SLC5, SLC17, SLC6, SLC16* et *SLC22*, chap 5) ont également montré une forte expansion et diversification dans les génomes des pétoncles *P. yessoensis* (Xun *et al.*, 2020) et *C. farreri* (Li *et al.*, 2017; Wang *et al.*, 2022) et sont apparues fortement corrélées à l'accumulation de toxines après exposition à *Alexandrium spp*. En particulier, la glande digestive des bivalves présenterait une très grande diversité de ces transporteurs, ce qui pourrait contribuer à l'évolution adaptative des bivalves pour tolérer et survivre dans des environnements contenant des microalgues toxiques (Xun *et al.*, 2020). Cette expansion rapide et la nouveauté fonctionnelle des SLC dans le génome des bivalves aurait entraîné d'importantes altérations au niveau des sites de reconnaissance des protéines (Hong, 2017; Xun *et al.*, 2020), expliquant la grande diversité des substances trafiquées à travers la membrane ou la capacité des transporteurs à interagir avec différents substrats.

Bien que les preuves de la littérature soient fortement biaisées en faveur de l'implication des transporteurs SLC dans l'entrée des phycotoxines, la dépuration rapide de l'AD initialement assimilée par les cellules digestives via ce type de transporteurs dans les dépurateurs rapides ne peut être exclue, ce qui pourrait également expliquer les différences très importantes dans les concentrations finales en AD trouvées entre les coquilles Saint-Jacques et les moules dans ce travail. Cette preuve renforce également l'hypothèse de Mauriz et Blanco (2010) puisque certains

des transporteurs SLC trouvés régulés positivement chez *M. edulis* dans cette étude, semblent être beaucoup plus efficaces pour excréter la toxine que ceux de *P. maximus*. De plus, après la caractérisation du processus d'absorption de l'AD dans les glandes digestives de *M. galloprovincialis*, Blanco *et al.* (2021) ont conclu que même si les transporteurs impliqués dans l'absorption de la toxine ont des caractéristiques similaires parmi les dépurateurs lents et rapides de l'AD, l'accumulation de toxine devrait être sensiblement plus élevée dans les premiers, comme cela s'est produit dans ce travail chez *P. maximus* , avec une absorption d'AD lors d'une incubation *in vitro* de 2h des glandes digestives, de près de 20 fois supérieure à celle de *M. edulis*.

L'analyse intégrative combinant l'absorption d'AD, les caractéristiques subcellulaires et l'activation des gènes ciblés nous amènent à formuler l'hypothèse d'une faible capacité de reconnaissance de la toxine par les cellules digestives et une excrétion moins efficace de la toxine par les SLC chez *P. maximus*. A l'inverse, la plus faible accumulation d'AD dans la glande digestive des moules a montré une relation complexe avec l'activation des iGR et avec l'expression de presque toutes les protéines SLC, ce qui pourrait indiquer une implication potentielle des récepteurs du glutamate dans la reconnaissance de la toxine sur la face externe de la membrane cellulaire, déclenchant ainsi son influx, mais un transport par efflux beaucoup plus efficace de cette toxine à travers les cellules digestives des moules.

Bien que l'expression des transporteurs membranaires de type ABC n'ait pas été mesurée dans ce travail, une étude plus approfondie comparant les dépurateurs rapides et lents de l'AD serait fortement souhaitable. Chez les organismes aquatiques, les protéines ABC ont montré une protection efficace contre les effets délétères causés par l'exposition à une variété de composés toxiques (Jeong *et al.*, 2017), mais leur implication potentielle sur l'excrétion de phycotoxines chez les bivalves (Huang *et al.*,

2014*;* Lozano *et al.*, 2015*;* Xu *et al.*, 2014). Des études antérieures en ARN-seq ont révélé qu'une grande variété de transporteurs ABC régulés à la hausse pouvaient être impliquée dans le processus de translocation et de détoxification des PST accumulés chez *C. gigas* (Matt *et al.*, 2018), *P. yessoensis* (Xun *et al.*, 2020) et *C. farreri* (Wang *et al.*, 2022), ainsi que l'acide okadaïque dans le pétoncle *Argopecten irradians* (Chi *et al.*, 2018), et la tétrodotoxine (TTX) dans le poisson *T. rubripes* (Zhang *et al.*, 2022). D'autres études transcriptomiques n'ont identifié que la régulation différentielle du nombre de membres de ce groupe de transporteurs après exposition à *Pseudo-nitzschia* toxique, comme dans le cas de *M. galloprovincialis* (Pazos *et al.*, 2017) et *A. opercularis* (Ventoso *et al.*, 2019) suggérant son implication dans l'absorption ou l'excrétion de l'AD dans la glande digestive de ces organismes. Schultz *et al.* (2013) ont émis l'hypothèse que l'absorption de l'AD par l'intestin antérieur et le transfert dans l'hépatopancréas et l'hémolymphe étaient régulés par des transporteurs ABC unidirectionnels chez les crabes dormeurs *Metacarcinus magister*. Cependant, cela contredit les conclusions de Blanco *et al.* (2021) puisque dans la glande digestive de *M. galloprovincialis*, le mécanisme d'absorption de l'AD semble être indépendant de l'ATP, du H^+ ou du Na^+, mais dépendre du Cl^- ou d'autres anions. La plupart des SLC évalués dans cette étude, bien qu'ils soient dépendants du Na^+, sont également dépendants du Cl^-, ce qui renforce les conclusions de Blanco *et al.* (2021) pointant l'implication de ces transporteurs dans le trafic de l'AD chez les bivalves.

L'AD accumulé dans les tissus des bivalves peut subir des processus de métabolisation par lesquels ils est modifié chimiquement, que ce soit en isomères plus ou moins toxiques par rapport à la molécule d'origine (Vale et Sampayo, 2001; Takata *et al.*, 2009). Ces biotransformations peuvent résulter, soit du métabolisme digestif, soit d'un processus de détoxification enzymatique active (Wright *et al.*, 1990b; Costa

et al., 2005; Basti *et al.*, 2018). Pour les cinq espèces de cette étude, 3 mollusques bivalves (*P. maximus, A. opercularis* et *D. trunculus*), 1 gastéropode (*C. fornicata*) et 1 tunicate (*Asterocarpa sp.*), les modifications du profil toxinique ont été comparées avec certains paramètres subcellulaires liés à l'accumulation et/ou à la longue rétention de l'AD (chapitre 3). L'analyse intégrative a révélé que les mécanismes subcellulaires évalués sur des animaux contaminés pourraient impliquer une biotransformation intracellulaire de l'AD, puisqu'une relation étroite et significative a été trouvée entre l'autophagie, la vacuolation des cellules digestives, et le profil isomérique de la toxine des invertébrés.

Par conséquent, une activation significative de certaines protéines candidates liées au métabolisme des xénobiotiques était attendue dans ce travail après exposition à l'AD de la glande digestive de *P. maximus* et *M. edulis*. Néanmoins, aucun gène codant pour les enzymes impliquées dans la défense antioxydante/la détoxification étudiés ici n'ont montré de modification significative de leur taux de transcrits du à l'effet de la toxine, ni chez la moule, ni chez la coquille Saint-Jacques. Cependant il existe un grand nombre de gènes codant pour des enzymes antioxydantes et nous n'en avons ciblé que quatre. Il se peut également que l'activité de ces enzymes ne soit pas régulée au niveau transcrptionnelle. Un grand nombre de gènes ou de protéines impliqués dans la détoxification et le métabolisme des antioxydants ont été identifiés lorsque plusieurs espèces de bivalves ont été exposées à des microalgues toxiques ou à leurs toxines respectives. Parmi les familles d'enzymes de détoxification les plus fréquemment signalées figurent les cytochromes P450, les aldo-céto réductases, les glutathion S-transférases (GST), les sulfotransférases (ST), la glutathion peroxydase (GPx), la superoxyde dismutase (SOD) et la protéine heat-chock de 70 kDa. (HSP70). La plupart de ces enzymes ont été identifiées comme étant activées dans

les tissus de pétoncles (Lou *et al.*, 2020*;* Wang *et al.*, 2022) et d'huîtres (Fabioux *et al.*, 2015*;* Matt *et al.*, 2018) exposés à des algues productrices de PST. Notamment, la GST et la ST ont montré une forte régulation à la hausse dans les transcriptomes de *M. galloprovincialis* (Pazos *et al.*, 2017) et *A. opercularis* (Ventoso *et al.*, 2019) en réponse à l'accumulation de l'AD dans la glande digestive, ce qui indique leurs effets potentiels sur la médiation des effets nocifs liés à l'absorption de l'AD. Même lorsque les preuves moléculaires de ce travail indiquent que la biotransformation n'est pas la principale voie d'élimination de l'AD chez les coquilles Saint-Jacques et les moules, certaines évidences indiquent un métabolisme de l'AD spécifique à l'espèce puisque des changements de variabilité dans les niveaux des isomères de cette toxine ont été détectés chez des poissons et des bivalves (Vale et Sampayo, 2001*;* Takata *et al.*, 2009). Par ailleurs, l'étude de Costa *et al.* (2005) a montré quelques informations sur la biotransformation de l'AD liée à l'augmentation apparente du taux global de détoxification de l'AD chez la seiche *Sepia officinalis*, où les isomères de l'AD représentent un pourcentage significatif du profil de toxine dans les branchies, ce qui suggère que cet organe a une fonction importante dans la détoxification. Ces éléments suggèrent que l'implication de la batterie enzymatique dans la biotransformation de l'AD ne peut être exclue dans les scénarios de contamination naturelle.

Ce travail a répondu à la principale question posée au début de ce travail de t hèse concernant les mécanismes physiologiques potentiellement impliqués dans l'accumulation et la longue rétention de l'AD chez *P. maximus*. Cependant, il a également généré toute une série de nouvelles questions et hypothèses qui devraient être abordées dans les recherches futures afin d'élargir les connaissances sur ces mécanismes et de proposer des solutions pour accélérer la dépuration de l'AD chez les coquilles. L'une des perspectives de ce travail qui semble particulièrement

pertinente serait l'analyse transcriptomique (ARN-seq) des différents tissus de *P. maximus*, mais particulièrement de la glande digestive, dans un scénario de contamination naturelle avec une exposition à des cellules *Pseudo-nitzschia* productrices d'AD. À ce jour, il n'y a pas d'analyse similaire en raison de la difficulté de cultiver des souches toxiques de *Pseudo-nitzschia*, en plus de la difficulté de récupérer des coquilles St-Jaques complètement décontaminées de l'AD qui peuvent être utilisées comme des témoins "négatifs" de contamination dans les expériences de contamination.

La pleine compréhension de la reconnaissance de l'AD médiée par les récepteurs sur la membrane plasmique des espèces affectées est également essentielle pour aller plus loin dans la proposition d'alternatives pour résoudre ce problème. La comparaison *in silico* des récepteurs impliqués dans l'autophagie et la reconnaissance du glutamate identifiés chez les invertébrés et les mammifères avec ceux impliqués dans la reconnaissance potentielle de l'AD chez *P. maximus* est essentielle pour identifier les différences évolutives pouvant donner lieu à la reconnaissance de la toxine chez les espèces contaminées. Une alternative pourrait être de tester des récepteurs candidats grâce à la deorphanisation des récepteurs impliqués dans l'autophagie et le glutamate chez les invertébrés marins susceptibles d'accumuler de l'AD, dont les ligands et la fonction sont encore inconnus. Des stratégies de criblage ont été développées au fil des années afin d'identifier des ligands naturels hautement sélectifs pour les récepteurs orphelins (Wise *et al.*, 2004*;* Parmentier et Detheux, 2006*;* Schwartz *et al.*, 2018) qui pourraient être applicables dans la poursuite de l'étude dans ce domaine.

Les résultats de ce travail ont renforcé les évidences indiquant que le transport de l'AD (entrée ou sortie) est médié par des protéines de transport membranaire appartenant à plusieurs sous-familles qui sont très développées et diversifiées dans les

génomes/transcriptomes des pétoncles, qui sont les espèces les plus sensibles à la longue rétention d'AD (Xun *et al.*, 2020*;* Wang *et al.*, 2022*;* Pazos *et al.*, 2017*;* Ventoso *et al.*, 2019, 2021). L'étude plus approfondie du channelome par des approches RNA-seq ou protéomique est essentielle pour comprendre l'ensemble des canaux ioniques, porines, et protéines SLC exprimés dans les cellules digestives de *P. maximus* pour leur caractérisation ultérieure afin de comprendre leur implication dans le transport de la toxine. L'introduction de gènes hétérologues ou l'inactivation de l'expression de gènes liés à l'autophagie, aux récepteurs du glutamate et aux transporteurs membranaires par des stratégies de génie génétique telles que l'ARN d'interférence et CRISPR-Cas9 pourraient être utiles pour comprendre la fonction de certaines des protéines candidates analysées dans le présent et d'autres études. Reprenant ainsi l'énorme défi de la génération précédente de connaissances transcriptomiques et protéomiques de ces gènes chez *P. maximus*.

L'analyse intégrative réalisée dans cette étude renforce fortement nos connaissances pour la compréhension des mécanismes physiologiques impliqués dans l'absorption et l'élimination de cette toxine chez les bivalves présentant des capacités différentes de métabolisation de l'AD. L'évolution adaptative s'associe probablement à une combinaison d'acquisition de nouveaux gènes et de modification de gènes existants entraînée par une sélection positive dans l'environnement avec l'AD, impliquant le rôle diversifié des mécanismes physiologiques dans la régulation de l'accumulation de cette toxine chez les bivalves. Des études au niveau transcriptomique et protéomique sont essentielles pour élucider les SLC susceptibles d'être sous sélection positive et éventuellement impliquées dans l'adaptation spécifique à l'espèce/ à la lignée pour faire face à des efflorescences de *Pseudo-nitzschia* toxique. Les résultats de ce travail

fournissent des informations inédites pour aller plus loin dans la proposition de procédures visant à accélérer la dépuration de l'AD chez *P. maximus*.

BILAN DE LA THÈSE

Publications (1)

García-Corona, J.L., Hegaret, H., Deléglise, M., Marzari, A., Rodríguez-Jaramillo, C., Foulon, V., Fabioux, C. (2022). First subcellular localization of the amnesic shellfish toxin, domoic acid, in bivalve tissues: Deciphering the physiological mechanisms involved in its long-retention in the king scallop *Pecten maximus*. *Harmful Algae*, 116, 102251. https://doi.org/10.1016/j.hal.2022.102251.

Publications en préparation (7)

Garcia-Corona, J.L., Fabioux, C., Blanco, J., Martínez-Rincón, R.O., Hegaret, H. The fate of the Amnesic Shellfish Poisoning (ASP) toxin, domoic acid in marine fish and invertebrates. *Article de revue.*

García-Corona, J.L., Deléglise, M., Vanmaldergem, J., Petek, S., Terre-Terrillon, A., Bressolier, L., Fabioux, C., Hegaret, H. Kinetics of the subcellular localization of the Amnesic Shellfish Poisoning toxin, domoic acid, in the king scallop *Pecten maximus* in a contamination and decontamination scenario. *Article original.*

García-Corona, J.L., Fabioux, C., Lassudrie-Duchesne, M., Derrien, A., Terre-Terrillon, A., Delaire, T., Hegaret, H. Comparative study of domoic acid accumulation, isomer content and associated digestive subcellular processes in five marine invertebrate species. *Article original.*

García-Corona, J.L., Hegaret, H., Blanco, J., Bidault, A., Fleury, E., Rossignoli, A.E., Calvo, E., Fabioux, C. The *in vitro* exposure of the digestive gland to the Amnesic Shellfish Toxin, domoic acid, reveals differences in activation of molecular and subcellular mechanisms between the slow-depurator *Pecten maximus* and the fast *Mytilus edulis*. *Article original.*

García-Corona, J.L., Hegaret, H., Fabioux, C. Impacts of *Pseudo-nitzschia* and domoic acid transfer in marine ecosystems. *Chapitre du livre*.

Roux, P., **García-Corona, J.L.**, Ragueneau, S., Schapira, M., Siano, R., Pernet, F., Queau, I., Malestroit, P., Tallec, K., Fleury, F. Ecophysiological response of the cupped oyster *Crassostrea gigas* exposed to the green dinoflagellate *Lepidodinium chlorophorum. Article original.*

Cueto-Vega, R., Flye-Sainte-Marie, J., **García-Corona, J.L.**, Palacios-Lau, F., Aguirre-Velarde, A., Jean, F., Gil-Kodaka, P., Mendoa, J., Thouzeau, G. Trade-off between growth and reproduction in scallop *Argopecten purpuratus* (L.) exposed to medium-term hypoxia and acidification. *Article original.*

Publications annexes à la thèse (7)

García-Corona, J. L., Mazón-Suástegui, J. M., Acosta-Salmón, H., Díaz-Castro, S. C., Amezquita-Arce, P., Rodríguez-Jaramillo, C. (2019). Super-low-frequency electromagnetic radiation affects early development of Pacific oysters (*Crassostrea gigas*). *Aquaculture Research*, 50(9): 2729–2734. https://doi.org/10.1111/are.14219.

Mazón-Suástegui, J. M., López-Carvallo, J. A., Rodríguez-Jaramillo, C., Arcos-Ortega, G. F., Abasolo-Pacheco, F., **García-Corona, J.L.** (2020). Ultra-diluted bioactive compounds enhance energy storage and oocyte quality during gonad conditioning of Pacific calico scallop *Argopecten ventricosus* (Sowerby II, 1842). *Aquaculture Research*, 52(4): 1490–1500. https://doi.org/10.1111/are.15002.

García-Corona, J.L.; Rodríguez-Jaramillo, C; Mazón-Suástegui, J.M; Ramírez-Luna, S. and R. Riosmena-Rodríguez. 2022. Retrospective analysis of the

morphophysiological and reproductive condition of two populations of Catarina Scallop *Argopecten ventricosus* In: Riosmena-Rodríguez, R. (ed.). La Paz Bay: Biodiversity, Ecological and Social Processes. Autonomous University of Baja California Sur, Mexico. ISBN: 978-607-8654-64-2.

Rodríguez-Jaramillo, C., **García-Corona, J. L.**, Zenteno-Savín, T., Palacios, E. (2022). The effects of experimental temperature increase on gametogenesis and heat stress parameters in oysters: Comparison of a temperate-introduced species (*Crassostrea gigas*) and a native tropical species (*Crassostrea corteziensis*). *Aquaculture,* 561, 738683. https://doi.org/10.1016/j.aquaculture.2022.738683.

Rodríguez-Jaramillo, C., **García-Corona, J.L.,** Estrada, N., Palacios, E. (2023). Changes in carbohydrates and N-Acetylglucosamine (Glcnac) in response to an experimental increase of temperature in tissues of two oyster species, the temperate Introduced *Crassostrea gigas* and the native tropical *Crassostrea corteziensis. Journal of Aquaculture & Fisheries,* 7, 9. https://doi.org/10.24966/AAF-5523/100056.

Vanmaldergem, J., **García-Corona, J. L.**, Deléglise, M., Fabioux, C., Hegaret, H. (2023). Effect of the antioxidant N-acetylcysteine on the depuration of the amnesic shellfish poisoning toxin, domoic acid, in the digestive gland of the king scallop *Pecten maximus*. *Aquatic Living Resources*, 36, 14. https://doi.org/10.1051/alr/2023011.

García-Corona, J.L., Arcos-Ortega, G.F., Rodríguez-Jaramillo, C., López-Carvallo, J.A., Mazón-Suástegui, J.M. (2023). Examination of the effects of highly-diluted bioactive compounds on gametogenesis in relation to energy budget and oocyte

quality in mussel (*Modiolus capax*) broodstock. *Aquaculture*, 578, 740080. https://doi.org/10.1016/j.aquaculture.2023.740080.

Présentations orales en conférences nationales (3)

Garcia-Corona, J.L., Fabioux, C., Hegaret, H., Fleury, E., Lassudrie, M. Physiological and molecular mechanisms involved in domoic acid contamination/decontamination in the king scallop *Pecten maximus*. Conférence virtuelle du GdR Phycotox 2020.

García-Corona, J.L., Hegaret, H., Deléglise, M., Marzari, A., Rodríguez-Jaramillo, C., Foulon, V., Fabioux, C. First subcellular localization of the amnesic shellfish toxin, domoic acid, in bivalve tissues: Deciphering the physiological mechanisms involved in its long-retention in the king scallop *Pecten maximus*. Conférence GdR Phycotox 2022. Brest/Plouzané (France).

García-Corona, J.L., Deléglise, M., Vanmaldergem, J., Petek, S., Terre-Terrillon, A., Bressolier, L., Fabioux, C., Hegaret, H. A King's tale: Is autophagy the mechanism behind the long-retention of the amnesic shellfish poisoning toxin, domoic acid, in king scallops *Pecten maximus?* Conférence GdR Phycotox & GIS Cyano 2023, Nantes (France).

Présentations orales en conférences internationales (3)

Garcia-Corona, J.L., Hegaret, H., Fleury, E., Lassudrie, M., Fabioux, C**.** Domoic acid *in situ* detection in tissues of the king scallop *Pecten maximus*: deciphering the subcellular mechanisms involved in contamination during blooms of the toxic diatom *Pseudo-nitzschia spp*. 19th International Conference on Harmful Algae, La Paz,

Mexico, 2021, en distanciel**. *Prix Maureen Keller pour la meilleure présentation orale étudiant*.**

Garcia-Corona, J.L., Hegaret, H., Lassudrie, M., Derrien, A., Fleury, E., Fabioux, C. Immunohistochemistry as a tool to decipher the mechanisms involved in the accumulation and long retention of the phycotoxin domoic acid in the king scallop *Pecten maximus.* Physiomar & ANZMBS, Nelson, New Zealand, 2021, en distanciel.

García-Corona, J.L., Hegaret, H., Blanco, J., Bidault, A., Fleury, E., Calvo, E., Fabioux, C. Differential activation of subcellular and molecular mechanisms by the Amnesic Shellfish Poisoning toxin, domoic acid, between the slow-depurator *Pecten maximus* and the fast *Mytilus edulis*. 115th National Shellfisheries Association Conference, Baltimore, MD, USA, 2023.

Encadrement des étudiants (5)

Adeline MARZARI, Master1 Sciences de la Mer et du Littoral, Mention Biologie, Parcours Biologie des Populations, Année universitaire 2020-2021.

Marie CALVEZ, 1ere année DUT Génie Biologique option Analyses Biologiques et Biochimiques, Année universitaire 2020-2021.

Laura BRESSOLIER, Master1 Sciences de la Mer et du Littoral, Mention Biologie, Parcours Biologie des Populations, Année universitaire 2021-2022.

Eva CALVO, Master2 Sciences, Technologies, Health, Mention Biology and Health, Parcours Genetic, Genomics and Biotechnology, Année universitaire 2021-/2022.

Tome DELAIRE, Licence 3 Sciences de la vie et de la terre, Parcours Biologie environnement, Année universitaire 2021-2022.

Formations (6)

- L'écotoxicologie aquatique : une boîte à outils pour évaluer l'impact de la pollution. Association mésoaméricaine d'écotoxicologie et de chimie environnementale. 22-25 mars 2021. Mexique-EN LIGNE.
- SEA-EU DOC training Event: Career Development for Doctoral Students. 17-21 May 2021, 17-21 mai 2021, Malte-EN LIGNE.
- DocuSciences, Formation à la médiation de problématiques scientifiques, sociales & environnementales par l'usage des techniques du cinéma documentaire. 25-27 mai et 9-10 juin 2021, Institut Universitaire Européen de la Mer, Brest, France.
- The Problem-solving Skills for Higher Education Learners. 23-27 mai 2022, Université de Split, Croatie.
- MOOC-Ethique de la recherche. 21 mars au 16 juin, 2023. Université de Lyon-ONLINE.

Enseignements (1)

8 heures de TP/TD durant l'année universitaire 2022/2023 pour la formation «Marine Genomics» du Master en Sciences de la Mer et du Littoral | Institut Universitaire Européen de la Mer / Master Sciences de la mer | Sorbonne Université.

Séjours de Recherche (1)

Séjour de recherche (financement ISBlue (1,6k€) obtenu suite à la réponse à l'appel à projet : "mobilités sortantes doctorant") sous tutelle académique du Dr. Juan BLANCO pour développer les expérimentations du projet "Study of the contamination and decontamination process with domoic acid on bivalves during harmful algal blooms of *Pseudo-nitzschia* sp., au Centro de Investigacións Mariñas du 04 au 12 février 2022, en Galice, Espagne.

Financements obtenus (2)

- Projet IUEM (2,5k€) (2021): CoDDa_Subcellular mechanisms involved in domoic - acid (DA) contamination/decontamination in the king scallop *Pecten maximus.*

- Bourse mobilité sortante ISBlue (1,782€) pour participation à la conférence annuelle de la NSA à Baltimore (Etats-Unis).

Sciences et Sociétés (9)

- Conférencier invité «Biología y Bases Científicas y Tecnológicas para el Cultivo de Bivalvos Marinos» pour la communauté étudiante de la carrière Technique en Aquaculture du Centro Multimodal de Estudios Científicos y Tecnológicos del Mar y Aguas Continentales le 12 novembre 2020-EN LIGNE, Mexico City, Mexique.
- Conférencier invité «Mareas rojas: asesinos seriales del mar» pour le programme de vulgarisation scientifique «En sus marcas, listos, ciencia!» du Consejo Sudcaliforniano de Ciencia y Tecnologia le 15 avril 2021- EN LIGNE, La Paz, Mexique.
- Conférencier invité lors de la Rencontre du Réseau Thématique CONACYT «Océan, climat et changement global» Atelier franco-mexicain «Océans 2021»

organisé par l'Ambassade de France au Mexique du 28 au 30 juin 2021- EN LIGNE, Mexico, Mexique.

- Réalisation de matériel de diffusion scientifique dans la modalité podcast «La toxina amnesica, ácido domoico» pour le Centro de Investigaciones Biológicas del Noroeste, le 9 novembre 2021- EN LIGNE, La Paz, Mexique.
- Projection de la capsule vidéo «La coquille Saint-Jacques face aux algues toxiques » lors des Journées de l'École Doctorale Sciences de la Mer et du Littoral du 16 au 18 novembre 2021 à Oceanopolis, Brest, France.
- Conférencier principal «Estado Actual de la Pesca y Acuacultura de Moluscos Bivalvos: Retos y Perspectivas» pour la communauté étudiante de la carrière Technique en Aquaculture du Centro Multimodal de Estudios Científicos y Tecnológicos del Mar y Aguas Continentales, lors de la célébration de la journée mondiale de l'aquaculture le 30 novembre 2021- EN LIGNE, Mexique.
- Conférencier invité «The fate of the amnesic toxin, domoic acide, in the king scallop *Pecten maximus*» lors du séminaire de l'Academia de Biotecnologia du Centro de Investigaciones Biológicas del Noroeste, le 9 décembre 2021- EN LIGNE, La Paz, Mexique.
- Jeune chercheur ambassadeur «The One Planet Summit for the Ocean» Organisé par l'UNESCO et la Présidence de la République française du 9 au 11 février 2022. Brest, France.
- Conférencier invité «Development of a novel immunohistochemical technique for the *in situ* detection of the phycotoxin domoic acid in bivalve tissues» lors du séminaire de l'Academia de Desarrollo de Tecnologias du Centro Interdisciplinario de Ciencias Marinas-IPN, le 3 mars 2022- EN LIGNE, La Paz, Mexique.

- Conférencier principal «El rol de los jovenes investigadores en la revolucion azul: el futuro de las ciencias ambientales marinas» lors de la 2eme Semaine de biologie marine, organisée par l'Université de Guadalajara le 12 octobre 2022- EN LIGNE, Jalisco, Mexique.

REFERENCES

— A —

Adams, N.G., Lesoing, M., Trainer, V.L. 2000. Environmental conditions associated with domoic acid in razor clams on the Washington coast. *Journal of Shellfish Research,* 19:1007–1015.

Ajani, P., Murray, S., Hallegraeff, G., Lundholm, N., Gillings, M. *et al.* 2013. The diatom genus *Pseudo-nitzschia* (Bacillariophyceae) in New South Wales, Australia: morphotaxonomy, molecular phylogeny, toxicity, and distribution. *Journal of Phycology,* 49: 765–785.

Allam, B., Espinosa, P. E. 2016. Bivalve immunity and response to infections: Are we looking at the right place? *Fish & Shellfish Immunology,* 53, 4–12. https://doi.org/10.1016/j.fsi.2016.03.037

Altwein, D.M., Foster, K., Doose, G., Newton, R. 1995. The detection and distribution of the marine neurotoxin domoic acid on the Pacific coast of the United States. *Journal of Shellfish Research,* 14:217– 222.

Álvarez, G., Rengel, J., Araya, M., Álvarez, F., Pino, R., Uribe, E., Díaz, P.A., Rossignoli, A.E., López-Rivera, A., Blanco, J. 2020. Rapid Domoic Acid Depuration in the Scallop *Argopecten purpuratus* and Its Transfer from the Digestive Gland to Other Organs. *Toxins,* 12, 698. https://doi.org/10.3390/toxins12110698.

Álvarez, G., Uribe, E., Regueiro, J., Martin, H., Gajardo, T., Jara, L., Blanco, J. 2015. Depuration and anatomical distribution of domoic acid in the surf clam *Mesodesma donacium*. *Toxicon*, 102, 1–7. https://doi.org/10.1016/j.toxicon.2015.05.011.

Amzil, Z., Fresnel, J., Le Gal, D., Billard, C. 2001. Domoic acid accumulation in French shellfish in relation to toxic species of *Pseudo-nitzschia multiseries* and *P. pseudodelicatissima*. *Toxicon*, 39(8), 1245–1251. https://doi.org/10.1016/s0041-0101(01)00096-4.

Amzil, Z., Sibat, M., Royer, F., Masson, N., Abadie, E., 2007. Report on the first detection of pectenotoxin-2, spirolide-A and their derivatives in French shellfish. *Marine Drugs,* 5, 168–179.

Anderson, D., Fachon, E., Hubbard, K., Lefebvre, K., Lin, P., Pickart, R., Richlen, M., Sheffield, G., Van Hemert, C. (2022). Harmful Algal Blooms in the Alaskan Arctic: An Emerging Threat as the Ocean Warms. *Oceanography.* The Oceanography Society. https://doi.org/10.5670/oceanog.2022.121.

Andjelkovic, S.M. Vandevijvere, J. Van Klaveren, H. Van Oyen, J. Van Loco. 2012. Exposure to domoic acid through shellfish consumption in Belgium, *Environmental International*, 49: 115–119.

Arévalo, F., Bermudez de la Puente, M., Salgado, C. 1998. ASP toxicity in scallops: individual variability and distribution. In: Reguera, B., Blanco, J., Fernández, M.L., Wyatt, T. (Eds.), Harmful Microalgae. Santiago de Compostela: Xunta de Galicia and the IOC of UNESCO, pp. 499–502.

Auro, M.E. Cochlan, W.P. 2013. Nitrogen utilization and toxin production by two diatoms ofthe *Pseudo-nitzschia pseudodelicatissima* complex: *P. cuspidata* and *P. fryxelliana. Journal of Phycology,* 49, 156–169.

Ayache, N., Hervé, F., Lundholm, N., Amzil, Z., Caruana, A. M. N. 2019. Acclimation of the Marine Diatom *Pseudo-nitzschia australis* to Different Salinity Conditions: Effects on Growth, Photosynthetic Activity, and Domoic Acid Content. In T. Mock (Ed.), Journal of Phycology (Vol. 56, Issue 1, pp. 97–109). Wiley. https://doi.org/10.1111/jpy.12929.

Ayache, N., Hervé, F., Martin-Jézéquel, V., Amzil, Z., Caruana, A. M. N. 2018. Influence of sudden salinity variation on the physiology and domoic acid production by two strains of *Pseudo-nitzschia australis*. In T. Mock (Ed.), *Journal of Phycology*, 55(1), 186–195. https://doi.org/10.1111/jpy.12801.

Ayaz, F., Eker-Develi, E., Sahin, M. 2018. First report of *Nitzschia navis-varingica* in the Mediterranean Sea and growth stimulatory effects of *Nitzschia navis-varingica*, *Chrysochromulina alifera* and *Heterocapsa pygmaea* on different mammalian cell types. *Molecular Biology Reports,* 45, 571–579.

— B —

Baden, D. G., Trainer, V. L. 1993. Mode of Action of Toxins of Seafood Poisoning. *Algal Toxins in Seafood and Drinking Water,* 49–74. https://doi.org/10.1016/b978-0-08-091811-2.50008-3.

Balbi, T., Cortese, K., Ciacci, C., Bellese, G., Vezzulli, L., Pruzzo, C., Canesi, L. 2018. Autophagic processes in *Mytilus galloprovincialis* hemocytes: effects of *Vibrio tapetis*. *Fish & Shellfish Immunology,* 73, 66–74. https://doi.org/10.1016/j.fsi.2017.12.003

Baranska, A., Shawket, A., Jouve, M., Baratin, M., Malosse, C., Voluzan, O., Vu Manh, T.-P., Fiore, F., Bajénoff, M., Benaroch, P., Dalod, M., Malissen, M., Henri, S., Malissen, B. 2018. Unveiling skin macrophage dynamics explains both tattoo persistence and strenuous removal. *Journal of Experimental Medicine,* 215(4), 1115–1133. https://doi.org/10.1084/jem.20171608.

Bargu, S., Silver, M.W. 2003. First field evidence of krill grazing on the toxic diatom genus *Pseudo- nitzschia* in Monterey Bay, California. Bulletin of Marine Science. 72(3): 629–638.

Bargu, S., Powell, C.L., Coale, S.L., Busman, M., Doucette, G.J., Silver, M.W. 2002. Krill: a potential vector for domoic acid in marine food webs. *Marine Ecology Progress Series*, 237: 209–216. https://doi.org/10.3354/meps237209.

Bargu, S., Powell, C.L., Wang, Z., Doucette, G.J., Silver, M.W. 2008. Note on the occurrence of *Pseudo-nitzschia australis* and domoic acid in squid from Monterey Bay, CA (USA). Harmful Algae 2008, 7, 45–51.

Basti, L., Hegaret, H., & Shumway, S.E. (2018). Harmful Algal Blooms and Shellfish. In Shumway, S.E., Burkholder, J.M., Morton, S.L., eds. Harmful Algal Blooms a Compendium Desk Reference, pp.135–191. John Wiley & Sons Inc., Hoboken, NJ.

Bates S.S., Garrison D.L., Horner R.A., 1998. Bloom dynamics and physiology of domoic-acid-producing Pseudo-nitzschia species. In: Physiological ecology of harmful algal multiseries.In: Harmful algal blooms 2000 (Ed. by G.M. Hallegraeff, S.I. Blackburn, C.J. Bolch & R.J. Lewis), pp. 320–323. Intergovernmental Oceanographic Commission of UNESCO, Paris.

Bates S.S., Trainer, V.L. 2006. The ecology of harmful diatoms. In: Granéli E, Turner J, editors. Ecology of harmful algae. Heidelberg (Germany): Springer. p. 81–93.

Bates SS. 1997. Toxic phytoplankton on the Canadian east coast: implications for aquaculture. *Bull Aquacult Assoc Canada* 97(3):9–18. Available from: http://www.glf.dfo-mpo.gc.ca/dapr-radp/ docs/bates_bull_aquacult_assoc_can_1997.pdf.

Bates SS. 2004. Amnesic shellfish poisoning: domoic acid production by *Pseudo-nitzschia* diatoms. *Aqua Info Aquaculture Notes*. Available from: http://www.gov.pe.ca/photos/original/ af_domoic_acid.pdf/.

Bates, S.S. Richard, D.J.A. 2000a. Shellfish harvest area closure due to domoic acid – Mill River, Prince Edward Island. *Harmful Algae News,* 21, 6–7.

Bates, S.S., 2000b. Domoic acid producing diatoms: another genus added! *Journal of Phycology,* 36, 978–985.

Bates, S.S., Hubbard, K.A., Lundholm, N., Montresor, M., Leaw, C.P. 2018. *Pseudo-nitzschia, Nitzschia,* and domoic acid: new research since 2011. *Harmful Algae*, 79, 3-43. https://doi.org/10.1016/j.hal.2018.06.001.

Bates, S.S., Trainer, V.L. 2006. Diatoms. In: Graneli, E., Turner, J.T. (Eds.), *Ecology of Harmful Algae,* pp. 81–93.

Baugh, K.A., Bush, J.M., Bill, B.D., Lefebvre, K.A., Trainer, V.L. 2006. Estimates of specific toxicity in several *Pseudo-nitzschia* species from the Washington coast,

based on culture and field studies, Afr. *African Journal of Marine Science*. 28: 403–407.

Baustian, M.M., Bargu, S., Morrison, W., Sexton, C., Rabalais, N.N. 2018. The polychaete, *Paraprionospio pinnata*, is a likely vector of domoic acid to the benthic food web in the northern Gulf of Mexico. *Harmful Algae*, 79, 44–49. https://doi.org/10.1016/j.hal. 2018.06.002.

Bejarano, A.C., VanDola, F.M., Gulland, F.M., Rowles, T.K., Schwacke, L.H. 2008. Production and toxicity of the marine biotoxin domoic acid and its effects on wildlife: a review. *Human and Ecological Risk Assessment*. https://doi.org/10.1080/10807030802074220.

Bejarano, A.C., VanDola, F.M., Gulland, F.M., Rowles, T.K., Schwacke, L.H. 2008. Production and toxicity of the marine biotoxin domoic acid and its effects on wildlife: a review. *Human and Ecological Risk Assessment*. https://doi.org/10.1080/10807030802074220.

Ben Haddouch, A., Taleb, H., Elmortaji, H., Ben Brahim, S., Ennafah, B., Menchih, K., Boumaz, A., Mzaki, F., Radi, A., Loutfi, M. 2016. Accumulation and tissue distribution of domoic acid in the common cuttlefish, *Sepia officinalis* from the south Moroccan coast. *American Academic Scientific Research Journal for Engineering, Technology, and Sciences,* 15(1), 252–264.

Beninger, P. G., & Le Pennec, M. (2016). Structure and function in scallops. In: S. E. Shumway, & G. J. Parsons (Eds.), Scallops: Biology, ecology, aquaculture, and fisheries (pp. 85–159). Elsevier.

Besiktepe, S., Ryabushko, L., Ediger, D., Yilmaz, D., Zenginer, A., Ryabushko, V., Lee, R. 2008. Domoic acid production by *Pseudo-nitzschia calliantha* Lundholm, Moestrup et Hasle (Bacillariophyta) isolated from the Black Sea. *Harmful Algae,* 7, 438–442.

Bill. B., Lundholm. N., Connell, L., Baugh, K.A., Trainer, V.L. 2005. Domoic acid in *Pseudo- nitzschia cuspidata* from Washington State coastal waters. Abstract from the 3rd Symposium on Harmful Algae in the US. Monterey, CA. Oct. 2–7, 2005, p 77.

Bill, B.D., Cox, F.H., Horner, R.A., Borchert, J.A., Trainer, V.L, 2006. The first closure of shellfish harvesting due to domoic acid in Puget Sound, Washington, USA. *African Journal of Marine Science,* 28, 435–440

Blanco, J., Acosta, C. P., Mariño, C., Muñiz, S., Martín, H., Moroño, Á., Correa, J., Arévalo, F., Salgado, C. 2006a. Depuration of domoic acid from different body compartments of the king scallop *Pecten maximus* grown in raft culture and natural bed. *Aquatic Living Resources,* 19(3), 257–265. http://dx.doi.org/10.1051/alr:2006026

Blanco, J., Acosta, C., Bermúdez de la Puente, M., Salgado, C., 2002a. Depuration and anatomical distribution of the amnesic shellfish poisoning (ASP) toxin domoic acid in the king scallop *Pecten maximus*. *Aquatic Toxicology*, 60 (1-2), 111–121. https://doi.org/10.1016/s0166-445x(01)00274-0.

Blanco, J., Bermúdez, M., Arévalo, F., Salgado, C., Moroño, A. 2002b. Depuration of mussels (*Mytilus galloprovincialis*) contaminated with domoic acid. *Aquatic Living Resources*, 15, 53–60. https://doi.org/10.1016/S0990-7440(01)01139-1.

Blanco, J., Livramento, F., Rangel, I. M., 2010. Amnesic shellfish poisoning (ASP) toxins in plankton and molluscs from Luanda Bay, Angola. *Toxicon*, 55(2–3), 541–546. https://doi.org/10.1016/j.toxicon.2009.10.008.

Blanco, J., Mariño, C., Martín, H., Álvarez, G., & Rossignoli, A. E. 2021a. Characterization of the Domoic Acid Uptake Mechanism of the Mussel (*Mytilus galloprovincialis*) Digestive Gland. *Toxins*, 13:7, 458. https://doi.org/10.3390/toxins13070458.

Blanco, J., Mauríz, A. & Álvarez, G. 2020. Distribution of Domoic Acid in the Digestive Gland of the King Scallop *Pecten maximus*. *Toxins,* 12(371): 1-11. http://dx.doi.org/10.3390/toxins12060371

Blanco, J., Moroño, A., Arévalo, F., Correa, J., Salgado, C., Rossignoli, A., Lamas, P., 2021b. Twenty-Five Years of Domoic Acid Monitoring in Galicia (NW Spain): Spatial, Temporal and Interspecific Variations. *Toxins,* 13(11):756. https://doi.org/10.3390/toxins13110756.

Bogan, Y., Bender, K., Hervas, A., Kennedy, D., Slater, J., Hess. P. 2007c. Spatial variability of domoic acid concentration in king scallops *Pecten maximus* off the southeast coast of Ireland. *Harmful Algae*. 6(1): 1-14. https://doi.org/10.1016/j.hal.2006.05.004

Bogan, Y. M., Kennedy, D. J., Harkin, A. L., Gillespie, J., Vause, B. J., Beukers-Stewart, B. D., Hess, P., Slater, J.W. 2007a. Variation in domoic acid concentration in king scallop (*Pecten maximus*) from fishing grounds around the Isle of Man. *Harmful Algae*, 6, 81–92. https://doi.org/10.1016/j.hal.2006.07.002.

Bogan, Y.M., Harkin, A.L., Gillespie, J., Kennedy, D.J., Hess, P., Slater, J.W. 2007b. The influence of size on domoic acid concentration in king scallop, *Pecten maximus* (L.). *Harmful Algae*, 6, 15–28. https://doi.org/10.1016/j.hal.2006.05.005.

Bouchouicha-Smida, D., Bates, S.S., Lundholm, N., Lambert, C., Mabrouk, H.H., Sakka Hlaili, A. 2015. Viability, growth and domoic acid toxicity of the diatom *Nitzschia bizertensis* following filtration by the mussel *Mytilus sp*. *Marine Biology,* 162, 0. https://doi.org/10.1007/s00227-015-2758-x.

Braid, H.E., Deeds, J., DeGrasse, S.L., Wilson, J.J., Osborne, J., Hanner, R.H. 2012. Preying on commercial fisheries and accumulating paralytic shellfish toxins: a dietary analysis of invasive *Dosidicus gigas* (Cephalopoda Ommastrephidae) stranded in Pacific Canada. *Marine Biology,* 159, 25–31.

Bresnan, E., Fryer, R. J., Fraser, S., Smith, N., Stobo, L., Brown, N., Turrell, E. 2017. The relationship between *Pseudo-nitzschia* (Peragallo) and domoic acid in Scottish shellfish. *Harmful Algae,* 63, 193–202. https://doi.org/10.1016/j.hal.2017.01.004

Bricelj, V.M., Shumway, S.E. 1998. Paralytic Shellfish Toxins in Bivalve Molluscs: Occurrence, Transfer Kinetics, and Biotransformation. *Reviews in Fisheries Science*, 6(4), 315–383. https://doi.org/10.1080/10641269891314294.

Brodie, E.C., Gulland, F.M.D., Greig, D.J., Hunter, M., Jaakola, J., Leger, J., Leighfield, T.A., Van Dolah, F.M. 2006. Domoic acid causes reproductive failure in California sea lions (*Zalophus californianus*). *Marine Mammal Science,* 22(3), 700–707. https://doi.org/10.1111/j.1748-7692.2006.00045.x.

Buck, K.R., Uttalcooke, L., Pilskaln, C.H., Roelke, D.L., Villac, M.C., Fryxell, G.A., Cifuentes, l. Chavez, F.P. 1992. Autoecology of the diatom *Pseudo-nitzschia australis*, a domoic acid producer, from Monterey Bay, California. *Marine Ecology Progress Series,* 84: 293–302.

Busse L.B., Venrick E.L., Antrobus R., Miller P.E., Vigilant V., Silver, M.V., Mengelt, C., mydlarz l. Prezelin, B.B. 2006. Domoic acid in phytoplankton and fish in San Diego, CA, USA. *Harmful Algae,* 5: 91–101.

— C —

Campbell, D.A., Kelly, M.S., Busman, M., Bolch, C.J., Wiggins, E., Moeller, P.D.R., Morton, S.L., Hess, P., Shumway, S.E. 2001. Amnesic shellfish poisoning in the king scallop, *Pecten maximus*, from the west coast of Scotland. *Journal of Shellfish Research,* 20, 75–84.

Campbell, D.A., Kelly, M.S., Busman, M., Wiggins, E., Fernandes, T.F. 2003. Impact of preparation method on gonad domoic acid levels in the scallop, *Pecten maximus* (L.). *Harmful Algae,* 2, 215e222.

Canesi, L., Ciacci, C., Balbi, T. 2016. Invertebrate Models for Investigating the Impact of Nanomaterials on Innate Immunity: The Example of the Marine Mussel *Mytilus* spp. *Current Bionanotechnology,* 2(2), 77-83. https://doi.org/10.2174/2213529402666160601102529.

Canesi, L., Gallo, G., Gavioli, M., Pruzzo, C. 2002. Bacteria-hemocyte interactions and phagocytosis in marine bivalves. *Microscopy Research and Technique*, 57(6), 469–476. https://doi.org/10.1002/jemt.10100

Carella, F., Feist, S., Bignell, J., De Vico, G. 2015. Comparative pathology in bivalves: aetiological agents and disease processes. *Journal of Invertebrate Pathology*, 131, 107–120. https://doi.org/10.1016/j.jip.2015.07.012

Caruana, A.M.N., Ayache, N., Raimbault, V., Rétho, M., Hervé, F., Bilien, G., Amzil, Z., Chomérat, N. 2019. Direct evidence for toxin production by *Pseudo-nitzschia plurisecta* (Bacillariophyceae) and extension of its distribution area. *European Journal of Phycology,* 54, 585–594.

Cavalcante, K.P., 2011. Taxonomia da diatomácea potencialmente tóxica Pseudo-nitzschia Peragallo (Bacillariophyceae) em áreas de maricultura de Santa Catarina. M.Sc. Thesis. Univesidade Federal do Paraná, Curitiba, Brazil, https://acervodigital.ufpr.br/bitstream/handle/1884/25674/DISSERTACAO%20Cavalcante%20(2011).pdf? sequence=1&isAllowed=y

Cerino, F., Orsini, L., Sarno, D., Dell'Aversano, C., Tartaglione, L., Zingone, A. 2005. The alternation of different morphotypes in the seasonal cycle of the toxic diatom *Pseudo- nitzschia galaxiae*. *Harmful Algae,* 4:33–38.

César-Razquin, A., Snijder, B., Frappier-Brinton, T., Isserlin, R., Gyimesi, G., Bai, X., Reithmeier, Reinhart A., Hepworth, D., Hediger, Matthias A., Edwards, Aled M., Superti-Furga, G. 2015. A call for systematic research on solute carriers. *Cell,* 162, 478e487.

Chi, C., Giri, S.S., Jun, J.W., Kim, S.W., Kim, H.J., Kang, J.W., Park, S.C. 2018. Detoxification- and immune-related transcriptomic analysis of gills from Bay scallops (*Argopecten irradians*) in response to algal toxin okadaic acid. *Toxins,* 10, 308.

Chi, C., Zhang, C., Liu, J., Zheng, X. 2019. Effects of marine toxin domoic acid on innate immune responses in bay scallop. *Journal of Marine Science and Engineering,* 7(11), 407. https://doi.org/10.3390/jmse7110407.

Chinabut, S., Somsiri, T., Limsuwan, C., Lewis, S. 2006. Problems associated with shellfish farming, *Revue scientifique et technique*, 25, 627–635.

Choi, K.D., Lee, J.S., Lee, J.O., Oh, K.S., Shin, I.S. 2009. Investigation of domoic acid in shellfish collected from Korean fish retail outlets. *Food Science and Biotechnology*, 18: 842–848.

Clark, S., Hubbard, K.A., Anderson, D.M., McGillicuddy, D.J., Ralston, D.K., Townsend, D.W. 2019. *Pseudo-nitzschia* bloom dynamics in the Gulf of Maine: 2012–2016. *Harmful Algae,* 88: 101656.

Corpet, F. 1988. Multiple sequence alignment with hierarchical clustering. *Nucleic Acids Research,* 16(22): 10881–10890. https://doi.org/10.1093/nar/16.22.10881.

Costa, P. Costa, M.H. 2012. Development and application of a novel histological multichrome technique for clam histopathology. *Journal of Invertebrate Pathology*, 110, 411-414. http://dx.doi.org/10.1016/j.jip.2012.04.013

Costa, P. R., Rosa, R., Duarte-Silva, A., Brotas, V., Sampayo, M. A. M. 2005. Accumulation, transformation and tissue distribution of domoic acid, the amnesic shellfish poisoning toxin, in the common cuttlefish, *Sepia officinalis*. *Aquatic Toxicology*, 74(1), 82–91. https://doi.org/10.1016/j.aquatox.2005.01.011

Costa, P., Costa, M.H. 2012. Development and application of a novel histological multichrome technique for clam histopathology. *Journal of Invertebrate Pathology*, 110, 411–414. https://doi.org/10.1016/j.jip.2012.04.013.

Costa, P.R., Garrido, S. 2004a. Domoic acid accumulation in the sardine *Sardina pilchardus* and its relationship to *Pseudo-nitzschia* diatom ingestion. *Marine Ecology Progress Series,* 284, 261–268. https://doi.org/10.3354/meps284261.

Costa, P.R., Rodrigues, S., Botelho M.J., Sampayo M.A.M. 2003. A potential vector of domic acid: the swimming crab *Polybius henslowii* Leach (Decapoda-Brachyura). *Toxicon,* 42, 135-141. https://doi.org/10.1016/S0041-0101(03)00107-7.

Costa, P.R., Rosa, R., Duarte-Silva, A., Brotas, V., Sampayo, M.A.M. 2005a. Accumulation, transformation and tissue distribution of domoic acid, the amnesic shellfish poisoning toxin, in the common cuttlefish, *Sepia officinalis*. *Aquatic Toxicology,* 74, 82–91. https://doi.org/10.1016/j.aquatox.2005.01.011.

Costa, P.R., Rosa, R., Pereira, J., Sampayo, M.A.M. 2005b. Detection of domoic acid, the amnesic shellfish toxin, in the digestive gland of *Eledone cirrhosa* and *E. moschata* (Cephalopoda, Octopoda) from the Portuguese coast. *Aquatic Living Resources,* 18(4), 395–400. https://doi.org/10.1051/alr:2005041.

Costa, P.R., Rosa, R., Sampayo, M.A.M. 2004b. Tissue distribution of the amnesic shellfish toxin, domoic acid, in *Octopus vulgaris* from the Portuguese coast. *Marine Biology,* 44: 971–976. https://doi.org/10.1007/s00227-003-1258-6.

Cuervo, A. M. 2004. Autophagy: Many paths to the same end. *Molecular and Cellular Biochemistry,* 263(1/2), 55–72. https://doi.org/10.1023/b:mcbi.0000041848.57020.57.

— D —

D'Agostino, V.C., Degrati, M., Sastre, V., Santinelli, N., Krock, B., Krohn, T., Dans, S.L., Hoffmeyer, M.S. 2017. Domoic acid in a marine pelagic food web: Exposure of southern right whales *Eubalaena australis* to domoic acid on the Península Valdés calving ground, Argentina. *Harmful Algae,* 68, 248–257. https://doi.org/10.1016/j.hal.2017.09.001.

Dao, H. V., Takata, Y., Omura, T., Sato, S., Fukuyo, Y., Kodama, M. 2009. Seasonal variation of domoic acid in a bivalve *Spondylus versicolor* in association with that in plankton samples in Nha Phu Bay, Khanh Hoa, Vietnam. *Fisheries Science,* 75(2), 507–512. https://doi.org/10.1007/s12562-009-0057-5.

Dao, H.V., Phan, V.B., Teng, S.T., Uchida, H., Leaw, C.P., Lim, P.T., Suzuki, T., Pham, K.X., 2015. *Pseudo-nitzschia fukuyoi* (Bacillariophyceae), a domoic acid-producing species from Nha Phu Bay, Khanh Hoa Province, Vietnam. *Fisheries Science,* 81, 533–539.

Dao, V.H., Lim, P.T., Ky, P.X., Takata, Y., Teng, S.T., Omura, T., Fukuyo, Y., Kodama, M. 2014. Diatom *Pseudo-nitzschia* cf. *caciantha* (Bacillariophyceae), the most likely source of domoic acid contamination in the thorny oyster *Spondylus versicolor* Schreibers 1793 in Nha Phu Bay, Khanh Hoa Province, Vietnam. *Asian Fisheries Science*, 27, 16–29.

Davies, M.S. Hawkins, S.J. 1998. Mucus from Marine Molluscs. pp. 1–71. In: Blaxter J.H.S., Southward A.J., & Tyler P.A. (eds), Advances in Marine Biology, Academic Press.

Del Rio, R., Bargu, S., Baltz, D., Fire, S., Peterson, G. and Wang, Z. 2010. Gulf menhaden (Brevoortia patronus): A potential vector of domoic acid in coastal Louisiana food webs. *Harmful Algae,* 10(1): 19–29. https://doi.org/10.1016/j.hal.2010.05.006.

Delegrange, A., Lefebvre, A., Gohin, F., Courcot, L., Vincent, D. 2018. *Pseudo-nitzschia sp.* diversity and seasonality in the southern North Sea, domoic acid levels and associated phytoplankton communities. *Estuarine, Coastal and Shelf Science*, 214, 194–206. https://doi.org/10.1016/j.ecss.2018.09.030

Dizer, H., Fischer, B., Harabawy, A.S.A., Hennion, M.C., Hansen, P.D. 2001. Toxicity of domoic acid in the marine mussel *Mytilus edulis*. *Aquatic Toxicology,* 55: 149-156. https://doi.org/10.1016/s0166-445x(01)00178-3.

Dong, H. C., Lundholm, N., Teng, S. T., Li, A., Wang, C., Hu, Y., Li, Y. 2020. Occurrence of *Pseudo-nitzschia* species and associated domoic acid production along the Guangdong coast, South China Sea. *Harmful Algae,* 98, 101899. https://doi.org/10.1016/j.hal.2020.101899.

Douglas, D.J., Kenchington, E.R., Bird, C.J., Pocklington, R., Bradford, B., Silvert, W. 1997. Accumulation of domoic acid by the sea scallop (*Placopecten magellanicus*) fed cultured cells of toxic *Pseudo-nitzschia multiseries*. *Canadian Journal of Fisheries and Aquatic Sciences,* 54 (4), 907–913. https://doi.org/10.1139/f96-333.

Drum, A.S., Siebens, T.L., Crecelius, E.A., Elston, R.A. 1993. Domoic acid in the Pacific razor clam *Siliqua patula* (Dixon, 1789). *Journal of Shellfish Research*, 12, 443–450.

Dusek Dusek Jennings, E., Parker, M. S., Simenstad, C. A., 2020. Domoic acid depuration by intertidal bivalves fed on toxin-producing *Pseudo-nitzschia multiseries*. *Toxicon,* 6, 100027. https://doi.org/10.1016/j.toxcx.2020.100027.

Dzulhelmi, M.N., Usup, G. 2017. Screening of toxic marine Nitzschia species (Bacillariophyceae) in Malaysia. Indonesian Journal of Marine Environmental Sciences and Technologies. 10, 97–102.

— E —

EFSA. (2009). Panel on Contaminants in the Food Chain. Scientific Opinion of the Panel on Contaminants in the Food Chain on a request from the European Commission on marine biotoxins in shellfish—Domoic acid. EFSA J., 1181, 1–61.

— F —

Fabioux, C., Sulistiyani, Y., Haberkorn, H., Hégaret, H., Amzil, Z., Soudant, P. 2015. Exposure to toxic *Alexandrium minutum* activates the detoxifying and antioxidant systems in gills of the oyster *Crassostrea gigas*. *Harmful Algae,* 48, 55–62. https://doi.org/10.1016/j.hal.2015.07.003.

FAO. 2020. The State of World Fisheries and Aquaculture 2020. Sustainability in action. Rome. https://doi.org/10.4060/ca9229en

Fehling, J., Davidson, K., Bolch, C.J., Bates, S.S. 2004. Growth and domoic acid production by *Pseudo-nitzschia seriata* (Bacillariophyceae) under phosphate and silicate limitation. *Journal of Phycology,* 40:674–683.

Ferdin, M.E., Kvitek, R.G., Bretz, C.K., Powell, C.L., Doucette, G.J., Lefebvre, K.A. Coale, S., Silver, M.W. 2002. *Emerita analoga* (Stimpson) – possible new indicator species for the phycotoxin domoic acid in California coastal waters. *Toxicon,* 40:1259–1265.

Fernandes, L. F., Cavalcante, K. P., Proença, L. A. D. O., Schramm, M. A. 2013. Blooms of *Pseudo-nitzschia pseudodelicatissima* and *P. calliantha*, and associated domoic acid accumulation in shellfish from the South Brazilian coast. *Diatom Research,* 28(4), 381–393. https://doi:10.1080/0269249x.2013.821424.

Fernandes, L.F., Hubbard, K.A., Richlen, M., Smith, J., Bates, S.S., Ehrman, J., Léger, C., Mafra Jr, L.L., Kulis, D., Quilliam, M., Erdner, D., Libera, K., McCauley, L., Anderson, D.M. 2014. Diversity and toxicity of the diatom *Pseudo-nitzschia peragallo* in the Gulf of Maine, Northwestern. *Atlantic Ocean. Deep-Sea Res,* II 103, 139–162.

Fernández M.L., Shumway S.E., Blanco J., 2003. Management of shellfish resources. In: Hallegraeff G.M., Anderson A.D., Anderson D.M. (Eds.) Manual on Harmful Marine Microalgae. UNESCO Publishing, Paris, pp. 657-692.

Fire, S.E., Silver M.W. 2005. Domoic acid in the Santa Cruz wharf fishery. *California Fish and Game,* 91: 179–192.

Flannagan, R. S., Jaumouillé, V., Grinstein, S. 2012. The Cell Biology of Phagocytosis. *Annual Review of Pathology: Mechanisms of Disease*, 7(1), 61–98. https://doi.org/10.1146/annurev-pathol-011811-132445.

Fraga, S., Alvarez, M.J., Miguez, A., Fernandez, M.L., Costas, E., Lopez-Rodas, V. 1998. *Pseudo-nitzschia* species isolated from Galician waters: toxicity, DNA content and lectin binding assay. In: Reguera, B., Blanco, J., Fernandez, M.L., Wyatt, T. (Eds.), Harmful Algae. Xunta de Galicia and the IOC of UNESCO, Paris, pp. 270–273.

Fritz, L., Quilliam, M.A., Wright, J.L.C., Beale, A.M., Work, T.M. 1992. An outbreak of domoic acid poisoning attributed to the pennate diatom *Pseudo nitzschia australis*. *Journal of Phycology,* 28: 439–442.

Fryxell, G.A., Hasle, G.R. 2002. Taxonomy of Harmful Diatoms. In: Hallegraeff, G.M., Anderson, D.M., Cembella, A.D. (Eds.), Manual on Harmful Marine Microalgae, 2nd Edition. IOC Monographs on Oceanographic Methodology, No. 11. UNESCO, Paris, in press.

Fuentes, M.S., Wikfors, G.H. 2013. Control of domoic acid toxin expression in *Pseudo-nitzschia multiseries* by copper and silica: relevance to mussel aquaculture in New England (USA). *Marine Environmetal Research,* 83, 23–28.

Funk, J.A., Janech, M.G., Dillon, J.C., Bissler, J.J., Siroky, B.J., Bell, P.D. 2014. Characterization of Renal Toxicity in Mice Administered the Marine Biotoxin Domoic Acid. *Journal of the American Society of Nephrology,* 25(6), 1187–1197. https://doi:10.1681/asn.2013080836.

— G —

Gai, F.F., Hedemand, C.K., Louw, D.C., Grobler, K., Krock, B., Moestrup, Ø., Lundholm, N., 2018. Morphological, molecular and toxigenic characteristics of Namibian *Pseudo-nitzschia* species – including *Pseudo-nitzschia bucculenta sp*. *Harmful Algae,* 76, 80–95.

Gallacher, S., Howard, G., Hess, P., MacDonald, E., Kelly, M.C., Bates, L.A., Brown, N., MacKenzie, M., Gillibrand, P., Turrell, W.R. 2001. The occurrence of amnesic shellfish poisons in shellfish from Scottish waters. In: Hallegraeff, G.M., Black- burn,

S.I., Bolch, C.J., Lewis, R.J. (Eds.), Harmful Algal Blooms. IOC of UNESCO, France, pp. 30–33.

García-Corona, J. L., Hégaret, H., Deléglise, M., Marzari, A., Rodríguez-Jaramillo, C., Foulon, V., Fabioux, C., 2022. First subcellular localization of the amnesic shellfish toxin, domoic acid, in bivalve tissues: Deciphering the physiological mechanisms involved in its long-retention in the king scallop *Pecten maximus*. *Harmful Algae*, 116. https://doi.org/10.1016/j.hal.2022.102251.

García-Corona, J.L., Deléglise, M., Vanmaldergem, J., Petek, S., Terre-Terrillon, A., Bressolier, L., Fabioux, C., Hegaret, H. in prep a. Kinetics of the subcellular localization of the Amnesic Shellfish Poisoning toxin, domoic acid, in the king scallop *Pecten maximus* in a contamination and decontamination scenario.

García-Corona, J.L., Fabioux, C., Lassudrie-Duchesne, M., Derrien, A., Terre-Terrillon, A., Delaire, T., Hegaret, H. in prep b. Comparative study of domoic acid accumulation, isomer content and associated digestive subcellular processes in five marine invertebrate species.

Garrison D.L., Conrad S.M., Eilers P.P., Waldron, E.M. 1992. Confirmation of domoic acid production by *Pseudo-nitzschia australis* (Bacillariophyceae) cultures. *Journal of Phycology,* 28: 604–607.

Gether, U., Andersen, P.H., Larsson, O.M., Schousboe, A., 2006. Neurotransmitter transporters: molecular function of important drug targets. *Trends in Pharmacology Science,* 27, 375e383.

Gilgan, M.W. 1996. Fish Inspection Services, Department of Fisheries and Oceans, Canada. Unpublished data.

Gilgan, M.W., Burns B.G., Landry, G.J. 1990. Distribution and magnitude of domoic acid contamination of shellfish in Atlantic Canada. In: E. Graneli, B. Sundstrom, L. Edler, D.M. Anderson (Eds.), Toxic Marine Phytoplankton. Elsevier, N.Y. pp. 469-474.

Goldberg, J. 2003. Domoic Acid in the Benthic Food Web of Monterey Bay, California. Master's thesis, California State University, Moss Landing, CA.

Goldstein, T., Mazet, J.A.K., Zabka, T.S., Langlois, G., Colegrove, K.M., Silver, M., Bargu-Ates, S., Van Dolah, F., Leighfield, T., Conrad, P.A., Barakos, J., Williams, D.C., Dennison. S., Haulena, M.A., Gulland, F.M.D. 2008. Novel symptomatology and changing of domoic acid toxicosis in California sea lions (*Zalophus californianus*): an increasing risk to marine mammal health. *Proceedings of the Royal Society of London*, 1632: 267–276.

Gómez-Robles, E., Rodríguez-Jaramillo, C., Saucedo, P.E. 2005. Digital image analysis of lipid and protein histochemical markers for measuring oocyte

development and quality in pearl oyster *Pinctada mazatlanica* (Hanley, 1856). Journal of Shellfish Research, 24(4), 1197-1202. http://dx.doi.org/10.2983/0730-8000(2005)24[1197:DIAOLA]2.0.CO;2.

Gordon, S., 2016. Phagocytosis: An Immunobiologic Process. *Immunity,* 44(3), 463–475. https://doi.org/10.1016/j.immuni.2016.02.026.

Granéli, E., Turner, J.T. (Eds.). (2006). Ecology of Harmful Algae. *Ecological Studies.* https://doi.org/10.1007/978-3-540-32210-8.

Grattan, L.M., Holobaugh, S., Morris, J.G. 2016. Harmful algal blooms and public health. *Harmful Algae,* 57: 2–8.

Grimmelt, B., Nijjar, M.S., Brown, J., Macnair, N., Wagner, S., Johnson, G.R., Amend, J.F. 1990. Relationship between domoic acid levels in the blue mussel (*Mytilus edulis*) and toxicity in mice. *Toxicon,* 28:501–508.

— H —

Ha, D.V., Takata, Y., Sato, S., Fukuyo, Y., Kodama, M. 2006. Domoic acid in a bivalve *Spondylus cruentus* in Nha Trang Bay, Khanh HoaProvince, Vietnam. *Coastal Marine Science*, 30(1): 130–132. https://doi.org/10.15083/00040763.

Halestrap, A.P. 2013. The *SLC16* gene family-structure, role and regulation in health and disease. *Molecular Aspects of Medicine,* 34, 337e349. https://doi.org/10.1016/j.mam.2012.05.003.

Hallegraeff, G. M. (1993). A review of harmful algal blooms and their apparent global increase. In Phycologia (Vol. 32, Issue 2, pp. 79–99). Informa UK Limited. https://doi.org/10.2216/i0031-8884-32-2-79.1.

Hallegraeff, G.M. 2010. Ocean climate change, phytoplankton community response, and harmful algal blooms, a formidable predictive challenge. *Journal of Phycology,* 46: 220–235.

Hallegraeff, G.M. 2017. Marine phycotoxins and seafood safety. In: Witczak, A., Sikorski, Z.E. (Eds.), Toxins and Other Harmful Compounds in Foods. CRC Press, Taylor & Francis Group, Boca Raton, Florida, pp. 63–84.

Hallegraeff, G.M., 2004. Harmful algal blooms: a global overview. In: Hallegraeff, G.M., Anderson, D.M., Cembella, A. (Eds.), Manual on Harmful Marine Microalgae. UNESCO, Paris, pp. 25e50.

Hallegraeff, G.M., 2014. In: Rossini, G.P. (Ed.), Harmful Algae and Their Toxins: Progress, Paradoxes and Paradigm Shifts, Toxins and Biologically Active Compounds from Microalgae. CRC, Press, Boca Raton, FL, pp. 3–20.

Hallegraeff, G.M., Anderson, D.M., Cembella, A.D., Enevoldsen, H.O. 1995. Manual on harmful marine microalgae. UNESCO, Paris (France), IOC Manual Guide. 33:1–551.

Hampson, D.R., Manalo, J.L. 1998. The Activation of Glutamate Receptors by Kainic Acid and Domoic Acid. *Natural toxins,* 6: 153-158.

Harðardóttir, S., Pančić, M., Tammilehto, A., Krock, B., Møller, E.F., Nielsen, T.G., Lundholm, N. 2015. Dangerous relations in the Arctic marine food web: interactions between toxin producing *Pseudo-nitzschia* diatoms and *Calanus copepodites*. *Marine Drugs,* 13, 3809–3835.

Hay, B.E., Grant, C.M., McCoubrey, D.-J., 2000. A review of the marine biotoxin monitoring programme for non-commercially harvested shellfish. Part 1: Tech- nical report. A report prepared for the NZ Ministry of Health by AquaBio Consultants Ltd. NZ Ministry of Health. Available at http://www.moh.govt.nz/moh.nsf/0/5486048e2cc88b67cc256a50000ca20a/$FILE/MarineBiotoxinReport Dec2000.pdf.

Haya, K., Martin, J.L., Burridge, L.E., Waiwood, B.A., Wildish, J. 1991. Domoic acid in shellfish and plankton from the bay of Fundy, New Brunswick, Canada. *Journal of Shellfish Research*, 10, 113–118.

Hector, A., 2015. The new statistics with R: an introduction for biologists, 1st ed. Oxford University Press, New York.

Hediger, M.A., Clémençon, B., Burrier, R.E., Bruford, E.A. 2013. The ABCs of membrane transporters in health and disease (SLC series): introduction. *Molecular Aspects of Medicine,* 34, 95e107. https://doi.org/10.1016/j.mam.2012.12.009.

Hégaret, H., Smolowitz, R. M., Sunila, I., Shumway, S. E., Alix, J., Dixon, M., Wikfors, G. H. 2010. Combined effects of a parasite, QPX, and the harmful-alga, *Prorocentrum minimum* on northern quahogs, *Mercenaria mercenaria*. *Marine Environmental Research,* 69(5), 337–344. https://doi.org/10.1016/j.marenvres.2009.12.008.

Higgins, M.J., Sader, J.E., Mulvaney, P., Wetherbee, R. 2003. Probing the surface of living diatoms with atomic force microscopy: the nanostructure and nanomechanical properties of the mucilage layer. *Journal of Phycology,* 39, 722–734.

Hindson, C., Chevillet, J., Briggs, H., Gallichotte, E. N., Ruf, I. K., Hindson, B. J., Vessella, R., Tewari, M. 2013. Absolute quantification by droplet digital PCR versus analog real-time PCR. *Nature Methods,* http://10: 1003–1005. https://doi.org/10.1038/nmeth.2633.

Hoagland, P., Anderson, D.M., Kaoru, Y., White, A.W., 2002. The economic effects of harmful algal blooms in the United States: estimates, assessment issues, and information needs. Estuaries 25, 819–837.

Hoagland, P., Scatasta, S. 2006. The economic effects of harmful algal blooms. In Ecology of Harmful Algae. Edited by: Graneli, E., Turner, J. The Netherlands: Springer-Verlag, Dordrecht.

Höglund, P.J., Nordstrom, K.J., Schioth, H.B., Fredriksson, R., 2010. The solute carrier families have a remarkably long evolutionary history with the majority of the human families present before divergence of Bilaterian species. *Molecular Biology and Evolution,* 28: 1531e1541.

Hong, M. 2017. Biochemical studies on the structure–function relationship of major drug transporters in the ATP-binding cassette family and solute carrier family. *Advanced Drug Delivery Reviews,* 116: 3–20. https://doi.org/10.1016/j.addr.2016.06.003.

Horner, R.A., Kusske, M.B., Moynihan, B.P., Skinner, R.N. Wekell, J.C. 1993a. Retention of Domoic Acid by Pacific Razor Clams, *Siliqua patula* (Dixon, 1789): Preliminary Study. *Journal of Shellfish Research,* 12, 451-456.

Horner, R.A., Postel, J.R. 1993b. Toxic diatoms in western Washington waters (U.S. west coast). Hydrobiologia, 269: 197–205. https://doi.org/10.1007/BF00028018.

Huang, C. X., Dong, H. C., Lundholm, N., Teng, S. T., Zheng, G. C., Tan, Z. J., Lim, P.T., Li, Y. 2019. Species composition and toxicity of the genus *Pseudo-nitzschia* in Taiwan Strait, including *P. chiniana sp*. nov. and *P. qiana sp*. nov. *Harmful Algae,* 84, 195–209. http://doi:10.1016/j.hal.2019.04.003.

Huang, L., Wang, J., Chen, W.-C., Li, H.-Y., Liu, J.-S., Jiang, T., Yang, W.-D. 2014. P-glycoprotein expression in *Perna viridis* after exposure to *Prorocentrum lima*, a dinoflagellate producing DSP toxins. *Fish & Shellfish Immunology,* 39, 254e262. https://doi.org/10.1016/j.fsi.2014.04.020.

Husson, B., Hernández-Fariñas, T., Le Gendre, R., Schapira, M., Chapelle, A. 2016. Two decades of *Pseudo-nitzschia spp*. blooms and king scallop (*Pecten maximus*) contamination by domoic acid along the French Atlantic and English Channel coasts: Seasonal dynamics, spatial heterogeneity and interannual variability. *Harmful Algae,* 51, 26–39. https://doi.org/10.1016/j.hal.2015.10.017.

— J —

James, K.D., Gillman, M., Fernández-Amandi, M., López- Rivera, A., Fernández Puente, P., Lehane, M., Mitrovic, S., Furey, A. 2005. Amnesic shellfish poisoning toxins in bivalve molluscs in Ireland. *Toxicon,* 46, 852–858. https://doi.org/10.1016/j.toxicon.2005.02.009.

James, K.D., Gillman, M., Fernández-Amandi, M., López- Rivera, A., Fernández Puente, P., Lehane, M., Mitrovic, S., Furey, A., 2005. Amnesic shellfish poisoning toxins in bivalve molluscs in Ireland. *Toxicon,* 46, 852–858. https://doi.org/10.1016/j.toxicon.2005.02.009.

Jensen, S.-K., Lacaze, J.-P., Hermann, G., Kershaw, J., Brownlow, A., Turner, A., Hall, A. 2015. Detection and effects of harmful algal toxins in Scottish harbour seals and potential links to population decline. *Toxicon,* 97, 1–14.

Jeong, C.B., Kim, H.S., Kang, H.M., Lee, J.S. 2017. ATP-binding cassette (ABC) proteins in aquatic invertebrates: evolutionary significance and application in marine ecotoxicology*. Aquatic Toxicology,* 185, 29–39.

Jones, T. O., Whyte, J. N. C., Ginther, N. G., Townsend, L. D., Iwama, G. K. 1995. Haemocyte changes in the pacific oyster, *Crassostrea gigas*, caused by exposure to domoic acid in the diatom *Pseudonitzschia pungens f. multiseries. Toxicon,* 33(3), 347–353. https://doi.org/10.1016/0041-0101(94)00170-

Jones, T.O., Whyte, J.N.C., Ginther, N.G., Townsend, L.D., Iwama, G.K., 1995. Haemocyte changes in the pacific oyster, *Crassostrea gigas*, caused by exposure to domoic acid in the diatom *Pseudo-nitzschia pungens* f. multiseries. *Toxicon,* 33 (3), 347–353. https://doi.org/10.1016/0041-0101(94)00170-.

— K —

Kaniou-Grigoriadou, I., Mouratidou, T., Katikou, P. 2005. Investigation on the presence of domoic acid in Greek shellWsh. *Harmful Algae,* 4:717–723.

Kawatsu, K., Hamano, Y. 2000. Determination of domoic acid in Japanese mussels by enzyme immunoassay. Journal of AOAC INTERNATIONAL, 83, 1384–1386.

Kim, J.H., Wang, P., Park, B.S., Kim, J.H., Patidar, S.K., Han, M.S, 2018. Revealing the distinct habitat ranges and hybrid zone of genetic sub-populations within *Pseudo- nitzschia pungens* (Bacillariophyceae) in the West Pacific area. *Harmful Algae,* 73, 72–83.

Kim, Y., Ashton-Alcox, K.A. Powell, E.N. 2006. Histological Techniques for Marine Bivalve Molluscs: update. NOAA Technical Memorandum NOS NCCOS 27, Maryland.

Kimura, O., Kotaki, Y., Hamaue, N., Haraguchi, K., Endo, T. 2011. Transcellular transport of domoic acid across intestinal Caco-2 cell monolayers. *Food and Chemical Toxicology*, 49, 2167–2171.

Koepsell, H. 2013. The SLC22 family with transporters of organic cations, anions and zwitterions. *Molecular Aspects of Medicine,* 34 (2013) 413–435.

Kotaki, Y., 2008. Ecobiology of ASP producing diatoms. In: Botana, L.M. (Ed.), Seafood and Freshwater Toxins: Pharmacology, Physiology and Detection. CRC Press, Boca Raton, FL pp. 383–396.

Kotaki, Y., Koike, K., Yoshida, M., Thuoc, C.V., Huyen, N.T.M., Hoi, N.C., Fukuyo, Y., Kodama, M. 2000 Domoic acid production in *Nitzschia sp*. isolated from a shrimp-culture pond in Do Son,Vietnam. *Journal of Phycology,* 36:1057–1060.

Kreuder, C., Miller, M.A., Lowenstine, L.J., Conrad, P.A., Carpenter, T.E., Jessup, D.A., Mazet, J.A.K. 2005. Evaluation of cardiac lesions and risk factors associated with myocarditis and dilated cardiomyopathy in southern sea otters (*Enhydra lutris nereis*). *American Journal of Veterinary Research*, 66(2), 289–299. https://doi.org/10.2460/ajvr.2005.66.289.

Krogstad, F.T.O., Griffith, W.C., Vigoren, E.M., Faustman, E.M. 2009. Re-evaluating blue mussel depuration rates in 'Dynamics of the phycotoxin domoic acid: accumulation and excretion in two commercially important bivalves.' *Journal of Applied Phycology,* 21(6): 745–746. https://doi.org/10.1007/s10811-009-9410-4.

Kruppa, A. J., Kendrick-Jones, J., Buss, F. 2016. Myosins, Actin and Autophagy. *Traffic*, 17(8): 878–890. https://doi.org/10.1111/tra.12410.

Kudela, R.M., Berdalet, E., Bernard, S., Burford, M., Fernand, L., Lu, S., Roy, S., Usup, G., Tester, P., Magnien, R., Anderson, D., Cembella, A.D., Chinain, M., Hallegraeff, G., Reguera, B., Zingone, A., Enevoldsen, H., Urban, E. 2015. Harmful Algal Blooms. A Scientific Summary for Policy Makers. IOC/UNESCO, Paris, France.

Kvitek, R.G., Goldberg, J.D., Smith, G.J., Doucette, G.J., Silver, M.W. 2008. Domoic acid contamination within eight representative species from the benthic food web of Monterey Bay, California, USA. Marine Ecology Progress Series, 367, 35–47. https://doi.org/10.3354/meps07569.

Kvrgić, K., Lešić, T., Džafić, N., Pleadin, P. 2022. Occurrence and Seasonal Monitoring of Domoic Acid in Three Shellfish Species from the Northern Adriatic Sea. *Toxins,* 14(1), 33; https://doi.org/10.3390/toxins14010033.

— L —

La Barre, S., Bates, S.S., Quilliam, M.A. 2014. Domoic acid. In. Outstanding marine molecules: chemistry, biology, analysis. Edited by S. La Barre and J.-M. Kornprobst. Wiley-VCH Verlag GmbH & Co. KgaA, Weinheim, Germany, pp. 189–216.

Lage, S., Raimundo, J., Brotas, V., Costa, P.R., 2012. Detection and sub-cellular distribution of the amnesic shellfish toxin, domoic acid, in the digestive gland of *Octopus vulgaris* during periods of toxin absence. *Marine Biology Research,* 8 (8), 784–789.

Langella, M. 2005. Mechanisms of synaptic plasticity in the vertical lobe of *Octopus vulgaris*. PhD thesis. UK: The Open University.

Lapworth, C.J., Hallegraeff, G.M., Ajani, P.A., 2001. Identification of domoic acid-producing *Pseudo-nitzschia* species in Australian waters. In: Hallegraeff, G.M., Blackburn, S.I., Bolch, C.J., Lewis, R.J. (Eds.), Harmful Algal Blooms 2000. IOC UNESCO, Paris, pp. 38–41, in press.

Lassudrie, M., Soudant, P., Richard, G., Henry, N., Medhioub, W., da Silva, P. M., Donval, A., Bunel, M., Le Goïc, N., Lambert, C., de Montaudouin, X., Fabioux, C., Hégaret, H. 2014. Physiological responses of Manila clams *Venerupis* (=*Ruditapes*) *philippinarum* with varying parasite *Perkinsus olseni* burden to toxic algal *Alexandrium ostenfeldii* exposure. *Aquatic Toxicology,* 154, 27–38. https://doi.org/10.1016/j.aquatox.2014.05.002.

Lassus P. Chomérat, N. Hess, P. Nézan, E. 2016. Toxic and Harmful Micro-algae of the World Ocean / Micro-algues toxiques et nuisibles de l'océan mondial. Denmark, International Society for the Study of Harmful Algae/ Intergovernmental Oceanographic Commission of UNESCO. IOC Manuals and Guides, 68. (Bilingual English/French).

Lawrence, J., H. Loreal, H. Toyofuku, P. Hess, K. Iddya, and L. Ababouch. 2011. Assessment and Management of Biotoxin Risks in Bivalve Molluscs. FAO Fisheries and Aquaculture Technical Paper 551. FAO, Rome: p. 337.

Leandro, L.F., Teegarden, G.J., Roth, P.B., Wang, Z. and Doucette, G.J. 2010. The copepod *Calanus finmarchicus*: a potential vector for trophic transfer of the marine algal biotoxin, domoic acid. *Journal of Experimental Marine Biology and Ecology,* 382: 88–95.

Leblad, R. B., Lundholm, N., Goux, D., Veron, B., Sagou, R., Taleb, H., Nhhala, H., Er-Raioui, H. 2013. *Pseudo-nitzschia peragallo* (Bacillariophyceae) diversity and domoic acid accumulation in tuberculate cockles and sweet clams in M'diq Bay, Morocco. *Acta Botanica Croatica,* 72, 35–47.

Lee, Y.H., Chang, Y.C., Yan, H.Y., Chiao, C.C. 2013. Early visual experience of background contrast affects the expression of NMDA-like glutamate receptors in the optic lobe of cuttlefish, *Sepia pharaonis*. *Journal of Experimental Marine Biology and Ecology,* 447, 86–92. https://doi.org/10.1016/j.jembe.2013.02.014.

Lefebvre K.A., Dovel S.L., Silver M.W. 2001. Tissue distribution and neurotoxic effects ofdomoic acid in a prominent vector species, the northern anchovy *Engraulis mordax*. *Marine Biology,* 138: 693–700.

Lefebvre, K. A., Bargu, S., Kieckhefer, T., Silver, M. W. 2002a. From sanddabs to blue whales: the pervasiveness of domoic acid. *Toxicon,* 40(7), 971–977. https://doi.org/10.1016/s0041-0101(02)00093-4 .

Lefebvre, K. A., Robertson, A. 2010. Domoic acid and human exposure risks: A review. *Toxicon,* 56(2), 218–230. http://dx.doi.org/10.1016/j.toxicon.2009.05

Lefebvre, K.A., Dovel, S.L. Silver, M.W. 2001. Tissue distribution and neurotoxic effects of domoic acid in a prominent vector species, the northern anchovy *Engraulus mordax*. *Marine Biology,* 138: 693–700.

Lefebvre, K.A., Frame, E.R., Kendrick, P.S. 2012. Domoic acid and fish behavior: A review. *Harmful Algae,* 13, 126-130. https://doi.org/10.1016/j.hal.2011.09.011.

Lefebvre, K.A., Hendrix, A., Halaska, B., Duignan, P., Shum, S., Isoherranen, N., Marcinek, D.J., Gulland, F.M.D. 2018. Domoic acid in California sea lion fetal fluids indicates continuous exposure to a neuroteratogen poses risks to mammals. *Harmful Algae,* 79:53-57. https://doi.org/10.1016/j.hal.2018.06.003.

Lefebvre, K.A., Powell, C.L., Busman, M., Doucette, G.J., Moeller, P.D.R., Silver, J.B., Miller, P.E., Hughes, M.P., Singaram, S., Silver, M.W., Tjeerdema, R.S. 1999. Detection ofdomoic acid in northern anchovies and California sea lions associated with an unusual mortality event. *Natural Toxins,* 7:85–92

Lefebvre, K.A., Quakenbush, L., Frame, E., Huntington, K.B., Sheffield, G., Stimmelmayr, R., Bryan, A., Kendrick, P., Ziel, H., Goldstein, T., Snyder, J.A., Gelatt, T., Gulland, F., Dickerson, B., Gill, V. 2016. Prevalence of algal toxins in Alaskan marine mammals foraging in a changing arctic and subarctic environment. *Harmful Algae,* 55, 13–24. https://doi.org/10.1016/j.hal.2016.01.007.

Lefebvre, K.A., Silver M.W., Coale, S.L., Tjeerdema, R.S. 2002b. Domoic acid in planktivorous fish in relation to toxic *Pseudo-nitzschia* cell densities. *Marine Biology*, 140: 625–631.

Lefebvre, K.A., Tilton, S.C., Bammler, T.K., Beyer, R.P., Srinouanprachan, S., Stapleton, P.L., Farin, F.M., Gallagher, E.P. 2009. Gene expression profiles in zebrafish brain after acute exposure to domoic acid at symptomatic and asymptomatic doses. *Toxicological Sciences,* 107, 65e77. https://doi.org/10.1093/toxsci/kfn207.

Lelong, A., Hégaret, H., Soudant, P., Bates, S.S. 2012. *Pseudo-nitzschia* (Bacillariophyceae) species, domoic acid and amnesic shellfish poisoning: revisiting previous paradigms. *Phycologia,* 51 (2), 168–216. https://doi.org/10.2216/11-37.1.

Lema, K.A., Latimier, M., Nézan, É., Fauchot, J., Le Gac, M., 2017. Inter and intra-specific growth and domoic acid production in relation to nutrient ratios and

concentrations in *Pseudo-nitzschia*: phosphate an important factor. *Harmful Algae,* 64, 11.

Lerma, J., Paternain, A.V., Naranjo, J.R., Mellstrom, B. 1993. Functional kainate-selective glutamate receptors in cultured hippocampal neurons. *Proceedings of the National Academy of Sciences,* USA 90: 11688–11692.

Li, Y., Huang, C.X., Xu, G.S., Lundholm, N., Teng, S.T., Wu, H., Tan, Z. 2017. *Pseudo-nitzschia simulans sp*. nov. (Bacillariophyceae), the first domoic acid producer from Chinese waters. *Harmful Algae*, 67, 119–130.

Li, Y.; Sun, X.; Hu, X.; Xun, X.; Zhang, J.; Guo, X.; Jiao, W.; Zhang, L.; Liu, W.; Wang, J.; *et al.* 2017. Scallop genome reveals molecular adaptations to semi-sessile life and neurotoxins. Nature Communications, 8, 1721.

Liefer, J.D., Robertson, A., MacIntyre, H.L., Smith, W.L., Dorsey, C.P. 2013. Characterization of a toxic *Pseudo-nitzschia spp*. bloom in the Northern Gulf of Mexico associated with domoic acid accumulation in fish. *Harmful Algae,* 26, 20–32.

Lim, H.G., Teng, S.T., Leaw, C.P., Lim, P.T. 2013. Three novel species in the *Pseudo-nitzschia Pseudodelicatissima* complex: *P. batesiana sp.* nov., *P. lundholmiae sp*. nov. and *P. fukuyoi sp.* nov. (Bacillariophyceae), from the Strait of Malacca, Malaysia. Jouranl of Phycology, 49(5): 902-16. https://doi.org/10.1111/jpy.12101.

Lima, P.A., Nardi, G., Brown, E.R. 2003. AMPA/kainate and NMDA-like glutamate receptors at the chromatophore neuromuscular junction of the squid: role in synaptic transmission and skin patterning. *European Journal of Neuroscience*, 17, 507–516. https://doi.org/10.1046/j.1460-9568.2003.02477.x.

Lin, L., Yee, S.W., Kim, R.B., Giacomini, K.M. 2015. SLC transporters as therapeutic targets: emerging opportunities. Nature Reviews Drug Discovery, 4:543e60.

Lincoln, J.A., Turner, J.T., Bates, S.S., Léger, C., Gauthier, D.A. 2001. Feeding, egg production, and egg hatching success of the copepods *Acartia tonsa* and *Temora longicornis* on diets of the toxic diatom Pseudo-nitzschia multiseries and the non-toxic diatom *Pseudo-nitzschia* pungens. *Hydrobiologia*, 453, 107–120. https://doi.org/10.1023/a:1013163816771.

Litaker, R. W., Stewart, T. N., Eberhart, B.-T. L., Wekell, J. C., Trainer, V. L., Kudela, R. M., Miller, P.E., Roberts, A., Hertz, C., Johnson, T.A., Frankfurter, G., Smith, G.J., Schnetzer, A., Schumacker, J., Bastian, J.L., Odell, A., Gentien, P., Le Gal, D., Hardison, D.R., & Tester, P. A. (2008). Rapid Enzyme-linked Immunosorbent Assay for Detection of the Algal Toxin Domoic Acid. *Journal of Shellfish Research,* 27(5), 1301–1310. https://doi.org/10.2983/0730-8000-27.5.1301

Liu, H., Kelly, M.S., Campbell, D.A., Dong, S.L., Zhu, J.X., Fang, J.G., Wang, S.F. 2007a. Exposure to domoic acid affects larval development of king scallop *Pecten maximus* (Linnaeus, 1758). *Aquatic Toxicology*, 81, 152–158. https://doi.org/10.1016/j.aquatox.2006.11.012.

Liu, H., Kelly, M.S., Campbell, D.A., Dong, S.L., Zhu, J.X., Wang, S.F. 2007b. Ingestion of domoic acid and its impact on king scallop *Pecten maximus* (Linnaeus, 1758). *Journal of Ocean University of China*, 6, 175–181. https://doi.org/10.1007/s11802-007-0175-6.

Liu, H., Kelly, M.S., Campbell, D.A., Fang, J., Zhu, J. 2008. Accumulation of domoic acid and its effect on juvenile king scallop *Pecten maximus* (Linnaeus, 1758). *Aquaculture,* 284(1-4), 224–230. https://doi.org/10.1016/j.aquaculture.2008.

Lopes, V. M., Lopes, A. R., Costa, P., Rosa, R. 2013. Cephalopods as vectors of harmful algal bloom toxins in marine food webs. *Marine Drugs,* 11, 3381–3409. https://doi.org/10.3390/md11093381.

Lopes, V.M., Rosa, R., Costa, P.R. 2018. Presence and persistence of the amnesic shellfish poisoning toxin, domoic acid, in octopus and cuttlefish brains. *Marine Environmental Research,* 133, 45–48. https://doi.org/10.1016/j.marenvres.2017.12.001.

López-Rivera, A., Pinto, M., Insinilla, A., Isla, B. S., Uribe, E., Alvarez, G., Lehane, M., Furey, A., James, K.J. 2009. The occurrence of domoic acid linked to a toxic diatom bloom in a new potential vector: The tunicate *Pyura chilensis* (piure). *Toxicon,* 54(6), 754–762. https://doi.org/10.1016/j.toxicon.2009.05.033.

Lou, J.R., Cheng, J., Xun, X.G., Li, X., Li, M.L., Zhang, X.C., Li, T.T., Bao, Z.M., Hu, X.L. 2020. Glutathione S-transferase genes in scallops and their diverse expression patterns after exposure to PST-producing dinoflagellates. *Marine Life Science & Technology,* 2, 252–261.

Louw, D. C., Doucette, G. J., Lundholm, N. 2018. Morphology and toxicity of *Pseudo-nitzschia* species in the northern Benguela Upwelling System. *Harmful Algae,* 75, 118–128. doi:10.1016/j.hal.2018.04.008

Louw, D.C., Doucette, G.J., Voges, E. 2016. Annual patterns, distribution and long-term trends of *Pseudo-nitzschia* species in the northern Benguela upwelling system. Journal of Plankton Research. https://doi.org/10.1093/plankt/fbw079.

Lozano, V., Martínez-Escauriaza, R., Perez-Paralle, M.L., Pazos, A.J., Sanchez, J.L., 2015. Two novel multidrug resistance associated protein (MRP/ABCC) from the Mediterranean mussel (*Mytilus galloprovincialis*): characterization and expression patterns in detoxifying tissues. Canadian Journal of Zoology, 93, 567e578. https://doi.org/10.1139/cjz-2015-0011.

Lund, J., Barnett, H., HatWeld, C., Gauglitz, E., Wekell, J., Rasco, B. 1997 Domoic acid uptake and depuration in Dungeness crab (*Cancer magister* Dana 1852). *Journal of Shellfish Research,* 16:225–231.

Lundholm, N. (Ed.), 2018. Bacillariophyceae. In: IOC-UNESCO Taxonomic Reference List of Harmful Micro Algae. Accessed at http://www.marinespecies.org/hab.

Lundholm, N., Andersen, P., Jorgensen, K., Thorbjornsen, B. R., Cembella, A., Krock, B. 2005 Domoic acid in Danish blue mussels due to a bloom of *Pseudo-nitzschia seriata*. *Harmful Algae,* 29: 8–10.

Lundholm, N., Churro, C., Fraga, S., Hoppenrath, M., Iwataki, M., Larsen, J., Mertens, K., Moestrup, Ø., Zingone, A. 2009. IOC-UNESCO Taxonomic Reference List of Harmful Micro Algae. Accessed at https://www.marinespecies.org/hab.

Lundholm, N., Moestrup, Ø. 2000. Morphology of the marine diatom *Nitzschia navis-varingica sp.* nov., another producer of the neurotoxin domoic acid. *Joural of Phycology*. 36, 1162–1174.

Lundholm, N., Skov, J., Pocklington, R. & Moestrup, O. (1997): Studies on the marine planktonic diatom *Pseudo-nitzschia*. 2. Autecology of *P. pseudodelicatissima* based on isolates from Danish coastal waters. *Phycologia,* 36: 381–388.

Lundholm, N., Skov, J., Pocklington, R., Moestrup, Ø. 1994. Domoic acid, the toxic amino acid responsible for amnesic shellfish poisoning, now in *Pseudonitzschia seriata* (Bacillariophyceae) in Europe. *Phycologia,* 33: 475-478.

— M —

MacKenzie, A., White, D.A., Sim, P.G., Holland, A.J. 1993, Domoic acid and the New Zealand Greenshell mussel (*Perna canaliculus*). In: Smayda T.J., Shimizu Y. (Eds.) Toxic phytoplank- ton blooms in the sea. Elsevier Sci. Publ. B.V, Amsterdam., pp. 607-612.

Madhyastha, M.S., Novaczek, I., Ablett, R.F., Johnson, G., Nijjar, M.S., Sims, D.E. 1991. *In vitro* study of domoic acid uptake by digestive gland tissue of blue mussel (*Mytilus edulis* L.). Aquatic Toxicology, 20, 73–82.

Mafra Jr., L.L., Bricelj, V.M., Fennel, K. 2010a. Domoic acid uptake and elimination kinetics in oysters and mussels in relation to body size and anatomical distribution of toxin. Aquatic Toxicology, 100, 17–29. https://doi.org/10.1016/j.aquatox.2010.07.0.

Mafra Jr., L.L., Bricelj, V.M., Ouellette, C., Bates, S.S., 2010b. Feeding mechanics as the basis for differential uptake of the neurotoxin domoic acid by oysters,

Crassostrea virginica, and mussels, *Mytilus edulis*. Aquatic Toxicology, 97, 160–171.

Malhi, N., Turnbull, A., Tan, J., Kiermeier, A., Nimmagadda, R., McLeod, C. 2014. A national survey of marine biotoxins in wild-caught abalone in Australia. *Journal of Food Protection,* 77, 1960–1967. https://doi.org/10.4315/0362-028X.JFP-14-221.

Maneiro, I., Iglesias, P., Guisande, C., Riveiro, I., Barreiro, A., Zervoudaki, S., Granéli, E. 2005. Fate of domoic acid ingested by the copepod *Acartia clausi*. *Marine Biology,* 148(1), 123–130. https://doi:10.1007/s00227-005-0054-x.

Martin, J.L., Haya, K., and Wildish, D.J. 1993. Distribution and domoic acid content of *Nitzchia pseudodelicatissima* in the Bay of Fundy. In Toxic phytoplankton blooms in the sea. Edited by T.J. Smayda and Y. Shimizu. Elsevier Science Publishers B.V., Amsterdam, The Netherlands. pp. 613–618.

Martin, J.L., Haya, K., Burridge, L.E., Wildish, D.J. 1990. *Nitzschia pseudodelicatissima* a source of domoic acid in the Bay of Fundy, eastern Canada. Marine Ecology Progress Series, 67: 177– 182. https://doi:10.1127/nova_hedwigia/2018/0502.

Mat, A. M., Klopp, C., Payton, L., Jeziorski, C., Chalopin, M., Amzil, Z., Tran, D., Wikfors, G. H., Hégaret, H., Soudant, P., Huvet, A., Fabioux, C. 2018. Oyster transcriptome response to Alexandrium exposure is related to saxitoxin load and characterized by disrupted digestion, energy balance, and calcium and sodium signaling. *Aquatic Toxicology,* 199, 127–137. https://doi.org/10.1016/j.aquatox.2018.03.030.

Mathers, N.F., 1976. The effects of tidal currents on the rhythm of feeding and digestion in Pecten maximus L. *Journal of Experimental Marine Biology and Ecology,* 24 (3), 271–283. https://doi.org/10.1016/0022-0981(76)90059-9.

Mauriz, A., Blanco, J. 2010. Distribution and linkage of domoic acid (amnesic shellfish poisoning toxins) in subcellular fractions of the digestive gland of the scallop *Pecten maximus*. *Toxicon,* 55(2-3), 606–611. https://doi.org/10.1016/j.toxicon.2009.10.

Mazzillo, F.F.M., Staaf, D.J., Field, J.C., Carter, M.L., Ohman, M.D. 2011. A note on the detection of the neurotoxin domoic acid in beach-stranded *Dosidicus gigas* in the Southern California Bight. CalCOFI Rep. 52, 109–115.

McCabe, R.M., Hickey, B.M., Kudela, R.M., Lefebvre, K.A., Adams, N.G., Bill, B.D., Gulland, F.M.D., Thomson, R.E., Cochlan, W.P., Trainer, V.L. 2016. An unprecedented coastwide toxic algal bloom linked to anomalous ocean conditions. *Geophysical Research Letters,* 43, (10), 366–10,376. https://doi.org/10.1002/2016GL070023.

McGinness, K.L., Fryxell, G.A., Mceachran, J.D. 1995. *Pseudo-nitzschia* species found in digestive tracts of northern anchovies (*Engraulis mordax*). *Canadian Journal of Zoology,* 73:642–647.

McHuron, E.A., Greig, D.J., Colegrove, K.M., Fleetwood, M., Spraker, T.R., Gulland, F.M.D., Harvey, J.T., Lefebvre, K.A., Frame, E.R. 2013. Domoic acid exposure and associated clinical signs and histopathology in Pacific harbor seals (*Phoca vitulina richardii*). *Harmful Algae,* 23, 28–33. https://doi.org/10.1016/j.hal.2012.12.008.

McKenzie, J.D., Bavington, C. (2002). Measurement of Domoic Acid in King Scallops processed in Scotland. Final Report for The Food Standards Agency Scotland. https://www.foodstandards.gov.scot/downloads/Domoic_Acid_in_King_Scallops.pdf

McMillan, D.B., Harris, R.J., 2018. The Animal Cell. In An Atlas of Comparative Vertebrate Histology (pp. 3–25). Elsevier. https://doi.org/10.1016/b978-0-12-410424-2.00001-9.

Meredith, D., Christian, H., 2008. The *SLC16* monocaboxylate transporter family. *Xenobiotica*, 38, 1072e1106.

Miller, M.A., Moriarty, M.E., Duignan, P.J., Zabka, T.S., Dodd, E., Batac, F.I., Young, C., Reed, A., Harris, M.D., Greenwald, K., Kudela, R.M., Murray, M.J., Gulland, F.M.D., Miller, P.E., Hayashi, K., Gunther-Harrington, C.T., Tinker, M.T., Toy-Choutka, S. 2021. Clinical Signs and Pathology Associated With Domoic Acid Toxicosis in Southern Sea Otters (*Enhydra lutris nereis*). *Frontiers in Marine Science*, 8. https://doi.org/10.3389/fmars.2021.585501

Miyaji, T., Echigo, N., Hiasa, M., Senoh, S., Omote, H., Moriyama, Y. 2008. Identification of a vesicular aspartate transporter. Proceedings of the National Academy of Sciences, U.S.A. 105, 11720e117244. https://doi.org/10.1073/pnas.0804015105.

Mizushima, N., Ohsumi, Y., Yoshimori, T. 2002. Autophagosome Formation in Mammalian Cells. *Cell Structure and Function,* 27(6): 421–429. https://doi.org/10.1247/csf.27.421.

Moore, M. N. 2004. Diet restriction induced autophagy: A lysosomal protective system against oxidative- and pollutant-stress and cell injury. *Marine Environmental Research,* 58(2-5), 603–607. https://doi.org/10.1016/j.marenvres.2004.03.

Moore, M. N. 2008. Autophagy as a second level protective process in conferring resistance to environmentally-induced oxidative stress. *Autophagy,* 4(2), 254–256. https://doi.org/10.4161/auto.5528

Moreau, P., Moreau, K., Segarra, A., Tourbiez, D., Travers, M.-A., Rubinsztein, D. Renault, T. 2015. Autophagy plays an important role in protecting Pacific oysters

from OsHV-1 and *Vibrio aestuarianus* infections. *Autophagy,* 11, 516–526. https://doi.org/10.1080/15548627.2015.1017188

Mos, L. 2001. Domoic acid: a fascinating marine toxin. 2001. *Environmental Toxicology and Pharmacology*, 9: 79–85.

Moschandreou, K.K., Baxevanis, A.D., Katikou, P., Papaefthimiou, D., Nikolaidis, G., Abatzopoulos, T.J. 2012. Interand intraspecific diversity of *Pseudo-nitzschia* (Bacillariophyceae) in the northeastern Mediterranean. European Journal of Phycology, 47, 321–339.

— N —

Naar, J., Kubanek, J., Bourdelais, A., Richard, D., Tomas, C., Baden, D.G., Wright, J.L.C. 2002. Chemical characterization of marine biotoxins involved in an epizootic event of zoo animals in Newport, Kentucky. In: Xth International Conference on Harmful Algae, UNESCO, St. Pete Beach, Florida, p. 211.

Negri, R.M., Montoya, N.G., Carreto, J.I., Akselman, R., Inza, D., 2004. *Pseudo-nitzschia australis, Mytilus edulis, Engraulis anchoita,* and domoic acid in the Argentine Sea. In: Steidinger, K.A., Landsberg, J.H., Tomas, C.R., Vargo, G.A. (Eds.), Harmful Algae 2002. Florida Fish and Wildlife Conservation Commission. Florida Institute of Oceanography, and Intergovernmental Oceanographic Commission of UNESCO, St. Petersburg, FL, USA, pp. 139–141.

Nézan, E., Antoine, E., Fiant, L., Amzil, Z., Billard, C. 2006. Identification of *Pseudo-nitzschiaaustralis* and *P. multiseries* in the Bay of Seine. Was there a relation to presence of domoic acid in king scallops in autumn 2004? *Harmful Algae News,* 31, 1-3.

Nézan, E., Chomérat, N., Bilien, G., Boulben, S., Duval, A., Ryckaert, M. 2010. *Pseudo-nitzschia australis* on French Atlantic coast-an unusual toxic bloom. *Harmful Algae News*, 41, 1-2.

Nigam, S.K. 2015. What do drug transporters really do? Nature Reviews Drug Discovery. 14, 29e44.

Nishimura, T., Murray, J. S., Boundy, M. J., Balci, M., Bowers, H. A., Smith, K. F., Harwood, D. T., Rhodes, L. L. 2021. Update of the Planktonic Diatom Genus Pseudo-nitzschia in Aotearoa New Zealand Coastal Waters: Genetic Diversity and Toxin Production. Toxins, 13(9): 637. https://doi.org/10.3390/toxins13090637.

Novaczek, I., Madhyastha, M. S., Ablett, R. F., Donald, A., Johnson, G., Nijjar, M. S., Sims, D. E. 1992. Depuration of Domoic Acid from Live Blue Mussels (*Mytilus edulis*). *Canadian Journal of Fisheries and Aquatic Sciences,* 49(2), 312–318. https://doi.org/10.1139/f92-035

Novaczek, I., Madhyastha, M.S., Ablett, R.F., Johnson, G., Nijjar, M.S., Sims, D.E. 1991. Uptake, disposition and depuration of domoic acid by blue mussels (*Mytilus edulis*). *Aquatic Toxicology,* 21, 103e118.

— O —

O'Dea, S.N., 2012. Occurrence, Toxicity, and Diversity of *Pseudo-nitzschia* in Florida Coastal Waters. University of South Florida ProQuest Dissertations Publishing. 1515837.

O'Dea, S.N., Flewelling, L.J., Wolny, J., Brame, J., Henschen, K., Scott, P., Hubbard, K.A., Wren, J., Jones, C., Knight, C., Brooks, C., 2013. Florida's first shellfish closure due to domoic acid. In: Seventh Symposium on Harmful Algae in the U.S. Sarasota, FL. p. 103.

Olesen, A. J., Leithoff, A., Altenburger, A., Krock, B., Beszteri, B., Eggers, S. L., Lundholm, N. 2021. First Evidence of the Toxin Domoic Acid in Antarctic Diatom Species. *Toxins,* 13(2): 93. https://doi.org/10.3390/toxins13020093.

Orive, E., Pérez-Aicua, L., David, H., García-Etxebarria, K., Laza-Martínez, A., Seoane, S., Miguel, I., 2013. The genus *Pseudo-nitzschia* (Bacillariophyceae) in a temperate estuary with description of two new species: *Pseudo-nitzschia plurisecta* sp. nov. and *Pseudo-nitzschia abrensis* sp. nov. *Journal of Phycology*, 49, 1192–1206.

Orsini, L., Sarno, D., Procaccini, G., Poletti, R., Dahlmann, J., Montresor, M. 2002. Toxic *Pseudo-nitzschia multistriata* (Bacillariophyceae) from the Gulf of Naples: morphology, toxin analysis and phylogenetic relationships with other *Pseudo-nitzschia species*. Eur J Phycol 37:247–257.

Owen, G. 1977. Lysosomes, peroxisomes and bivalves. *Science Progress*, 60(239), 299–318.

Owen, G., 1972. Lysosomes, peroxisomes and bivalves. *Science Progress,* 60 (239), 299–318.

— P —

Pan, Y., Parsons, M.L., Busman, M., Moeller, P.D.R., Dortch, Q., Powell, C.L., Doucette, G.J. 2001. *Pseudo-nitzschia sp*. cf. *pseudodelicatissima* a confirmed producer of domoic acid from the northern Gulf of Mexico. Marine Ecology Proggres Ser. 220:83–92.

Parmentier, M., Detheux, M. 2007. Deorphanization of G-Protein-Coupled Receptors. In Ernst Schering Foundation Symposium Proceedings. 163–186. Springer Berlin Heidelberg. https://doi.org/10.1007/2789_2006_008.

Pazos, A.J., Ventoso, P., Martínez-Escauriaza, R., Pérez-Parallé, M.L., Blanco, J., Triviño, J.C., Sánchez, J.L. 2017. Transcriptional response after exposure to domoic acid-producing *Pseudo-nitzschia* in the digestive gland of the mussel *Mytilus galloprovincialis*. *Toxicon*, 140, 60–71. https://doi.org/10.1016/j.toxicon.2017.10.002.

Pazos, A.J., Ventoso, P., Martínez-Escauriaza, R., Pérez-Parallé, M.L., Blanco, J., Triviño, J.C., Sánchez, J.L. 2017. Transcriptional response after exposure to domoic acid-producing *Pseudo-nitzschia* in the digestive gland of the mussel *Mytilus galloprovincialis*. *Toxicon*, 140, 60–71. https://doi.org/10.1016/j.toxicon.2017.10.002.

Pednekar, S.M., Bates, S.S., Kerkar, V., Prabhu Matondkar, S.G. 2018. Environmental factors affecting the distribution of *Pseudo-nitzschia* in two monsoonal estuaries of western India and effects of salinity on growth and domoic acid production by *P. pungens*. *Estuaries and Coasts,* 41, 1448–1462.

Penna, A., Casabianca, S., Perini, F., Bastianini, M., Riccardi, E., Pigozzi, S., Scardi, M., 2013. Toxic *Pseudo-nitzschia spp*. in the northwestern Adriatic Sea: characterization of species composition by genetic and molecular quantitative analyses. Journal of Plankton, Res. 35, 352–366.

Perl, T.M., Bedard, L., Kosatsky, T., Hockin, J.C., Todd, E.C., Remis, R.S. 1990. An out- break of toxic encephalopathy caused by eating mussels contaminated with domoic acid. *The New England Journal of Medicine,* 322, 1775–1780. https://doi.org/10.1056/NEJM199006213222504.

Perl, T.M., Bédard, L., Kosatsky, T., Hockin, J.C., Todd, E.C.D., Remis, R.S., 1990. An Outbreak of Toxic Encephalopathy Caused by Eating Mussels Contaminated with Domoic Acid. *N. Engl. J. Med.* 322(25): 1775–1780. https://doi:10.1056/NEJM199006213222504.

Picot, S., Morga, B., Faury, N., Chollet, B., Dégremont, L., Travers, M.A., Renault, T., Arzul, I., 2019. A study of autophagy in hemocytes of the Pacific oyster *Crassostrea gigas*. *Autophagy,* 1–9. https://doi.org/10.1080/15548627.2019.1596.

Pistocchi, R., Guerrini, F., Pezzolesi, L., Riccardi, M., Vanucci, S., Ciminiello, P., Dell'Aversano, C., Forino, M., Fattorusso, E., Tartaglione, L., Milandri, A., Pompei, M., Cangini, M., Pigozzi, S., Riccardi, E. 2012. 2012. Toxin levels and profiles in microalgae from the North-Western Adriatic Sea –

Pitcher, G.C., Cembella, A.D., Krock, B., Macey, B., Mansfield, L., Probyn, T. 2014. Identification of the marine diatom *Pseudo-nitzschia* multiseries (Bacillariophyceae) as a source of the toxin domoic acid in Algoa Bay, South Africa. African Journal of Marine Sciencies. 36, 523–528.

Pizarro, G., Frangópulos, M., Krock, B., Zamora, C., Pacheco, H., Alarcón, C., Toro1, C., Pinto, M., Torres, R., Guzmán, L. 2017. Watch out for ASP in the Chilean Subantarctic region. In: Proença, L.A.O., Hallegraeff, G.M. (Eds.), Marine and Fresh- Water Harmful Algae. Proceedings of the 17th International Conference on Harmful Algae. International Society for the Study of Harmful Algae, and Intergovernmental Oceanographic Commission of UNESCO, Paris, pp. 30–33.

Powell, C., Ferdin, M., Busman, M., Kvitek, R., Doucette, G. 2002. Development of a protocol for determination of domoic acid in the sand crab (*Emerita analoga*): a possible new indicator species. *Toxicon,* 40:485–492.

Powell, C.L., Ferdinb, M.E., Busmana, M., Kvitekb, R.G., Doucettea, G.J. 2002. Development of a protocol for determination of domoic acid in the sand crab (*Emerita analoga*): a possible new indicator species. *Toxicon,* 40: 485-492.

Pulido, O.M. 2008. Domoic Acid Toxicologic Pathology: A Review. *Marine Drugs,* 6, 180-219. https://doi.org/10.3390/md20080010.

— Q —

Quilliam, M. A., Sim, P. G., McCulloch, A. W., McInnes, A. G. (1989). High-Performance Liquid Chromatography of Domoic Acid, a Marine Neurotoxin, with Application to Shellfish and Plankton. *International Journal of Environmental Analytical Chemistry,* 36(3), 139–154. https://doi.org/10.1080/03067318908026867.

— R —

R Core Team (2018). R: A language and environment for statistical computing. R Foundation for Statistical Computing,Vienna, Austria. URL https://www.R-project.org/.

R Core Team (2020). R: a language and environment for statistical computing. R Foundation for Statistical Computing, Vienna, Austria. URL https://www.R-project.org/.

Ramsdell, J.S. 2007. The molecular and integrative basis to domoic acid toxicity. In: Botana L (ed), Phycotoxins: Chemistry and Biochemistry, Blackwell Publishing Professional, Cambridge, MA, USA, 223–50.

Reimer, R.J. 2013. *SLC17*: a functionally diverse family of organic anion transporters. Molecular Aspects of Medicine. 34 (2e3), 350e359. https://doi.org/10.1016/j.mam.2012.05.004.

Reizopoulou, S., Strogyloudi, E., Giannakourou, A., Granéli, E., Pagou, K. 2012. Toxin accumulation in benthic populations under blooms of *Dinophysis acuminata* and *Pseudo-nitzschia multiseries.* In: Pagou, P., Hallegraeff, G. (Eds.), Proceedings of

the 14th International Conference on Harmful Algae. International Society for the Studyof Harmful Algae and Intergovernmental Oceanographic Commission of UNESCO, Paris, pp. 178–180.

Rhodes, L., Adamson, Scholin, C. 2000. *Pseudo-nitzschia multistriata* (Bacillariophyceae) in New Zealand. New Zealand Journal of Marine. Freshwater Researchers. 34: 463–7.

Rhodes, L., Scholin, C., Garthwaite, I., Haywood, A., Thomas, A. 1998 Domoic acid producing *Pseudo-nitzschia* species educed by whole cell DNA probe-based and immunochemical assays. In: Reguera B, Blanco J, Fernández ML, Wyatt T (eds) Harmful algae. Xunta de Galicia and IOC-UNESCO, Paris, pp 274–277.

Rhodes, L., White, D., Syhre, M., Atkinson, M. 1996. *Pseudonitzschia* species isolated from New Zealand coastal waters: domoic acid production *in vitro* and links with shellfish toxicity. In: Yasumoto T, Oshima Y, Fukuyo Y, eds. Harmful and Toxic Algal Blooms. IOC of UNESCO: pp 155–158.

Rivera-Vilarelle, M., Valdez-Velázquez, L.L., Quijano-Scheggia, S.I., 2018. Description of *Pseudo-nitzschia* cuspidata var. manzanillensis var. nov. (Bacillariophyceae): mor- phology and molecular characterization of a variety from the central Mexican Pacific. Diatom Res. 33, 55–68.

Rodríguez-Jaramillo, C., García-Corona, J.L., Zenteno-Savín, T., Palacios, E., 2022. The effects of experimental temperature increase on gametogenesis and heat stress parameters in oysters: Comparison of a temperate-introduced species (*Crassostrea gigas*) and a native tropical species (*Crassostrea corteziensis*). *Aquaculture,* 561, 738683. https://doi.org/10.1016/j.aquaculture.2022.738683.

Roelke, D.L., Fryxell, G.A., Cifuentes, L.A. 1993. Effects on the oyster *Crassostrea virginica* caused by exposure to the toxic diatom *Nitzschia pungens f. multiseries. J*. Shellfish Res. 12, 143.

Romero, M.L.J., Kotaki, Y., Lundholm, N., Thoha, H., Ogawa, H., Relox, J.R., Terada, R., Takeda, S., Takata, Y., Haraguchi, K., Endo, T., Lim, P.T., Kodama, M., Fukuyo, Y. 2011. Unique amnesic shellfish toxin composition found in the South East Asian diatom *Nitzschia navis-varingica*. *Harmful Algae,* 10, 456–462.

Romero, M.L.J., Kotaki, Y., Relox, J.R., Lundholm, N., Takata, Y., Kodama, M., Fukuyo, Y., 2012. Two new ASP toxin production types in strains of *Nitzschia navis-varingica* from the Philippines. *Estuarine and Coastal Marine Science*, 67–69.

Romero, M.L.J., Lirdwitayaprasit, T., Kotaki, Y., Lundholm, N., Relox, Jr, R.J., Furio, E.F., Terada, R., Yokoyama, T., Kodama, M., Fukuyo, Y. 2008. Isolation of ASP toxinproducing *Nitzschia from Thailand*. *Marine Research,*. Indonesia 33, 225–228.

Roth, M.A., Obaidat, B. Hagenbuch, OATPs, OATs and OCTs: the organic anion and cation transporters of the SLCO and SLC22A gene superfamilies, Br. J. Pharmacol. 165 (2012) 1260–1287.

Rowland-Pilgrim, S., Swan, S. C., O'Neill, A., Johnson, S., Coates, L., Stubbs, P., Dean, K., Parks, R., Harrison, K., Teixeira Alves, M., Walton, A., Davidson, K., Turner, A. D., & Maskrey, B. H. 2019. Variability of Amnesic Shellfish Toxin and *Pseudo-nitzschia* occurrence in bivalve molluscs and water samples–Analysis of ten years of the official control monitoring programme. *Harmful Algae,* 87: 101623). https://doi.org/10.1016/j.hal.2019.101623.

Rust, L., Gulland, F., Frame, E., Lefebvre, K. 2014. Domoic acid in milk of free living California marine mammals indicates lactational exposure occurs. *Marine Mammal Science,* 30(3), 1272–1278. https://doi.org/10.1111/mms.12117.

Ryabushko, L.I., Besiktepe, S., Ediger, D., Yilmaz, D., Zenginer, A., Ryabushko, V.I., Lee, R.I. 2008. Toxic diatom of *Pseudo-nitzschia calliantha* Lundholm, Moestrup et Hasle from the Black Sea: morphology, taxonomy, ecology. Mar. Ecol. J. ECOSI, 51–60.

— S —

Sahraoui, I., Bates, S.S., Bouchouicha, D., Mabrouk, H.H., Hlaili, A.S. 2011. Toxicity of *Pseudo-nitzschia* populations from Bizerte Lagoon, Tunisia, southwest Mediterranean, and firstreport of domoic acid production by *P. brasiliana*. Diatom Res. 26, 293–303. https://doi.org/10.1080/0269249X.2011.597990.

Sakka Hlaili, A., Sahraoui Khalifa, I., Bouchouicha-Smida, D., Melliti Garali, S., Ksouri, J., Chalghaf, M., Bates, S.S., Lundholm, N., Kooistra, W.H.C.F., de la Iglesia, P., Diogène, J. 2016. Toxic and potentially toxic diatom blooms in Tunisian (SW Mediterranean) waters: review of ten years of investigations. Adv. Environ. Res. 48, 51–69.

Sakka Hlaili, A., Sahraoui Khalifa, I., Bouchouicha-Smida, D., Melliti Garali, S., Ksouri, J., Chalghaf, M., Bates, S.S., Lundholm, N., Kooistra, W.H.C.F., de la Iglesia, P., Diogène, J., 2016. Toxic and potentially toxic diatom blooms in Tunisian (SW Mediterranean) waters: review of ten years of investigations. Advances in Environmental Research, 48, 51–69.

Santiago-Morales, I.S., García-Mendoza, E. 2011. Growth and domoic acid content of *Pseudo-nitzschia australis* isolated from northwestern Baja California, Mexico, cultured under batch conditions at different temperatures and two Si:NO3 ratios. *Harmful Algae,* 12, 82–94.

Schaffer, P., Reeves, C., Casper, D.R., Davis, C.R. 2006. Absence of neurotoxic effects in leopard sharks, *Triakis semifasciata*, following domoic acid exposure. *Toxicon*, 47 (7), 747-752. https://doi.org/10.1016/j.toxicon.2006.01.030.

Schnetzer, A., Lampe, R.H., Benitez-Nelson, C.R., Marchetti, A., Osburn, C.L., Tatters, A.O. 2017. Marine snow formation by the toxin-producing diatom, *Pseudo-nitzschia australis*. *Harmful Algae*, 61, 23–30. https://doi.org/10.1016/j.hal.2016.11.008.

Schnetzer, A., Miller, P.E., Schaffner, R.A., Stauffer, B., Jones, B., Weisberg, S.B., DiGiacomo, P.M., Berelson, W. and Caron, D.A. 2007. Blooms of *Pseudo-nitzschia* and domoic acid in the San Pedro Channel and Los Angeles harbor areas of the Southern California Bight, 2003–2004. *Harmful Algae,* 6: 372–387.

Scholin C.A., Gulland F., Doucette G.J., Benson S., Busman M., Chavez F.P., Cordaro J., DeLong R., De Vogelaere A., Harvey J., Haulena M., Lefebvre K., Lipscomb T., Loscutoff S., Lowenstine L.J., Martin R.I., Miller P.E., McLellan W.A., Moeller P.D.R., Powell C.L., Rowles T., Silvagnl P., Silver M., Spraker T., Trainer V., Van Dolah F.M. 2000, Mortality of sea lions along the central California coast linked to a toxic diatom bloom. *Nature,* 403, 80-84.

Schultz, I. R., Skillman, A., Sloan-Evans, S., Woodruff, D. 2013. Domoic acid toxicokinetics in Dungeness crabs: New insights into mechanisms that regulate bioaccumulation. *Aquatic Toxicology*, 140–141, 77–88). https://doi.org/10.1016/j.aquatox.2013.04.011.

Schwartz, J., Dubos, M.P., Pasquier, J., Zatylny-Gaudin, C., Favrel, P. 2018. Emergence of a cholecystokinin/sulfakinin signalling system in Lophotrochozoa. Scientific Reports, (8):1. https://doi.org/10.1038/s41598-018-34700-4.

Shanks, A.L., Morgan, S.G., MacMahan, J., Reniers, A.J.H.M., Kudela, R., Jarvis, M., Brown, J., Fujimura, A., Ziccarelli, L., Griesemer, C. 2016. Variation in the abundance of *Pseudo-nitzschia* and domoic acid with surf zone type. *Harmful Algae,* 55, 172–178.

Shubin, A. V., Demidyuk, I. V., Komissarov, A. A., Rafieva, L. M., Kostrov, S. V. 2016. Cytoplasmic vacuolization in cell death and survival. *Oncotarget,* 7(34), 55863–55889. https://doi.org/10.18632/oncotarget.10150.

Shumway, E. 1990. A Review of the Effects of Algal Blooms on Shellfish and Aquaculture. Journal of World Aquaculture Society, 21(2): 65-104.

Shumway, S.E., Allen, S.M., Boersma, P.D. 2003. Marine birds and harmful algal blooms: sporadic victims or under-reported events? *Harmful Algae,* 2, 1–17. https://doi.org/10.1016/S1568-9883(03)00002-7.

Sierra-Beltrán, A.S., Palafox-Uribe, M., Grajales-Montiel, J., Cruz-Villacorta, A., Ochoa, J.L. 1997. Sea bird mortality at Cabo San Lucas, Mexico: Evidence that toxic

diatom blooms are spreading. *Toxicon,* 35(3), 447–453. https://doi:10.1016/s0041-0101(96)00140.

Silvagni, P.A., Lowenstine, L.J., Spraker, T., Lipscomb, T.P., Gulland, F.M.D. 2005. Pathology of Domoic Acid Toxicity in California Sea Lions (*Zalophus californianus*). *Veterinary Pathology,* 42(2), 184–191. https://doi.org/10.1354/vp.42-2-184

Silvert, W., Subba R.D.V. 1992. Dynamic model of the flux of domoic acid, a neurotoxin, through a *Mytilus edulis* population. *Canadian Journal of Fisheries and Aquatic Sciences*, 49, 400- 405. https://doi.org/10.1139/f92-045.

Sison-Mangus, M.P., Jiang, S., Tran, K.N., Kudela, R.M. 2014. Host-specific adaptation governs the interaction of the marine diatom, *Pseudo-nitzschia* and their microbiota. ISME Journal, 8, 63–76.

Skepper, J.N., Powell, J.M. 2008. Immunogold Staining of Epoxy Resin Sections for Transmission Electron Microscopy (TEM). *CSH Protocols*, 3(6), 1-4. http://dx.doi.org/10.1101/pdb.prot5015

Smith, E. A., Papapanagiotou, E. P., Brown, N. A., Stobo, L. A., Gallacher, S., Shanks, A. M. 2006. Effect of storage on amnesic shellfish poisoning (ASP) toxins in king scallops (*Pecten maximus*). *Harmful Algae,* 5(1), 9–19. http://doi:10.1016/j.hal.2005.02.002.

Smith, E.A., Grant, F., Ferguson, C.M.J., Gallacher, S. 2001 Biotransformations of paralytic shellfish toxins by bacteria isolated from bivalve molluscs. *Environ Microbiol*, 67:2345–2353.

Smith, Q.R. 2000. Transport of glutamate and other amino acids at the blood-brain barrier. Journal of Nutrition, 130, 1016–1022.

Song, W., Li, D., Tao, L., Luo, Q., Chen, L. 2020. Solute carrier transporters: the metabolic gatekeepers of immune cells. *Acta Pharmaceutica B*, 10(1), 61–78. https://doi.org/10.1016/j.apsb.2019.12.006.

Stauffer, B.A., Gellene, A.G., Schnetzer, A., Seubert, E.L., Oberg, C., Sukhatme, G.S., Caron, D.A. 2012. An oceanographic, meteorological and biological 'perfect storm' yields a massive fish kill. *Marine Ecology Progress Series,* 468, 231–243.

Steffansen, B., Nielsen, C.U., Brodin, B., Eriksson, A.H., Andersen, R., Frokjaer, S. 2004. Intestinal solute carriers: an overview of trends and strategies for improving oral drug absorption. *European Journal of Pharmaceutical Sciences,* 21, 3e16.

Stewart, J.E., Marks, L.J., Gilgan, M.W., Pfeiffer, E., Zwicker, B.M. 1998. Microbial utilization ofthe neurotoxin domoic acid: blue mussels (*Mytilus edulis*) and soft shell clams (*Mya arena*) as sources of microorganisms. Canadian *Journal of Microbiology*, 44, 456–464.

Stonik, I. V., Orlova, T. Yu., Chikalovets, I. V., Aizdaicher, N. A., Aleksanin, A. I., Kachur, V. A., Morozova, T. V. 2019. *Pseudo-nitzschia species* (Bacillariophyceae) and the domoic acid concentration in *Pseudo-nitzschia* cultures and bivalves from the northwestern Sea of Japan, Russia. In Nova Hedwigia (Vol. 108, Issues 1–2, pp. 73–93). Schweizerbart.

Sykes, A.V., Almansa, E., Ponte, G., Cooke, G.M., Andrews, P.L.R. 2020. Can Cephalopods Vomit? Hypothesis Based on a Review of Circumstantial Evidence and Preliminary Experimental Observations. *Frontiers in Physiology,* 11. https://doi.org/10.3389/fphys.2020.00765.

— T —

Takahashi, E., Yu Q., Eaglesham G., Connell D.W., Mcbroom J., Costanzo S. Shaw G.R. 2007. Occurrence and seasonal variations of algal toxins in water, phytoplankton and shellfish from north stradbroke island, queensland, australia. M*arine environmental research,* 64: 429–442.

Takahashi, E., Yu, Eaglesham, Q., Connel, D.W.G., McBroom, J., Costanzo, S. Shaw, G.R. 2007 Occurrence and seasonal variations of algal toxins in water, phytoplankton and shellfish from north Stradbroke Island, Queensland, Australia. Mar. Environ. Res. 64: 429–442.

Takata, Y., Sato, S., Ha, D. V., Montojo, U. M., Lirdwitayaprasit, T., Kamolsiripichaiporn, S., Kotaki, Y., Fukuyo, Y., Kodama, M., 2009. Occurrence of domoic acid in tropical bivalves. *Fisheries Science,* 75(2), 473–480. https://doi.org/10.1007/s12562-009-0073-5.

Tammilehto, A., Nielsen, T.G., Krock, B., Møller, E.F., Lundholm, N., 2015. Induction of domoic acid production in the toxic diatom Pseudo-nitzschia seriata by calanoid copepods. Aquat. Toxicol. Amst. Neth. 159, 52–61. https://doi.org/10.1016/j.aquatox.2014.11.026.

Tammilehto, A., Nielsen, T.G., Krock, B., Møller, E.F., Lundholm, N. 2012. Calanus spp.–Vectors for the biotoxin, domoic acid, in the Arctic marine ecosystem? *Harmful Algae,* 20, 165–174.

Tan, S.N., Teng, S.T., Lim, H.C., Kotaki, Y., Bates, S.S., Leaw, C.P., Lim, P.T. 2016. Diatom *Nitzschia navis-varingica* (Bacillariophyceae) and its domoic acid production from the mangrove environments of Malaysia. *Harmful Algae,* 60, 139–149. https://doi.org/10.1016/j.hal.2016.11.003.

Tatters, A.O., Fu, F.-X., Hutchins, D.A. 2012. High CO_2 and silicate limitation synergistically increase the toxicity of *Pseudo-nitzschia fraudulenta*. PLoS ONE 7, e32116.

Teng, S.T., Lim, H.C., Lim, P.T., Dao, V.H., Bates, S.S., Leaw, C.P. 2014. *Pseudo-nitzschia kodamae* sp. nov. (Bacillariophyceae), a toxigenic species from the Strait of Malacca, Malaysia. *Harmful Algae,* 34, 17–28.

Teng, S.T., Lim, H.C., Lim, P.T., Rivera-Vilarelle, M., Quijano-Scheggia, S., Takata, Y., Quilliam, M.A., Wolf, M., Bates, S.S., Leaw, C.P. 2015. A non-toxigenic but morphologically and phylogenetically distinct new species of *Pseudo-nitzschia*, *Pseudo-nitzschia sabit* sp. nov. (Bacillariophyceae). Journal of Phycology, 51, 706–725.

Teng, S.T., Lim, H.C., Lim, P.T., Rivera-Vilarelle, M., Quijano-Scheggia, S., Takata, Y., Quilliam, M.A., Wolf, M., Bates, S.S., Leaw, C.P. 2015. A non-toxigenic but morphologically and phylogenetically distinct new species of *Pseudo-nitzschia*, *Pseudo-nitzschia sabit* sp. nov. (Bacillariophyceae). Journal of Phycology, 51, 706–725.

Tenorio, C., Álvarez, G., Quijano-Scheggia, S., Perez-Alania, M., Arakaki, N., Araya, M., Álvarez, F., Blanco, J., Uribe, E. 2021. First Report of Domoic Acid Production from *Pseudo-nitzschia multistriata* in Paracas Bay (Peru). *Toxins,* 13(6): 408. https://doi.org/10.3390/toxins13060408.

Tewari, K. 2022. A Review of Climate Change Impact Studies on Harmful Algal Blooms. *Phycology,* 2(2): 244–253. https://doi.org/10.3390/phycology2020013.

Thoha, H., Kotaki, Y., Panggabean, L., Lundholm, N., Ogawa, H., Lim, P.T., Takata, Y., Kodama, M., Fukuyo, Y. 2012. Screening of diatoms that produce ASP toxins in Southernmost Asian waters. *Coastal Mararine Sciemce*, 35, 34–38.

Thomas, K. M., LeBlanc, D. M., Quilliam, M. A. 1998. The 112th AOAC International Annual Meeting and Exposition, AOAC, Montreal.

Thorel, M., Fauchot, J., Morelle, J., Raimbault, V., Le Roy, B., Miossec, C., Kientz-Bouchart, V., Claquin, P. 2014. Interactive effects of irradiance and temperature on growth and domoic acid production of the toxic diatom *Pseudo-nitzschia australis* (Bacillariophyceae). *Harmful Algae,* 39, 232–241.

Todd, E.C.D. 1993 Domoic acid and amnesic shellfish poisoning – a review. *Journal of Food Protection,* 56, 69–83.

Torres de la Riva, G., Johnson, C.K., Mazet, J.A.K, Frances, Gulland, F.M.D., Langlois, G., Heyning, J., Rowles, T. 2006. Marine Mammal Strandings Along the Southern California Coast Associated With Domoic Acid Producing Algal Blooms. IAAAM Confeence Proceedings. Davis, CA.

Trainer, V. L., Bates, S. S., Lundholm, N., Thessen, A. E., Cochlan, W. P., Adams, N. G., Trick, C. G. 2012. *Pseudo-nitzschia* physiological ecology, phylogeny, toxicity, monitoring and impacts on ecosystem health. *Harmful Algae*, 14, 271–300. http://dx.doi.org/doi:10.1016/j.hal.2011.10.025

Trainer, V. L., Cochlan, W.P., Erickson, A., Bill, B.D., Cox, F.H., Borchert, J.A., Lefebvre, K.A. 2007 Recent domoic acid closures of shellfish harvest areas in Washington State inland waterways, *Harmful Algae,* 6: 449–459.

Trainer, V., L. Moore, B. Bill, N. Adams, N. Harrington, J. Borchert, D. da Silva, and B.T. Eberhart. 2013. Diarrhetic shellfish toxins and other lipophilic toxins of human health concern in Washington State. *Marine Drugs,* 1: 1815–1835.

Trainer, V.L. Bill, B.D. 2004. Characterization of a domoic acid binding site from Pacific razor clam. *Aquatic Toxicology*, 69, 125–132. http://dx.doi.org/10.1016/j.aquatox.2004.04.012

Trainer, V.L., Adams, N.G., Bill, B.D., Stehr, C.M., Wekell, J.C. 2000a. Domoic acid production near California coastal upwelling zones, June 1998. *Limnology and Oceanography,* 45, 1818–1833.

Trainer, V.L., Adams, N.G., Wekell, J.C. 2000b. Domoic acid-producing *Pseudo-nitzschia* species off the US. West coast associated with toxification events. In: Hallegraeff, G.M. (Ed.), Proceedings of the Ninth International Conference on Harmful Algal Blooms.

Trainer, V.L., Bates, S.S., Lundholm, N., Thessen, A.E., Cochlan, W.P., Adams, N.G. 2012. *Pseudo-nitzschia* physiological ecology, phylogeny, toxicity, monitoring and impacts on ecosystem health. *Harmful Algae,* 14, 271–300. https://doi.org/10.1016/j.hal.2011.10.025.

Trainer, V.L., Bates, S.S., Lundholm, N., Thessen, A.E., Cochlan, W.P., Adams, N.G., 2012. *Pseudo-nitzschia* physiological ecology, phylogeny, toxicity, monitoring and impacts on ecosystem health. *Harmful Algae,* 14, 271–300. https://doi.org/10.1016/j.hal.2011.10.025.

Trainer, V.L., Bates, S.S., Lundholm, N., Thessen, A.E., Cochlan, W.P., Adams, N.G. 2012. *Pseudo-nitzschia* physiological ecology, phylogeny, toxicity, monitoring and impacts on ecosystem health. *Harmful Algae,* 14, 271–300. https://doi.org/10.1016/j.hal.2011.10.025.

Trainer, V.L., Bates, S.S., Lundholm, N., Thessen, A.E., Cochlan, W.P., Adams, N.G., 2012. *Pseudo-nitzschia* physiological ecology, phylogeny, toxicity, monitoring and impacts on ecosystem health. *Harmful Algae,* 14, 271–300. https://doi.org/10.1016/j.hal.2011.10.025.

Trainer, V.L., Bill, B.D., 2004. Characterization of a domoic acid binding site from Pacific razor clam. *Aquatic Toxicology,* 69, 125–132. https://doi.org/10.1016/j.aquatox.2004.04.012.

Trainer, V.L., Cochlan, W.P., Erickson, A., Bill, B.D., Cox, F.H., Borchert, J.A., Lefebvre, K.A. 2007. Recent domoic acid closures ofshellfish harvest areas in

Washington State inland waterways. *Harmful Algae*, 6, 449–459. https://doi.org/10.1016/j.hal.2006.12.001.

Trainer, V.L., Hickey B.M., BATES S.S. 2008. Toxic diatoms. Oceans and human health: risks and remedies from the sea (Ed. by P.J. Walsh, S.L. Smith, L.E. Fleming, H. Solo-Gabrielle & W.H. Gerwick), pp. 219–237. Elsevier Science Publishers, New York.

Trainer, V.L., Hickey, B., Bates, S.S. 2008. Toxic diatoms. In: Walsh PJ, Smith SL, Fleming LE, Solo-Gabriele H, Gerwick WH, editors. Oceans and human health: risks and remediesfrom the sea.NewYork (NY): Elsevier. p. 219–237.

Trainer, V.L., Pitcher, G.C., Reguera, B., Smayda, T.J. 2010. The distribution and impacts of harmful algal bloom species in eastern boundary upwelling systems. *Progress in Oceanography,* 85(1-2), 33–52. https://doi.org/10.1016/j.pocean.2010.02.003.

Trick, C.G., Bill, B.D., Cochlan, W.P., Wells, M.L., Trainer, V.L., Pickell, L.D. 2010. Iron enrichment stimulates toxic diatom production in high-nitrate, low-chlorophyll areas. *Proceedings of the National Academy of Sciences,* 107, 5887–5892. https://doi.org/10.1073/pnas.0910579107.

Turner, A. D., Lewis, A. M., Bradley, K., Maskrey, B. H. 2021. Marine invertebrate interactions with Harmful Algal Blooms – Implications for One Health. *Journal of Invertebrate Pathology,* 186, 107555). https://doi.org/10.1016/j.jip.2021.107555.

Twiner, M.J., Flewelling, L.J., Fire, S.E., Bowen-Stevens, S.R., Gaydos, J.K., Johnson, C.K., Landsberg, J.H., Leighfield, T.A., Mase-Guthrie, B., Schwacke, L., Van Dolah, F.M., Wang, Z., Rowles, T.K. 2012. Comparative analysis of three brevetoxin-associated bottlenose dolphin (*Tursiops truncatus*) mortality events in the Florida panhandle region (USA). PLoS ONE 7, e42974.

— U —

Ujević, I., Ninčević-Gladan, Ž., Roje, R., Skejić, S., Arapov, J., Marasović, I. 2010. Domoic Acid - A New Toxin in the Croatian Adriatic Shellfish Toxin Profile. *Molecules*, 15(10): 6835–6849. https://doi.org/10.3390/molecules15106835.

— V —

Vale, P., Botelho, M.J., Rodrigues, S.M., Gomes, S.S., Sampayo, M.A.M. 2008. Two decades of marine biotoxin monitoring in bivalves from Portugal (1986-2006): A review of exposure assessment. *Harmful Algae,* 7:11-25.

Vale, P., Sampayo, M. A. M. 2002. Evaluation of marine biotoxin's accumulation by *Acanthocardia tuberculatum* from Algarve, Portugal. *Toxicon,* 40(5), 511–517. http://doi:10.1016/s0041-0101(01)00246-x.

Vale, P., Sampayo, M.A.M. 2001. Domoic acid in Portuguese shellfish and fish. *Toxicon,* 39:893–904. https://doi.org/10.1016/s0041-0101(00)00229-4.

Van Dolah, F.M. 2000. Marine algal toxins: origins, health effects, and their increased occurrence. EHP, 108: 133–141.

Ventoso, P., Pazos, A.J., Blanco, J., Pérez-Parallé, M.L., Triviño, J.C., Sánchez, J.L., 2021. Transcriptional Response in the Digestive Gland of the King Scallop (*Pecten maximus*) after the Injection of Domoic Acid. *Toxins,* 13, 339. https://doi.org/10.3390/toxins13050339.

Ventoso, P., Pazos, A.J., Pérez-Parallé, M.L., Blanco, J., Triviño, J.C., Sánchez, J.L. 2019. RNA-Seq Transcriptome Profiling of the Queen Scallop (*Aequipecten Opercularis*) Digestive Gland after Exposure to Domoic Acid-Producing *Pseudo-nitzschia*. *Toxins,* 11, 97. https://doi.org/10.3390/toxins11020097.

Veschasit, O., Meksumpun, S., Thawonsode, N., Lirdwitayaprasit, T. 2017. Accumulation of domoic acid in marine organisms from Sriracha Bay, Chonburi province, Thailand. *ScienceAsia,* 43, 207–216.

Vieira, A. C., Alemañ, N., Cifuentes, J. M., Bermúdez, R., Peña, M. L., Botana, L. M. 2015. Brain Pathology in Adult Rats Treated With Domoic Acid. *Veterinary Pathology* (52(6): 1077–1086. https://doi.org/10.1177/0300985815584074.

Vieira, A. C., Martínez, J. M. C., Pose, R. B., Queijo, Á. A., Posadas, N. A., López, L. M. B. 2015. Dose-response and histopathological study, with special attention to the hypophysis, of the differential effects of domoic acid on rats and mice. *Microscopy Research and Technique.* 78(5), 396–403). https://doi.org/10.1002/jemt.22486.

Vieira, A., Cifuentes, J., Bermúdez, R., Ferreiro, S., Castro, A., Botana, L. (2016). Heart Alterations after Domoic Acid Administration in Rats. *Toxins,* 8, 3-68. MDPI AG. https://doi.org/10.3390/toxins8030068.

Vigilant, V.L., Silver, M.W. 2007. Domoic acid in benthic flatfish on the continental shelf of Monterey Bay, California, USA*. Marine Biology,* 151(6), 2053–2062. https://doi.org/doi:10.1007/s00227-007-0634-z.

Villac, M.C., Roelke, D.L., Chavez, F.P., Cifuentes, L.A., Fryxell, G.A. 1993. *Pseudo-nitzschia australis* Frenguelli and related species from the west coast of the USA: occurrence and domoic acid production. Journal of Shellfish Research, 12:457–465.

— W —

Wang, L., Ye, X., Zhao, T. 2019. The physiological roles of autophagy in the mammalian life cycle. *Biological Reviews*, 94, 503–516. https://doi.org/10.1111/brv.12464

Wang, Y., Li, M., Lou, J., Xun, X., Chang, L., Wang, Y., Zhang, Q., Lu, L., Wang, H., Hu, J., Bao, Z., Hu, X. 2022. Transcriptome and Network Analyses Reveal the Gene Set Involved in PST Accumulation and Responses to Toxic Alexandrium minutum Exposure in the Gills of Chlamys farreri. *International Journal of Molecular Sciences,* 23(14): 7912). https://doi.org/10.3390/ijms23147912.

Wekell, J. C., Trainer, V. L., Ayres, D., Simons, D. 2002. A study of spatial variability of domoic acid in razor clams: recommendations for resource management on the Washington coast. *Harmful Algae,* 1(1), 35–43. http://doi:10.1016/s1568-9883(02)00004-5.

Wekell, J.C., Gauglitz Jr., E.J., Barnett, H.J., Hatfield, C.L., Eklund, M. 1994b. The occurrence of domoic acid in razor clams (*Siliqua patula*), Dungeness crab (*Cancer magister*), and anchovies (*Engraulis mordax*). *Journal of Shellfish Research,* 13, 587–593.

Wekell, J.C., Gauglitz, E.J., Barnett, H.J., Hatfield, C.L., Simons. D., Ayres, D. 1994a. Occurrence of domoic acid in Washington state razor clams (*Siliqua patula*) during 1991–1993. *Natural Toxins,* 2: 197– 205.

Wekell, J.C., Hurst, J., Lefebvre, K.A. 2004. The origin of the regulatory limits for PSP and ASP toxins in shellfish. Journal of Shellfish Research, 23: 927–930.

Whale, A.S., Cowen, S., Foy, C.A., Huggett, J.F. 2013. Methods for applying accurate digital PCR analysis on low copy DNA samples. PLoS ONE, 8(3): e58177. https://doi.org/10.1371/journal.pone.0058177.

Whyte, J.N.C., Ginther, N.G., Townsend, T.D. 1995, Accumulation and depuration of domoic acid by the mussel, *Mytilus californianus*. In: Lassus P., Arzul G., Erard E., Gentien P., Marcaillou C. (Eds.) Harmful marine algal blooms. Technique et documentation-Lavoisier, Intercept Ltd, París, pp. 531-537.

Wise, A., Jupe, S. C., Rees, S. 2004. The Identification of Ligands at Orphan G-Protein Coupled Receptors. *Annual Review of Pharmacology and Toxicology*, 44(1): 43–66). https://doi.org/10.1146/annurev.pharmtox.44.101802.121419.

Wohlgeschaffen, G. D., Mann, K. H., Subba Rao, D. V., Pocklington, R. 1992. Dynamics of the phycotoxin domoic acid: accumulation and excretion in two commercially important bivalves. *Journal of Applied Phycology,* 4(4), 297–310. https://doi.org/10.1007/bf02185786

Woods, A., 2016. Domoic acid production in *Pseudo-nitzschia* (Bacillariophyceae) as a general response to unbalanced growth: the role of photo-oxidative stress. Master's Thesis. Monterey Bay. Capstones and Theses, Paper 575. California State University 86 p.

Work, T.M., Beal, A.M., Fritz, L., Quilliam, M.A., Silver, M., Buck, K., Wright, J.L.C. 1993. Domoic acid intoxication of brown pelicans and cormorants in Santa Cruz, California. In: Smayda, T.J., (Ed.), Toxic Phytoplankton Blooms in the Sea, Elsevier, Amsterdam, pp. 643–649.

Wright, J.L., Bird, C.J., de Freitas, A.S., Hampson, D., McDonald, J., Quilliam, M.A., 1990a. Chemistry, biology, and toxicology of domoic acid and its isomers. Canada Diseases Weekly Report = Rapport Hebdomadaire des Maladies au Canada. Pp. 21-26.

Wright, J.L.C., Falk, M., McInnes, A.G., Walter, J.A., 1990b. Identification of isodomoic acid D and two new geometrical isomers of domoic acid in toxic mussels. *Canadian Journal of Chemistry,* 68(1), 22–25. https://doi.org/10.1139/v90-005.

— X —

Xu, Y.-Y., Liang, J.-J., Yang, W.-D., Wang, J., Li, H.-Y., Liu, J.-S. 2014. Cloning and expression analysis of P-glycoprotein gene in Crassostrea ariakensis. *Aquaculture*, 418e419, 39e47. https://doi.org/10.1016/j.aquaculture.2013.10.004.

Xun, X., Cheng, J., Wang, J., Li, Y., Li, X., Li, M., Lou, J., Kong, Y., Bao, Z., Hu, X. 2020. Solute carriers in scallop genome: Gene expansion and expression regulation after exposure to toxic dinoflagellate. *Chemosphere,* 241, 124968). https://doi.org/10.1016/j.chemosphere.2019.124968.

— Y —

You, G., Morris, E.M.. 2007. Overview of drug transporter families, in: G. You, E.M. Morris, B. Wang (Eds.), Drug Transporters: Molecular Characterization and Role in Drug Disposition, John Wiley & Son Inc. 2007, pp. 1–11.

Yurchenko, O., Kalachev, A. 2019. Morphology of nutrient storage cells in the gonadal area of the Pacific oyster, *Crassostrea gigas* (Thunberg, 1793). *Tissue Cell,* 56, 7–13. https://doi.org/10.1016/j.tice.2018.11.004.

— Z —

Zabaglo, K., Chrapusta, E., Bober, B., Kaminski, A., Adamski, M., Bialczyk, J. 2016. Environmental roles and biological activity of domoic acid: A review. *Algal Research*, 13, 94–101. http://dx.doi.org/10.1016/j.algal.2015.11.020

Zaman, L., Arakawa, O., Shimosu, A., Onoue, Y., Nishio, S., Shida, Y., Noguchi, T. 1997. Two new isomers of domoic acid from a red alga, Chondria armata. *Toxicon,* 35(2), 205-212. https://doi.org/10.1016/S0041-0101(96)00123-7

Zar, J. H., 2010. Biostatistical Analysis. 5th Ed. Pearson, Westlake Village, CA, 251 pp.

Zarrella, I., Herten, K., Maes, G. E., Tai, S., Yang, M., Seuntjens, E., Ritschard, E. A., Zach, M., Styfhals, R., Sanges, R., Simakov, O., Ponte, G., Fiorito, G. 2019. The survey and reference assisted assembly of the *Octopus vulgaris* genome. *Scientific Data,* 6(1). https://doi.org/10.1038/s41597-019-0017-6

Zeng, Q., Liu, J., Wang, C., Wang, H., Zhang, L., Hu, J., Bao, L., Wang, S. 2021. High-quality reannotation of the king scallop genome reveals no 'gene-rich' feature and evolution of toxin resistance. *Computational and Structural Biotechnology Journal,* 19. 4954–4960. https://doi.org/10.1016/j.csbj.2021.08.038.

Zhang, H., Li, P., Wu, B., Hou, J., Ren, J., Zhu, Y., Xu, J., Si, F., Sun, Z., Liu, X. 2022. Transcriptomic analysis reveals the genes involved in tetrodotoxin (TTX) accumulation, translocation, and detoxification in the pufferfish Takifugu rubripes. *Chemosphere*, 303, 134962. https://doi.org/10.1016/j.chemosphere.2022.134962.

Zhao, Y. G., Codogno, P., Zhang, H. 2021. Machinery, regulation and pathophysiological implications of autophagosome maturation. *Nature Reviews Molecular Cell Biology.* http://dx.doi.org/10.1038/s41580-021-00392-4

Zheng, G., Wu, H., Guo, M., Peng, J., Zhai, Y., Tan, Z. 2022. First observation of domoic acid and its isomers in shellfish samples from Shandong Province, China. *Journal of Oceanology and Limnology*, 40(6) 2231–2241. https://doi.org/10.1007/s00343-022-2104-3.

Zhu, Z., Qu, P., Fu, F., Tennenbaum, N., Tatters, A.O., Hutchins, D.A. 2017. Understanding the blob bloom: warming increases toxicity and abundance of the harmful bloom diatom *Pseudo-nitzschia* in California coastal waters. *Harmful Algae,* 67, 36–43.

COLLEGE DOCTORAL BRETAGNE SCIENCES DE LA MER ET DU LITTORAL

Université de Bretagne Occidentale

Titre: Mécanismes physiologiques impliqués dans la contamination et la lente dépuration de la toxine amnésiante, l'acide domoïque, chez la coquille St-Jacques *Pecten maximus*

Mots clés : *Pecten maximus, Pseudo-nitzschia*, acide domoïque, dépuration, autophagie, transporteurs membranaires.

Résumé: L'acide domoïque (AD) est une neurotoxine produite par les diatomées du genre *Pseudo-nitzschia* qui est responsable de l'intoxication par des toxines amnésiantes (ASP) chez l'homme. La coquille St-Jacques *Pecten maximus* est une ressource de grande valeur fréquemment exposée aux proliférations de *Pseudo-nitzschia*, capable d'accumuler de grandes quantités d'AD, et de les retenir pendant des mois voire des années, par rapport à d'autres bivalves à dépuration rapide. Ce travail avait pour objectif d'identifier les principaux mécanismes physiologiques impliqués dans la cinétique d'accumulation et la lente dépuration de l'AD chez *P. maximus*. Le développement d'une technique d'immunohistochie anti-AD a permis de visualiser qu'une partie de l'AD reste piégée dans des autophagosomes répartis dans le cytoplasme des cellules digestives des coquilles Saint-Jacques. Le suivi temporel de l'AD à l'échelle subcellulaire a révélé une forte implication de l'autophagie dans la longue rétention de l'AD chez *P. maximus,* alors que ce lien n'a pas pu être identifié aussi clairement chez d'autres dépurateurs rapides. L'exposition *in vitro* des glandes digestives de *P. maximus* et des moules *Mytilus edulis* à l'AD dissout a révélé une forte sur-expression des transcrits liés à l'autophagie chez les coquilles et une surexpression des récepteurs du glutamate (GR) et des transporteurs membranaires des solutés (SLC) chez la moule, ce qui pourrait confirmer l'hypothèse d'une différence de reconnaissance et d'assimilation et /ou d'excrétion de l'AD entre les dépurateurs lents et rapides. Ce travail a permis de progresser dans nos connaissances des mécanismes physiologiques impliqués dans la longue rétention de l'AD chez les coquilles Saint-Jacques *P. maximus* et représente une avancée majeure pour explorer, dans le futur, des stratégies visant à accélérer la décontamination chez cette espèce.

Title: Physiological mechanisms involved in the contamination and long retention of the Amnesic Shellfish Poisoning toxin, domoic acid, in the king scallop *Pecten maximus*

Keywords: *Pecten maximus, Pseudo-nitzschia*, domoic acid, depuration, autophagy, membrane transporters.

Abstract: Domoic acid (DA) is a neurotoxin produced by diatoms of the genus *Pseudo-nitzschia* and is responsible for Amnesic Shellfish Poisoning (ASP) in humans. The king scallop *Pecten maximus* is a high valuable resource frequently exposed to *Pseudo-nitzschia* blooms, and capable of accumulating high amounts of DA, retaining it for months or even a few years, compared to other fast-depurator bivalves. This work aimed to decipher what are the main physiological mechanisms involved in the kinetics of accumulation and slow depuration of DA in the scallop *P. maximus* in comparison to fast-depurator species. The development of an anti-DA immunohistochemical technique allowed to visualize that part of the DA-signal was trapped within autophagosomes distributed within the cytoplasm of the scallops digestive cells. The subcellular time-tracking of DA revealed a strong implication of autophagy in slow DA-depuration, which did not seem to occur as much in other fast depurating species. Furthermore, an *in vitro* exposure of digestive gland slices of scallops *P. maximus* and mussels *Mytilus edulis* to dissolved DA revealed a strong upregulation of autophagy-related transcripts in the scallops, and an overexpression of glutamate receptors (GR) and membrane solute-carriers (SLC) genes in mussels, which could support differences in recognition and assimilation/excretion of DA between slow and fast depurators. This work provides new evidence about physiological mechanisms involved in the long retention of DA in *P. maximus* and represents the baseline to explore procedures to accelerate decontamination in this species.